. 125, April 1, 1981
nplete in one issue

ISSN 0003–2670

NALYTICA CHIMICA ACTA

International journal devoted to all branches of analytical chemistry

ELSEVIER SCIENTIFIC PUBLISHING COMPANY

ANALYTICA CHIMICA ACTA

International journal devoted to all branches of analytical chemistry
Revue internationale consacrée à tous les domaines de la chimie analytique
Internationale Zeitschrift für alle Gebiete der analytischen Chemie

PUBLICATION SCHEDULE FOR 1981 (incorporating the section on Computer Techniques and Optimization).

	J	F	M	A	M	J	J	A	S	O	N	D
Analytica Chimica Acta	123	124/1	124/2	125	126	127	128	129	130/1	130/2	131	132
Section on Computer Techniques and Optimization		133/1			133/2			133/3			133/4	

Scope. *Analytica Chimica Acta* publishes original papers, short communications, and reviews dealing with every aspect of modern chemical analysis, both fundamental and applied. The section on *Computer Techniques and Optimization* is devoted to new developments in chemical analysis by the application of computer techniques and by interdisciplinary approaches, including statistics, systems theory and operation research. The section deals with the following topics: Computerized acquisition, processing and evaluation of data. Computerized methods for the interpretation of analytical data including chemometrics, cluster analysis, and pattern recognition. Storage and retrieval systems. Optimization procedures and their application. Automated analysis for industrial processes and quality control. Organizational problems.

Submission of Papers. Manuscripts (three copies) should be submitted as designated below for rapid and efficient handling:

Papers from the Americas to: Professor Harry L. Pardue, Department of Chemistry, Purdue University, West Lafayette, IN 47907, U.S.A.

Papers from all other countries to: Dr. A. M. G. Macdonald, Department of Chemistry, The University, P.O. Box 363, Birmingham B15 2TT, England.

For the section on *Computer Techniques and Optimization:* Dr. J. T. Clerc, Universität Bern, Pharmazeutisches Institut, Sahlistrasse 10, CH-3012 Bern, Switzerland.

American authors are recommended to send manuscripts and proofs by INTERNATIONAL AIRMAIL.

Submission of an article is understood to imply that the article is original and unpublished and is not being considered for publication elsewhere. Upon acceptance of an article by the journal, the author(s) resident in the U.S.A. will be asked to transfer the copyright of the article to the publisher. This transfer will ensure the widest dissemination of information under the U.S. Copyright Law.

Information for Authors. Papers in English, French and German are published. There are no page charges. Manuscripts should conform in layout and style to the papers published in this Volume. Authors should consult Vol. 121, p. 353 for detailed information. Reprints of this information are available from the Editors or from: Elsevier Editorial Services Ltd., Mayfield House, 256 Banbury Road, Oxford OX2 7DE (Great Britain).

Reprints. Fifty reprints will be supplied free of charge. Additional reprints (minimum 100) can be ordered. An order form containing price quotations will be sent to the authors together with the proofs of their article.

Advertisements. Advertisement rates are available from the publisher.

Subscriptions. Subscriptions should be sent to: Elsevier Scientific Publishing Company, P.O. Box 211, 1000 AE Amsterdam, The Netherlands. The section on *Computer Techniques and Optimization* can be subscribed to separately.

Publication. *Analytica Chimica Acta* (including the section on *Computer Techniques and Optimization*) appears in 11 volumes in 1981. The subscription for 1981 (Vols. 123–133) is Dfl. 1639.00 plus Dfl. 198.000 (postage) (total approx. U.S. $942.00). The subscription for the *Computer Techniques and Optimization* section only (Vol. 133) is Dfl. 149.00 plus Dfl. 18.00 (postage) (total approx. U.S. $86.00). Journals are sent automatically by airmail to the U.S.A. and Canada at no extra cost and to Japan, Australia and New Zealand for a small additional postal charge. All earlier volumes (Vols. 1–121) except Vols. 23 and 28 are available at Dfl. 164.00 (U.S. $84.00), plus Dfl. 13.00 (U.S. $6.50) postage and handling, per volume.

Claims for issues not received should be made within three months of publication of the issue, otherwise they cannot be honoured free of charge.

Customers in the U.S.A. and Canada who wish to obtain additional bibliographic information on this and other Elsevier journals should contact Elsevier/North Holland Inc., Journal Information Center, 52 Vanderbilt Avenue, New York, NY 10017. Tel: (212) 867-9040.

ANALYTICA CHIMICA ACTA
VOL. 125 (1981)

ANALYTICA CHIMICA ACTA

International journal devoted to all branches of analytical chemistry

ELSEVIER SCIENTIFIC PUBLISHING COMPANY

Anal. Chim. Acta, Vol. 125 (1981)

Analytica Chimica Acta, 125 (1981) 1—11
Elsevier Scientific Publishing Company, Amsterdam — Printed in The Netherlands

LUMINESCENCE ANALYSIS OF COMPLEX ORGANIC MATERIALS BASED ON RESOLVED LINE SPECTRA PRODUCED BY SELECTIVE LASER EXCITATION

L. A. BYKOVSKAYA, R. I. PERSONOV* and Yu. V. ROMANOVSKII

Institute of Spectroscopy, USSR Academy of Sciences, Troitsk, Moscow r-n, 142092 (USSR)

(Received 7th November 1980)

SUMMARY

Selective methods of obtaining the resolved line spectra of the solutions of complex molecules, along with the peculiarities of these spectra, are considered. At sufficiently low temperatures (4.2 K), broad-band absorption and luminescence spectra of the solutions of organic compounds are often broadened, mainly inhomogeneously. Excitation of the luminescence by tunable lasers can eliminate this broadening. The spectra obtained consist of dozens of narrow ($\Delta\nu \approx 1$ cm^{-1}) vibrational lines. Some examples of selective excitation for the spectrofluorimetric analysis of complex organic materials are given: identification (at the 10^{-11} g ml^{-1} level) and determination of individual polynuclear hydrocarbons in certain materials without preliminary separation is demonstrated by the determination of benzopyrene and perylene in gasoline and the detection of perylene in a solid paraffin.

In many cases luminescence methods of analysis of complex organic products present difficulties. The large width of a luminescence band (hundreds of cm^{-1}) results in the overlapping of spectra of individual components in a mixture. Even with preliminary extraction and chromatographic separation of the mixture, the fractions obtained are usually multicomponent and thus the difficulties of determining individual components are not eliminated.

The situation is considerably improved if quasi-line spectra can be obtained by the Shpol'skii method [1—3]. In this method, a crystalline matrix (one of a number of short-chain n-paraffins) is chosen; a quasi-line spectrum is obtained in this matrix at low temperatures. In a number of cases, such spectra allow the determination of individual compounds in a complex mixture. This method is currently used to determine polynuclear aromatic hydrocarbons (in particular carcinogenic ones) in various products. However, there are certain serious limitations to the use of n-paraffin matrices. Many compounds dissolve poorly in these nonpolar solvents, and various compounds which do dissolve have broad-band spectra under these conditions. Finally, even when this method is applicable, different n-paraffins have to be used for obtaining quasi-line spectra of various compounds.

0003—2670/81/0000—0000/$02.50

The present paper is devoted to a highly sensitive method of luminescence analysis which is applicable to a greater number of compounds and a large selection of solvents (both crystalline and glassy). The method is based on selective laser excitation of a certain type of luminescent centre in a complex mixture with inhomogeneously broadened spectra. This reveals (at low temperatures) a detailed line structure. These spectra, obtained with the use of tunable-laser excitation, allow identification and determination of several individual components in a complex mixture. In some cases, the method permits the direct analysis of the product under investigation without any preliminary separation and without using any solvents. The principles of selective spectroscopy of complex molecules are briefly outlined below, together with examples of identification and determination of some luminescent components in gasoline and solid paraffin.

PRINCIPLES OF SELECTIVE SPECTROSCOPY FOR COMPLEX MOLECULES IN SOLUTIONS

Considerable progress has been achieved in the understanding of the nature of the broad spectral bands of complex molecules in solution. In many cases [4, 5] at sufficiently low temperatures the inhomogeneous broadening is of such importance, that methods for eliminating it were developed [6].

A molecule in solution is similar to an impurity centre in a crystal. Therefore, each vibronic transition in a molecule should lead to a spectral band consisting of a narrow phonon-less line (p.l.l.) and a broad phonon wing (p.w.) (Fig. 1a). The relative intensity of the p.l.l. is determined by a Debye-Waller factor [7, 8]: $\alpha = I_{\text{p.l.l.}}/(I_{\text{p.l.l.}} + I_{\text{p.w.}}) = \exp[-2\,M\,(T)]$, where $I_{\text{p.l.l.}}$ and $I_{\text{p.w.}}$ are the integral intensities of the p.l.l. and p.w., respectively. The value 2 M depends on the strength of the electron–phonon coupling of the molecule with the solvent, on the character of the phonon spectrum of the solvent and on the temperature T [7, 8]. The weaker the electron–phonon coupling and the lower the temperature, the greater is the p.l.l. intensity. However, in many cases even at low temperature and weak electron–phonon coupling, a p.l.l. is not observed in the spectrum because of inhomogeneous broadening. The differences in the local conditions for individual molecules in a solid solution lead to the statistical scatter in their spectral positions. Therefore, though in the spectrum of each molecule the p.l.l. intensity at the maximum may considerably exceed the p.w. intensity, the summation of many optical bands of this type gives a broad structureless band (Fig. 1b). However, this inhomogeneous broadening can be eliminated and the fine structure of the spectrum revealed by selective excitation.

Fluorescence spectra

In the fluorescence spectrum, inhomogeneous broadening can be eliminated by means of selective laser excitation in the appropriate region of the absorp-

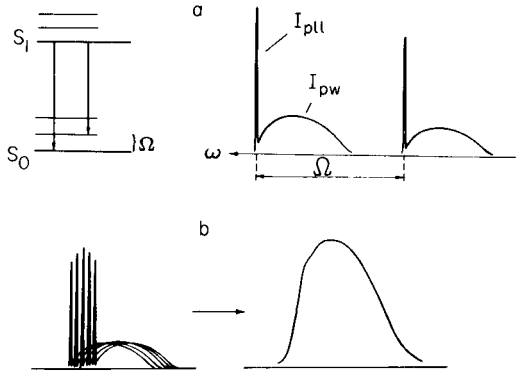

Fig. 1. Formation of fluorescence bands: (a) vibronic bands of one molecule; (b) an inhomogeneously broadened band.

tion spectrum [4—6]. In this case the laser excites mainly those molecules which have the absorption p.l.l. at this frequency. Therefore narrow lines are observed in the fluorescence spectrum pertaining to these molecules. Some examples are shown in Fig. 2. It can easily be seen that the transition from normal to monochromatic excitation results in a dramatic change in the character of the spectrum, from broad bands to narrow lines, which are accompanied by broad wings on the long-wavelength side. These results prove the inhomogeneous character of the spectral broadening and demonstrate that it can be eliminated by selective excitation. This method has enabled resolved line spectra of various classes of compounds in a great variety of solvents to be obtained, not only for neutral molecules, but also for their ionic forms. The main peculiarities of these spectra are briefly considered below.

First, it should be emphasized that a system of narrow phonon-less lines in the fluorescence spectra under selective excitation is determined by the vibronic levels of the molecules under investigation and is practically independent of the solvent. In contrast, the broad wings depend considerably on the solvent. At the same time, the long-wavelength wings near the p.l.l. are not purely phonon-like. Their nature is more complicated, for they include a true p.w., but also a contribution from the radiation (both p.l.l. and p.w.) of non-resonantly excited centres. (These centres are the molecules which absorb laser radiation not at a p.l.l., but at a p.w.) Therefore, the Debye-Waller factor observed is less than the true one. The observed factor α' can be shown to be connected with the true factor α by the relationship $\alpha' = \alpha^2$, if the value of the inhomogeneous broadening (usually 100—300 cm^{-1}) exceeds the p.w. homogeneous width, and if α is the same for absorption and emission. This means that the intensity of the lines observed in the spectra under selective excitation is rather sensitive to the variation of α caused, for example, by variation of the electron—phonon coupling in various solvents or by temperature variations.

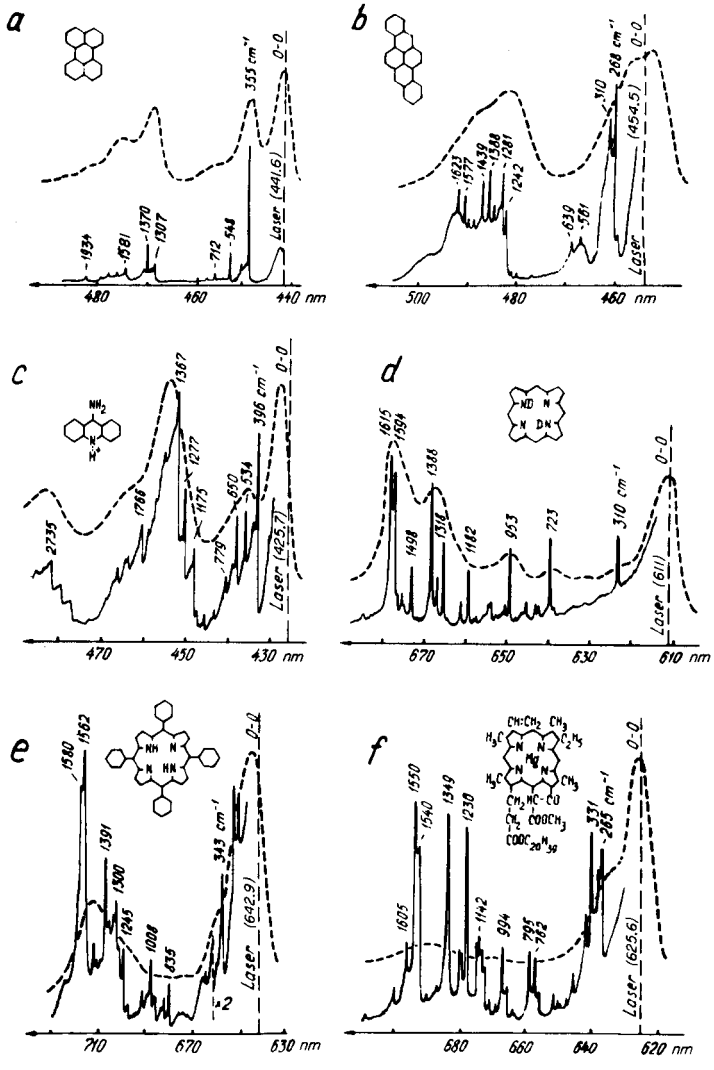

Fig. 2. Fluorescence spectra of solutions of organic compounds under normal (λ_{Hg} = 365.0 nm, broken lines) and laser (solid lines) excitation (T = 4.2 K): (a) perylene in ethanol; (b) 3,4,8,9-dibenzopyrene in polymethylmethacrylate; (c) 9-aminoacridinium ion in C_2H_5OH + HCl (pH 2); (d) porphorin-d_2 in C_2H_5OH + C_2H_5OD (e) tetraphenylporphorin in polystyrene; (f) protochlorophyll in ether.

Temperature increase causes the p.l.l. attenuation, i.e., a decrease of α and a greater decrease of α'. In many cases a p.l.l. in the fluorescence spectrum practically disappears when the temperature rises to 40—60 K. Therefore, resolved line spectra can be obtained only with the use of sufficiently low temperatures.

Measurements of the homogeneous width of a vibronic p.l.l. in the spectra under consideration give values of 1—5 cm^{-1}. (The homogeneous width of a

purely electronic line is considerably less; in the case of quasi-line spectra of molecular crystals of the impurity at 1.5—2 K, this width is of the order of 10^{-3} cm^{-1} [9, 10].) Accordingly, fluorescence line spectra can be obtained with the use of lasers with a line width of 1—2 cm^{-1}. Further narrowing of the laser line does not provide a significant improvement in the structure of the spectrum, but, at the same laser power, makes the undesirable "burning-out" of the centres more likely (see below). It is evident also that the width of vibronic lines determines the resolution required of the spectrometer.

An important feature of the spectra under consideration is their dependence on the excitation frequency [6, 11—16]. Gradual variation of the laser frequency within 100—200 cm^{-1} (i.e., within the limits of the value of the inhomogeneous broadening) during excitation in the region of the 0,0 transition leads only to the displacement of the whole spectrum along the frequency scale without much change in its structure. On increasing the laser frequency to the region of vibronic states, the fluorescence spectrum becomes a multiplet; in the region of the 0,0 transition a multiplet appears instead of a single line, which is afterwards repeated along the whole spectrum. The number of lines and their intensity distribution in the multiplet depend appreciably on the excitation frequency and are independent of the solvent. Without going into details concerning the nature of these multiplets [6, 11—16], they appear because in the region of vibronic transitions (under the conditions of inhomogenous broadening) the laser excites several types of centres, each to one of the vibrational sub-levels of the excited electronic state. The distances (in cm^{-1}) from the laser line to individual components of the 0,0 multiplet give the frequencies relevant to the molecule in its excited electronic state.

With further increase of the laser frequency, to cause excitation in the region of very high vibrational sub-levels of the excited electronic state (the region of overtones), the fluorescence spectrum loses its linear structure [12]. This is due to the fact that here the level widths and state density exceed considerably those in the region of the lowest vibronic states. Therefore, the laser affects practically all types of centres and the inhomogeneous broadening is not eliminated.

It can be concluded that in order to obtain a structured but simple spectrum, it is preferable to excite fluorescence in the region of a purely electronic transition.

Phosphorescence and absorption spectra

Selective excitation also enables inhomogeneous broadening to be eliminated and a line structure to be obtained in phosphorescence spectra. However, this requires monochromatic excitation of the phosphorescence directly in the region of the $T_1 \leftarrow S_0$ transition [6, 17].

Line structure can also be revealed in absorption spectra. This can be achieved by "burning-out" narrow gaps in the broad-band absorption spectrum [6, 18]. This is based on the selective photophysical or photochemical

modification of the centres which resonantly absorb laser radiation. The modification of the centres leads to the displacement of their absorption spectrum. As a result, in the inhomogeneously broadened absorption bands of the sample, narrow stable gaps appear at the laser frequency and at the frequencies of all vibronic transitions of the burnt-out centres. The totality of these gaps, the burnt-out spectrum [19], corresponds to a line absorption spectrum of the burnt-out molecules. Burnt-out spectra may be used for analytical purposes for both luminescent and non-luminescent compounds.

EXPERIMENTAL

The experimental set-up is shown schematically in Fig. 3. Each sample under investigation (0.5—1 ml) in a quartz cuvette (d = 1 mm) was placed in an optical helium cryostat with quartz windows. All measurements were made at 4.2 K.

For selective excitation of fluorescence, a tunable dye laser pumped by a nitrogen laser was used. Various dyes (PBO, POPOP, coumarin-47, -120 or -30, rhodamine-110, -6G or -B, oxazine-17, cresylviolet) were used to produce laser radiation in the region 390—680 nm. The laser operated with the frequency of 12—15 Hz. The average density of the laser excitation power on the sample was $\simeq$1 mW cm^{-2}. The width of the exciting line was 2 cm^{-1}.

Fluorescence spectra were recorded by a double diffraction spectrometer DFS-24 (linear dispersion 0.46 nm mm^{-1} at an aperture of f/5).

As was noted above, selective burning-out of molecules may occur under laser irradiation. As a result, the intensity of the fluorescence lines decreases in the course of recording a spectrum, so that the recorded spectrum does not give the true intensity distribution. In the experiments under consideration, a low density of the laser radiation power was used so that burning-out usually did not play an important role. It was appreciable only in the study of metal-free porphyrins where burning-out proceeds extremely easily and

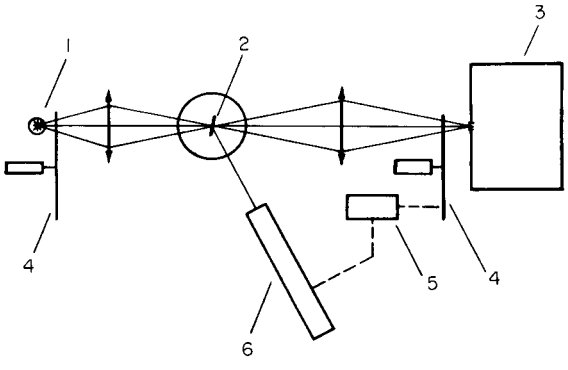

Fig. 3. Diagram of experimental set-up: (1) filament lamp, (2) sample in liquid helium cryostat, (3) DFS-24 spectrometer, (4) chopper, (5) electronic operating circuit for laser, (6) dye laser.

is connected with the displacement of two protons at the centre of the molecule. To eliminate any distortions, a special system was provided for restoration of the burnt-out centres by irradiating the sample with intense white light. This irradiation was done quasi-continuously and was synchronized with the spectrum recording. A chopper passed the intense light from a powerful filament lamp onto the sample during those intervals when a second chopper obstructed the spectrometer slit. The system of synchronization turns on the laser at the moment when the restoring light is cut off and the recording system is opened.

EXAMPLES OF ANALYTICAL APPLICATIONS

The methods described above can be used successfully for spectroscopic analysis of complex organic materials. For example, it has been demonstrated [20] that individual compounds (pyrene, anthracene, chrysene, etc.) can be determined at the ng ml^{-1} level in aqueous glycerol solutions, with fluorescence excitation by the u.v. lines of an argon laser.

In the present paper, some analytical possibilities of luminescence excitation by a tunable laser are discussed. For this purpose, the spectra of motor gasoline and solid commercial paraffin were studied. It should be stressed that in both cases the spectroscopic analysis was done on the product in its original form, without any preliminary separation.

Qualitative analysis

Figure 4(a) shows a section of the fluorescence spectrum of a motor gasoline in the visible region, under conventional u.v. excitation at 4.2 K. Although several maxima are present, it is rather difficult to identify indi-

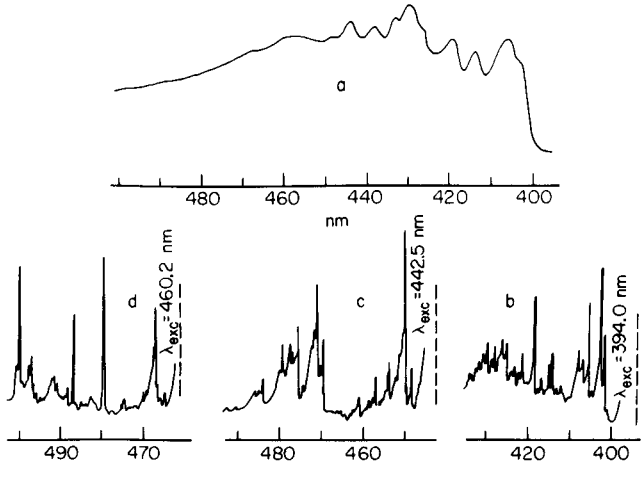

Fig. 4. Fluorescence spectra of gasoline at 4.2 K: (a) normal u.v. excitation; (b, c, d) selective tunable dye laser excitation.

vidual compounds in gasoline by means of this spectrum. Quite a different picture is observed in the spectrum when fluorescence is excited by a tunable laser. In this case, highly resolved spectra are observed with dozens of lines 1—5 cm^{-1} wide. The structure of these line-spectra is strongly dependent on the excitation frequency. The number of various spectra which can be obtained in this way is determined by the chosen tuning step of the laser and can be rather large. Figure 4 (b, c, d) shows three such spectra.

Owing to the large number and narrowness of the lines, fluorescence spectra obtained under selective excitation permit the reliable identification of individual compounds in a complex mixture. The identification of all fluorescent compounds in gasoline was not attempted, but a gasoline sample was analyzed for two polynuclear aromatic hydrocarbons, 3,4-benzopyrene and perylene. For this purpose, preliminary experiments were carried out with laser frequencies which would provide the most effective fluorescence excitation of these compounds and the sharpest spectral structure. The excitation conditions can be chosen with reference solutions or directly on the object under study; in the latter case, the compound being determined must be introduced in a sufficiently large concentration (10^{-4}—10^{-5} g ml^{-1})

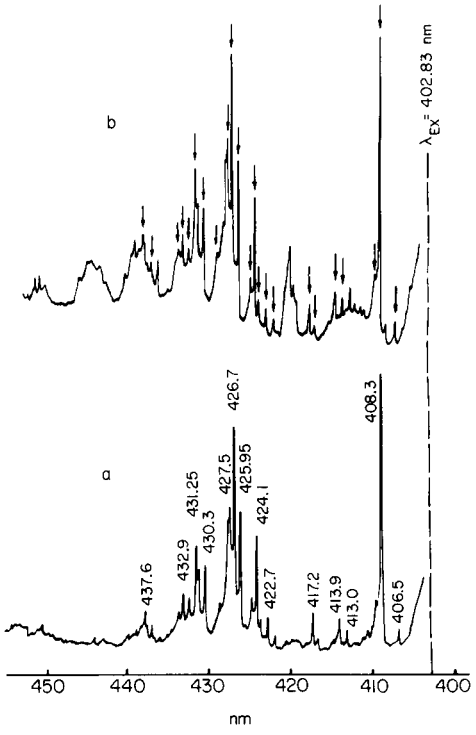

Fig. 5. Identification of 3,4-benzopyrene in gasoline from the fluorescence spectrum obtained under selective laser excitation at 4.2 K: (a) reference sample of 3,4-benzopyrene in gasoline (10^{-4} g ml^{-1}); (b) a portion of the gasoline spectrum, in which the 3,4-benzopyrene lines are marked by arrows.

that its luminescence will appreciably exceed the intrinsic luminescence of the sample. The spectrum recorded under these conditions was used as a reference spectrum.

Figure 5 shows the fluorescence spectrum of reference 3,4-benzopyrene and a section of the luminescence spectrum of a gasoline under excitation by the same laser line at 402.8 nm. It can be seen that all intense lines of 3,4-benzopyrene are present in the gasoline spectrum. The measurements show that more than 20 lines in both spectra coincide within the limits of experimental error (0.1 nm). The presence of 3,4-benzopyrene in gasoline is beyond doubt. The presence of perylene in gasoline was established in a similar way.

Identification of perylene in solid paraffin was considered as the second example. Figure 6 shows the fluorescence spectrum of paraffin with conventional excitation, and a fragment of the laser-excited fluorescence spectrum (laser line 441.6 nm); in the latter, narrow lines which belong to perylene are clearly revealed.

In addition to these lines, other lines of perylene are present at longer wavelength. To identify perylene in paraffin, the spectrum obtained under excitation as described previously [4, 5] was used as a reference.

Quantitative analysis

Small concentrations of fluorescent compounds can be determined using the selective excitation spectra, by various techniques. Among them the method of standard additions is of particular interest because it provides for a similar composition of constituents in the sample under study and in reference samples. This is important for quantitative measurements of the fluorescence spectra of multicomponent mixtures because systematic errors from the influence (e.g., fluorescence quenching, reabsorption) of other components of the mixture on the line intensities of the substance being determined can be avoided.

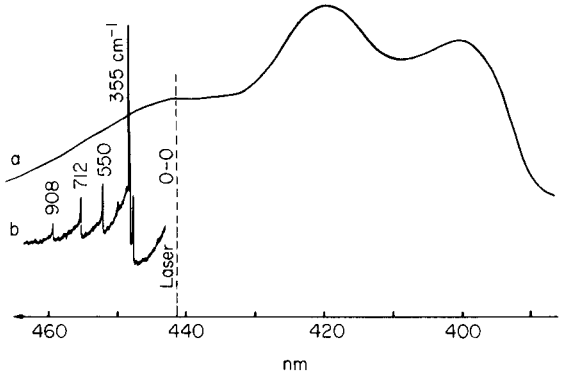

Fig. 6. Fluorescence spectra of commercial solid paraffin at 4.2 K: (a) normal u.v. excitation; (b) selective laser excitation.

In order to diminish random errors connected with variations in the experimental conditions (e.g., sample freezing which is difficult to control) on line intensities, the relative intensity of lines should be measured. In this case, the intensity ratio of the analytical line to the reference line (or band) is measured. A line which does not belong to the compound being determined can be chosen as a reference line.

The method is exemplified by the determination of perylene in gasoline. Five 1-ml portions of gasoline were taken and perylene was added to four of them to give added concentrations of 2.5×10^{-8}, 5×10^{-8}, 10×10^{-8} and 18×10^{-8} g ml^{-1}. Fluorescence was excited by laser radiation at 441.6 nm and the intense 448.6-nm line in the fluorescence spectrum of perylene was chosen as the analytical line, and the 447.1-nm line in the gasoline spectrum served as the reference. Figure 7 shows recordings of these lines in the spectrum of gasoline and a calibration plot. The perylene concentration in gasoline was measured to be 5×10^{-8} g ml^{-1} by standard addition as indicated.

The concentration of 3,4-benzopyrene in gasoline was determined in a similar way. For three different gasoline grades the values obtained were within the range $(1—2) \times 10^{-7}$ g ml^{-1}.

Limit of detection and accuracy are important characteristics of any analytical method. In the analysis of complex mixtures, the character of which may vary considerably, these characteristics may vary appreciably in different cases and must be established for each particular case. The possibility of detecting an analytical line and the precision of measuring its intensity obviously depend on the background in the spectrum. Also important is the absorption cross-section of the compound being determined at the laser frequency and the quantum yield of its fluorescence.

To describe the general characteristics of the method, the results obtained with model solutions of perylene in ethanol are presented. The 448.6-nm line

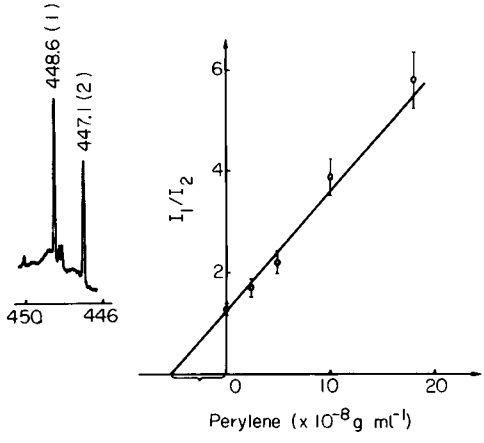

Fig. 7. Pair of lines and calibration graph used for the determination of perylene in gasoline.

was easily observed down to 10^{-11} g ml^{-1}. The average error at 10^{-8} g ml^{-1} was less than 20%. The limit of detection and the accuracy may be improved by using more powerful and more stabilized lasers and a signal accumulating technique.

REFERENCES

1 E. V. Shpol'skii, A. A. Il'ina and L. A. Klimova, Dokl. Akad. Nauk SSSR, 87 (1952) 935.
2 E. V. Shpol'skii, Uspekhi Fiz. Nauk, 80 (1963) 255.
3 E. V. Shpol'skii and R. I. Personov, Zavod. Lab., 4 (1962) 428.
4 R. I. Personov, E. I. Al'shits and L. A. Bykovskaya, Pis'ma v Zh. Eksper. Teor, Fiz., 15 (1972) 609; Opt. Commun., 6 (1972) 169.
5 R. I. Personov, E. I. Al'shits, L. A. Bykovskaya and B. M. Kharlamov, Zh. Eksper. Teor. Fiz., 65 (1973) 1825.
6 R. I. Personov, Izv. Akad. Nauk. SSSR, Ser. Fiz., 42 (1978) 242, and references therein.
7 A. Maradudin, in F. Seitz and D. Turnbull (Eds.), Solid State Physics, Suppl. 3, J. Wiley, 1963, Ch. 8.
8 K. K. Rebane, Impurity Spectra of Solids, Plenum, NY, 1970, Ch. 2.
9 S. Volker, R. M. Macfarlane, A. Z. Genack, H. P. Trommsdorff and J. H. van der Waals, J. Chem. Phys., 67 (1977) 1759.
10 A. A. Gorokhovskii and L. A. Rebane, Izv. Akad. Nauk SSSR, Ser. Fiz., 44 (1980) 859.
11 R. I. Personov and E. I. Al'shits, Chem. Phys. Lett., 33 (1975) 85.
12 E. I. Al'shits, R. I. Personov, A. M. Fyndyk and V. I. Stogov, Opt. Spektrosk., 39 (1975) 274.
13 I. I. Abram, R. A. Auerbach, R. R. Birge, B. E. Kohler and J. M. Stevenson, J. Chem. Phys., 63 (1975) 2473.
14 K. Cunningam, J. M. Morris, J. Fünfschilling and D. F. Williams, Chem. Phys. Lett., 32 (1975) 581.
15 K. K. Rebane, R. A. Avarmaa and A. A. Gorokhovskii, Izv. Akad. Nauk SSSR, Ser. Fiz., 39 (1975) 1793.
16 J. H. Eberly, W. C. McCalgin, K. Kawaoka and A. P. Marchetti, Nature, 251 (1974) 215.
17 E. I. Al'shits, R. I. Personov and B. M. Kharlamov, Chem. Phys. Lett., 40 (1976) 116; Opt. Spektrosk., 41 (1976) 803.
18 B. M. Kharlamov, R. I. Personov and L. A. Bykovskaya, Opt. Commun., 12 (1974) 191.
19 B. M. Kharlamov, L. A. Bykovskaya and R. I. Personov, Opt. Spektrosk., 42 (1977) 783; Chem. Phys. Lett., 50 (1977) 407.
20 J. C. Brown, M. C. Edelson and G. J. Small, Anal. Chem., 50 (1978) 1394.

Analytica Chimica Acta, 125 (1981) 13—19
Elsevier Scientific Publishing Company, Amsterdam — Printed in The Netherlands

DIRECT DETERMINATION OF SELECTED POLYNUCLEAR AROMATIC HYDROCARBONS IN A COAL LIQUEFACTION PRODUCT BY SYNCHRONOUS LUMINESCENCE TECHNIQUES

T. VO-DINH* and P. R. MARTINEZ[a]

Health and Safety Research Division, Oak Ridge National Laboratory, Oak Ridge, TN 37830 (U.S.A.)

(Received 8th September 1980)

SUMMARY

Synchronous fluorescence and the room-temperature phosphorescence methods were used to determine selected polynuclear aromatic hydrocarbons in a coal liquid (solvent-refined coal) product without a preseparation step. The procedure identified and quantified ten polynuclear aromatic compounds including anthracene, 2,3-benzofluorene, benzo[a]pyrene, benzo[e]pyrene, carbazole, dibenzothiophene, fluoranthene, fluorene, perylene, and pyrene. Standard deviations for repeated determinations ranged from 10—30% for concentrations in the range of 0.1—6 mg g^{-1}. The data obtained by these methods agree with results by other methods within the estimated experimental uncertainty.

Determinations of organic substances in coal-derived products generally involve separation methods coupled with measurement techniques such as gas chromatography with mass spectrometry (g.c.—m.s.) or high-performance liquid chromatography with fluorimetry, because coal liquids are known to contain a large number of organic species and this extreme complexity has prevented the use of conventional luminescence methods at room temperature. In this work, ten polynuclear aromatic (PNA) compounds in raw solvent-refined coal (SRC II) sample were identified and quantified by synchronous luminescence and room-temperature phosphorescence techniques.

Unlike previous work which dealt mainly with synthetic mixtures [1, 2] or real samples that had been fractionated [3], this study involved determinations in a raw coal liquid that had not been subjected to any prior fractionation or separation procedures. This work was part of a round-robin analysis organized jointly by the National Bureau of Standards (NBS) and the Department of Energy (DOE) to evaluate the efficacy of various techniques utilized by different laboratories. No information about the composition and nature of this sample was available to the participating laboratories prior to their own determinations. Our contribution to this program was to determine the applicability of two simple luminescence techniques at room temperature for identification as well as determination of target PNA compounds in a raw coal liquid sample.

[a]Present address: Alcoa Company, Alcoa, Tennessee, U.S.A.

EXPERIMENTAL

Spectroscopic techniques

The synchronous luminescence technique has been described previously [1, 4, 5]. In the synchronous method, the luminescence signal is recorded while both λ_{em} and λ_{ex} are scanned simultaneously with a fixed interval, $\Delta\lambda$, between them. The principal features of this method are a narrowing of the spectral band, and a decrease of spectral interferences from other luminescent species that would otherwise interfere with the emission being monitored. Room-temperature phosphorimetry (r.t.p.) is based on the detection of the phosphorescence emission at room temperature from organic compounds adsorbed on solid substrates. Although different types of sample supports could be used, filter paper was employed exclusively in this work. In the room-temperature phosphorescence measurements, both fixed-excitation and synchronous excitation methods were used. Several heavy-atom salts including thallium acetate, lead acetate, cesium iodide, and sodium bromide were used to increase the phosphorescence of PNA compounds [2].

Instrumentation and procedures

A Perkin-Elmer spectrofluorimeter (Model 43A) was used for all spectroscopic measurements. Fluorescence measurements of liquid solutions were done with standard 1 cm × 1 cm silica cells. The procedures for room-temperature phosphorescence assay [2] are depicted schematically in Fig. 1. The r.t.p. measurements employed filter paper circles of 0.6 cm diameter mounted on finger-type sample holders. Sample solutions of 3 μl were spotted on the filter paper that had been impregnated with an appropriate heavy-atom salt solution. After a 5-min drying period under an infrared lamp, the phosphorescence was measured using the spectrofluorimeter equipped with a phosphoroscopic attachment. Warm, dry air was passed through the sample compartment during the measurements to prevent moisture from quenching the phosphorescence. For synchronous luminescence, both excitation and emission monochromators were locked together and scanned simultaneously. The spectral bandpass was 1 nm for synchronous fluorescence

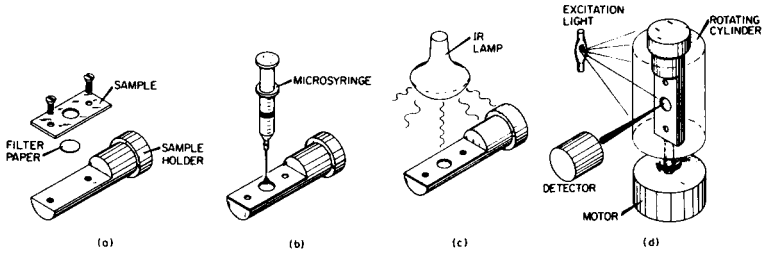

Fig. 1. Experimental procedure for r.t.p. determinations: (a) sample holder preparation; (b) sample delivery; (c) sample drying operation; (d) spectroscopic measurement.

measurements and 5 nm for r.t.p. measurements. The synchronous fluorescence measurements required a narrower bandpass in order to prevent excessive excitation light scatter because of the generally small value of $\Delta\lambda$ = 3 nm used. The 5-nm spectral bandpass used for r.t.p. was large enough to provide sufficient sensitivity, while being adequate for the resolution of most r.t.p. spectra.

RESULTS AND DISCUSSIONS

Figure 2 shows a portion of the synchronous fluorescence (s.f.) spectrum for 8 μg ml^{-1} of the SRC II sample in ethanol with $\Delta\lambda$ = 3 nm. The various bands were associated with acenaphthene, anthracene, benzo[a]pyrene (BaP), perylene, and 2,3-benzofluorene. The spectrum in Fig. 2 does not show the emission band of fluorene that occurs at 304 nm. Three peaks in the spectrum which did not match the s.f. spectra of our current library were assigned as unidentified (U) species.

A higher spectral resolution (1 nm) was used for precise identification and accurate quantification of the PNA compounds. At this higher resolution, some spectral bands were further resolved. For instance, the peak assigned to BaP was further resolved into a doublet. The capacity for multi-component determinations by the synchronous approach is illustrated in Fig. 2 where five compounds were readily determined in only one scan with the use of $\Delta\lambda$ = 3 nm.

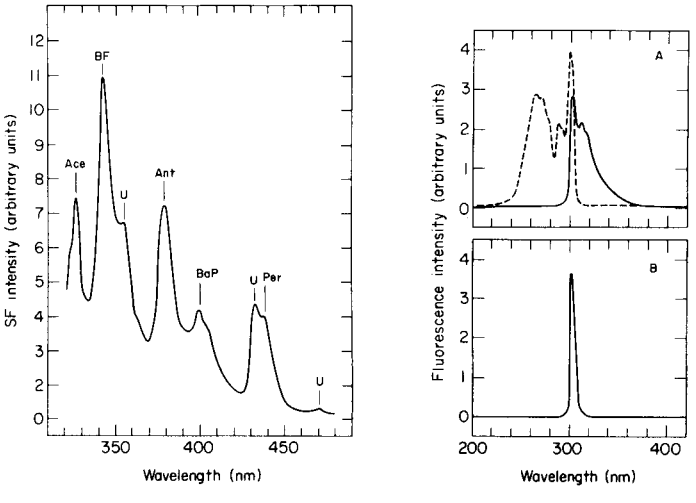

Fig. 2. Portion of the synchronous fluorescence profile of the SRC II sample using $\Delta\lambda$ = 3 nm. Ace, acenaphthene; BF, 2,3-benzofluorene; Ant, anthracene; BaP, benzo[a]pyrene; Per, perylene; U, unidentified species.

Fig. 3. Conventional and synchronous fluorescence spectra of fluorene. (A) Conventional spectra: (---) excitation; (—) emission. (B) synchronous spectrum ($\Delta\lambda$ = 3 nm).

The synchronous measurement of anthracene, 2,3-benzofluorene, benzo-[a]-pyrene, fluorene, and perylene produced fluorescence peaks at 378 nm, 342 nm, 404 nm, 304 nm and 438 nm, respectively. For a compound such as fluorene that has a strong O-O absorption band (Fig. 3), a small $\Delta\lambda$ value matching the Stokes shift of a PNA compound is recommended because it produces a simplified synchronous spectrum with one intense emission band. For a compound such as benzo[a]pyrene, which has a weak O-O absorption band (Fig. 4), an alternative value of $\Delta\lambda$ can be used to match the O-O emission band with the more intense second absorption band. As examples, $\Delta\lambda$ values of 20, 38, and 80 nm were used for benzo[a]pyrene, pyrene, and fluoranthene, respectively.

Most of the quantitative work on the PNA compounds was done with the standard addition technique. The synchronous fluorescence spectra of the SRC II sample enriched with known amounts of 2,3-benzofluorene and pyrene are shown in Figs. 5 and 6, respectively. Note that only the first peak of the doublet in Fig. 6 matches the synchronous spectrum of pyrene; this peak is superimposed on an unidentified band. These two emission peaks, however, are sufficiently resolved to permit the determination of pyrene. Except for acenaphthene, the determination of the other compounds did not present any serious problems. It was found that naphthalene and its alkyl derivatives also exhibit synchronous bands at the same spectral region as acenaphthene. Naphthalene analogs known to be present in many coal-derived products can, therefore, interfere with acenaphthene determination.

Three compounds, 2,3-benzofluorene, fluoranthene, and pyrene, could be readily determined by room-temperature phosphorescence using fixed

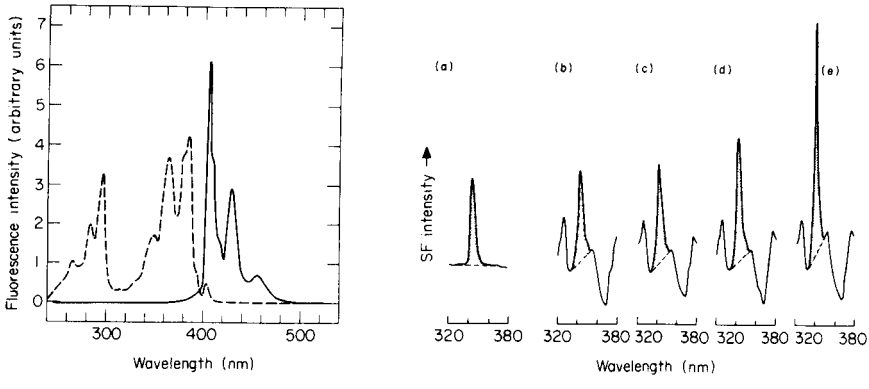

Fig. 4. Conventional fluorescence excitation and emission spectra of benzo[a]pyrene: (---) excitation; (—) emission.

Fig. 5. The synchronous fluorescence spectra of 2,3-benzofluorene (BF) and of the SRC II sample spiked with various amounts of BF for $\Delta\lambda$ = 3 nm: (a) pure 2,3-benzofluorene sample; (b) pure SRC II sample; (c) SRC II sample with 10^{-8} M 2,3-benzofluorene; (d) SRC II sample with 4×10^{-8} M 2,3-benzofluorene; (e) SRC II sample with 1.6×10^{-7} M 2,3-benzofluorene.

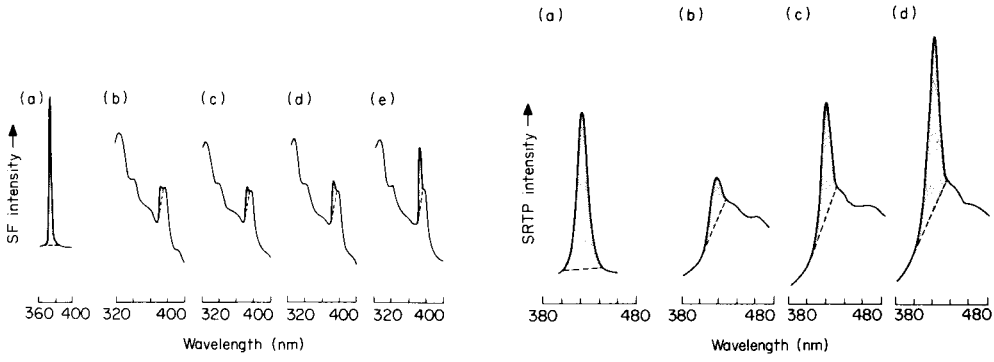

Fig. 6. The synchronous fluorescence spectra of pyrene and of SRC II sample spiked with various amounts of pyrene ($\Delta\lambda$ = 38 nm): (a) pure pyrene sample; (b) pure SRC II sample; (c) SRC II sample with 8×10^{-8} M pyrene; (d) SRC II sample with 2×10^{-7} M pyrene; (e) SRC II sample with 8×10^{-7} M pyrene.

Fig. 7. The synchronous r.t.p. spectra of dibenzothiophene (DBT) and of the SRC II sample spike with various amounts of DBT ($\Delta\lambda$ = 88 nm): (a) pure dibenzothiophene sample; (b) pure SRC II sample; (c) SRC II sample with 6×10^{-7} M dibenzothiophene; (d) SRC II sample with 1.2×10^{-6} M dibenzothiophene.

excitation at 321 nm, 365 nm, and 343 nm, respectively. Thallium acetate was also used for most of the compounds being investigated. Cesium iodide was used as the heavy-atom perturber for 2,3-benzofluorene, and lead acetate was used for fluoranthene and pyrene. The selectivity of these heavy-atom salts was discussed in a previous paper [2].

The synchronous excitation method was also applied for room-temperature phosphorescence. This approach was most helpful for the determination of benzo[e]pyrene, carbazole and dibenzothiophene which would otherwise be difficult to characterize unambiguously. The synchronous phosphorescence determination of carbazole and dibenzothiophene used $\Delta\lambda$ values of 68 nm and 88 nm, respectively. Figure 7 shows the synchronous r.t.p. spectra of the SRC II sample enriched with dibenzothiophene.

Recommended experimental conditions for the SRC II sample are given in Table 1. Synchronous scanning for room-temperature phosphorescence is used only when the conventional fixed excitation method cannot identify the compounds unambiguously. Although the synchronous excitation method could be used for 2,3-benzofluorene, fluoranthene, and pyrene, these compounds could be readily determined with fixed wavelength excitation.

Standard deviations of measurements performed under conditions in Table 1 fall between 10% and 30%. The SRC II sample has been characterized by more than a dozen different methods applied in eight laboratories [6, 7]. Most of the assays involved a prefractionation step prior to measurement. In addition to synchronous luminescence and room-temperature

TABLE 1

Conditions[a] for synchronous fluorescence and phosphorescence determinations of PNA in the SRC II sample

Compound	Synchronous fluorescence $\Delta\lambda$ (nm)	Room-temperature phosphorescence	
		λ_{ex} (nm)	$\Delta\lambda$ (nm)
Anthracene	3	N[b]	N
2,3-Benzofluorene	3	321	—
Benzo[a]pyrene	3 and 20	N	N
Benzo[e]pyrene	N	—	207
Carbazole	N	—	68
Dibenzothiophene	N	—	88
Fluoranthene	80	365	—
Fluorene	3	N	N
Perylene	3	N	—
Pyrene	38	342	—

[a]T = 25°C. [b]N means not detected by this method in the SCR II sample.

phosphorescence, only two laser-induced luminescence techniques at low temperatures, viz. laser-excited Shpolskii spectroscopy l.e.S.s. [8] and fluorescence line narrowing spectroscopy [9], and a direct-insertion capillary column g.c.—m.s. method are techniques that involved measurement without prior separation.

Table 2 gives the results of the determinations compared with results

TABLE 2

Results of the direct determination of PNA compounds in the SRC II sample by synchronous fluorescence (s.f.) and room-temperature phosphorescence (r.t.p.)

Compound	S.f.	Concentration (mg/g)		
		R.t.p.	NBS Data[a]	L.e.S.s.
Anthracene	1.7 ± 0.2	N[b]	NA[c]	NA
2,3-benzofluorene	1.8 ± 0.2	1.8 ± 0.6	NA	NA
Benzo[a]pyrene	0.13 ± 0.03	N	0.134	0.145
Benzo[e]pyrene	N	0.12 ± 0.03	0.143	0.126
Carbazole	N	4 ± 1	1.96	NA
Dibenzothiophene	N	1.0 ± 0.3	1.02	NA
Fluoranthene	5 ± 1.5	5 ± 1.5	3.30	NA
Fluorene	1.5 ± 0.3	N	NA	NA
Perylene	0.02 ± 0.006	N	0.026	NA
Pyrene	6 ± 2	3.6 ± 0.6	6.0	4.605

[a]The NBS data are of a preliminary nature (h.p.l.c. and/or g.c.—m.s.). The standard deviations of the NBS results range within 5—10% [7]. [b]N, emission not detected or not resolved. [c]NA, data not available.

obtained by g.c.—m.s. and/or high-performance liquid chromatography [6] and the l.e.S.s. technique at low temperatures (15 K).

Except for carbazole, the results obtained by synchronous fluorescence (s.f.) and r.t.p. are in reasonable agreement with most of the data reported by the other laboratories at the round-robin meeting [6]. The techniques described above do not require elaborate fractionation devices, low temperature equipment, cryogenic refrigerant, or laser excitation sources. The fact that the determinations can be done rapidly in a cost-effective manner makes the techniques attractive for screening large numbers of samples. The possibility for mechanized sampling and real-time determinations is presently under investigation. Potential applications in other areas such as quality control, process control, and environmental monitoring are yet to be explored.

This work was sponsored by the Office of Health and Environmental Research, U.S. Department of Energy, under contract W-7405-eng-26 with the Union Carbide Corporation. We thank H. S. Hertz of the National Bureau of Standards for providing the SRC II sample and the results of the NBS determinations. We also thank Y. Yang, A. P. D'Silva, V. A. Fassel, and M. Ilas for communicating their pre-publication results. The authors acknowledge the helpful assistance of G. H. Miller in repeating the determination of benzo[a]pyrene and benzo[e]pyrene.

REFERENCES

1 T. Vo-Dinh, Anal. Chem., 50 (1978) 396.
2 T. Vo-Dinh and J. R. Hooyman, Anal. Chem., 51 (1979) 1915.
3 T. Vo-Dinh, R. B. Gammage and P. R. Martinez, Anal. Chim. Acta, 118 (1980) 313.
4 J. B. F. Lloyd and J. W. Evett, Anal. Chem., 49 (1977) 1710.
5 T. Vo-Dinh, Synchronous Excitation Spectroscopy, in E. L. Wehry (Ed.), Modern Fluorescence Spectroscopy, Vol. 4, Plenum, New York, in press.
6 Surrogate Materials Program Meeting, January 15, 1980, Oak Ridge National Laboratory, Oak Ridge, TN.
7 H. S. Hertz, National Bureau of Standards, Washington, DC 20234, private communications, 1980.
8 Y. Yang, A. P. D'Silva, V. A. Fassel and M. Iles, Anal. Chem., 52 (1980) 1350.
9 J. C. Brown, J. A. Duncanson, Jr. and G. J. Small, Anal. Chem., 52 (1980) 1711.

Analytica Chimica Acta, 125 (1981) 21—28
Elsevier Scientific Publishing Company, Amsterdam — Printed in The Netherlands

SPECTROFLUORIMETRIC KINETIC DETERMINATION OF COPPER BASED ON THE AUTOXIDATION OF 2,2'-DIPYRIDYL KETONE AZINE OR HYDRAZONE OR PHENYL-2-PYRIDYL KETONE HYDRAZONE

F. GRASES and F. GARCIA-SANCHEZ

Department of Analytical Chemistry, Faculty of Sciences, University of Palma de Mallorca (Spain)

M. VALCARCEL*

Department of Analytical Chemistry, Faculty of Sciences, University of Cordoba (Spain)

(Received 19th September 1980)

SUMMARY

Kinetic methods for determination of ppm levels of copper are based on its catalytic effect on the autoxidation of the hydrazone and the azine of 2,2'-dipyridyl ketone and the hydrazone of phenyl-2-pyridyl ketone. The reaction is followed by measuring the rate of appearance of fluorescence. The methods suffer very few interferences.

In recent studies [1] it was found that the unsubstituted hydrazones and azines of 2,2'-dipyridyl ketone, phenyl-2-pyridyl ketone and dipyridylglyoxal suffer aerial oxidation at pH $\geqslant$ 7 that is catalyzed by copper(II), cobalt(II), mercury(II), gold(III) and platinum(IV), forming products that have an intense blue fluorescence. In all cases the reaction rate is readily measurable under normal experimental conditions, so that kinetic methods can be established for the determination of these cations.

In a previous paper [2], the catalytic action of copper(II) in the autoxidation of 2,2'-dipyridyl ketone hydrazone has been exhaustively studied. The fluorescent products formed were isolated and characterized and a non-kinetic method was described for the determination of traces of copper, as well as mercury. Only two previous kinetic fluorimetric methods for the determination of copper(II) have been reported; one is based on the quenching action of copper(II) in the reaction of hydrogen peroxide with lucigenin [3] and the other on the reaction of copper with benzamido(*p*-dimethylbenzylidene)acetic acid [4].

EXPERIMENTAL

Synthesis of reagents

2,2'-Dipyridyl ketone hydrazone (DPKH) was synthesized as described previously [2].

The synthesis of 2,2'-dipyridyl ketone azine (DPKA) was as follows. 2,2'-

0003—2670/81/0000—0000/$02.50

Dipyridyl ketone (2 g) was dissolved in 12 ml of hot absolute ethanol and mixed with 0.27 ml of 100% hydrazine hydrate. Two drops of 11 M HCl were added and the mixture was refluxed for 1 h. It was cooled to 0°C and the yellow precipitate that appeared was recrystallized from 1:1 ethanol–water. (Calculated for $C_{22}H_{16}N_6$, 72.5% C, 4.4% H, 23.1% N; found, 72.65% C, 4.3% H, 23.1% N.) The i.r. spectrum was as expected.

For the synthesis of phenyl-2-pyridyl ketone hydrazone (FPKH), phenyl-2-pyridyl ketone (5 g) was dissolved in the minimum quantity of hot absolute ethanol and refluxed with 1.5 g of 100% hydrazine monohydrate for 15 h. The solution, once cool, was shaken and the oily mass that separated was recrystallized from ethyl acetate. (Calculated for $C_{12}H_{11}N_3$, 73.0% C, 5.6% H, 21.3% N; found 72.9% C, 5.5% H, 21.2% N.) The i.r. spectrum confirmed the identification.

Reagents and instrumentation

Stock solutions included an aqueous 1 g l^{-1} solution of DPKH, a 30% ethanolic 1 g l^{-1} solution of DPKA, a 2% ethanolic 1 g l^{-1} solution of FPKH, and a copper(II) sulfate solution (0.9730 g Cu l^{-1}), standardized iodimetrically [5]. Buffer solutions of pH 6.3, 4.0 and 9.0 were prepared according to Clark and Lubs [6].

The fluorescence measurements were accomplished on a FIKA 55 MK II spectrofluorimeter fitted with an apparatus for kinetic measurements that permits direct recording of fluorescence–time curves at fixed excitation and emission wavelengths. In all the experiments the speed of movement of the recorder chart paper was 1 cm min^{-1}.

Procedures for determination of copper(II)

With DPKH. In a 50-ml beaker, 0.3 ml of 5.0×10^{-3} M DPKH, 2 ml of pH 6.3 buffer and the necessary volume of cation to ensure a final concentration of copper between 0.1 and 1 ppm were added, giving a final volume of 4 ml, achieved if necessary by addition of deionized water. After 30 s had elapsed since the cation was added, recording of the intensity–time curve was started (λ_{ex} = 359 nm, λ_{em} = 430 nm). From the curve obtained, the rate of reaction was calculated by the initial rate (tangent) method the fixed time method, or the fixed % change procedure, as outlined later.

With DPKA. In a 50-ml beaker, 1.0 ml of 2.7×10^{-5} M DPKA, 2 ml of pH 4.0 buffer and the necessary volume of cation to ensure a final concentration of copper between 0.2 and 0.5 ppm were added, giving a final volume of 4 ml, achieved if necessary by addition of deionized water. The intensity–time curve was recorded as for DPKH (λ_{ex} = 347 nm, λ_{em} = 430 nm).

With FPKH. In a 50-ml beaker, 1.0 ml of 4.1×10^{-4} M FPKH, 2 ml of pH 9.0 buffer and the necessary volume of cation to ensure a final concentration of copper between 0.12 and 0.60 ppm were added, with any necessary water to give a final volume of 4 ml. The intensity–time curve was recorded as for DPKH (λ_{ex} = 308 nm, λ_{em} = 435 nm).

RESULTS AND DISCUSSION

The excitation and emission spectra of the reagents and the reaction products in aqueous media in the presence of copper(II) are shown in Fig. 1. In all cases in the absence of the cation, the fluorescence is hardly detectable.

Effects of reaction variables

Influence of pH. The product of the reaction of DPKH in the presence of copper(II) shows maximum fluorescence intensity in very acidic media (pH ca. 0.6), but in these media the reaction is extremely slow [1]. Figure 2 shows how the initial reaction rate grows as the acidity diminishes; pH 6.3 was chosen so that the initial reaction rate was adequate for ease and precision of measurement, and the sensitivity was as great as possible without working in alkaline solution, thus eliminating the inconveniences, especially of interferences, that occur in basic conditions.

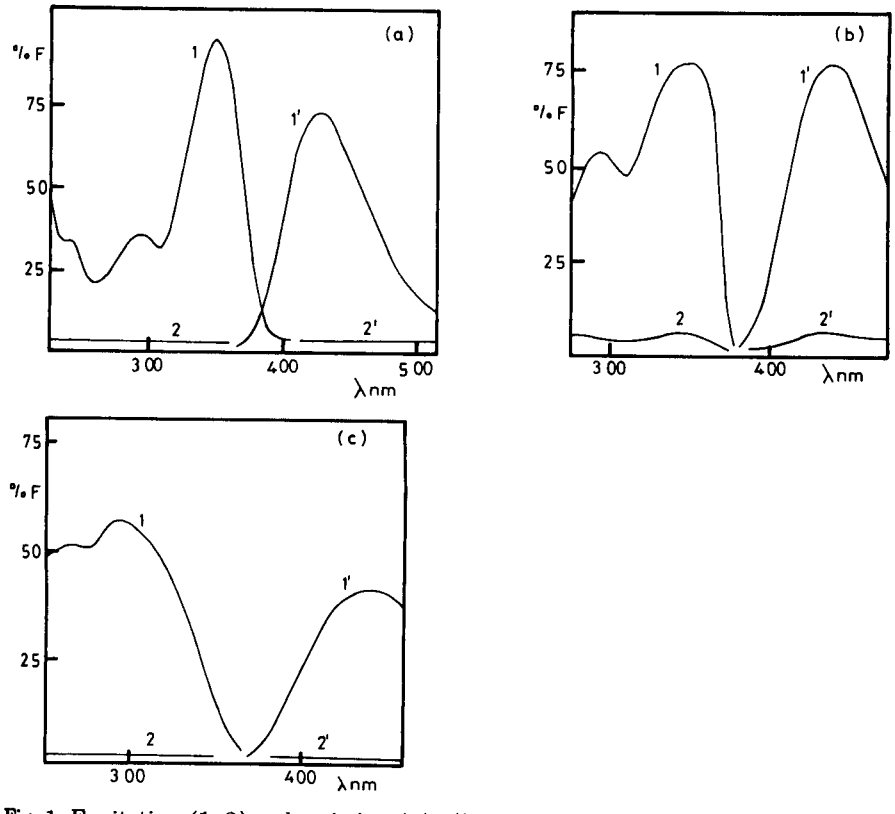

Fig. 1. Excitation (1, 2) and emission (1', 2') spectra: (a) 4×10^{-7} M DPKH in the presence (1, 1') and absence (2, 2') of 0.01 ppm Cu(II), pH 0.6, sensitivity $\times 40$, λ_{ex} = 349 nm, λ_{em} = 435 nm; (b) 2.2×10^{-5} M DPKA in the presence (1, 1') and absence (2, 2') of 1 ppm Cu(II), pH 1.9, sensitivity $\times 4$, λ_{ex} = 349 nm, λ_{em} = 435 nm; (c) 4×10^{-5} M FPKH in the presence (1, 1') and absence (2, 2') of 1 ppm Cu(II), pH = 12, sensitivity $\times 20$, λ_{ex} = 308 nm, λ_{em} = 435 nm.

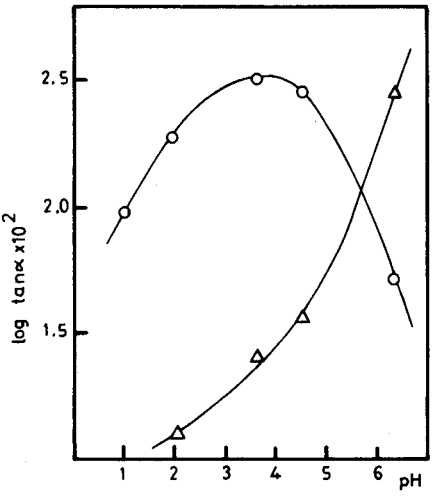

Fig. 2. Influence of pH on the initial rate: (△) [DPKH] = 3.75×10^{-4} M, [Cu^{2+}] = 0.7 ppm, sensitivity × 100, λ_{ex} = 349 nm, λ_{em} = 475 nm; (○) [DPKA] = 3.4×10^{-5} M, [Cu^{2+}] = 1 ppm, sensitivity × 100, λ_{ex} = 349 nm, λ_{em} = 435 nm.

Figure 2 also shows that the initial reaction rate of DPKA in the presence of copper is greatest around pH 4, which was chosen for the determination of copper.

The maximum fluorescence intensity of the product formed from FPKH in the presence of copper always appears at pH ca. 12. However, studies of the influence of pH on the stability of aqueous solutions of FPKH [1] showed that at pH $\geqslant$ 10, the formation of the fluorescent product was considerable in the absence of added copper. Thus such a high pH was avoided; pH 9 was chosen for the determination.

Influence of reagent concentration. To optimize the concentration of each reagent, its initial concentration was varied while the concentrations of the other components were kept constant, and the initial reaction rate was measured for each concentration. The log—log plots of the initial rate against the initial reagent concentration are linear, and their slope enables the orders of reaction to be established. The optimum concentrations of reagents are those for which the relative standard deviation of measurements of the initial rate is as small as possible. This will happen at concentrations where the order of reaction with respect to the reagent is as near zero as possible, under which conditions small variations in the concentration of reagent will not affect the initial reaction rate.

The results are shown in Fig. 3. DPKH shows no region in which the order of reaction is zero, but around 3.75×10^{-4} M it is a minimum. For DPKH and FPKH, in a very small interval around 6.75×10^{-6} M and 1.2×10^{-4} M, respectively, the reaction rate is zero with respect to the reagent. The three mentioned concentrations were therefore chosen for the determination of copper.

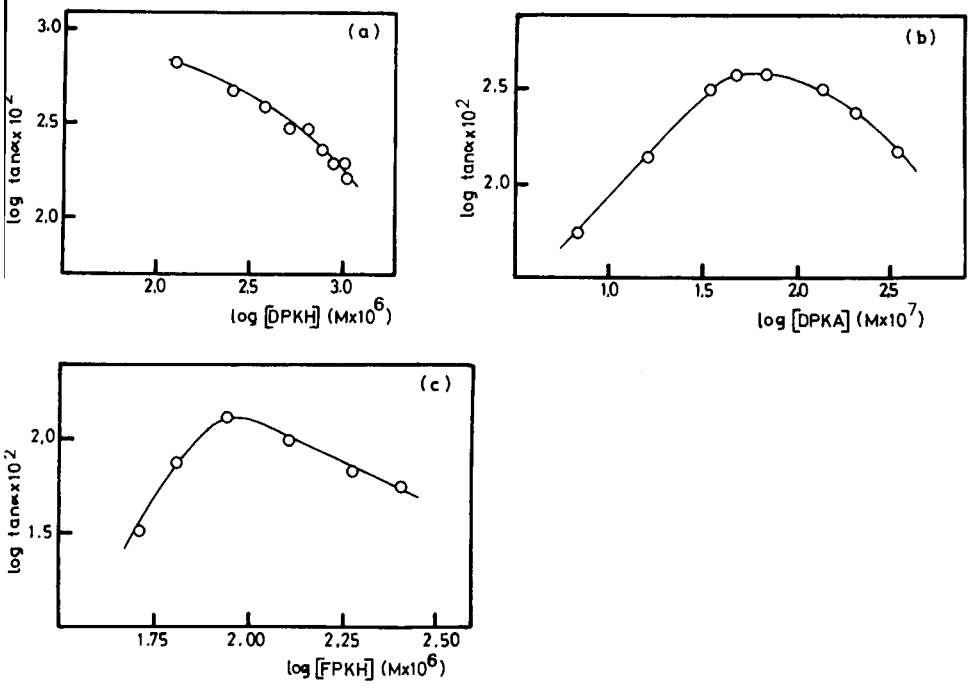

Fig. 3. Log—log plots of the effect of concentration of reagent on the initial rate: (a) $[Cu^{2+}]$ = 0.7 ppm, pH 6.3, sensitivity × 100, λ_{ex} = 349 nm, λ_{em} = 435 nm; (b) $[Cu^{2+}]$ = 0.5 ppm, pH 4.0, sensitivity × 100, λ_{ex} = 349 nm, λ_{em} = 435 nm; (c) $[Cu^{2+}]$ = 0.2 ppm, pH 9.0, sensitivity × 20, λ_{ex} = 308 nm, λ_{em} = 435 nm.

Calibration

The intensity of the fluorescence—time curves were obtained for solutions containing different quantities of copper(II) under the optimum conditions of pH and of reagent concentration. To these curves, various well established methods of preparing calibration graphs were applied. For DPKH, the tangent method gave a linear calibration graph for 0.1—1 ppm copper(II). The plot was logarithmic because the order of reaction with respect to the cation is not an integer. The relative standard deviation was 2% (n = 11, α = 0.05). For the fixed time method, a time interval of 2 min was chosen. The calibration graph was linear for 0.2—1 ppm copper(II) and the relative standard deviation (S_r) was 3% (n = 11, α = 0.05). For the fixed intensity approach, the inverse of the time required to reach a fluorescence of 12% full scale deflection was plotted against the concentration of copper; the graph was linear between 0.5 and 1 ppm copper, and the S_r was 2% (n = 11, α = 0.05).

Similar approaches were used for DPKA and FPKH. For the former the tangent method gave a linear calibration graph for 0.2—0.5 ppm copper (S_r = 3.5%, n = 11, α = 0.05). The fixed time method (2 min interval) also gave a linear calibration for 0.2—0.5 ppm copper (S_r = 7.5%, n = 11, α = 0.05).

For the fixed intensity method, where the inverse of the time needed to reach a 12% fluorescence was measured, linear calibration was observed for 0.25—0.50 ppm copper (S_r = 7%, n = 11, α = 0.05). For FPKH, the tangent method gave a linear calibration of 0.12—0.60 ppm copper (S_r = 3%, n = 11, α = 0.05). For the fixed time method, a 2-min interval was again chosen, and the calibration graph was linear for 0.12—0.60 ppm copper (S_r = 5%, n = 11, α = 0.05). For the fixed intensity method when the inverse of the time needed to reach a 12% fluorescence was again plotted against the concentration of copper, the graph was linear for 0.2—0.6 ppm copper (S_r = 6.5%, n = 11, α = 0.05).

Of the three ways in which the kinetic data were treated, measurements of the initial rates are recommended, since generally, the range of application and precision are greater and the effects of foreign ions which do not have a linear relation between fluorescence intensity and concentration, are considerably reduced. This probably happens because, when the rate measurements are made in the initial stages of the reactions, the time elapsed is not sufficient for the interfering effects to be noticeable.

The experimental rate information obtained for the various systems is summarized in Table 1.

Study of interferences

The effects of other ions are shown in Table 2. None of the three methods suffers more than a few interferences.

Nature of fluorescence

Studies made to determine the nature of the reaction of copper(II) with DPKH, DPKA and FPKH indicated that the reagents alone were converted to fluorescent products only slowly, so that the transformation was not

TABLE 1

Summary of kinetic data: V_0 is the initial rate

DPKH—Cu(II) system
$V_0 \propto [H^+]^{1/5}$, $2 < pH < 4.5$; $V_0 \propto [H^+]^{1/2}$, $4.5 < pH < 6.3$.
$V_0 \propto [DPKH]^{-1/2}$, 1.3×10^{-4} M $< [DPKH] < 6.3 \times 10^{-4}$ M.
$V_0 \propto [Cu^{2+}]^{4/3}$, 0.1 ppm $< [Cu^{2+}] <$ 1 ppm.
DPKA—Cu(II) system
$V_0 \propto [H^+]^{1/4}$, $1 < pH < 3$; $V_0 \propto [H^+]^0$, $3.5 < pH < 4.5$; $V_0 \propto [H^+]^{-1/2}$, $5 < pH < 6.3$.
$V_0 \propto [DPKA]$, 6.8×10^{-7} M $< [DPKA] < 4.0 \times 10^{-6}$ M; $V_0 \propto [DPKA]^0$, 4.0×10^{-6} M $< [DPKA] < 1.0 \times 10^{-5}$M.
$V_0 \propto [Cu^{2+}]$, 0.2 ppm $< [Cu^{2+}] <$ 0.5 ppm.
FPKH—Cu(II) system
$V_0 \propto [FPKH]^3$, 5.0×10^{-5} M $< [FPKH] < 7.9 \times 10^{-5}$ M; $V_0 \propto [FPKH]^0$, 7.9×10^{-5} M $< [FPKH] < 1.0 \times 10^{-4}$ M.
$V_0 \propto [Cu^{2+}]$, 0.1 ppm $< [Cu^{2+}] <$ 0.6 ppm.

TABLE 2

Influence of foreign ions in the kinetic determination of copper(II) by the tangent method for the three reagents

Tolerable concentrations (ppm)[a]							
DPKH[b]		DPKA[c]	FPKH[d]	DPKH[b]		DPKA[c]	FPKH[d]
Ion added				Ion added			
Mg	10	10	3	Mn(II)	2 (max)	2	0.5
Ca	10	10	3	Be	2.5	2	0.5
Ba	10	10	3	Al	5	5	0.5
Sr	10	10	3	Fe(III)	5	3	0.5
Pb	10	10	3	Cr(III)	5	5	0.1 (max)
Zn	10	10	0.5	Au(III)	2.5	0.05 (max)	0.4
Cd	10	10	1	Ga(III)	5	5	0.5
Hg(II)	10	10	0.4	NO_3^-	10	10	3
UO_2^{2+}	10	10	—	SO_4^{2-}	10	10	3
Pd	—	—	0.2 (max)	F^-	10	10	3
Co(II)	5	2.5 (max)	0.4	$H_2PO_4^-$	10	10	3
Ni(II)	5	0.5 (max)	0.4				

[a]Except where indicated, these are the maximum concentrations tested, not the maximum tolerable concentrations. [b]For 0.7 ppm Cu, tolerable error 2%. [c]For 0.4 ppm Cu, tolerable error 3.5%. [d]For 0.35 ppm Cu, tolerable error 3%.

detected until several weeks after solution preparation. This transformation was favoured by higher temperatures, and the presence of oxidizing agents ($KBrO_3$, H_2O_2, etc.) rapidly ensured that the fluorescent product is formed. Dissolved oxygen favoured the formation of the fluorescent product in the presence of copper(II). These facts, together with other data obtained for similar reactions [1] lead to the conclusion that these are autoxidation processes, catalyzed by the metal ion. For DPKH, the fluorescent product which results from its reaction in the presence of copper has been isolated [2]. A study of its i.r. and mass spectra confirmed that autoxidation occurs and that an azo derivative is probably formed.

Conclusion

Although the non-kinetic method previously described [2], based on the DPKH system, is more sensitive, the kinetic fluorimetric determination of copper with one of the three reagents mentioned offers the advantage of being much quicker. Thus each measurement is accomplished in 3—4 min, while the non-kinetic method requires at least 90 min. The level of interference is as low as that found in the non-kinetic method.

Of the three kinetic methods proposed, that based on the autoxidation of DPKH with copper(II) as catalyst is undoubtedly the best. It has the highest sensitivity, the smallest relative error, and the lowest level of interferences.

REFERENCES

1 F. Grases, Doctoral Thesis, University of Palma de Mallorca, 1978.
2 F. Grases, F. Garcia-Sanchez and M. Varcárcel, Anal. Chim. Acta, 119 (1980) 359.
3 V. G. Drokov and L. I. Dubovenko, Ukr. Khim. Zh., 40 (1974) 549.
4 E. A. Bozhevol'nov, S. U. Kreingol'd and L. I. Sosenkova, Tr., Vses. Nauch. Issled. Inst. Khim. Reaktivov Osobo Chist. Khim. Veshchestv., 30 (1967) 176.
5 A. I. Vogel, A Text-book of Quantitative Inorganic Analysis, Longmans, London, 1961.
6 W. M. Clark and H. A. Lubs, in L. Meites (Ed.), Handbook of Analytical Chemistry, McGraw-Hill, New York, 1963.

Analytica Chimica Acta, 125 (1981) 29—35
Elsevier Scientific Publishing Company, Amsterdam — Printed in The Netherlands

FLOW INJECTION SPECTROPHOTOMETRIC DETERMINATION OF BORON IN PLANT MATERIAL WITH AZOMETHINE-H

F. J. KRUG, J. MORTATTI, L. C. R. PESSENDA, E. A. G. ZAGATTO and H. BERGAMIN F°*

Centro De Energia Nuclear Na Agricultura, USP, 13.400-Piracicaba, S. Paulo (Brasil)

(Received 29th September 1980)

SUMMARY

A simple, fast method for the determination of boron in plant extracts is described. The method utilizes injection of 1.0 ml of an acid plant digest into a 0.1 M hydrochloric acid stream, with further addition of a buffer—masking solution and azomethine-H as the colour-forming reagent. Effects of pH, kinetics of colour reaction development, sample volume, reagent composition and interferences are described. The proposed method allows the analysis of plant extracts with boron contents in the range 0.1—6.0 ppm at a rate of 60 determinations per hour, with a reagent consumption of 2 mg of azomethine-H per sample. The precision is good (r.s.d. <1%) and the results agree with those obtained by the curcumin method.

Several automated procedures for the spectrophotometric determination of boron have been proposed, both for continuous flow and batch analysers [1]. However, in continuous flow systems, either evaporation or the development of chemical reactions under very acidic conditions makes automation difficult. Specific and sensitive colour-forming reagents such as curcumin and carminic acid are therefore unsuitable for the determination of boron with such systems [2, 3]. In contrast, with the azomethine-H reagent the reactions are carried out under slightly acidic conditions, and despite the long reaction time for colour formation the development of automated procedures in air-segmented flow systems has presented no difficulties [2—4].

Azomethine-H was first suggested as a reagent for boron determinations in 1961 [5]. In aqueous solutions, the reagent is yellowish and dissociates according to

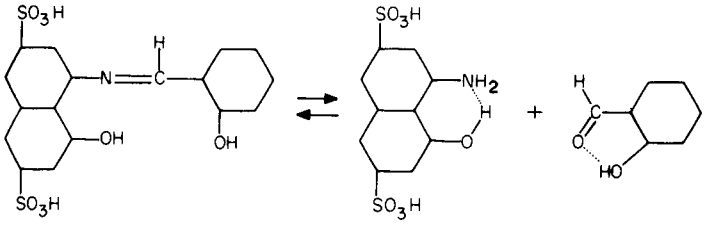

Boric acid displaces this equilibrium towards the left, increasing the yellow

colour intensity proportionally to the boron concentration. This displacement is very slow when the recommended pH values [2—7] are used.

The aim of this work was to develop a flow injection procedure for the determination of boron in plant material with azomethine-H as the colour-forming reagent. A detailed investigation made it possible to improve the kinetics of the colour reaction.

EXPERIMENTAL

Apparatus

A Technicon AA-II peristaltic pump with tygon pumping tubes was employed. A model 25 Beckman spectrophotometer, connected to a model 24-25 ACC Beckman recorder, was equipped with a Hellma flow cell (type 178, light path 10 mm, inner volume 80 μl). The potentiometric assembly consisted of a G202B glass electrode, a K401 calomel reference electrode, a model 64 pH meter and a REC 61 recorder provided with a REA 112 high-sensitivity unit (all from Radiometer, Copenhagen). The flow-through potentiometric chamber was similar to that already described [8].

The manifold was made with polyethylene tubing of the non-collapsible wall type (0.8 mm i.d.). The coils were made by winding suitable tubing lengths on a glass tube support (2-cm o.d.). All connectors were made from perspex, the tubing insertion holes being slightly conical. The multiple proportional injector, also made from perspex, was operated manually by means of a lever, and consisted of two fixed external plates and a central sliding plate assembled tightly together by means of two screws with springs [9]. Silicone rubber sheets with the same holes as the plates were used to avoid leakage.

The flow system for boron determinations is presented in Fig. 1, which shows also the injector (I) in the sampling position. In this position, the sample (S) is aspirated to fill the sample loop (L) which defines exactly the sample injected volume, its excess being directed to waste (W). Line C is the sample carrier stream and lines A and B are the reagent streams. After a time interval long enough to prevent carry-over, the injector is commutated and the selected sample volume is introduced into the carrier streams. This sample injection originates a well defined sample zone [10] which is directed towards detection. At point x, the sample zone meets the buffer—masking reagent, and mixing, pH adjustment and masking occur in coil R_1 (50 cm long). At the next confluence point y, the azomethine-H solution is added continuously, the colour-forming reaction occurring in coil R_2 (300 cm long). The absorbance of the zone is then measured at 420 nm and discarded.

Reagents, standards and samples

The reagents were analytical grade and distilled-deionized water was always used. The solutions, including samples and standards, were stored in polyethylene flasks.

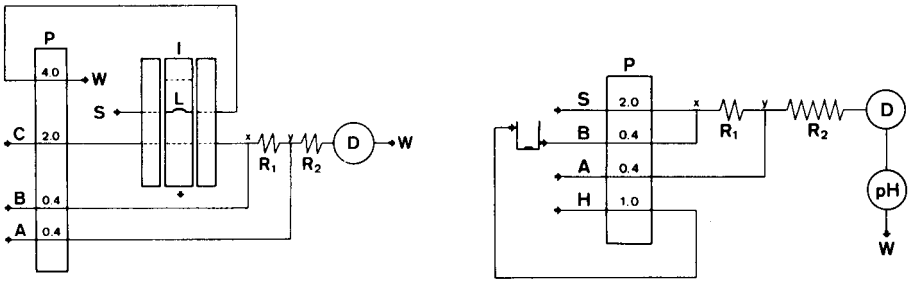

Fig. 1. Flow diagram of the proposed system. P is the peristaltic pump with indication of flow rates, in ml min^{-1}; C is the sample carrier stream; B is the buffer—masking reagent; A is the colour-forming reagent; S is the sample under aspiration filling the sample loop L and I is the injector in the sampling position. R_1 and R_2 are the reaction coils, x and y are confluence points, D is the detector and W denotes waste. For details, see text.

Fig. 2. Flow diagram of the system used for investigation of the effect of pH on colour formation. S is the sample, B is the phosphate buffer initially at pH 8.2; A is a 0.5% (w/v) azomethine-H reagent; H is a 1 M HCl solution and pH represents the assembly for pH measurements. Other symbols are referred to in Fig. 1. For details, see text.

The azomethine-H reagent was synthesized as described by Capelle [5]. The colour reagent (line A, Fig. 1) was prepared daily by dissolving 0.5 g of azomethine-H and 2.0 g of ascorbic acid in about 40 ml of warm water (ca. 50°C) and making the volume up to 100 ml with water. The buffer—masking reagent (line B) was prepared by dissolving 132 g of $(NH_4)_2HPO_4$ and 25 g of disodium-EDTA in 500 ml of water. The sample carrier stream (line C) was 0.1 M hydrochloric acid solution. Boron standards were prepared by dilution of a 100 ppm B (as H_3BO_3) stock solution in 0.1 M HCl.

Samples were prepared by ashing 100 mg of ground cotton leaves at 550°C and dissolving with 10 ml of 0.1 M HCl solution.

Preliminary tests

Different pH values ranging from 4.50 to 6.35 have been suggested for the colour development reaction [2—7]. In order to study the influence of pH, the system shown in Fig. 2 was used. Boron standard solutions (0.0, 1.0 and 5.0 ppm B) were pumped at a rate of 2.0 ml min^{-1}, receiving the reagents B and A at points x and y. The pH of reagent B was continuously decreased by the addition of a hydrochloric acid solution (D). The pH-measuring assembly [8] was placed after the flow cell.

A stopped-flow procedure [11] was employed to investigate the kinetics of the colour-formation reaction under different pH conditions. The sample carrier stream (C, Fig. 1) was replaced by a 2.0 ppm boron standard and the pump was stopped when the measured signal reached a constant value. Different reaction coil lengths (50 and 500 cm) were used in order to attain two sample residence times (about 6 and 60 s).

Effects of the azomethine-H, ascorbic acid and EDTA concentrations were also studied with the system shown in Fig. 1. In all cases, boron standard (1.0 ml) ranging from 0.0 to 3.0 ppm B were injected into 0.1 M hydrochloric acid solution, the sample carrier stream having the same acidity as the standards. The necessary concentration of EDTA in the buffer—masking reagent to overcome interferences caused by aluminium, copper, iron and zinc was checked. Other interfering ions [5] such as beryllium, chromium, gallium, mercury, tellurium, tin, titanium and vanadium occur at negligible levels in plant extracts, and therefore were not studied.

The accuracy of the proposed method was evaluated by standard additions of 10 and 20 μg of boron to four plant samples, and the results of the analysis of 13 plant extracts were compared with those obtained by the use of the curcumin method [12].

RESULTS AND DISCUSSION

The influence of pH on the colour reaction is shown in Fig. 3. The boron isoconcentration curves in Fig. 3A indicate than an increase in the pH causes an increase in colour formation (up to pH 8.0). Figure 3B shows the net absorbance values for 1.0 and 5.0 ppm B standards. The maximum difference between absorbances of blank and standards is found when the pH is about 7.3. This result, which differs from those already reported [2—7], is due to the effect of pH on the kinetics of the colour-forming reaction, as shown in Fig. 4. At pH 5.0, the maximum absorbance is attained in about 2 h (Fig. 4) whereas at pH 7.3, complete reaction appears to be achieved in about 2 min, with a reduction in the final absorbance. However, in flow injection systems, the available time for chemical reactions is usually very short, and so the use of a faster reaction generally leads to the development of a more sensitive method although the system may not be at equilibrium. The small irregularity in the pH 7.3 curve is probably due to the presence of sodium in the buffer—masking reagent; sodium ions also affect the colour formation [5]. After 5 min the colour becomes stable for at least 90 min.

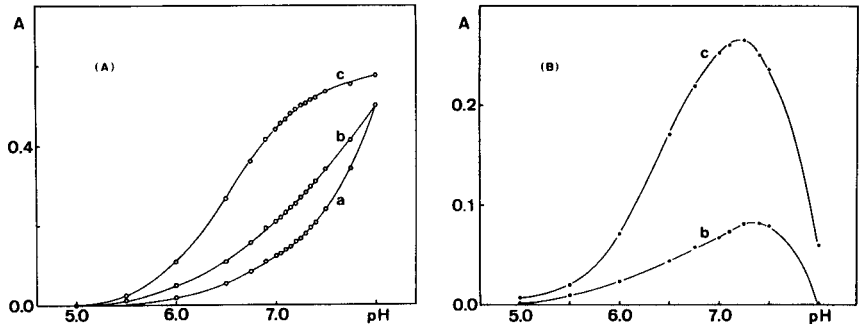

Fig. 3. Effect of pH on colour reaction. Curves a, b and c shown in (A) correspond to 0.0, 1.0 and 5.0 ppm B, respectively. Curves b and c shown in (B) correspond to 1.0 and 5.0 ppm B, respectively. For details, see text.

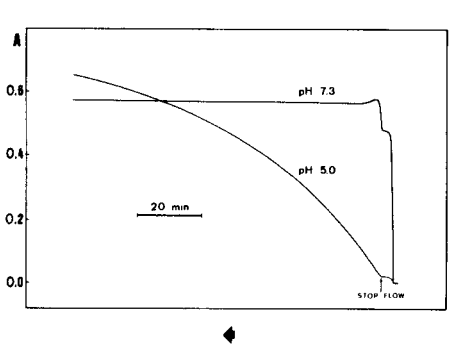

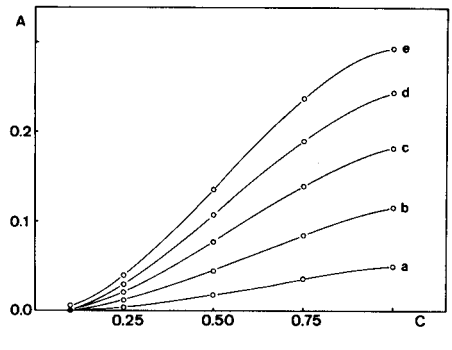

Fig. 4. Effect of pH on the kinetics of colour development. For details, see text.

Fig. 5. Effect of azomethine-H concentration. Curves a, b, c, d and e correspond to 1.0, 2.0, 3.0, 4.0 and 5.0 ppm B, respectively. A denotes absorbance and C the azomethine concentration in % (w/v).

The reaction coil length (R_2, Fig. 1) was then defined as 300 cm long, in order to permit a sample residence time of about 40 s, which corresponds to 75% of the reaction completion. When a 1.0-ml sample is injected, the sampling rate is about 60 determinations per hour, and the sensitivity is only 20% less than that corresponding to the infinite volume configuration (Fig. 2). It must be emphasized that, when hydrochloric acid is used as sample carrier stream (Fig. 1), the pH value in the flow cell output is around 7. If better sensitivity is desired, an adjustment to pH 7.3 must be made, either by alkali addition in reagent B or by increasing its buffer capacity, the latter being recommended.

The influence of azomethine-H concentration on colour formation is shown in Fig. 5. Increasing the reagent concentration increases the sensitivity,

TABLE 1

Interferences in the determination of boron

Sample	Boron found (ppm)			Sample	Boron found (ppm)		
	Without EDTA	EDTA 1%	5%		Without EDTA	EDTA 1%	5%
0.5 B + 10 Al	0.6	0.5	0.5	0.5 B + 10 Fe	6.0	0.6	0.5
0.5 B + 100 Al	0.7	0.5	0.5	0.5 B + 100 Fe	9.6	0.9	0.8
3.0 B + 10 Al	3.1	3.0	3.0	3.0 B + 10 Fe	8.5	3.0	3.0
3.0 B + 100 Al	3.1	3.0	3.0	3.0 B + 100 Fe	11.9	3.0	3.0
0.5 B + 10 Cu	3.6	0.5	0.5	0.5 B + 10 Zn	0.5	0.5	0.5
0.5 B + 100 Cu	8.6	0.5	0.5	0.5 B + 100 Zn	— [a]	— [a]	— [a]
3.0 B + 10 Cu	6.1	3.0	3.0	3.0 B + 10 Zn	3.0	3.0	3.0
3.0 B + 100 Cu	10.3	3.0	3.0	3.0 B + 100 Zn	2.2	2.2	2.2

[a]Negative signal.

TABLE 2

Comparison of procedures for the determination of boron in plant extracts: values are expressed as ppm B in the extracts

Sample	Flow injection method	Manual curcumin method [12]	Sample	Flow injection method	Manual curcumin method [12]
01	1.88	1.68	08	4.00	3.82
02	3.16	3.17	09	3.38	3.08
03	3.28	3.48	10	3.20	2.92
04	4.16	4.10	11	3.32	2.97
05	2.18	1.96	12	2.18	1.95
06	3.76	3.44	13	4.18	3.95
07	4.34	4.37			

but concentrations of azomethine-H higher than 0.75% (w/v) cause drift in the baseline. A 0.5% (w/v) azomethine-H concentration was chosen, meaning a consumption of about 2 mg of azomethine-H per determination. This corresponds to 20% of the consumption of reagent in other automatic methods [2, 3]. The effect of ascorbic acid concentrations ranging from 0 to 5% was investigated, the maximum colour formation being obtained with 2% (w/v) in a 0.5% (w/v) azomethine-H solution.

Table 1 shows the interferences caused by aluminium, copper, iron and zinc, and their suppression by EDTA. Interferences of aluminium (100 μg ml^{-1}), copper (100 μg ml^{-1}) and iron (10 μg ml^{-1}) were eliminated with 5% (w/v) EDTA, while iron and zinc in higher concentrations caused severe interferences, especially when the boron content was low. Considering that the aluminium and iron contents in the plant extracts are generally in the range 1—10 ppm, and that the copper and zinc contents are between 0.1 and 1.0 ppm, a 5% (w/v) EDTA concentration is sufficient.

TABLE 3

Standard additions in plant extracts

Sample	Boron content (μg)			Recovery (%)
	Originally measured	Added	Found	
31	18.5	10.0	28.5	100.0
32	12.3	10.0	21.9	98.2
33	9.2	10.0	19.2	100.0
34	6.2	10.0	15.8	97.5
31	18.5	20.0	38.5	100.0
32	12.3	20.0	31.0	96.0
33	9.2	20.0	28.7	98.3
34	6.2	20.0	26.2	100.0

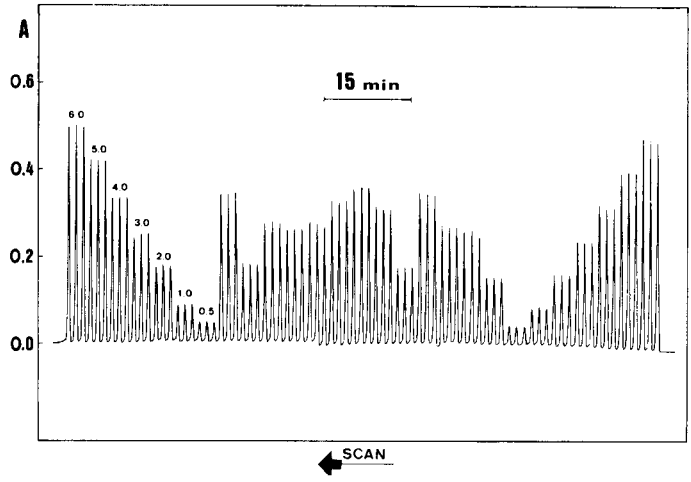

Fig. 6. Routine analysis of plant extracts, recorded with the manifold shown in Fig. 1. From left to right: a series of boron standards (6.0—0.5 ppm B), the samples and a second set of standards: all measurements in triplicate.

Table 2 shows that the proposed method compares well with the curcumin method [12]. Table 3 shows the results of the standard addition experiment. Both these sets of experiments prove the good accuracy of the proposed method. A typical run for the routine determination of boron in plant extracts (Fig. 6) shows the linearity of the calibration graph, the precision of the measurements (r.s.d. <1%) and the stability of the system.

Partial support of this project by CNPq (Conselho Nacional de Desenvolvimento Científico e Tecnológico) is greatly appreciated. The authors thank Peter B. Vose for reading the original manuscript, and S. S. Jørgensen for his participation in the earlier stage of this work.

REFERENCES

1 G. Östling, Anal. Chim. Acta, 78 (1975) 507.
2 W. D. Basson, R. G. Bohmer and D. A. Stanton, Analyst, 94 (1969) 1135.
3 R. A. Edwards, Analyst, 105 (1980) 139.
4 W. D. Basson, P. P. Pille and A. L. Du Preez, Analyst, 99 (1974) 168.
5 R. Capelle, Anal. Chim. Acta, 24 (1961) 555.
6 G. D. Shucker, T. S. Magliocca and Yao-Sin Su, Anal. Chim. Acta, 75 (1975) 95.
7 B. Wolf, Commun. Soil Sci. Plant Anal., 2 (1971) 363.
8 J. Růžička, E. H. Hansen and E. A. G. Zagatto, Anal. Chim. Acta, 88 (1977) 1.
9 H. Bergamin F°, E. A. G. Zagatto, B. F. Reis and F. J. Krug, Anal. Chim. Acta, 101 (1978) 17.
10 J. Růžička and E. H. Hansen, Anal. Chim. Acta, 99 (1978) 37.
11 J. Růžička and E. H. Hansen, Anal. Chim. Acta, 106 (1979) 207.
12 O. C. Bataglia, J. P. F. Teixeira, P. R. Furlani, A. M. C. Furlani and J. R. Gallo, Circ. Inst. Agron. Norte (Braz.), 87 (1978) 16.

Analytica Chimica Acta, 125 (1981) 37—43
Elsevier Scientific Publishing Company, Amsterdam — Printed in The Netherlands

MERGING ZONES IN FLOW INJECTION ANALYSIS
Part 5. Simultaneous Determination of Aluminium and Iron in Plant Digests by a zone-sampling approach

E. A. G. ZAGATTO, A. O. JACINTHO, L. C. R. PESSENDA, F. J. KRUG, B. F. REIS and H. BERGAMIN F°*

Centro de Energia Nuclear na Agricultura, USP, 13.400 Piracicaba, S. Paulo (Brasil)

(Received 23rd October 1980)

SUMMARY

A flow injection procedure is proposed for the simultaneous determination of aluminium and iron in plant material. The method is based on a flow configuration involving zone sampling and merging zones. Aluminium is determined spectrophotometrically with eriochrome cyanine R as reagent and iron by atomic absorption spectrometry. The advantages of this method over other procedures already reported are discussed. The effects of reagent composition for the aluminium determination are described in detail. The zone-sampling approach permits an easier pH control in the aluminium determinations so interferences caused by variations in sample acidity are avoided without the need for very concentrated buffers. The merging zones configuration greatly reduces the consumption of reagents. The proposed method permits the analysis of about 120 samples (240 determinations) per hour, with good precision (r.s.d. <2%) in both the aluminium and iron channels. The results agree with those obtained by inductively-coupled argon plasma spectrometry.

In a recent publication [1], the zone-sampling approach to flow injection systems was proposed: the sample is injected into a first carrier stream and after a time interval Δt, an aliquot of the resulting sample zone is introduced into a second carrier stream. That paper indicated that the approach could be used in conjunction with the merging zones configuration [2] and also outlined the feasibility of simultaneous determinations when the required dispersions were very different.

The spectrophotometric flow injection determination of aluminium in plant material with the eriochrome cyanine R reagent requires a high degree of sample dispersion [3]. The atomic absorption spectrometry (a.a.s.) of iron in nitric—perchloric acid plant digests is usually performed without sample dilution when an air—acetylene flame is employed. Previous papers [1, 4] demonstrated that a flow injection system in conjunction with atomic absorption spectrometry is very beneficial for routine determinations of calcium, magnesium and potassium in plant material.

This paper reports the development of a flow injection procedure based on the zone-sampling approach for the simultaneous determination of aluminium and iron in plant material. The sample is injected into an un-

0003—2670/81/0000—0000/$02.50

segmented carrier stream of water, creating a well-defined sample zone which is transported through a second injection port towards the nebuliser of an atomic absorption spectrometer for the iron determination. A small portion of the dispersed zone is taken and introduced into a second carrier stream, creating another sample zone which is processed while going towards a spectrophotometric flow cell for the aluminium determination. An interesting feature in this design is the injection of acidic samples into water, which is not usually employed in flow injection analysis, mainly to avoid the refractive index effect [5] and the establishment of pH gradients in the sample zone. These phenomena are not relevant in the a.a.s. determination of iron in plant digests and are transferred only to a slight extent to the second carrier stream. In the aluminium determination, which is strongly pH-dependent [3], the initial dispersion of the sample zone with water permits a better pH control without the requirement of very concentrated buffers and/or the use of an initial neutralizing agent [3].

The merging zones configuration is employed to reduce the consumption of reagents.

EXPERIMENTAL

Apparatus

The peristaltic pump and all components of the manifold were the same as used in earlier work [3]. The injector-commutator, similar to that used previously [1], consisting of three 2:3:2 commutation sections [6], was electronically operated. Details of the electronics are furnished elsewhere [1, 7].

A Varian spectrophotometer model 634, furnished with a Hellma flow cell (type 178; inner volume, 80 μl; light path, 10 mm) was employed for aluminium determinations at 535 nm. For iron measurements, a Perkin-Elmer atomic absorption spectrometer model 306, equipped with a multi-element (Fe, Zn, Cu, Mn) hollow-cathode lamp and a burner for air—acetylene flame, was used; the conditions for maximum sensitivity were followed, and a damping factor of 1.3 was set. Both instruments were connected to Radiometer REC 61 recorders with REA 112 high-sensitivity units. Interfacing of the atomic absorption spectrometer with the flow injection system was the same as already described [4].

Flow diagram

The flow diagram of the system used is shown in Fig. 1, with the injector-commutator (I) in the sampling position. The sample (S) is aspirated to fill the first sample loop (L_S) which defines exactly the volume to be injected, and the excess is discarded (W). When the injector-commutator is switched to the injection position: then simultaneously (a) the selected volume of sample is introduced into the water carrier stream C_S; (b) the second sample loop (L'_S) is moved to the same path; and (c) the reducing reagent (R) starts

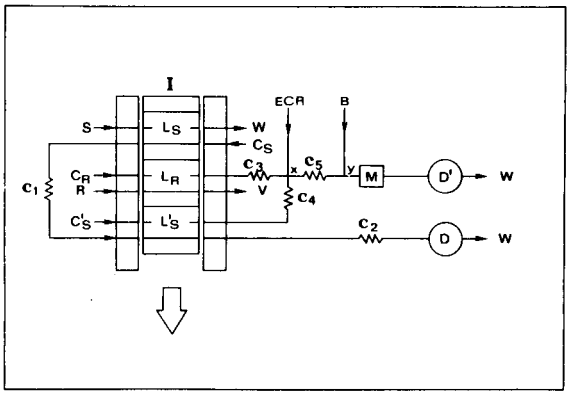

Fig. 1. Flow diagram of the system. Symbols, dimensions and operation are described in the text.

to fill the corresponding loop (L_R). The merging zones configuration allows the excess of reagent to be recovered in vessel V. The injection of the sample gives a sample zone which is directed through the dispersion coil C_1, the second sample loop L'_S and the transmission line C_2 towards the atomic absorption spectrometer (D). Switching of the injector-commutator back to the position specified in Fig. 1 to start a new cycle, is done while the sample zone is passing through loop L'_S. This simple movement causes the simultaneous introduction of both the sample portion inside L'_S and the selected volume of reducing reagent into their corresponding carrier streams (C'_S and C_R). The two zones merge at point X, where the eriochrome cyanine R reagent is added. The reduction of iron(III) by ascorbic acid to avoid its interference takes place under acidic conditions in the reaction coil C_5, where the coloured aluminium—eriochrome cyanine R complex is also formed. Sodium acetate in line B, which acts as a buffer in the presence of the acidic sample, is then added to the sample zone at point Y, and in the following chamber (M) mixing is improved to allow absorbance measurement in detector D' under better conditions. Details of the chemical processes involved in the aluminium determinations have already been discussed [3].

The system was designed to permit a sampling rate of about 120 samples per hour with a carry-over less than 1% in both analytical channels. The initial injection volume of sample was chosen to be 500 μl (L_S = 100 cm) and the dispersion coils C_1 and C_2 were kept as short as possible (15 and 80 cm, respectively) to avoid large sample dispersion inside the iron channel. The sample aspiration rate (3.0 ml min^{-1}) was sufficient to wash and fill the sample loop completely and the first sample carrier stream C_S (6.0 ml min^{-1}) was chosen according to the criteria discussed earlier [4]. The second sample loop was 40 cm long (200 μl); preliminary experiments showed that when this loop was too small, the results became erratic. The pumping rates in the aluminium channel were fixed in order to permit the addition of reagents

under good hydrodynamic mixing conditions. Synchronization lines C_3 and C_4 (15 cm and 5 cm) and volume of reagent injected (100 μl) were defined according to a procedure already described [8]. The reaction coil C_5 was sufficient to permit reduction of the iron(III) and full development of the colour reaction, as indicated in a preliminary experiment involving a stopped-flow procedure [9]. The mixing chamber M was cylindrical (8 mm i.d., 6 mm high, inner volume, ca. 300 μl) and had little effect on sampling rate. This was due to the very small dead volume as the stirring bar occupied a significant portion inside the chamber. The connection lines between this chamber and both point Y (Fig. 1) and the flow cell D′ were 30 cm long.

The resting time of the injector-commutator in the injection position, which corresponds to the Δt value [1], was chosen in order to achieve the required concentration in the re-sampled aliquot, and the sampling time was defined to permit a maximum sampling rate with less than 1% carry-over.

Reagents, standards and samples

All chemicals were analytical grade and distilled-deionized water was always used.

The 1% (w/v) eriochrome cyanine R stock solution was prepared in water, the pH being adjusted to 3.0 with glacial acetic acid. It stayed stable for several months. The working reagent solutions were prepared by dilution of this stock with water. The 1 M sodium acetate solution was prepared by dissolving 82.037 g of the anhydrous salt in 1 l of water. The 1% ascorbic acid aqueous solution was prepared just before use in deoxygenated water.

The 1000-ppm aluminium stock solution was prepared by dissolving 17.514 g of $KAl(SO_4)_2 \cdot 12H_2O$ in 1 l of 0.001 M HCl solution, and the 1000-ppm iron stock solution by dissolving 1.000 g of iron wire (Merck) in about 50 ml of 4 M HCl solution, and diluting to 1 l with water. To achieve similar acidity to the samples [3], mixed working standards ranging from 0.00 to 15.00 ppm (for both aluminium and iron) were prepared in 0.25 M perchloric acid.

The plant digests were prepared by wet digestion with nitric and perchloric acids, as in earlier work [3].

Preliminary tests

The total dispersion factor in the iron channel was estimated by using a 3.00-ppm iron standard, which was first injected into a 0.25 M $HClO_4$ carrier stream and then employed in an infinite volume situation [9], the total dispersion factor being the ratio between absorbances corresponding to the top peak and the achieved plateau. A dye solution (0.02% eriochrome cyanine R solution, pH adjusted to 4.7 with 1 M sodium acetate solution) and a buffer solution (0.1 M acetic acid plus 0.1 M sodium acetate at about pH 4.7) were employed to determine all dispersion factors related to the aluminium determination, using a procedure already described [1].

The system in Fig. 1 was employed to study the effect of reagent concentrations in the aluminium determinations. A calibration graph was obtained for each situation with aluminium standards ranging from 0.00 to 15.00 ppm Al: all measurements were performed in triplicate.

The effect of concentration of reagent B (Fig. 1) was investigated by using sodium acetate concentrations ranging from 0.25 to 2.0 M. A 0.02% eriochrome cyanine R solution was used as colour reagent. Two extra standards (9.00 ppm Al plus 9.00 ppm Fe), prepared in triplicate with different acidities (0.15 M and 0.35 M in perchloric acid), were also used to check the buffering conditions.

Eriochrome cyanine R concentrations ranging from 0.01% to 0.04% (w/v) were tested to investigate the effect of the colour reagent concentration, using a 1 M sodium acetate solution.

Three mixed standards (9.00 ppm Al plus 50.00 ppm Fe(III)) were employed to study the masking of iron(III) interference in the aluminium determination; the concentration of eriochrome cyanine R was 0.02% (w/v). Ascorbic acid concentrations ranging from 2.5 to 0.25% (w/v) were tested.

The stability of the system was checked by repeating the determination of a 9.00 ppm Al—9.00 ppm Fe standard during two hours. A 1% (w/v) ascorbic acid solution was used. The precision of the proposed method was estimated by running a typical sample (4.70 ppm Al—7.25 ppm Fe) ten times. The accuracy was tested by analysing nine samples which had already been analysed by inductively-coupled argon plasma spectrometry [10].

RESULTS AND DISCUSSION

The Δt value was chosen as 8 s. In this situation, the mean concentration of the aliquot sampled at the second injection port L'_S (Fig. 1) is about 65% of the maximum concentration at that point. The total attenuation factor (including dispersion and dilution by confluent streams) in the aluminium determination was 0.022 and the partial attenuation factor in the aluminium channel was 0.132. The total dispersion factor in the iron determination

TABLE 1

Effect of reagent concentration on the determination of aluminium

Parameters of the calibration curve	Sodium acetate conc.[a] (M)				Eriochrome cyanine R conc.[b] (% w/v)			
	0.25	0.5	1.0	2.0	0.01	0.02	0.03	0.04
Blank value (A)	0.133	0.089	0.083	0.042	0.044	0.083	0.144	0.178
Slope (A ppm^{-1})	0.050	0.052	0.057	0.064	0.030	0.057	0.073	0.080
Regression coeff. (n = 18)	0.9986	0.9994	0.9981	0.9976	0.9956	0.9976	0.9981	0.9945

[a]With 0.02% (w/v) eriochrome cyanine R. [b]With 1.0 M sodium acetate.

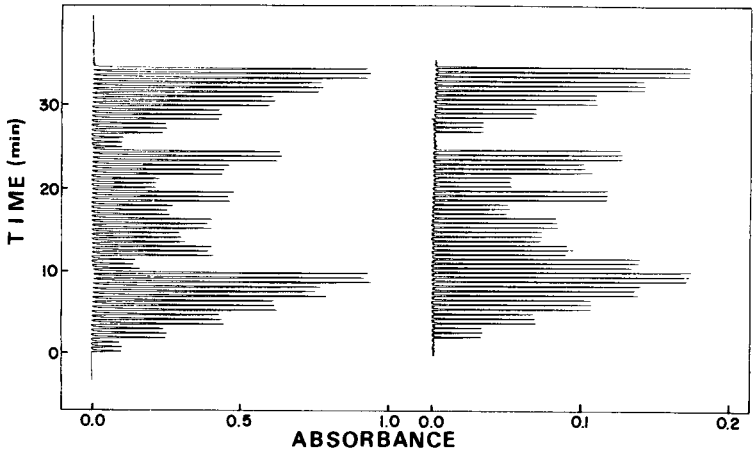

Fig. 2. Routine run for the simultaneous determinations of aluminium (left) and iron (right) in plant digests. From bottom: six mixed standards (0.00, 3.00, 6.00, 9.00, 12.00 and 15.00 ppm Al and Fe), nine samples and the standards again. All measurements in triplicate.

was 0.659. In spite of the large difference between the two total attenuation factors, good precision was achieved because of the zone-sampling approach.

The sampling time was 24 s and therefore, 3600/(24 + 8) = 113 samples can be run per hour.

The influence of the concentrations of sodium acetate and eriochrome cyanine R on the aluminium calibration curves are summarized in Table 1. Only the blank values and the slopes of the curves are presented because good linearity was always achieved (Fig. 2). Increase of the buffer capacity (sodium acetate concentration) decreases the blank value and increases slightly the slope of the calibration curve. The 1.0 M concentration was chosen because in this situation no differences in peak height corresponding to different sample acidities were found. Higher sodium acetate concentrations are not recommended mainly because the mixing conditions are poorer and consequently the reproducibility decreases. It must be emphasized that the proposed system utilizes a very diluted acetate solution compared with that employed earlier [3]. The slope of the calibration curve increases as the eriochrome cyanine R concentration increases. The colour reagent concentration cannot, however, be increased at will because of the higher blank values. A 0.02% concentration was therefore chosen. Although a 0.05% (w/v) ascorbic acid solution was sufficient to mask 50 ppm Fe(III), a 1.0% concentration was chosen.

The proposed system is remarkably stable: after 2 h of continuously measuring a standard, no baseline drift was observed. Slight variations in peak heights (about 5% in both Al and Fe channels) were observed after two hours. Therefore, recalibration after running 100 samples is recommended.

The precisions of the aluminium and iron determinations are about 1.5% and 2.0%, respectively (expressed as the relative standard deviation). The

TABLE 2

Comparative results obtained after analysis of foliar material by the proposed method (f.i.a.) and by inductively-coupled argon plasma spectrometry (i.c.p.—a.e.s.). Data expressed in ppm in the final digest

Sample	Al (ppm)		Fe (ppm)	
	F.i.a.	I.c.p.—a.e.s.	F.i.a.	I.c.p.—a.e.s.
Gossypium sp.	1.10	1.10	11.85	11.90
Sorghum bicolor L.	5.25	5.15	8.00	8.10
Sorghum bicolor L.	3.70	3.70	6.40	6.60
Sorghum bicolor L.	5.25	5.30	7.25	7.30
Glycine hispida L.	3.20	3.00	4.55	4.55
Sorghum bicolor L.	6.30	6.10	9.75	9.70
Glycine hispida L.	2.50	2.45	4.60	4.50
Glycine hispida L.	6.00	5.95	8.55	8.20
Glycine hispida L.	9.25	9.40	10.45	10.50

analytical range of the aluminium method can be expanded by employing other Δt values. The sensitivity in the iron procedure can only be decreased when lower initial injected volumes are used. Table 2 indicates that the results obtained for actual samples by the proposed method agree with those obtained by inductively-coupled argon plasma spectrometry. No statistical difference was found at the 1% level.

Partial support of this project by CNPq (Conselho Nacional de Desenvolvimento Científico e Tecnológico) is greatly appreciated. The authors thank Diva Athiê for critical comments, J. Mortatti for helping with the Figures and N. M. C. Pereira for typing the original manuscript.

REFERENCES

1 B. F. Reis, A. O. Jacintho, J. Mortatti, F. J. Krug, E. A. G. Zagatto, H. Bergamin F° and L. C. R. Pessenda, Anal. Chim. Acta, 123 (1981) 221.
2 H. Bergamin F°, E. A. G. Zagatto, F. J. Krug and B. F. Reis, Anal. Chim. Acta, 101 (1978) 17.
3 B. F. Reis, H. Bergamin F°, E. A. G. Zagatto and F. J. Krug, Anal. Chim. Acta, 107 (1979) 309 (part 3).
4 E. A. G. Zagatto, F. J. Krug, H. Bergamin F°, S. S. Jørgensen and B. F. Reis, Anal. Chim. Acta, 104 (1979) 279.
5 H. Bergamin F°, B. F. Reis and E. A. G. Zagatto, Anal. Chim. Acta, 97 (1978) 427.
6 B. F. Reis, E. A. G. Zagatto, A. O. Jacintho, F. J. Krug and H. Bergamin F°, Anal. Chim. Acta, 119 (1980) 305.
7 H. Bergamin F°, B. F. Reis, A. O. Jacintho and E. A. G. Zagatto, Anal. Chim. Acta, 117 (1980) 81.
8 E. A. G. Zagatto, B. F. Reis, H. Bergamin F° and F. J. Krug, Anal. Chim. Acta, 109 (1979) 45.
9 M. F. Giné, H. Bergamin F°, E. A. G. Zagatto and B. F. Reis, Anal. Chim. Acta, 114 (1980) 191.
10 H. Bradbury, Jarrell-Ash Plasma Newsl., 1 (1978) 3.

Analytica Chimica Acta, 125 (1981) 45—53
Elsevier Scientific Publishing Company, Amsterdam — Printed in The Netherlands

DETERMINATION AND ON-SITE SAMPLING OF INORGANIC AND ORGANIC MERCURY IN AQUEOUS SAMPLES WITH ENZYME REACTORS

LARS ÖGREN

Analytical Chemistry, University of Lund, P.O. Box 740, S-220 07 Lund (Sweden)

(Received 4th November 1980)

SUMMARY

Micro reactors containing immobilized urease are used for the sampling and determination of mercury ions. When an aqueous sample is passed through the reactor, the mercury ions are collected and bound to the enzyme. The enzyme is partially inhibited and the amount of mercury ions is determined as a decrease in the enzyme activity. The enzyme activity is determined with an ammonia electrode when a urea solution is pumped through the reactor. The selectivity is very high and the operating range is 0—15 nM Hg^{2+} for 5-ml samples. The mercury can be stored for several days in the reactor before the measurements are made. Organo-mercury compounds give essentially the same response as inorganic mercury.

Many methods are available for the determination of traces of mercury. The main method, cold-vapour atomic absorption, has been the subject of a great number of papers during the last few years [1].

The enzyme inhibition method for mercury [2, 3] has some desirable properties which make further studies worth while. The instrumentation is simple, the sensitivity is very high, and as shown in this paper the method can be modified so that at least part of the sample storage problems are solved. Errors from losses or contamination during sample handling are very important for mercury and especially for organo-mercury compounds [4, 5]. The main disadvantage is that the enzymatic technique is not well established in analytical laboratories and that further work is necessary before routine application is feasible.

Principle

Immobilized urease is filled into small reactors (see Fig. 1) provided with luer end fittings. If a buffered urea solution is pumped through the reactor a fraction of the substrate will be converted to ammonia. The measurement is done with an ammonia electrode after addition of a stream of sodium hydroxide to make the solution alkaline. If the procedure is repeated with partially inhibited enzyme a smaller fraction of urea will be converted to ammonia. The decrease represents the inhibition caused by the mercury.

The enzyme reactors are easily removed from the measuring unit and can be transported to the sampling site. A sample, say 5 ml, is taken with a disposable syringe, mixed with buffer—NaCl and pressed through an enzyme reactor. Any mercury in the sample will bind very strongly to the enzyme and therefore losses will be small. The danger of contamination is also smaller than for a bottle of aqueous sample.

EXPERIMENTAL

Reactor design

The immobilized enzyme—glass (20 μl) is enclosed in a teflon cylinder as shown in Fig. 1. The packing is kept in place with polypropylene filters, woven with 8 threads per mm, the openings being 0.02—0.03 mm. The teflon body consists of three parts which can be pressed together inside a stainless steel tube (8 mm i.d., 10 mm o.d.) using a special tool made for the purpose. The ends are made as male and female luer fittings for connection to normal disposable syringes. End caps are used during storage to prevent drying.

Various other materials were tested and found to be unsuitable for different reasons. The silver filters used earlier [2] tended to clog with time, and nickel filters corroded and produced small amounts of nickel which inhibited the enzyme if given a sufficiently long time for reaction.

Various alternative body materials caused a special type of inhibition. It could be reversed after prolonged pumping of water or buffer. The materials tested were acid-etched Delrin (acetal polymer), PVC and plexiglas, as well as various glues and solvents for the glues. Most of the difficulties were traced to peroxides from the solvents or the materials. The all-teflon construction with polypropylene filters removed all those problems.

Immobilized enzyme

Urease (Sigma U-0251) was immobilized on porous glass (Corning 729 Å, CPG-10) by means of glutaraldehyde coupling as described earlier [6]. The glass was sieved after silanization and the fractions 120—140 or 140—170 mesh were used. The urease was inhomogeneous so that if small amounts were weighed and used the reactors might have widely different activities. Therefore a large amount of enzyme was dissolved in a buffer and a suitable fraction was used. Even so, it was found expedient to make two immobilizations at the same time, one with 1 mg of urease per g of alkylamino-glass

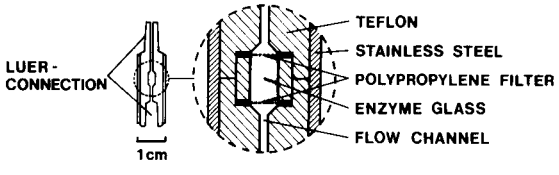

Fig. 1. Enzyme reactor. The central part is shown magnified four times.

and the other with 3 mg g^{-1}, and to use the preparation with the most suitable activity. The reactors with 3 mg of enzyme per g of glass are more stable as shown later, and should be used whenever possible. If the activity of the enzyme batch is very high, very curved calibration plots will be obtained, and to rectify this the enzyme—glass with the lower activity can be used instead. Before assessment of the final activity, 1 g of enzyme glass should be treated with 600 ml of 2 μM Hg^{2+} solution in 1 mM malic acid (hydroxysuccinic acid) buffer pH 5.3, washed with 400 ml of regeneration solution and finally with 400 ml of water.

Sudden losses of activity either of the prepared batch or of individual reactors after the final assembly were sometimes observed. Storage in 1 mM phosphate buffer pH 7, or in buffer containing 0.02% sodium azide did not help. The most likely cause is bacterial growth and therefore care was taken to use sterile solutions and to sterilize the equipment used in the preparation. This resulted in a marked improvement. It should be worthwhile to insert filters on both sides of the enzyme bed for sterile filtration of the solution, but this possibility has not been tested.

Chemicals

Regeneration of mercury-inhibited urease was done with a solution containing 10 mM thioacetamide and 10 mM EDTA in 0.1 M Tris-HCl buffer, pH 7.0. Regeneration with sodium iodide was tested in addition to the solutions studied earlier [2], but it was found that this could only remove part of the mercury bound to the enzyme.

The substrate solution was 15 mM urea (Aristar, BDH Chemicals) in 25 mM maleic acid (*cis*-butenedioic acid) adjusted to pH 6.15 with sodium hydroxide. Traces of heavy metals in the urea—buffer solution were removed by a column (10 mm i.d., length 95 mm) containing Chelex-100 ion-exchange resin (100—200 mesh) in the sodium form (Bio-Rad Laboratories).

A stock solution was prepared from weighed amounts of mercury(II) nitrate. A secondary stock solution was made each day by diluting the primary solution 400 times. The secondary stock solution was 25 μM in Hg^{2+}. Working standards in the range 1—50 nM Hg^{2+} were prepared by taking the appropriate amount from the secondary stock solution, adding 1% (v/v) of an 0.1 M malic acid buffer, pH 5.3, and dilute with water purified in a Millipore-Q-system. The concentrated buffer had been purified by passing it slowly through a column of Chelex-100. The sodium chloride was Merck Suprapur.

Apparatus

The flow diagram and the arrangement are shown in Fig. 2. The components within the broken lines were thermostatted. The assembly was mounted on the stainless steel lid of a circulation thermostat (Julabo, Model U2). Two modes of operation could be selected with a 6-port rotary valve (Altex Model 202). In the first, called "measure", the urea—buffer solution

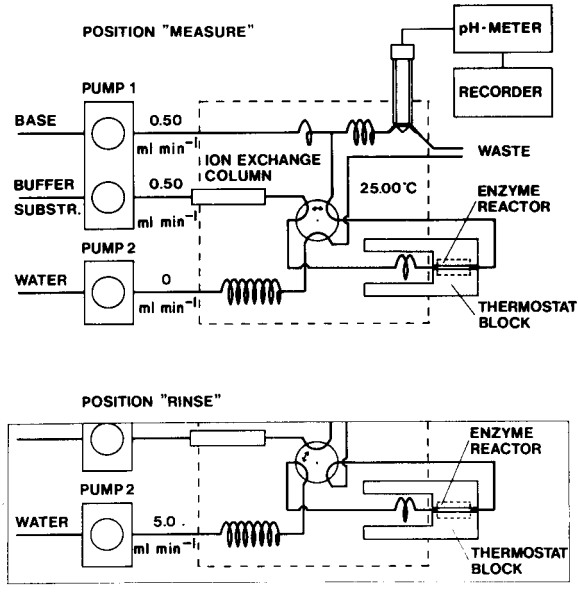

Fig. 2. Flow diagram of the measuring apparatus.

was pumped through the enzyme reactor and after mixing with 0.1 M sodium hydroxide the solution passed an ammonia electrode (EIL, Model 8002). The second position, "rinse", was used only for removing the reagents so that the reactor would be ready for use after disconnection.

The reactor is fastened on a male luer connector in the lid of the thermostat; the other connection is made from above. Heavy metal clamps can be closed around the reactor so that good thermal contact is established. The lower parts of the clamps dip into the water so that a thermal sink is obtained. If a reactor at 5°C is mounted in the clamp, its center will reach 24.5°C in 105 s and 24.99°C in 205 s if the water in the thermostat is at 25.00°C, according to theoretical calculations. In practice, temperature equilibrium is reached more quickly as thermostatted solutions are pumped through the reactor. The length of the heat-exchanger coils were adjusted until the solution reached thermal equilibrium within 0.01°C at normal pumping speed. Every turn of the coil in Fig. 2 corresponds to 200 mm. The tubings were made from teflon (0.5 mm i.d.).

In practice thermal equilibrium was reached faster than the time required for a steady-state electrode response, i.e. 4 min. The buffer—substrate and sodium hydroxide solutions were pumped with a multi-channel peristaltic pump (Ismatec, Model mp-ge).

Five successive activity measurements on the same reactor could be made with a standard deviation of 0.3%.

RESULTS

Sensitivity

The sensitivity increases if the amount of enzyme in the reactor is small. The linearity of the calibration curves will be improved when the fractional conversion of substrate, i.e. the amount of enzyme, decreases [2]. The reactors used in this study were filled with 20 μl of enzyme glass from a lot containing either 1 or 3 mg of urease per g of glass. These amounts should give almost linear calibration curves. The sensitivities of the two batches are of the order 0.6 or 0.3% inhibition per picomole of mercury in 10 mM NaCl (3.0 or 1.5% inhibition per nM for 5-ml samples).

The sensitivity also depends on the chloride concentration of the sample (Fig. 3). The sensitivity increases up to a plateau before a final slow increase. The latter is caused by mercury in the sodium chloride solutions. At 10 mM chloride concentration, the mercury is distributed [7] between $HgCl_2$ (90%), $HgCl_3^-$ (9%), $HgCl_4^{2-}$ (1%), $HgCl^+$ (0.003%) and Hg^{2+} (5×10^{-8}% or 5×10^{-18} M) at a total sample concentration of 10 nM. The favoured explanation for the chloride dependence is that the presence of strong complexes decreases the activity of Hg^{2+} to such a low level that binding to weaker non-inhibiting sites is prevented. The binding to walls and to the porous glass will also decrease. It was shown, by using sodium sulphate either alone or in combination with chloride, that the effect is not caused by changes in the ionic strength. The addition of chloride increases the selectivity slightly over copper and silver.

Figure 4 shows calibration curves made with samples containing 10 mM NaCl. Besides the increased sensitivity in the presence of chloride, there is also less leakage to a second reactor placed in series with the first. There is a

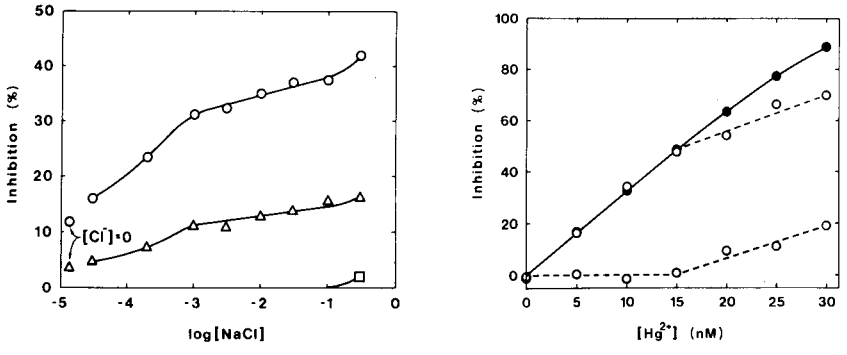

Fig. 3. Variation of the sensitivity as a function of the sodium chloride content of the sample solution. All solutions were 1 mM in malic acid buffer. (○) Samples containing 10 nM Hg^{2+}; (△) samples containing 5 nM Hg^{2+}; (□) blank solutions.

Fig. 4. Calibration curves of two enzyme reactors in series. (○) Samples containing 10 mM Cl^-: the upper curve marks the first reactor and the lower curve the second reactor. (●) The sum of the two reactors.

break-through around 50% inhibition caused by inhomogeneities in the flow. At the rapid flow rates used during sampling, there will be channeling in the packing. The presence of chloride also increases the precision of the measurements. The calibration curve, considering the sum from both reactors, is almost but not completely linear.

If two reactors are placed in series during sampling, mercury which passes the first will be collected in the second. The reactors are measured individually and the percent inhibition is calculated for each one. A correct result will be obtained if the inhibitions are added. A calibration curve made from the sum of two or more reactors can be constructed, provided that the deviations from linearity are small.

Figure 5 shows the decrease in activity with time for two reactors with different amount of enzyme. The reactors were thoroughly rinsed before the start. Nevertheless, at least part of the initial decrease is thought to be caused by desorption of enzyme not covalently bound to the glass. Part of the early inactivation and most of that occurring after one day is caused by an irreversible inactivation of enzyme molecules remaining immobilized in the bed. The effect is more pronounced for the reactor with the smaller amount of enzyme. After a week the activity stabilizes, and further decrease is of the order of 0.3—1% per day, supposing 4 h each day at room temperature and the remaining time in a refrigerator. The decrease follows the same curve for those parts of the batch stored in the refrigerator and packed later, except that the activity of the glass with the low enzyme loading decreases more rapidly for reactors that are kept at room temperature part of the day.

The sensitivity, however, has a time course completely different from that of the activity. The sensitivity remains essentially constant with time, except for a slight increase during the first day caused by losses of adsorbed enzyme. Therefore it is necessary to assume that the irreversibly inactivated urease

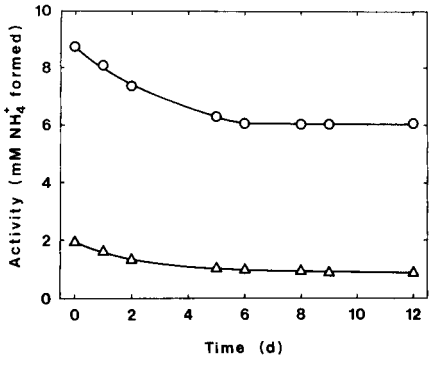

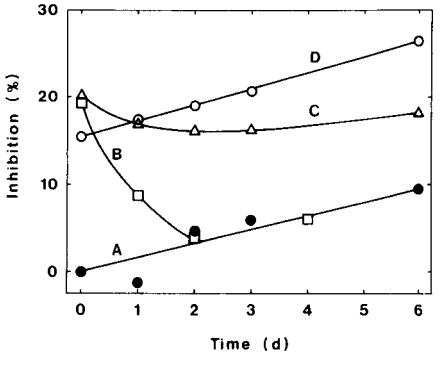

Fig. 5. Decrease in enzyme activity with time for reactors with high (○) and low (△) enzyme loading.

Fig. 6. Sensitivity measured with samples containing 5 nM Hg^{2+}, 10 mM Cl^- and 1 mM malic acid buffer. For explanation, see text.

TABLE 1

Measurements with different reactors prepared from the same enzyme batch. The samples were 5 ml; the solutions were 10 mM in sodium chloride and 1 mM in malic acid buffer.

Reactor	Hg^{2+} (nm)	Inhibition (%)	Sensitivity % inhibition/pmol Hg^{2+}
1	2.5	7.5	0.600
	2.5	6.4	0.512
2	5.0	13.4	0.536
	5.0	13.1	0.524
3	7.5	19.6	0.523
	7.5	17.7	0.472
4	10.0	28.2	0.564
	10.0	27.3	0.546
5	12.5	35.1	0.562
	12.5	35.6	0.570
6	15.0	47.8	0.637
	15.0	47.0	0.627
		Mean	0.556
		S.d.	0.048

molecules remain bound to the glass with their mercury binding sites intact. The mercury ions will bind equally well to active and inactive molecules.

The sensitivities of reactors with low and high loading were, respectively, 0.6 and 0.3% inhibition per picomole of mercury in the presence of 10 mM sodium chloride (3.0 and 1.5% inhibition per nM Hg^{2+} for 5-ml samples). The ratios of the loadings, the activities and the inverse sensitivities were 1:3, 1:7 and 1:2.

The sensitivity of reactors packed from the same batch was almost the same for all. Table 1 shows duplicate measurements on six different reactors. The largest single source of error is the variation in the amount of enzyme glass packed into a reactor.

Storage

Figure 6 shows the time course of reactors with low enzyme loading. The inhibition was calculated as a percentage of the activity relative to that at the start of the experiment. A reactor without any bound mercury was used as a blank (curve A); because of the mode of calculation the activity decrease will show up as increasing inhibition. Three reactors were treated with 5 ml of 5 nM Hg^{2+} in the presence of chloride. Curve B shows the result when the reactor had been regenerated 10 min before the inhibition. Curves C and D were obtained under identical conditions except that the regeneration had been made 24 and 96 h, respectively, before the inhibition. Traces of the regeneration reagent are trapped in pores or crevices and are slowly released by diffusion resulting in a removal of mercury. If the measurements are made immediately after sampling, freshly regenerated reactors can be used;

otherwise some days should elapse between regeneration and a final rinse. If this precaution is taken (curve D) the reactors can be stored for several days before measurement, if a blank correction is applied.

The slopes of the blank and consequently of the plots for inhibited reactors are very much smaller when enzyme—glass with the higher loading is used.

Both the sensitivity and the activity of a reactor can be restored almost completely if the regeneration is done within a few hours after the inhibition. This is not the case if the reactor has been stored in inhibited condition for about a week. The inhibited fraction will be irreversibly damaged; the amount of the deactivation is 25% after 24 h and almost 100% after a week. The reactors cannot be re-used unless they are regenerated very soon after the inhibition.

Organo-mercury compounds

Organo-mercury compounds cause inhibition as shown in Table 2. The response was found to be less than that for inorganic mercury, but it is not known if the difference is real or caused by losses of the volatile compounds. The standards were checked by flame atomic absorption spectrometry. The mercury concentration in the standards were in the millimolar range but even at this level losses were observed. The problems are of course magnified at the nanomolar level used in the reactor tests.

The organo-mercury compounds behaved in a similar way to inorganic mercury and the procedure for determinations was essentially the same. Addition of chloride to the sample increased the sensitivity in the same way as for inorganic mercury but the leakage from the first to the second reactor

TABLE 2

Sensitivity of an enzyme reactor towards organo-mercury compounds
(5-ml samples were taken and the sample injection rate was about 4 ml min^{-1}. (Cl^-) indicates that the samples were 10 mM in sodium chloride. All solutions were 1 mM in malic acid buffer.)

Sample	1st reactor inhibition (%)	2nd reactor inhibition (%)	Sum of inhibition (%)	Inhibition relative to Hg^{2+} (%)
5 nM Hg^{2+} (Cl^-)	16.4	0.8	17.2	100
10 nM Hg^{2+} (Cl^-)	36.3	−0.4	35.9	100
5 nM CH_3HgCl	6.0	0.0	6.0	35
5 nM CH_3HgCl (Cl^-)	13.0	1.2	14.2	83
10 nM CH_3HgCl	16.0	1.9	17.9	50
10 nM CH_3HgCl (Cl^-)	31.1	3.8	34.9	97
5 nM Ph—HgAc	4.2	−0.4	3.8	22
5 nM Ph—HgAc (Cl^-)	10.3	1.2	11.5	67
10 nM Ph—HgAc	17.6	1.9	19.5	54
10 nM Ph—HgAc (Cl^-)	23.5	2.7	26.2	73

was somewhat larger in the presence of chloride. This indicates that complexation with chloride causes a redistribution from weak non-inhibiting binding sites to stronger inhibiting sites with the result that the sensitivity increases. It can be assumed that the ligand exchange is slower for the organo-mercury compounds than for Hg^{2+} and this is supported by the observation that the flow rate during the sampling of organo-mercury compounds had to be kept low. The somewhat larger losses to the second reactor observed indicate that the flow rate is still too high to reach equilibrium within the first reactor.

The author thanks Professor Gillis Johansson for valuable discussions concerning this work. This work was supported by grants from the Swedish Board for Technical Development, STU.

REFERENCES

1 G. Horlick, Anal. Chem., 52 (1980) 290 R.
2 L. Ögren and G. Johansson, Anal. Chim. Acta, 96 (1978) 1.
3 B. Mattiasson, B. Danielsson, C. Hermansson and K. Mosbach, FEBS Lett., 85 (1978) 203.
4 I. Sanemasa, T. Deguchi, K. Urata, J. Tomooka and H. Nagai, Anal. Chim. Acta, 94 (1977) 421.
5 M. Stoeppler and W. Matthes, Anal. Chim. Acta, 98 (1978) 389.
6 G. Johansson and L. Ögren, Anal. Chim. Acta, 84 (1976) 23.
7 L. G. Sillén and A. E. Martell, Stability Constants of Metal-Ion Complexes, The Chemical Society, London, 1964, Suppl. No. 1, London, 1971.

Analytica Chimica Acta, 125 (1981) 55—64
Elsevier Scientific Publishing Company, Amsterdam — Printed in The Netherlands

AUTOMATIC ENZYMATIC DETERMINATION OF GLUCOSE WITH A POTENTIOMETRIC SULPHUR DIOXIDE PROBE

P. W. ALEXANDER* and P. SEEGOPAUL

Department of Analytical Chemistry, University of New South Wales, P.O. Box 1, Kensington, N.S.W. 2033 (Australia)

(Received 26th November 1980)

SUMMARY

An automatic, continuous-flow system for the determination of glucose is reported, with a sulphur dioxide probe used as the sensor for an indicator reaction with hydrogensulphite. In the presence of glucose oxidase, glucose is selectively oxidised to produce hydrogen peroxide at a rate proportional to the glucose concentration. The oxidation of hydrogensulphite by the hydrogen peroxide is rapidly monitored by the probe at sampling rates as high as 90 samples per hour. Proteins and reducing substances, such as cysteine, uric acid and ascorbic acid interfere only in large amounts. The method is applicable to biological fluids without prior separation steps.

The need for accurate and rapid glucose determinations in clinical work has resulted in the development of a wide variety of assay procedures, including fluorimetric, spectrophotometric, radioisotopic and electrochemical techniques. These methods are generally based on reduction or condensation reactions of glucose or on the more selective enzyme-catalysed reactions of glucose [1—3].

Enzymatic determination of glucose with electrochemical sensors has become commonly used since the advent of enzyme immobilisation technology [4]. Several amperometric [5—8], potentiometric [9, 10], and ion-selective electrode [11, 12] methods have been devised for glucose determinations. Of these methods, the use of gas-sensing probes for electrometric monitoring of enzyme—substrate reactions has considerable advantages [13, 14], with high selectivity being a significant feature. The most commonly used electrometric technique for glucose measurements is based on amperometric oxygen electrodes which are used to measure the oxygen consumed either in enzyme solutions [15] or via the enzyme immobilised at the electrode surface [16].

In a recent paper, the use of a gas-sensing sulphur dioxide probe for potentiometric enzyme determination was described [17]. In the study described here, the sulphur dioxide probe was utilised for potentiometric enzymatic determination of glucose in an automated continuous-flow system, and the method was applied in the analysis of serum, urine and cerebrospinal fluid.

EXPERIMENTAL

Reagents and solutions

All chemicals used were of analytical-reagent grade and solutions were made up either in distilled water or the appropriate buffer. Sodium metabisulphite solutions used as the base-line reagent were obtained by serial dilutions from freshly prepared 0.1 M metabisulphite solution.

Glucose oxidase (E.C. 1.1.3.4; Calbiochem) had a quoted specific activity of 123 I.U. mg^{-1}. For most of this work, enzyme solutions were prepared in 0.0667 M phosphate buffer of pH 5.6 made by dissolving 8.62 g of KH_2PO_4 and 0.473 g of Na_2HPO_4 in 1 l of distilled water; the pH of the buffer was changed by varying the amounts of the components [18]. The enzyme solutions were left to stand at room temperature (ca. 20°C) for at least 24 h so that any catalase impurity would be destroyed. Glucose oxidase activity in the range 3—4 I.U. ml^{-1} was used for this study. Glucose sample solutions were made up in distilled water from a 0.1 M stock D-(+)-glucose (BDH Analar) solution in distilled water which was refrigerated overnight for mutarotation equilibrium.

For interference studies, bovine serum albumin (BSA, Fraction V, Miles Research Lab. Inc.), cysteine, uric acid and ascorbic acid (all from Nutritional Biochemical Corporation) were used. For the control studies, Chemistry Control Serum I (Lot No. 0369N005A), Chemistry Control Serum II (Lot No. 0368N003AA), Chemistry Control for Spinal Fluid (Lot No. 0313P002A), and Chemistry Urine Control (Lot No. 0401N005A) were obtained from Hyland Lab. Human serum samples were obtained from the Prince Henry Hospital, Sydney.

Instrumentation

The system for glucose determination is shown in Fig. 1. It consisted of a Watson-Marlow pump running at 100 rpm, thermostatted mixing coils with hold-up time of less than 2 min for incubation of the enzymatic reaction mixture, an electrode assembly, a pH/mV meter and a mV recorder. Standard Technicon Tygon pump and transmission tubing and mixing coils were used in the system.

The sensing electrode assembly comprised an E.I.L. Model No. 8010-8 sulphur dioxide probe fitted with a flow-through cap designed with single inlet and outlet ports, giving a dead volume in the order of 100 μl. The filling solution (E.I.L. Part No. 8010 240) for the probe was modified by the addition of glucose, as previously reported [17]. Potentiometric output was continuously monitored with a Radiometer PHM62 pH/mV meter and recorded on a National VP-6511A recorder.

Procedure

For measurements in the automated system, the glucose or wash solutions were pumped into a continuously flowing stream of air-segmented enzyme

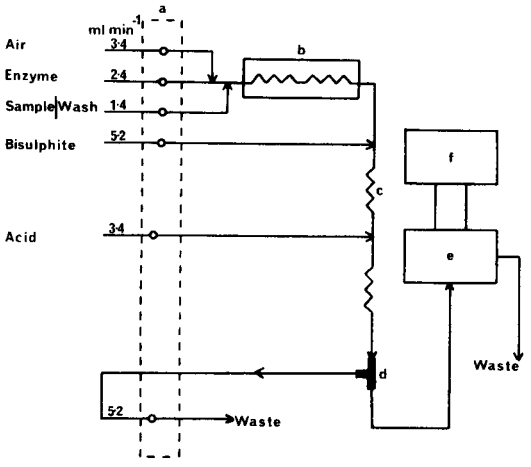

Fig. 1. Schematic diagram of the continuous flow apparatus for glucose determination, with the total flow rate of solution across the probe being 10.4 ml min^{-1}. (a) Peristaltic pump; (b) thermostatted coils for incubation; (c) mixing coil; (d) debubbler; (e) electrode assembly; (f) pH/mV meter and mV recorder.

solution. The sample-to-wash ratio was kept at a constant value of 1:1, with the sampling times varied from 60 to 10 s to give sampling rates of 30 to 180 samples per hour, respectively. The enzyme—substrate stream was incubated for a fixed period of less than 2 min at a pre-determined temperature, after which time the flowing solution was mixed with the sulphite and sulphuric acid. The effect of incubation time on the enzymatic reaction was investigated by varying the number of mixing coils used for incubation. Unless otherwise stated, the concentrations of the various reagents used were as follows: $1.0—5.0 \times 10^{-4}$ M $S_2O_5^{2-}$, 1.5 M H_2SO_4 and 3—4 I.U. ml^{-1} glucose oxidase activity in pH 5.6 phosphate buffer. The enzymatic reaction was quenched by the acid and, simultaneously, the unreacted sulphite was converted to sulphur dioxide. The activity of the indicator ion was displayed as a peak on the chart recorder and the glucose concentration was directly related to the potential via a calibration plot.

Recovery studies were done with aqueous solutions, urine samples and pooled human sera. A stock solution of glucose containing 10.0 g in 100 ml of distilled water was prepared. Aliquots (0—350 μl) of this solution were added to 25 ml of either water or urine, or to 5.0 ml of serum which was then diluted to 25 ml with distilled water. Each sample was fed through the flow system, the peak heights were measured and the glucose concentration was read off a calibration plot obtained from aqueous glucose standards.

For the interference studies, aliquots of the stock glucose solution were added to 25 ml of serum or urine samples followed by the addition of the reducing substances. The samples were then measured as above.

RESULTS

The experimental factors influencing both the enzyme-catalysed reaction and the indicator reaction were investigated, using the flow system shown in Fig. 1. The effects of pH, temperature, incubation period, enzyme activity, metabisulphite concentration and acid concentration were optimized. Interference effects and recoveries of glucose in aqueous, urine, and pooled sera samples were then determined.

Glucose calibration data

The flow system was used to detect sulphur dioxide produced in the following reaction sequence

$$\beta\text{-D-glucose} + H_2O + O_2 \xrightarrow[\text{oxidase}]{\text{glucose}} \text{D-gluconic acid} + H_2O_2$$

$$S_2O_5^{2-} + H_2O \rightarrow 2HSO_3^-$$

$$H_2O_2 + 2HSO_3^- \rightarrow S_2O_6^{2-} + 2H_2O$$

$$S_2O_5^{2-} + 2H^+ \rightarrow 2SO_2 + H_2O$$

The second reaction indicates that metabisulphite exists as hydrogensulphite in aqueous solutions. The enzyme activity was initially kept at 3.44 I.U. ml^{-1} with the metabisulphite and acid concentrations being 5.0×10^{-4} M and 1.5 M respectively. The results of sampling glucose standards in the concentration range 270—1400 mg l^{-1} are shown in Fig. 2. The probe responded to SO_2 produced by 60 glucose samples per hour with a 1:1 sample-to-wash ratio. Figure 2A shows calibrations with increasing and decreasing

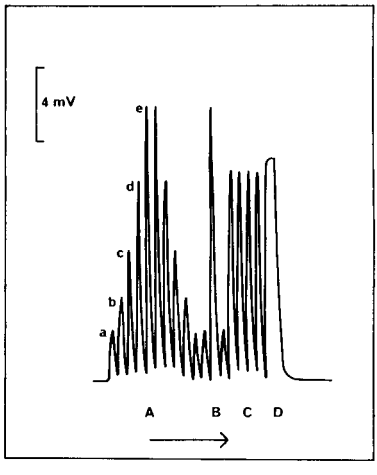

Fig. 2. Continuous recording of glucose samples at 60 per hour with a base-line concentration of 5.0×10^{-4} M $S_2O_5^{2-}$, 3.44 I.U. ml^{-1} glucose oxidase and 1.5 M H_2SO_4 at 30.5°C: [A] calibrations in direction of increasing and decreasing concentrations; [B] carry-over between consecutive samples; [C] replicate measurements; [D] steady-state potential. (a) 270; (b) 450; (c) 720; (d) 1080; (e) 1440 mg l^{-1} glucose.

concentrations, with linearity obtained for the concentration range given above. Carryover of 0.3% was observed, as shown in Fig. 2B. Approximately 94% of the steady-state potential was obtained with a relative standard deviation of 0.8%, as shown in Figs. 2C and 2D.

Figure 3 shows glucose calibration plots at sampling rates of 60, 90 and 120 sample per hour for glucose standards in the range 270—1440 mg l^{-1}. Linearity was obtained in the concentration range studied, but lower peak heights were obtained at the higher sampling rates because of the decreased sampling time allowed.

Optimization of kinetic parameters of the enzyme reaction

The effects of pH, buffer composition, temperature and oxygen have been determined previously [17]. When 0.1 M phosphate buffer was used, it was found that a pH of 5.6 gave greatest sensitivity, whereas acetic acid interfered with the performance of the SO_2 probe.

The temperature range required to maximise the rate of the enzyme-catalysed reaction was found to be 39—41°C. Figure 4 shows glucose calibration plots at various temperatures, obtained by measuring the potential changes given by glucose standards at various temperatures with a fixed enzyme activity of 3.44 I.U. ml^{-1}. Increased sensitivity was observed at the higher temperatures but linearity was poorer. Figure 5 shows the dependence of the glucose response on the incubation time determined for a fixed glucose concentration. At times greater than 200 s, the curve began to flatten.

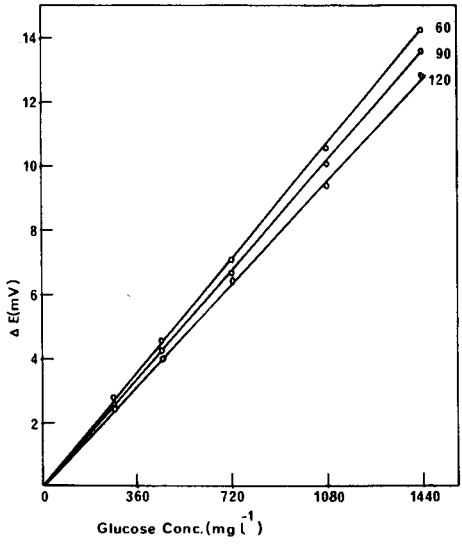

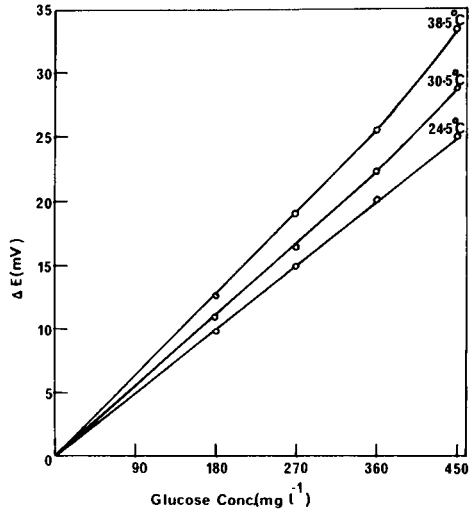

Fig. 3. Glucose calibrations at sampling rates of 60, 90 and 120 h^{-1} (1:1 sample-to-wash ratio) with 5.0×10^{-4} M $S_2O_5^{2-}$, 3.44 I.U. ml^{-1} enzyme and 1.5 M H_2SO_4 at 30.5°C.

Fig. 4. Glucose calibrations at various temperatures, at a sampling rate of 30 h^{-1} with 1.0×10^{-4} M $S_2O_5^{2-}$, 3.44 I.U. ml^{-1} enzyme and 1.5 M H_2SO_4.

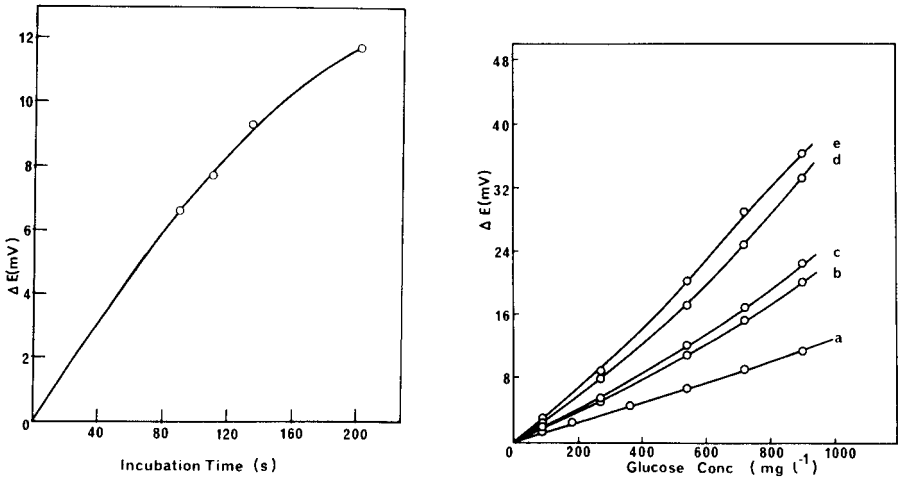

Fig. 5. Effect of incubation time at 30.5°C on the sensitivity of 530 mg l^{-1} glucose measurement at 60 samples per hour, using 4.0×10^{-4} M $S_2O_5^{2-}$, 3.44 I.U. ml^{-1} enzyme and 1.5 M H_2SO_4.

Fig. 6. Glucose calibrations at various enzyme concentrations using 2.0×10^{-4} M $S_2O_5^{2-}$ and 1.5 M H_2SO_4 at a sampling rate of 60 h^{-1}: (a) 1.19; (b) 3.08; (c) 3.44; (d) 4.92; (e) 5.90 I.U. ml^{-1} glucose oxidase.

The effect of enzyme concentration on sensitivity is shown in Fig. 6. Glucose calibration plots were measured by changing the enzyme activity fed into the system. An increase in sensitivity was observed for increasing enzyme activity but, simultaneously, there was a deviation from linearity. Enzyme activity in the range 3—4 I.U. ml^{-1} was subsequently used for the determination of glucose in biological fluids.

Indicator reaction conditions

The effects of acid and bisulphite concentrations were reported previously [17], with the optimum bisulphite concentration being $0.8—1.0 \times 10^{-4}$ M. The influences of bisulphite on the parameters of precision, percentage carry-over, and approach to steady-state potential were investigated; the results are given in Table 1. At 1.0×10^{-4} M bisulphite, 87% of the steady-state potential was observed with a r.s.d. of 0.75% at a sampling rate of 30 per hour. By contrast, with 5.0×10^{-4} M bisulphite, more than 99% of the steady-state potential was obtained with a r.s.d. of 0.40% at a sampling rate of 30 per hour. The sensitivity and response time of the probe were affected by the bisulphite concentration. Improved response times but poorer sensitivity were observed with high bisulphite concentrations.

Recovery and interference studies

Recovery of glucose added to human pooled sera and urine samples was

TABLE 1

Dependence of performance of automatic system for glucose determination on metabisulphite concentration

Conc. of $S_2O_5^{2-}$ ($\times 10^{-4}$ M)	% steady-state at various sampling rates[a]				% R.s.d.[b] at various sampling rates[a]			
	30	60	90	120	30	60	90	120
1.0	87	69	51	45	0.75	4.10	13.00	18.10
2.0	99	90	84	73	0.65	1.40	2.00	3.11
4.0	>99	93	87	79	0.50	0.84	1.30	1.80
5.0	>99	94	89	85	0.40	0.84	1.20	1.60

[a]30—120 samples per hour. [b]Calculated from 6 determinations.

determined by addition of glucose standard spikes to each sample. The samples were introduced into the system at 60 h^{-1} with the sample-to-wash ratio kept at 1:1. Table 2 gives the % recoveries of glucose, showing a range of 95.5—98.8% glucose recovered in the various media used. The recoveries obtained in the serum and urine samples were approximately the same as those obtained in the aqueous samples, indicating the lack of interferences in sera and urine in the method developed.

For interference studies, recovery of glucose from solutions containing various reducing substances (ascorbic acid, cysteine or uric acid) was determined. Table 3 shows the % error obtained for glucose measurements in the presence of these reducing substances. Errors in the range of 1.2—5.9% were obtained, indicating some interference from relatively large concentrations of the reducing agents.

Determination of glucose in albumin solutions

Glucose standards made up in solutions of various concentrations of bovine albumin were determined. Differences of <2% were obtained between the peak potentials for the glucose standards in the concentration range 160—460 mg l^{-1} in aqueous and 4% albumin solutions. Random sampling of glucose standards in 4% albumin solutions at 30 samples per hour

TABLE 2

Recovery of glucose after standard addition to human pooled serum and urine samples

Sample	Glucose added[b] (mg)	Glucose found (mg)	Recovery (%)	Sample	Glucose added[b] (mg)	Glucose found (mg)	Recovery (%)
Serum[a]	0	14.3	—	Urine	0	2.1	—
	9.0	23.0	96.7		20.0	21.2	95.5
	21.0	35.0	98.6		32.5	34.2	98.8

[a]Sample diluted by 1:5. [b]To a total volume of 25 ml.

TABLE 3

Effect of other reducing substances added to solutions containing glucose

Sample	Reducing substance added	Amount added (mg l^{-1})	Glucose found (mg l^{-1})	Error (%)
Urine	None	—	340	—
	Uric acid	350	320	−5.9
	Cysteine	300	332	−2.4
	Ascorbic acid	350	336	−1.2
Serum[a]	None	—	580	—
	Uric acid	300	547	−5.7
	Cysteine	300	557	−4.0
	Ascorbic acid	350	568	−2.1

[a]Sample diluted 1:5.

TABLE 4

Relative error in random sampling of glucose standards in 4% albumin solution (30 samples per hour, 1.0×10^{-4} M $S_2O_5^{2-}$, 3.44 I.U. ml^{-1} enzyme)

Glucose concentration (mg l^{-1})			Relative error (%)
Taken	Found	Difference	
160	161.7	+1.7	+1.1
245	246.3	+1.3	+0.5
380	374.0	−6.0	−1.6
460	453.8	−6.2	−1.4

gave relative errors in concentration of +0.5 to −1.6%, as shown in Table 4. The relative error was calculated on the basis of a standard glucose calibration in aqueous solution in the above concentration range. Glucose therefore was accurately determined in protein-loaded solutions.

Control studies

The accuracy of the method developed was determined by comparing results obtained for commercial controls with the values quoted by the manufacturer. Table 5 shows the results obtained for the determination of glucose in pre-assayed commercial quality control sera, urine control solutions and cerebrospinal fluid control solutions. Comparison of the results showed that the values obtained by the present method were slightly lower than the values quoted by the manufacturer. Poorer agreement was noted between the present method and the alkaline copper method quoted by the manufacturer for urine analysis. However, linear regression analysis of the results gave a correlation coefficient of 0.9983 ($y = 0.9525x + 1.86$).

TABLE 5

Analysis of commercial quality control sera for glucose

Reference sample	Method[a]	Mean value quoted (mg l^{-1})	Mean value[c] found (mg l^{-1})
Serum control I	Beckman Analyzer	890	900
	BMC Autoflo	910	
	AutoAnalyzer-SMA 12/60	910	
Serum control II	Beckman Analyzer	1940	1850
	AutoAnalyzer-SMA 12/60	1940	
Control for cerebro-spinal fluid analyses	Beckman Analyzer	570	550
Urine control	Alkaline Copper[b]	870	787

[a]Glucose oxidase methods, except for urine. [b]Alkaline copper method used by manufacturer. [c]Mean of 6 replicates with a maximum r.s.d. of 1.1%.

DISCUSSION

The use of the sulphur dioxide probe for the determination of glucose via the oxidation of bisulphite by the hydrogen peroxide produced in the enzymatic reaction gives a rapid and selective determination of glucose in various biological fluids. With this probe, a number of characteristics were found which simplify the method for glucose determination, viz. response times are rapid, a catalyst is not required for the coupling reaction, and comparatively large amounts of reducing substances and proteins do not interfere.

The response time allows samples to be analyzed at a rate of 90 per hour with less than 2% carryover and a precision of ±1.5%, while as little as 10 mg l^{-1} of glucose can be detected. The response time is similar to that of the continuous-flow system proposed by Llenado and Rechnitz [11]. Most of the previous methods mentioned, however, have not been studied in air-segmented, continuous flow systems and a direct comparison therefore is not possible. The most important factor controlling response time in the present analytical procedure is the concentration of bisulphite in the reagent stream. Improved sensitivity was obtained at low bisulphite concentrations but with a simultaneous decrease in the linear range and deterioration in electrode performance. This decline in response time with poor precision occurred because the peroxide oxidised the low bisulphite concentration at the lower limit of the Nernstian range (3.0×10^{-5}—3.0×10^{-2} M), and close to the detection limit of the probe, which is 5.0×10^{-6} M. The use of higher bisulphite concentrations, therefore, permitted faster sampling and better precision but with a marked loss in sensitivity.

A catalyst for the oxidation of bisulphite is not required as in other electrochemical techniques where molybdenum(VI) [10, 11] and peroxidase

[12] have been used to catalyse the oxidation of iodide. This is due to the rapid oxidation of bisulphite by the hydrogen peroxide liberated in the enzymatic reaction.

Large amounts of reducing substances, including cysteine, uric acid and ascorbic acid do not present any serious interference problem in the present system. More than 90% of glucose added to urine and serum samples was recovered in the presence of reducing substances in excess of the concentrations normally occurring. The lack of interference is due to the use of bisulphite as the coupling reagent. It is a stronger reducing agent than the naturally occurring reductants in urine and hence there is little interference with the bisulphite—hydrogen peroxide reaction.

The probe allows the determination of glucose in protein-loaded media without prior protein separation via precipitation or dialysis. Analysis of reference control samples containing both protein and reducing substances gave consistently low results by an average of 5% in comparison to manufacturers' data for other analytical methods. However, the results from the present method fell within the performance limits quoted by the manufacturer for enzymatic methods of analysis.

The sulphur dioxide electrode method proposed, therefore offers a simple and accurate means of monitoring glucose concentration in biological fluids. The technique should be applicable to the enzymatic determination of substrates such as uric acid, cholesterol and amino acids, via the hydrogen peroxide produced in the appropriate enzyme-catalysed reactions.

The authors gratefully acknowledge Miss J. Pickering of the Prince Henry Hospital for serum samples and the assistance from the Commonwealth Scholarship and Fellowship Plan (CSFP) for P.S.

REFERENCES

1 G. G. Guilbault, Handbook of Enzymatic Methods of Analysis, M. Dekker, New York, 1976, p. 264.
2 G. R. Cooper, C.R.C. Crit. Rev. Clin. Lab. Sci., 4 (1973) 101.
3 J. Okuda and I. Miwa, in D. Glick (Ed.), Methods of Biochemical Analysis, Vol. 21, Wiley—Interscience, New York, 1973, p. 155.
4 M. M. Fishman, Anal. Chem., 52 (1980) 185R.
5 G. J. Lubrano and G. G. Guilbault, Anal. Chim. Acta, 97 (1978) 229.
6 J. L. Fromette, B. Froment and D. Thomas, Clin. Chim. Acta, 95 (1979) 249.
7 D. R. Thevenot, R. Sternberg, P. R. Coulet, J. Laurent and D. C. Gautheron, Anal. Chem., 51 (1979) 96.
8 C. M. Wolff and H. A. Mottola, Anal. Chem., 50 (1978) 94.
9 H. V. Malmstadt and H. L. Pardue, Anal. Chem., 33 (1961) 1040.
10 L. Gorton and K. M. Bhatti, Anal. Chim. Acta, 105 (1979) 43.
11 R. A. Llenado and G. A. Rechnitz, Anal. Chem., 45 (1973) 2165.
12 G. Nagy, L. H. von Storp and G. G. Guilbault, Anal. Chim. Acta, 66 (1973) 443.
13 G. G. Moody and J. D. R. Thomas, Analyst, 100 (1975) 609.
14 P. L. Bailey and M. Riley, Analyst, 100 (1975) 145.
15 A. H. Kadish and D. A. Hall, Clin. Chem., 11 (1965) 869.
16 M. Koyama, Y. Sato, M. Aizawa and S. Suzuki, Anal. Chim. Acta, 116 (1980) 307.
17 P. W. Alexander and P. Seegopaul, Anal. Chim. Acta, 121 (1980) 61.
18 G. Toro and P. G. Ackermann, Practical Clinical Chemistry, Little, Brown and Co., Boston, 1975, p. 734.

Analytica Chimica Acta, 125 (1981) 65—72
Elsevier Scientific Publishing Company, Amsterdam — Printed in The Netherlands

A MICROCOMPUTER-BASED SYSTEM FOR POTENTIOMETRIC MEASUREMENTS WITH ION-SELECTIVE ELECTRODES

A. GUSTAVSSON* and P. NYLÉN[a]

The Royal Institute of Technology, Department of Analytical Chemistry, Fack, S-100 44 Stockholm 70 (Sweden)

(Received 15th August 1980)

SUMMARY

A comparison, on completely equal terms, of a microcomputer-based system with manual measurements is described in detail. The main features compared are the precision and accuracy of the results and the number of determinations per time unit. The example used is a standard addition measurement of fluoride in toothpaste. The microcomputer system and its interfacing to the peripheral units are also described. The microcomputer system for control, supervision and evaluation of the measurements results in a significant gain in precision and speed. Accuracy requires the use of a non-theoretical value of the Nernstian slope. The memory effect of the ion-selective electrode is large when the type of sample is changed.

Since the early 1970's there has been an increasing interest in the automation of chemical determinations. In the field of potentiometric titration, the first step was to include computers [1—3], but these were used only for calculating the results, and not for actual control of the measurements. The off-line character and cost of the systems made them valuable only for research. On-line characteristics for titration and standard addition systems were obtained by the use of minicomputers [4—7], which are much cheaper than large computers and make it possible to control and supervise the measurements. Some additional advantages for such systems were obtained by the introduction of microcomputers [8—10], which are again cheaper and easier to integrate with other components because of their electrical and mechanical construction.

The objective of this work was to study the advantages of a microcomputer-based system over manual standard additions, particularly with regard to the precision and accuracy of the results and the number of determinations per time unit. The example used for the comparison is a standard addition determination of fluoride in toothpaste.

---

[a]Present address: University of Stockholm, Institute of Physics, Vanadisvägen 9, S-113 46 Stockholm, Sweden.

THEORY

When it is necessary to eliminate a matrix effect in potentiometric determinations, the standard addition method is often used. A modified Gran-plot method is used to evaluate the measurements in this work.

The Nernst equation, sometimes modified, is valid for ion-selective electrodes. For the use of a fluoride electrode, modification of the equation will yield [3]

$$K[F^-] = 10^{(E'_F - E)/Q}$$

where K is a proportionality constant and $E'_F = E^0_F + m$ (m is an arbitrary constant). E^0_F and E have their usual meaning and Q is the slope of the conventional mV/pF plot [3]. A straight line will be obtained if $(V_0 + V_{ADD})10^{(E'_F - E)/Q}/V_0$ is plotted as a function of V_{ADD}; V_0 is the starting volume and V_{ADD} is the total added volume. The final result of the measurements is obtained as the intersection point of the straight line and the negative part of the V_{ADD} axis.

The value of Q is frequently taken as the theoretical value (predicted by thermodynamic theory), but this is not valid for ion-selective electrodes other than the hydrogen-ion glass electrode. The value of Q lies in the range 56–60 mV for the fluoride electrode investigated. The absolute need for using an experimentally determined (non-theoretical) Q value is often overlooked despite comments by several authors [11]. It is possible to attain high precision but only poor accuracy of the results if an incorrect Q value is used. The equation given by Ivaska [11] is useful for calculation of Q. There are three numerical methods suitable for solving the equation, the bisection, the Newton–Raphson and the secant method [12]. The secant method is best for solving the equation, because it gives four significant decimal digits with only one to four iterations (depending on the starting values). The disadvantages of the other methods are the slow convergence, ($\approx$3.3 iterations per decimal digit) in the bisection method, and the large amount of work needed for calculation of the derivative in the Newton–Raphson method.

EXPERIMENTAL

Hardware

The system used is outlined in Fig. 1. The parts of the system are a burette (Dosimat E412, Metrohm, Herisau), a mV-meter (S1016H, Systemteknik AB, Lidingö, Sweden), a Silent 700 terminal and an Intel 8080 microcomputer system. The reference electrode is of single-junction type (saturated calomel) and the fluoride-selective electrode is an Orion 94-09.

Burette. The additions, in steps of 0.1 ml, are obtained by sending a 0.4-s starting pulse to the burette every 1.0 s. A facility of the burette is that it always stops at 0.1 ml intervals. This start/stop procedure for each addition is preferred to continuous addition, because the time needed by the burette

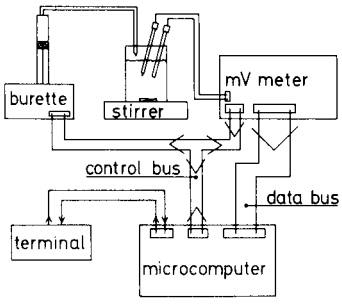

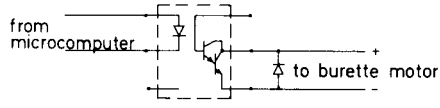

Fig. 1. Diagram of the hardware and data flow of the system.

Fig. 2. An optocoupler used as interface between the microcomputer and the burette motor.

for an addition drifts with time. An optocoupler (H11B2, General Electric) is used to interface the motor in the burette to the microcomputer (Fig. 2). A transient quenching diode is used (Fig. 2) to protect the darlington transistor (in the optocoupler) from being destroyed by transients from the motor.

Millivoltmeter. The output from the meter has TTL levels with positive logic in BCD format and is interfaced directly to a parallel port of the microcomputer. The least significant digit of the mV meter is a tenth of a mV. Via the control bus (Fig. 1), the microcomputer starts/stops the mV meter when reading it, reads the sign of the BCD number and checks if overrange of the meter has occurred.

Microcomputer. The microcomputer system (Fig. 3) is based on Intel 8080 microprocessor and uses three cards in the SBC series, the CPU card SBC 80/10 [13], the memory and I/O expansion card SBC 108 [14] and the arithmetic processing card SBC 310 [15]. A better choice today would be to use the AMC 95/6011 arithmetic processing unit board, which has all the common functions implemented. This gives a memory capacity of 8 kbytes PROM for the system monitor and utility routines and 9 kbytes RAM for system stack, user program and data storage. The microcomputer is equipped with a 3M DCD 1 data cassette drive [16] for program backup and data dump.

The total I/O capacity of the microcomputer is 4 parallel ports (Intel 8255) of three bytes each giving 96 bits in parallel and two ports (Intel 8251) for serial communication. One serial port is used for communication between the microcomputer and the terminal. Of the remaining I/O capacity, only two parallel ports are used. One port is used by the monitor for the data cassette drive communication and the other port for controlling the burette and the mV meter and for collecting data from the mV meter. The controlling function of a parallel port is easily achieved thanks to the flexibility of the 8255 circuit. It is possible to program half of one of the bytes of the port as input and the other half as output, and to set and reset single bits to obtain the control signals.

Software

Exponential routine. All arithmetic calculations are done with 32-bit floating point representation of the numbers. The arithmetic processing card (SBC 310), however, only does the four standard arithmetic operations in floating point format. The program involves exponential terms, so an exponential routine was implemented. The routine uses the equation

$$e^x \approx 2^{p+1}\,[0.5 + Y/(A - Y + BY^2)]$$

where p is the integer closest to $X/\ln 2$, Y is $2(X/\ln 2 - p)$ and in the range $-1 < Y \leqslant 1$, A = 5.7708162 and B = 0.05761803. The accuracy of the routine is at least 28 bits (7 decimal digits).

Program preparation. Without a large computer, programming for a microcomputer would be done by using the microcomputer development system (MDS) supplied by the manufacturer. However, when access to larger computers is available, the use of their storage capacity, system support and calculating speed is beneficial. The program was written in 8080 macro assembly language [17], edited and stored in a large host computer (CDC 6400) using the editor and file handler of the operating system. The program was then converted to machine code using the Intel MAC-80 cross-assembler, which runs as a standard Fortran program with the source code of the application program as its input and the machine code as the output. The program is then loaded into the microcomputer via a RS-232 serial link, and

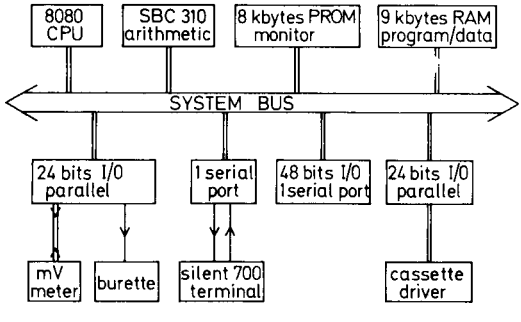

Fig. 3. Architecture of the microcomputer and system interface.

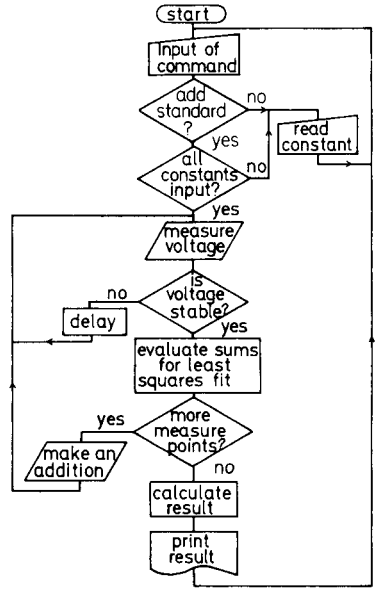

Fig. 4. Flow chart for the standard addition program.

is then directly usable. The benefit of this technique is its better turn-round time, capacity for handling long programs and lower cost, since an MDS is unnecessary.

Program. The program (Fig. 4) needs a memory area of ca. 4.4 kbyte. Before measurements are started, the necessary constants must be input. These constants are: (i) E'_x; (ii) the largest difference between two consecutive voltage measurements before the next addition; (iii) the number of electrons in the Nernst equation with appropriate sign for anions and cations; (iv) the number of points for the least-squares fit; (v) the volume of an addition; (vi) the concentration of the solution added; (vii) the molar weight of the species to be determined (fluoride in this case); (viii) the weight of the sample; (ix) the temperature; (x) the time between two consecutive measurements; (xi) the initial volume of the sample solution. The same constants can be used repeatedly without re-initiation, except for the weight of the sample. The control flag for input of the weight of the sample will be reset during the calculation of the result (Fig. 4). If the flag is reset and a determination started, the weight of the sample will be requested automatically. E'_x must be chosen in the vicinity of the starting value of E to obtain a line of about unit slope in evaluation of the measurements.

The theoretical value of Q was used in the program only to ensure direct comparison with the manual measurements which were made without correction for a non-theoretical value of Q. All timing in the program was done by use of a program loop of 0.1 s duration. The complete program is available from the authors on request.

Chemicals and samples

Distilled water and p.a. grade chemicals were used for making solutions.

The samples were ca. 1-g portions of toothpaste in 100 ml of distilled water. A sodium fluoride solution (32.69×10^{-3} M) were used for standard additions. The buffer used was 0.16 M phosphate pH 7.0 added in 1:1 ratio to the sample solution.

RESULTS AND DISCUSSION

The results are summarized in Table 1. Samples 1—5 contained sodium fluoride and water without and with buffer as indicated. Buffer was added here to stabilize the pH and to simulate the ionic strength of the toothpaste samples. Fluctuating potentials were more pronounced for unbuffered than for buffered samples. The fluctuating behavior of the electrode potential for unbuffered solutions (Table 1) is of course a well-known phenomenon at these low concentrations (0.5 mM sodium fluoride solution); the low standard deviation of the results, despite the fluctuations, is due to the increased time needed for the determination.

Samples 2 and 3 and samples 4 and 5 were taken from different solutions. The correct value for the synthetic samples was 0.09345% and for the tooth-

TABLE 1

Summary of the results

Sample[a]	$\bar{X} \pm s_{\bar{X}}$ (%)[b]	Number of runs	R.s.d. (%)	Error (%)	$\bar{X}$ after correction for slope[c]	Error (%)
1 Without buffer	0.09911 ± 0.00028	15	1.1	6.1		
2 With buffer	0.1028 ± 0.0010	10	3.0	10.0		
3 With buffer*	0.1044 ± 0.0007	10	2.2	11.7	0.09370	0.26
4 With buffer[d]	0.09573 ± 0.00028	4	0.6	2.4	0.09251	−1.0
5 With buffer	0.09729 ± 0.00057	4	1.2	4.1	0.09377	0.35
6 Toothpaste	0.1035 ± 0.0016	11	5.2	15.0		
7 Toothpaste*	0.1049 ± 0.0007	9	2.0	16.6	0.09286	2.0
8 Toothpaste[d]	0.1076 ± 0.0013	33	7.2	19.6		

[a]Samples 1—5 are sodium fluoride solutions containing 0.09345% fluoride. Sample 8 corresponds to manual measurements. Asterisks indicate that temperature correction was applied in the evaluation. [b]$\bar{X}$ is the mean value and $s_{\bar{X}}$ is the standard deviation of the mean. [c]These values are the $\bar{X}$ obtained when measurements are evaluated with a non-theoretical Q. [d]Use of E'_F = 100.0 mV instead of 15.0 mV.

paste ca. 0.09% (ca. 0.2% sodium fluoride) according to the manufacturer. The standard deviation for the manual measurement was 0.0077% and the pooled value for all the microcomputer-controlled measurements was 0.0029%.

To evaluate the fluctuations in the electrode potential under stirred conditions, a meter readable to 0.01 mV (Keithley, 190 Digital Multimeter) was used. Consecutive values (35 each) were measured with the stirrer on and off, for a single sample of ca. 1 g of toothpaste in 100 ml of water with several additions. The mean potentials were 6.36 ± 0.01 mV and 6.68 ± 0.001 mV for stirred and unstirred solutions, respectively. In stirred solution, fluctuations in the potentials of up to 1 mV were occasionally observed; this did not happen in unstirred solutions. A slow drift in the potential caused by gradual changes in the liquid junction potential of the reference electrode was lessened when a double-junction reference electrode was used. The electrode potential (E) spanned the range about +12 mV to −30 mV during a determination. Conditioning the electrode for a new type of solution, e.g. changing from toothpaste samples to unbuffered samples, required soaking for several hours.

Measuring the potential with stirring interrupted and the solution at rest provided a tenfold gain in precision and much more stable potentials compared with measurements in stirred solutions. The difference in the measured potentials in stirred and unstirred solutions (0.32 mV) did not cause difficulties because the stirring rate was constant enough during the measurements.

When temperature correction was applied, the temperature of the sample was measured to within 0.5°C and input for each sample; otherwise, the ambient temperature was measured only at the start of each series of measurements. Such temperature corrections gave results with better preci-

sion, but the error was still high (cf. samples 2/3 and 6/7). Thus the poor accuracy is not caused by using an uncorrected value for the temperature.

Samples 4 and 5 were run to show the need of a correctly chosen value of E'_F; the mean values are statistically different (95% certainty). By using an E'_F in the vicinity of the starting potential of the determination, a result with higher accuracy but lower precision is obtained, in comparison with 100.0 mV. The higher precision obtained with E'_F = 100.0 mV is of course due to the bias added (100.0 mV) to the measured potential value reducing the information content (accuracy) of the value.

An empirically determined value of Q [11] was used in evaluating some of the analyses (Table 1); this correction was done manually. It is clearly seen that this procedure gives results of greatly improved accuracy. Consequently, the main part of the error in the other results shown in Table 1 is due to the use of a theoretical (and incorrect) Q value. Much of the remaining error is due to the rounding error of the mV meter (0.05 mV), and a meter readable to 0.01 mV would give even better accuracy. The errors (2.0%) shown for the toothpaste are probably excessive because the results were compared with the manufacturer's statement of the sodium fluoride content ($\approx$0.2%).

The number of samples measured per unit time was 2—3 times greater with the microcomputer system than with the manual method if no correction for a non-theoretical value of Q was used. When the correction was incorporated in both methods, the time required for each sample with the microcomputer was a quarter of the time required for a manual determination.

Conclusions

Microcomputer-based standard addition systems offer several advantages compared with manual methods: (i) the gain in precision of the results; (ii) the increased speed of analyses; (iii) the decreased labour cost and release of skilled staff from routine work.

The above results show that an experimentally determined value of the slope Q, must be used in evaluating the data. Thermostatting of the sample vessel is not important, but to avoid potential drift the fluoride electrode should be carefully selected and a double-junction reference electrode should be used. The precision of the potential measurement is improved if stirring is interrupted, and could be improved further by using a voltmeter with 0.01 mV resolution.

The authors express their gratitude to Professor Folke Ingman for stimulating discussions and comments relating to the manuscript, to Professor Albin Lagerqvist for the stimulating working conditions and for his keen interest in the development of the microcomputer system, and to the National Swedish Board for Technical Development for providing the funds.

REFERENCES

1 D. Jagner, Anal. Chim. Acta, 50 (1970) 15.
2 M. J. D. Brand and G. A. Rechnitz, Anal. Chem., 42 (1970) 1172.
3 A. Johansson and S. Johansson, Analyst, 104 (1979) 1240 (and references therein).
4 T. Anfält and D. Jagner, Anal. Chim. Acta, 57 (1971) 177.
5 J. W. Frazer, A. M. Kray, W. Selig and R. Lim, Anal. Chem., 47 (1975) 869.
6 J. W. Frazer, W. Selig and L. P. Rigdon, Anal. Chem., 49 (1977) 1250.
7 L. P. Rigdon, G. J. Moody and J. W. Frazer, Anal. Chem., 50 (1978) 465.
8 S. Yamaguchi and T. Kusuyama, Fresenius Z. Anal. Chem., 295 (1979) 256.
9 L. P. Rigdon, C. L. Pomernacki, D. J. Balaban and J. W. Frazer, Anal. Chim. Acta, 112 (1979) 397.
10 D. Betteridge, E. L. Dagless, P. David, D. R. Deans, G. E. Penketh and P. Shawcross, Analyst, 101 (1976) 409.
11 A. Ivaska, Talanta, 27 (1980) 161 (and references therein).
12 G. Dahlqvist and Å. Björk, Numerical Methods, Prentice—Hall, 1974, p. 220.
13 System 80/10 Microcomputer Hardware Manual. Intel, 9800316 B, 1977.
14 i SBC 108 A/116 A Combination Memory and I/O Expansion Boards Hardware Reference Manual. Intel, 9800862-01, 1979.
15 SBC 310 High-speed Mathematics Unit, Hardware Reference Manual. Intel, 9800410 A, 1977.
16 P. Nylén, Monitor Routines for a 3M DCD 1 Cassette Drive, Intel User's Library, Ref. AB 131, 1978.
17 8080 Assembly Language Programming Manual, Intel, 98-004C Rev. C, 1976.

Analytica Chimica Acta, 125 (1981) 73—83
Elsevier Scientific Publishing Company, Amsterdam — Printed in The Netherlands

VOLTAMMETRIC STUDY OF THE ELECTROCHEMICAL REDUCTION OF LUCIGENIN IN AQUEOUS MEDIUM

R. J. MURPHY and G. SVEHLA*

Department of Analytical Chemistry, Queen's University, Belfast (Gt. Britain)

(Received 21st August 1980)

SUMMARY

The electrochemical reduction of lucigenin (bis-N-methylacridinium nitrate) in aqueous solution was studied by d.c. Tast polarography at a dropping mercury electrode, by cyclic voltammetry at an amalgamated gold electrode and at a hanging mercury drop electrode, and by microcoulometry. The effects of pH, lucigenin concentration and temperature were studied, and special methods were applied to study the suspected adsorption and catalytic (regeneration) currents. A spectrophotometric study is also reported. It was found that lucigenin is reduced in two separate one-electron steps. An adsorption pre-wave accompanies the first step, while the second, below pH 3.5, is catalytic, owing to the chemical regeneration of the intermediate reduction product at the electrode surface.

Chemiluminescence involving non-biological compounds was first discovered in the latter part of the 19th century. The chemiluminescence of lucigenin was reported in 1935 by Gleu and Petsch [1] who observed a blue-green chemiluminescence during the alkaline oxidation of lucigenin with hydrogen peroxide. Totter and Philbrook [2, 3] suggested that the emitting substance was N-methylacridone and briefly discussed the electrochemical reduction of lucigenin at the dropping mercury electrode (DME) in aqueous solution. The chemiluminescent reaction is greatly influenced by catalysts and inhibitors and this forms the basis of many analytical applications [4, 5]. The mechanisms of these catalytic reactions have been investigated [6, 7]. Some work has been reported on the electrochemistry of lucigenin. Voltammetric studies [8, 9] in aqueous dimethylsulphoxide (DMSO) mixtures have suggested a two-electron irreversible reduction to dimethylbiacridine; this takes place in two consecutive one-electron steps. For comparison, polarograms were run in aqueous solutions at pH 8 only, and the behaviour was reported to be similar to that in DMSO. According to the present findings, however, the reduction phenomena are much more complex than have been suggested; it was decided therefore to undertake a systematic study of the electrochemical reduction of lucigenin in aqueous medium.

EXPERIMENTAL

Reagents

Commercial preparations of lucigenin (bis-N-methylacridinium nitrate, >97% pure, Aldrich Chemical Co. Ltd.) were used for this study; aqueous 2×10^{-3} mol l^{-1} solutions were prepared daily and the appropriate dilutions made for each experiment, incorporating the required concentration of supporting electrolyte.

All supporting electrolytes, buffer solutions and maximum suppressors were prepared from analytical-grade reagents. Oxygen-free nitrogen was used for deaeration.

Apparatus

All polarographic measurements were done with a Polariter PO4 polarograph (Radiometer, Copenhagen) with the E65 dropping mercury electrode (DME) and drop-life timer and current sampler unit DLTI. The DME had the following characteristics: outflow velocity $m = 3.12$ mg s^{-1}; drop lifetime $t = 0.8$ s unless otherwise stated; height of mercury column $h = 60$ cm. The reference electrode was a saturated calomel electrode.

An instrument, similar in design to that described by Bezman and McKinney [10], was built and used in conjunction with a Hewlett-Packard 3310B function generator for cyclic voltammetric studies. A Hewlett-Packard 7035B X-Y recorder was used to record the cyclic voltammograms at low scan rates and a Hewlett-Packard 1201B storage oscilloscope at fast scan rates. A three-electrode, single-compartment cell (Metrohm) was fitted with a platinum foil auxiliary electrode, a saturated calomel reference electrode, and a micrometer-type hanging mercury drop electrode. In some instances the hanging mercury drop electrode was replaced with an amalgamated gold pin electrode.

For microcoulometric experiments a Manousek cell was used in conjunction with the PO4 polarograph. pH measurements were carried out with a Philips PW9414 pH meter with a combined glass/reference electrode. Visible and u.v. spectra were recorded using a Unicam SP8000 recording spectrophotometer.

Procedures

For polarography, an appropriate volume of lucigenin solution (2×10^{-3} mol l^{-1}) was mixed with the supporting electrolyte and a few drops of 0.4% Triton X-100, and diluted to 50 ml with distilled water; 20-ml aliquots of the solutions were deaerated with a stream of nitrogen for 10 min. Polarograms were recorded at the slowest possible speed (100 mV min^{-1}) with minimum damping and 85% blanking of the drop life to minimise the condenser current. Each wave was studied individually and the pH measured before and after the polarographic experiments. The polarograms were evaluated by the point method [11] for both the half-wave potential and the limiting current.

The cyclic voltammetric experiments were carried out with electrolytes similar to those used for polarography. At slow scan rates the voltammograms were recorded with the X-Y recorder. At fast scan rates the voltammograms were either photographed or visually examined on the oscilloscope using the "store" facility.

Microcoulometric experiments were carried out on 1-ml solutions, which contained initially $1—4 \times 10^{-4}$ mol l^{-1} of lucigenin in the supporting electrolyte. The solution was placed in the Manousek cell and the capillary was positioned in such a way that its tip was just below the surface of the solution. The deaerated solution was kept under a nitrogen atmosphere and mixed at intervals by a stream of nitrogen. The experiments were carried out at pH 4 and 9 for each of the three waves and the decrease in limiting current was obtained from a continuous recording during electrolysis and from polarograms recorded every 30 min under the same conditions. The electrolysis was carried out at a constant potential corresponding to the limiting diffusion current. After 20—25% conversion, the electrolysis was discontinued and the solution replaced with the pure supporting electrolyte to measure the residual current. After correction for the residual current, the results were evaluated by Gilbert and Rideal's logarithmic method [12].

Instantaneous current—time curves were recorded at intervals over the range 0 to −1.8 V to check for adsorption phenomena. Electrocapillary curves were then obtained by plotting the drop lifetime against the applied potential, both for lucigenin and for the supporting electrolyte alone. From the electrocapillary curves, appropriate potential values were selected, covering both distorted and undistorted regions, at which the current—time curves were measured. These curves were evaluated according to the guidelines given by Heyrovsky and Kuta [13].

The effects of pH and concentration on the u.v. and visible spectra of lucigenin were investigated. The buffer solution, adjusted to the appropriate concentration and pH, was used as a reference. All spectra were recorded at the slowest scan speed. The spectra of lucigenin were also recorded before and after electrolysis at the potentials and under the conditions of the microcoulometric experiments already described.

RESULTS

Polarography

The polarographic behaviour of lucigenin was investigated within the widest possible pH and concentration ranges for each wave. Two well-defined waves and a double wave were obtained. Wave I formed at $E_{1/2}$ = −0.19 V with, under certain conditions, a small post-wave at $E_{1/2}$ = −0.26 V. Above 10^{-4} mol l^{-1} a second, double wave appeared at $E_{1/2}$ = −0.44 V (Fig. 1). This was enumerated as wave II as the half-wave potentials of the two component waves were so close together that exact measurements of each wave were not possible under the conditions employed. Wave III formed at $E_{1/2}$ = −1.50 V; it was thought to be a catalytic wave (see below).

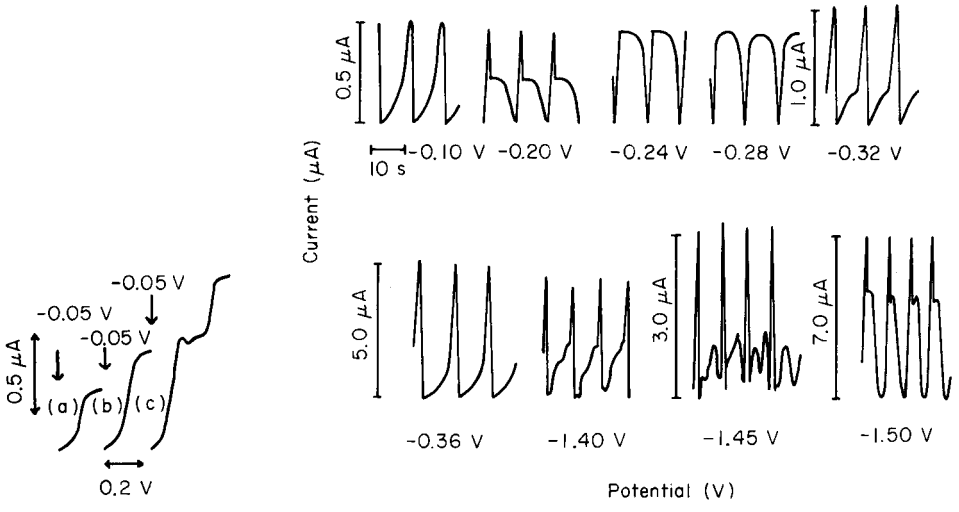

Fig. 1. Polarograms of (a) 5×10^{-5}, (b) 10^{-4}, (c) 2×10^{-4} mol l^{-1} lucigenin in 0.1 mol l^{-1} acetate buffer, pH 5.0.

Fig. 2. Instantaneous current—time curves of 1.4×10^{-3} mol l^{-1} lucigenin in 0.2 mol l^{-1} KCl/HCl, pH 4.24, at different DME potentials.

Current measurements were taken for each wave at various mercury column heights and the currents plotted as a function of the square root of the corrected height to test for diffusion control. This was carried out at several pH values and concentrations. The plot for wave I was curved, which was to be expected as it will be shown later that this wave is an adsorption pre-wave to wave II. Waves II and III both gave straight line plots indicating diffusion control.

The shape of the instantaneous current—time curves were studied for the three waves at various pH values and concentrations (Fig. 2). The curves are distorted in the region of the half-wave potential of wave I (—0.2 V) indicating an adsorption wave. Distortions also occurred at the half-wave potential of the double wave (wave II). The curves at —1.50 V associated with wave III were distorted in a peculiar way; this phenomenon would merit more detailed study.

Further evidence of adsorption was obtained by examination of the electrocapillary curves. The average drop lifetime was plotted as a function of the potential of the DME at different pH values and concentrations for lucigenin and also for the supporting electrolyte alone. A characteristic incision occurred between —0.20 and —0.40 V in the presence of the depolariser, whereas the curve was smooth at these potentials in its absence (Fig. 3).

Polarograms were obtained at different lucigenin concentrations and the wave heights plotted against concentration. Wave I gave a typical adsorption

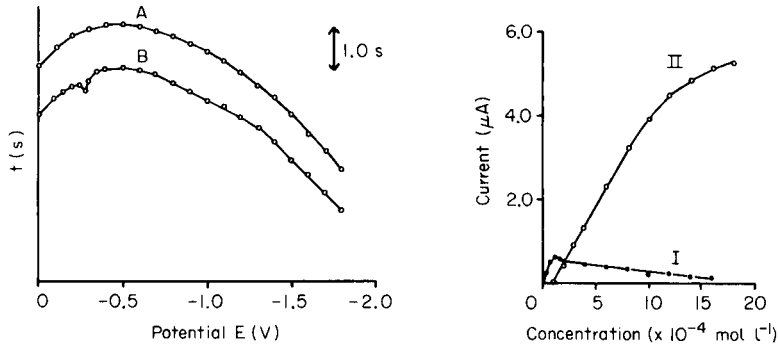

Fig. 3. Electrocapillary curves of mercury in 0.2 mol l^{-1} KCl/HCl, pH 4.06, in (A) the absence, and (B) the presence, of 8×10^{-4} mol l^{-1} lucigenin.

Fig. 4. Current—concentration plot for waves I and II of lucigenin.

plot (Fig. 4). The current measurements for wave II were for the total wave. Up to 10^{-3} mol l^{-1}, wave II alone increases linearly with concentration (Fig. 4). Its intercept with the concentration axis coincides with that concentration where wave I becomes fully developed. As a consequence the sum of the heights of waves I and II shows good linear proportionality with concentration up to 10^{-3} mol l^{-1}. This supports the view that wave I is an adsorption pre-wave to wave II. The plot for wave III shows two distinct linear portions, one up to 10^{-3} mol l^{-1}, above which the slope is greater (Fig. 5). The effect of concentration on the half-wave potentials was also studied. The half-wave potential of wave I moves linearly from —0.19 V to less negative potentials with increasing lucigenin concentration, reaching —0.14 V at 1.6×10^{-3} mol l^{-1}. The half-wave potential of wave II shifts from —0.44 V at 10^{-4} mol l^{-1} to —0.36 V at 3×10^{-4} mol l^{-1} but then remains constant at higher concentrations. The half-wave potential of wave III rapidly moves to more negative potentials with concentration changes up to 10^{-3} mol l^{-1} but changes only slightly above this concentration.

The effect of temperature on the wave heights and half-wave potentials of the three waves was studied at different pH values and lucigenin concentrations. The height of wave I was independent of temperature except for a slight decrease above 60°C. A post-wave formed at about 35°C and gradually increased in size with temperature. The half-wave potential of wave I shifted rapidly to less negative potentials up to 40°C and then remained constant over the next 20°C. The post-wave moved linearly to less negative potentials up to the highest temperature of 74°C. The effect of temperature on wave II was examined for the total wave and for each of the two component waves. The temperature—wave height plots are shown in Fig. 6. The half-wave potentials of these waves move to less negative potentials with increase in temperature. The height of wave III increased rapidly and almost linearly with temperature (Fig. 6) and the half-wave potential also shifted linearly to

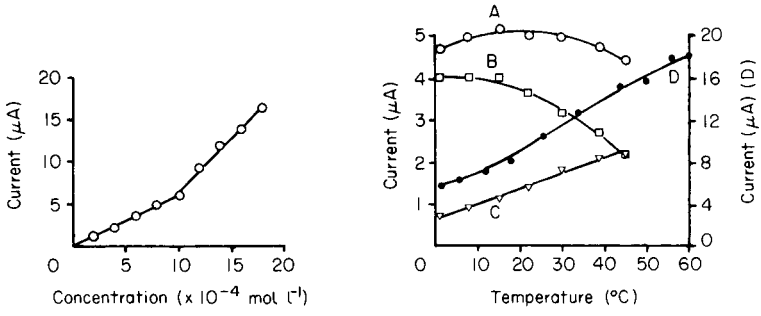

Fig. 5. Current—concentration plot for wave III of lucigenin.

Fig. 6. Temperature dependence of the height of wave II for 1.4×10^{-3} mol l^{-1} lucigenin at pH 9.0 in 0.1 mol l^{-1} KCl/0.05 mol l^{-1} boric acid/NaOH: (A) total wave; (B) main wave; (C) prewave. (D) Temperature dependence for wave III at pH 3.96 in 0.1 mol l^{-1} KCl/0.05 mol l^{-1} boric acid/HCl.

less negative potentials. Polarograms were obtained for 2×10^{-4}—1.8×10^{-3} mol l^{-1} lucigenin at different temperatures; the current—concentration plots obtained from these results are shown in Fig. 7. When evaluating these curves, one has to keep in mind the complexity of the phenomena involved. Theoretically, the height of adsorption waves should decrease, while those of diffusion waves should increase with temperature, provided that the surface area of the electrode is kept constant. This, however, is not the case in experiments where the drop lifetime is the same, as at higher temperatures the volume and therefore the surface area of the mercury drop increase. This is why the adsorption wave does not show the predicted behaviour, though at higher temperatures the decrease is clearly observable. The increase in electrode area and in diffusion rates do together cause the initial slight increase of wave height with temperature in the case of a diffusion wave (Fig. 6). The very fast increase of wave III with temperature does, however, indicate the catalytic nature of the wave.

The effect of pH on the half-wave potentials of the three waves was investigated in detail, as this can provide valuable information on the acid-base equilibria in which the oxidised and reduced species are involved. The half-wave potentials of waves I and II are unchanged throughout the pH range. The half-wave potential of wave III shifted to more negative potentials below pH 3.0 and to less negative potentials above pH 12.75. The half-wave potential—pH plot is shown in Fig. 8. From the theoretical point of view the slopes of this plot are more important than the actual values of the half-wave potential and the expected values are simple multiples of the Nernstian constant of 60 mV pH^{-1} with factors of 0 and 1, i.e., 0 and 60 mV pH^{-1}. The lines in Fig. 8 were drawn with slopes corresponding to the appropriate expected value and are not necessarily the best lines through the experimental points. The effect of pH on the wave heights of the three waves was

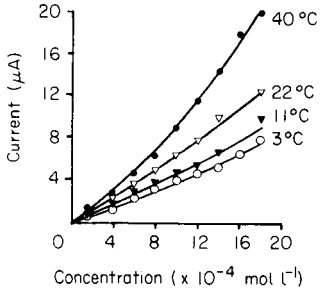

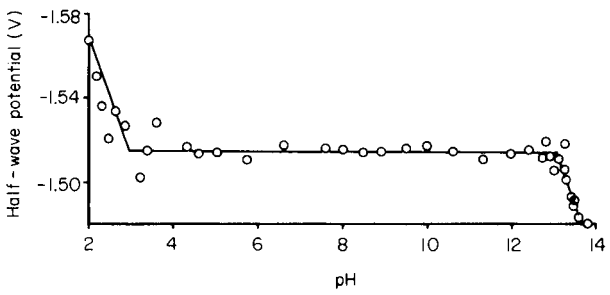

Fig. 7. Effect of temperature on the current—concentration curves for wave III in 0.1 mol l^{-1} KCl/0.05 mol l^{-1} boric acid/NaOH, pH 9.0.

Fig. 8. Effect of pH on the half-wave potential of wave III for 8×10^{-4} mol l^{-1} lucigenin.

also examined: waves I and II were found to be unaffected by change in pH.

The height of wave III was independent of pH down to pH 3.5. Between pH 3.5 and 3.0 there was a slight decrease of wave height, but below pH 3 the height started to increase rapidly, reaching about three times the original height at pH 2. At this stage, however, the decomposition of the supporting electrolyte began to affect the results, as it became increasingly difficult to separate wave III from the current originating from the decomposition of the supporting electrolyte (Fig. 9). Differential pulse polarography [14] indicated, however, that the increase in the wave height continues below pH 2. The significance of this effect will be discussed below.

All three waves were subjected to logarithmic analysis throughout the concentration and pH ranges. Wave I gave curved log $[i/(i_d - i)]$ vs. E plots, suggesting a quasi-reversible wave [15]. The slopes of similar plots for wave II increased initially with concentration from 20 mV to 42 mV, then decreased and levelled out from 7×10^{-4} mol l^{-1} at a value of 30 mV corresponding to $\alpha n = 2$. Microcoulometric experiments indicated a value of $n = 1$ for this wave. Wave III was found to be reversible except at high concentrations and low pH values, and the slope of the log $[i/(i_d - i)]$ vs. E plots gave a value for n of 1. This value is supported by the microcoulometric results for wave III.

Microcoulometry

Microcoulometric experiments were carried out in order to find the number of electrons taken up by a single molecule of lucigenin. Each wave was examined separately in acidic and alkaline media. The results were obtained by continuous recording of the current, with polarograms recorded at the beginning and end of electrolysis; and in different experiments by polarograms recorded at intervals during the electrolysis. The period of electrolysis was usually 240 min. The results were evaluated from the slope of the log i_1 vs. time plot using the Gilbert and Rideal equation [12]. Ultra-

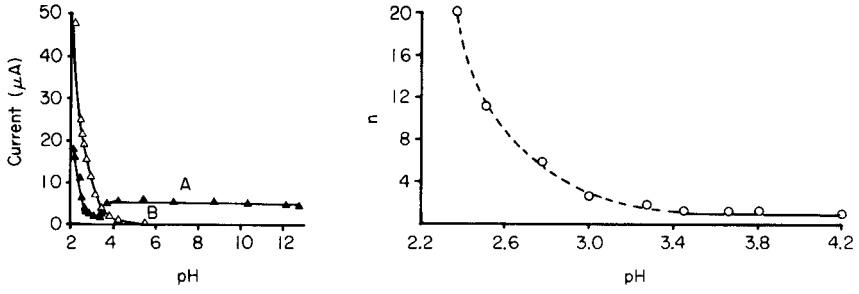

Fig. 9. Effect of pH on the height of wave III for 8×10^{-4} mol l^{-1} lucigenin in 0.1 mol l^{-1} KCl/0.05 mol l^{-1} boric acid: (A) lucigenin wave; (B) hydrogen wave.

Fig. 10. Variation of n with pH (0.1 mol l^{-1} KCl/0.05 mol l^{-1} boric acid buffer).

violet and visible spectra of the solutions were recorded before and after electrolysis.

Wave I, the adsorption prewave, was unchanged after electrolysis. Measurements for wave II were made on the total wave and gave values for n between 0.74 and 1.36. Wave III was examined at pH 4, 6, 8, 9 and 11, and in small pH increments between pH 2 and 4. By measuring polarograms recorded at intervals during the electrolysis, values of n for wave III were found in the range 0.95—1.36 for pH 3.5—11. These results would indicate an overall 2-electron reduction of lucigenin in this pH range. Below pH 3.5 the microcoulometric results for wave III are startling; the observed n values rise gradually (Fig. 10). The decomposition of the supporting electrolyte made it difficult to determine this value precisely, but values as high as 36 were observed at pH 2.2. This is strong evidence for the suggestion that wave III is a catalytic wave.

Cyclic voltammetry

Cyclic voltammetry was used to determine whether the reduction of lucigenin was reversible or not. Measurements were made at different pH values and concentrations in an aqueous medium. At concentrations below 10^{-4} mol l^{-1} only two peaks were observed, at —0.3 V and —1.7 V; above this concentration a third peak appeared at —0.5 V (Fig. 11A). When the frequency was reduced to 0.05 Hz, the peak at —0.5 V split to give two separate peaks (Fig. 11B). The peak potentials (E_p) are —0.44 V and —0.47 V, respectively, which confirms that wave II, found in d.c. polarography, is a double wave, but also illustrates the difficulty of resolving the two component waves. The effect of frequency (ν) on all three peaks was examined throughout the concentration range 10^{-5}—1.28×10^{-3} mol l^{-1} at different pH values; the frequency was varied between 0.1 and 50 Hz. Theoretically, there should be a $30/\alpha n$ mV cathodic shift in the E_p values for every 10-fold increase in the scan rate. This criterion was examined, and the variation of E_p/ν values with frequency was studied. The cathodic and anodic peak separation ($E_{pc} - E_{pa}$)

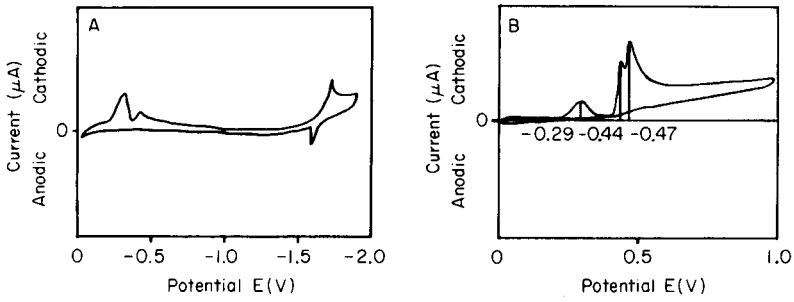

Fig. 11. Cyclic voltammograms of 1.28×10^{-3} mol l^{-1} lucigenin in 0.2 mol l^{-1} KCl/HCl, pH 3.0: (A) range 500 μA, frequency 5.0 Hz; (B) range 20 μA, frequency 0.05 Hz.

as well as the distance between the peak and half-peak potentials ($E_p - E_{p1/2}$) were also used to test reversibility. The cathodic peaks at −0.3 V and −0.5 V were found to originate from irreversible charge transfer through the whole frequency range; the process with the cathodic peak of −1.7 V was reversible or quasi-reversible, depending on frequency and lucigenin concentration [15].

Spectrophotometry

The effects of concentration and pH on the spectrum of lucigenin were studied. Typical u.v. and visible spectra are shown in Fig. 12. Very strong absorption occurs in the ultraviolet with a peak at 261 nm (molar absorptivity ϵ = 18425 l mol^{-1} cm^{-1}); further peaks appear at 352 nm (ϵ = 1810), 369 nm (ϵ = 3825) and 428 nm (ϵ = 1050 l mol^{-1} cm^{-1}), with shoulders at 335, 401 and 452 nm. Beer's law is valid at all the wavelengths corresponding to the absorption peaks; there is no variation in the molar absorptivities

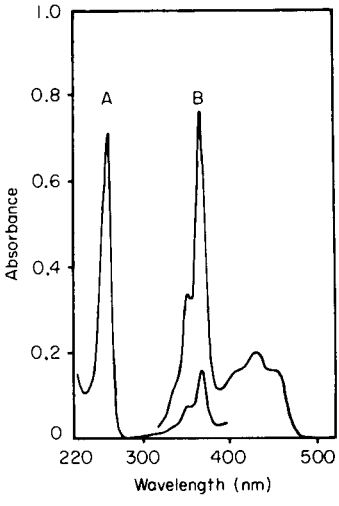

Fig. 12. Visible—u.v. spectrum of (A) 4×10^{-6} mol l^{-1} lucigenin pH 5.0; (B) 2×10^{-5} mol l^{-1} lucigenin pH 5.0.

between pH 5 and 9, and essentially no change between pH 0.7 and 13.0. Below pH 0.7 and especially above 13.0, decomposition occurs, a precipitate forms, and the molar absorptivities decrease considerably.

DISCUSSION

This section deals with characterisation of the polarographic waves, the behaviour of wave III at low pH values, and the mechanism of the electrochemical reduction of lucigenin in aqueous solution.

Wave I was shown to be an adsorption pre-wave to wave II. This was illustrated by the fact that the sum of the limiting currents of the two waves shows a good linear variation with concentration up to 10^{-3} mol l^{-1}. Wave II is a double wave with the half-wave potentials very close together. This was confirmed by cyclic voltammetry which also showed wave II to be irreversible. One electron is taken up in this reduction step. In the pH range 3.5—13.75, the results indicate that wave III is a reversible diffusion wave corresponding to a one-electron reduction. In this pH range the reduction of lucigenin therefore takes place through two consecutive one-electron steps. This supports the work already reported [8, 9] although a reversible cathodic reduction at −1.50 V was not mentioned earlier. The half-wave potentials of waves I and II were pH-independent but wave III was only independent of pH between pH 2.75 and 13.0. Below pH 2.75 the slope of the half-wave potential vs. pH plot was 60 mV pH^{-1} and above pH 13.0 it was −60 mV pH^{-1}. As shown experimentally the height of wave III is independent of pH down to pH 3.5. Below this value the wave height initially decreases, then increases from 5 μA at pH 3.5 to 18 μA at pH 2 for a 10^{-3} mol l^{-1} lucigenin solution. The latter figure represents a net wave height (obtained as the difference between measured currents for sample and blank), and therefore its precision is limited. While the experimental results indicate that this wave is diffusion-controlled above pH 3.5, diffusion cannot account for the increase in current below this pH.

Above pH 3.5 the experimental facts are consistent with the following reduction mechanism

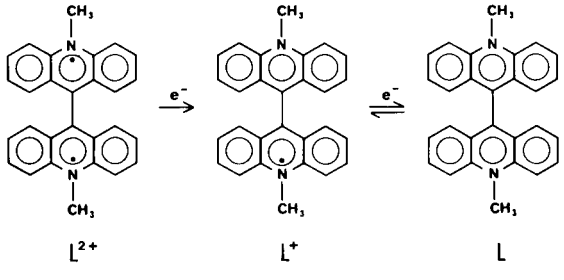

First the lucigenin cation L^{2+} takes up a single electron to form an intermediate monocation L^{+}, and then the uptake of a second electron produces dimethylbiacridone, L; the second reaction is reversible.

The increase in the limiting current of wave III at low pH values is most probably due to a catalytic regeneration wave. The reduction product dimethylbiacridone is capable of taking up a proton in an equilibrium reaction, $L + H^+ \rightleftharpoons LH^+$, followed by the regeneration of L^+ and the evolution of hydrogen gas, $LH^+ \rightarrow L^+ + \frac{1}{2}H_2$. Thus, further molecules of L^+, not supplied by diffusion, become available for reduction at the electrode surface, allowing an increased current to flow. The wave height increases with decreasing pH below pH 3.0. The gradual increase of the apparent number of electrons per molecule of lucigenin, involved in the reduction (cf. Fig. 10) demonstrates beyond doubt the equilibrium nature of the protonation reaction. The unusually large number of electrons obtained in the microcoulometric experiments shows that the current is catalytic, leading to the regeneration of the intermediate oxidised species, L^+. As stated earlier, the variation of the wave height with temperature agrees well with this supposition.

We thank Mr. F. McManus for helping in the cyclic voltammetric work. R. J. M. acknowledges financial assistance from the Department of Agriculture for Northern Ireland.

REFERENCES

1 K. Gleu and W. Petsch, Angew. Chem., 48 (1935) 57.
2 J. R. Totter, Photochem. Photobiol., 3 (1964) 231.
3 J. R. Totter and G. E. Philbrook, Photochem. Photobiol., 5 (1966) 177.
4 U. Isacsson and G. Wettermark, Anal. Chim. Acta, 68 (1974) 339.
5 L. I. Dubovenko, A. M. Guta, V. G. Drokov and A. P. Toomasyan, Org. Reagenty Anal. Khim, Tezisy Dokl. Vses Konf. 4th, 2 (1976) 82.
6 I. Nikokavouras, A. Vavayannis and G. Vassilopoulos, J. Prakt. Chem., 320 (1978) 43.
7 K. Maeda, T. Kashiwabara and M. Toluyama, Bull. Chem. Soc. Jpn., 50 (1977) 473.
8 K. D. Legg and D. W. Shive, Anal. Chem., 41 (1969) 1560.
9 S. Wada, K. Maeda and K. Nakada, Nippon Kagahu Kaishi, 5 (1977) 639.
10 R. Bezman and P. S. McKinney, Anal. Chem., 41 (1969) 1560.
11 H. H. Willard, L. L. Merritt, Jr. and J. A. Dean, Instrumental Methods of Analysis, 4th edn., Van Nostrand, New York, 1965, p. 692.
12 G. A. Gilbert and E. K. Rideal, Trans. Faraday Soc., 47 (1951) 369.
13 J. Heyrovsky and J. Kuta, Principles of Polarography, Czechoslovak Academy of Sciences, Prague, Academic Press, New York, 1966, pp. 311, 214.
14 R. J. Murphy and G. Svehla, Anal. Chim. Acta, to be published.
15 F. McManus, private communication, 1979.

Analytica Chimica Acta, 125 (1981) 85—91
Elsevier Scientific Publishing Company, Amsterdam — Printed in The Netherlands

COMPARISON BETWEEN A DIFFERENTIAL AMPEROMETRIC DETECTOR IN THE REDUCTIVE MODE AND A U.V. DETECTOR IN HIGH-PERFORMANCE LIQUID CHROMATOGRAPHY WITH VITAMIN K3 AS TEST COMPOUND

K. BRUNT*[a], C. H. P. BRUINS and D. A. DOORNBOS

Laboratory for Pharmaceutical and Analytical Chemistry, State University of Groningen, 9713 AW Groningen (The Netherlands)

(Received 15th September 1980)

SUMMARY

The amperometric detector is superior to the u.v. detector in terms of the limit of detection (less than 0.5 ng) and true linearity of response when vitamin K3 (menadione) is used as the test compound with a reversed-phase column. However, the high uncompensated resistance between the reference and working electrodes caused by the low conductivity of the mobile phase, restricts the upper limit of the linear range of the differential amperometric detector to about 200 ng of menadione.

Although many detectors for high-performance liquid chromatography (h.p.l.c.) are available [1], detector performance remains a bottleneck in h.p.l.c. Optical detectors currently dominate the field but interest in electrochemical detectors, especially amperometric detectors, is growing. Most investigators apply amperometric detectors in the oxidative rather than the reductive mode, because in the reductive mode reduction of dissolved oxygen, traces of metal ions and hydrogen ions can cause high background currents [2]. Teflon tubing is very permeable to oxygen, and therefore must be replaced by stainless steel tubing [3, 4]; but to minimize leaching of traces of electroactive metals, stainless steel components should be avoided and teflon or teflon-lined stainless steel tubing with a glass column used wherever possible [3, 4]. In order to compromise between entry of oxygen and entry of traces of metal ions into the system, some investigators have placed part or all the chromatographic system in a perspex or glass box purged with nitrogen or argon [3, 5]. Obviously this does nothing to improve the simplicity or ease of operation of the chromatographic system.

Most investigators who have applied amperometric detection in the reductive mode, have used some kind of mercury electrode because of its extended cathodic potential range. Detectors with a dropping mercury electrode [6—8], a hanging mercury drop electrode [9], a mercury pool

[a]Present address: Proefstation voor Aardappelverwerking-TNO, Rouaanstraat 27, 9723 CC Groningen, The Netherlands.

electrode [10] or a mercury-plated electrode [3, 5, 11] have been described. Very few investigators have used graphite electrodes in amperometric detector flow cells in the reductive mode [4, 12].

A differential amperometric detector [13, 14] is very suitable in principle for operating in the reductive mode because it provides continuous compensation even for high background currents. Accordingly, no special precautions are required to prevent oxygen from dissolving in the mobile phase, provided that the solution does not degas in the detector flow cell.

In this paper a comparison is made between the performances of the differential amperometric detector with glassy carbon electrodes in the reductive mode and a commercial u.v. detector. With the electrochemical detector, no special precautions were taken, and the simplicity and ease of operation of the chromatographic system were retained. As the test compound 2-methyl-1,4-naphthoquinone (menadione, vitamin K3) was chosen for two reasons: menadione has a high molar absorptivity (17200 l mol^{-1} cm^{-1}, at 250 nm) [15] and it is also easily reducible [16, 17].

EXPERIMENTAL

Apparatus

The liquid chromatograph was constructed from individual components. A high-pressure Spectra-Physics pump (model 740) and a low-pressure FMI laboratory pump (model RP-154) were used. Samples were injected by a Rheodyne valve (model 70-10) with a 20-μl sample loop.

The differential amperometric detector was home-made to the previous design [13] with a minor alteration in the electronics: to prevent the output voltage of the current-to-voltage converters reaching the limit of their supply voltage (saturation) when high background currents had to be compensated, the amplifier gain was decreased by a factor of 10 by changing the value of the feedback resistor from 10 MΩ to 1 MΩ. In consequence, the time constant of the damping circuit decreased by a factor of 10 from 4.7 s to 0.47 s. This will be a change for the better as regards deformation of the chromatographic peak by the detector electronics [1]. The Kel-F flow cell with a 51-μm spacer [14] was used. All potentials were measured with respect to a saturated calomel reference electrode. The cell impedances were measured at 70 Hz with a Radiometer conductivity meter (type CDM-2). The u.v. detector used, was a fixed wavelength (254 nm) Chromatronix u.v. detector (model 220).

A Texas Instruments TI-52 pocket calculator was used for the fitting calculations (programs ST 1-08 and ST 1-09).

Chemicals

All chemicals were of analytical-reagent grade (Merck) and were used without further purification.

The menadione (2-methyl-1,4-naphthoquinone) was obtained from Hoffman-La Roche.

The composition of the mobile phase was methanol—water—1.0 M aqueous acetic acid (60 + 30 + 10) adjusted to pH 5.5 with pellets of sodium hydroxide. The stationary phase was a Nucleosil RP-8 (5-μm particles) column (15 cm long, 4.6 mm internal diameter).

RESULTS AND DISCUSSION

Figure 1 shows the steady-state voltammetric wave of a 50-ng menadione sample. An excellent linear relationship existed between the amount of menadione introduced in 20-μl samples and the detector response over the range 0—200 ng of menadione (0—380 nA) when the potential of the working electrodes was held at −275 mV vs. SCE and the flow rate was 0.8 ml min^{-1}. Because of the high content of methanol in the eluent, the uncompensated resistance between the working electrode and the reference electrode in both thin-layer flow cells was rather high (about 80 kΩ). This resulted in a considerable voltage drop in the sample cell of the differential amperometric detector during the passage of large menadione samples and thus restricted the upper limit of the linear dynamic range. Gradually increasing curvature of the calibration was observed above 200 ng of menadione.

A disadvantage of the differential amperometric detector was that after a few days of operation, the vitreous carbon electrodes became plated with a thin metal film because of the reduction of metals leached from the stainless steel tubing and the pump. This metal film could be removed by electrochemical dissolution in a 0.1 M nitric acid solution at +1.0 V vs. a platinum electrode.

In principle, the problems of this electrode contamination and of the restricted upper limit of the linear dynamic range caused by the high uncompensated resistance could be solved by using a mobile phase which contained ethanol instead of methanol and to which some disodium-EDTA had been added. The mobile phase must contain less organic solvent if menadione is to be eluted with the more hydrophobic ethanol. In consequence, the uncompensated resistance will decrease considerably. The presence of disodium-EDTA in the mobile phase will suppress the high background

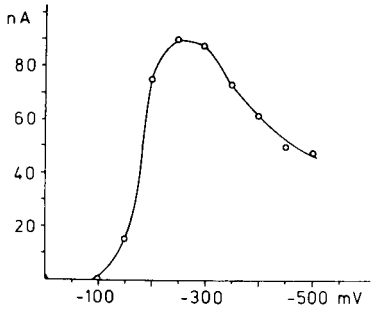

Fig. 1. Steady-state voltammetric wave of 50 ng of menadione (20 μl samples).

currents by chelating the metals leached from the stainless steel tubing and so shifting the reduction waves corresponding to the metals to more negative potentials. Some very promising results were obtained by using a mobile phase composed of ethanol—water—0.1 M aqueous acetic acid (45 + 45 + 10) adjusted to pH 5.5 to which 0.5 g l^{-1} EDTA was added. The uncompensated resistance decreased to about 25 kΩ and the upper limit of the linear dynamic range shifted to about 900 ng of menadione. However, the viscosity of a water—ethanol mixture (55 + 45) is considerable and caused insuperable problems with the standard flow restrictor of the Spectra-Physics pump used. Therefore in further experiments the methanol—water mobile phase was used again. Unfortunately, the disodium-EDTA was almost entirely insoluble in this mobile phase.

An ideal detector is one with an output that can be described over a very wide range by the expression $p = q\ c$, in which p is the detector response, q is the detector sensitivity and c is the concentration of the compound of interest. Because of the imperfections of its mechanical and electrical parts, no detector is truly linear. Fowlis and Scott [18] suggested the power function $p = q\ c^{\alpha}$ to describe the output of detectors which are approximately linear. For a truly linear detector, the response index α is one and the proximity of α to unity indicates the extent to which the detector response approaches true linearity; the response can be called linear if $0.98 < \alpha < 1.02$ [18]. By means of two curve-fitting programs, the responses of the differential amperometric detector were fitted to the expressions $p = q\ c$ and $p = q\ c^{\alpha}$; the results are presented in Table 1. Clearly, the upper limit of the linear dynamic range for this detector was about 200 ng of menadione; the lower limit was less than 0.5 ng of menadione (Fig. 2).

The same analysis and calculations were made for the u.v. detector. The results are shown in Fig. 3 and in Table 2. For the u.v. detector the lower

TABLE 1

Results of the linear curve-fitting and power curve-fitting calculations of the response of the differential amperometric detector as a function of the concentration of menadione

Sample range for menadione (ng)	Linear curve fitting[a]		Power curve fitting	
	$i = a\ c + b$	r^2	$i = d\ c^{\alpha}$	r^2
0.5—100	$i = 1.95c - 0.98$	0.9992	$i = 1.99c^{0.98}$	0.9989
0.5—120	$i = 1.95c - 0.97$	0.9995	$i = 1.98c^{0.99}$	0.9990
0.5—140	$i = 1.95c - 0.91$	0.9997	$i = 1.97c^{0.99}$	0.9991
0.5—160	$i = 1.94c - 0.78$	0.9997	$i = 1.97c^{0.99}$	0.9992
0.5—180	$i = 1.92c - 0.35$	0.9996	$i = 1.96c^{0.99}$	0.9992
0.5—200	$i = 1.92c - 0.20$	0.9997	$i = 1.96c^{0.99}$	0.9993
0.5—250	$i = 1.89c + 0.87$	0.9992	$i = 1.97c^{0.99}$	0.9994
0.5—300	$i = 1.85c + 2.45$	0.9985	$i = 1.97c^{0.99}$	0.9994

[a] i, detector response in nA; c, ng of menadione per 20-μl sample; r^2, squared correlation coefficient; a, b, d are constants; α, response index.

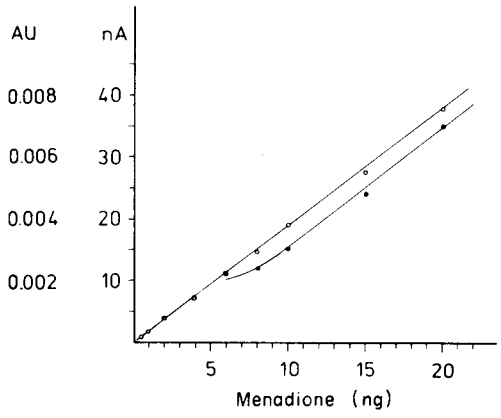

Fig. 2. Lower parts of the calibration curves of menadione with a u.v. detector (•) and the differential amperometric detector (○).

limit of the linear dynamic range was about 8 ng of menadione and the upper limit was more than 200 ng of menadione.

The responses of the u.v. detector and the differential amperometric detector at different menadione concentrations are compared in Fig. 3. The chromatograms recorded with the differential amperometric detector also show a peak of the dissolved oxygen in the sample; the lower limit of detection of the electrochemical detector is clearly demonstrated by Fig. 3.

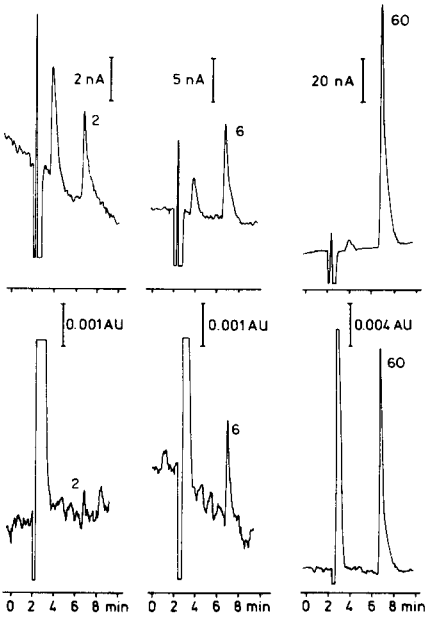

Fig. 3. Comparison between the response of the differential amperometric detector (above) and the u.v. detector (below) for menadione samples of 2 ng, 6 ng and 60 ng.

TABLE 2

Results of the linear curve-fitting and power curve-fitting calculations of the response of the u.v. detector as a function of the concentration of menadione

Sample range for menadione (ng)	Linear curve fitting[a]		Power curve fitting	
	$A = a\,c + b$	r^2	$A = d\,c^{\alpha}$	r^2
40—200	$A = 0.37c - 0.45$	0.9993	$A = 0.34c^{1.02}$	0.9988
20—200	$A = 0.37c - 0.40$	0.9995	$A = 0.33c^{1.02}$	0.9994
15—200	$A = 0.37c - 0.49$	0.9996	$A = 0.33c^{1.04}$	0.9991
10—200	$A = 0.37c - 0.52$	0.9997	$A = 0.29c^{1.05}$	0.9990
8—200	$A = 0.37c - 0.52$	0.9997	$A = 0.28c^{1.06}$	0.9991
6—200	$A = 0.37c - 0.40$	0.9996	$A = 0.31c^{1.03}$	0.9969
4—200	$A = 0.37c - 0.36$	0.9997	$A = 0.32c^{1.03}$	0.9975

[a] A, detector response in 10^{-3} AU; c, ng of menadione per 20-μl sample; r^2, squared correlation coefficient; a, b, d are constants; α, response index.

Although the linearity of the differential amperometric detector was somewhat better than the linearity of the u.v. detector, the correlation between the responses of the two detectors in the range 10—200 ng of menadione was good.

The results obtained for both detectors are in good agreement with the literature. Williams et al. [15] found a linear dynamic range of 5—2000 ng for menadione using a reversed-phase separation in combination with a u.v. detector. Ikenoya et al. [12] found a detection limit of 0.15—0.20 ng for some quinone derivatives, using an amperometric detector in combination with reversed-phase chromatography.

Conclusions

The differential amperometric detector is very effective in the reductive mode although its cathodic potential range is limited. The differential measuring principle compensates very well for the high background currents caused by dissolved oxygen and traces of metals leached by the eluent from the stainless steel parts of the chromatograph. It is not necessary to exclude oxygen from the system, but it would be advisable to avoid the reduction of metals at the working electrodes to avoid poisoning of the electrode surfaces. Excessive reduction of metal ions can be suppressed by adding a strong ligand to the mobile phase or by using teflon-lined stainless steel tubing and glass columns [3, 4].

Just as in the oxidative mode [13], the detector performance of the differential amperometric detector in the reductive mode is comparable with the performance of a commercial u.v. detector.

The authors are indebted to Mrs. T. Brunt-Velthuis for preparing the manuscript. The work is taken from the Ph.D. thesis of K. Brunt, Groningen, 1980.

REFERENCES

1 R. P. W. Scott, Liquid Chromatography Detectors, Elsevier, Amsterdam, 1977.
2 P. T. Kissinger, Anal. Chem., 49 (1977) 447A.
3 W. A. MacCrehan, R. A. Durst and J. M. Bellama, Anal. Lett., 10 (1977) 1175.
4 R. M. Wightman, E. C. Paik, S. Borman and M. A. Dayton, Anal. Chem., 50 (1978) 1140.
5 M. O. Funk, M. B. Keller and B. Levison, Anal. Chem., 52 (1980) 773.
6 J. G. Koen, J. F. K. Huber, H. Poppe and G. den Boef, J. Chromatogr. Sci., 8 (1970) 192.
7 R. Stillman and T. S. Ma, Mikrochim. Acta (Vienna), (1973) 491.
8 H. B. Hanekamp, W. H. Voogt, P. Bos and R. W. Frei, Anal. Lett., 12 (1979) 175.
9 G. H. Brilmyer, S. C. Lamey and J. T. Maloy, Anal. Chem., 47 (1975) 2304.
10 D. L. Rabenstein and R. Saetre, Anal. Chem., 49 (1977) 1036.
11 R. C. Buchta and L. J. Pappa, J. Chromatogr. Sci., 14 (1976) 213.
12 S. Ikenoya, K. Abe, T. Tsuda, Y. Yamano, O. Hiroshima, M. Ohmae and K. Kawabe, Chem. Pharm. Bull., 27 (1979) 1237.
13 K. Brunt and C. H. P. Bruins, J. Chromatogr., 172 (1979) 37.
14 K. Brunt, C. H. P. Bruins and D. A. Doornbos, in W. F. Smyth (Ed.), Electroanalysis in Hygiene, Environmental, Clinical and Pharmaceutical Chemistry, London, 17—20 April 1979, Elsevier, Amsterdam, 1980, p. 327.
15 R. C. Williams, J. A. Schmidt and R. A. Henry, J. Chromatogr. Sci., 10 (1972) 494.
16 G. J. Patriarche and J. J. Lingane, Anal. Chim. Acta, 49 (1970) 241.
17 J. C. Viré and G. J. Patriarche, Analusis, 6 (1978) 155.
18 J. A. Fowlis and R. P. W. Scott, J. Chromatogr., 11 (1963) 1.

Analytica Chimica Acta, 125 (1981) 93—99
Elsevier Scientific Publishing Company, Amsterdam — Printed in The Netherlands

DETERMINATION OF BISMUTH, LEAD AND TELLURIUM IN COPPER BY ATOMIC ABSORPTION SPECTROMETRY WITH INTRODUCTION OF SOLID SAMPLES INTO AN INDUCTION FURNACE

ADRIAN A. BAKER and JAMES B. HEADRIDGE*
Department of Chemistry, The University, Sheffield S3 7HF (Gt. Britain)
(Received 21st November 1980)

SUMMARY

Atomic absorption spectrometry with an induction furnace is used for the determination of bismuth (0.015—10 $\mu g\ g^{-1}$), lead (0.2—15 $\mu g\ g^{-1}$) and tellurium (0.04—5 $\mu g\ g^{-1}$) in 2—30-mg samples of copper and low-alloy copper dropped into the furnace. Calibration graphs of peak area versus mass of element were constructed by use of standardised alloys. The accuracy, precision and limits of detection of the method are described for numerous copper samples. With alloys containing more than 0.1 μg Bi g^{-1}, 0.2 μg Pb g^{-1} and 0.8 μg Te g^{-1}, average relative standard deviations are 7%, 6% and 8%, respectively. The limits of detection for bismuth, lead and tellurium are 0.01, 0.1 and 0.02 $\mu g\ g^{-1}$, respectively.

Antimony, arsenic, bismuth, selenium and tellurium, and, to a lesser extent, lead, markedly affect the annealability of copper used in wire production and can exert harmful effects at levels below 1 $\mu g\ g^{-1}$ [1—4]. Trace levels of these same impurities are also known to affect the electrical conductivity of copper but generally this happens at levels above those at which they affect the annealability. For example, lead is known to impair electrical conductivity at a concentration of 8 $\mu g\ g^{-1}$. Therefore there is a need to determine these trace elements at concentrations below 10 $\mu g\ g^{-1}$ and often below 1 $\mu g\ g^{-1}$. A method is required of good accuracy and reasonable precision with a limit of detection for bismuth, lead and tellurium of 0.1 $\mu g\ g^{-1}$ or better.

Many papers have been published on the determination of these trace elements in copper; a selection of the methods used is given in Table 1. It can be seen that the methods involving anodic stripping voltammetry and atomic absorption spectrometry (a.a.s.) with hydride generation or using a graphite cup atomizer have the required sensitivity, but these are all methods involving a preconcentration step. Furnace a.a.s. after dissolution, but without preconcentration, is not quite sensitive enough. However, a.a.s. with the introduction of solid copper samples into a constant-temperature induction furnace has the required sensitivity and is the method reported in this paper. The induction furnace is similar to that used by Headridge and coworkers for the determination of bismuth [19], lead [20], silver [21] and antimony

TABLE 1

Methods for the determination of bismuth, lead and tellurium in copper

Method	Limit of detection ($\mu g\ g^{-1}$)			Ref.
	Bi	Pb	Te	
Emission spectrography with a globule arc	0.2	0.1	2	5
Inductively-coupled plasma spectrometry after dissolution		9		6
Molecular absorption spectrometry:				
after solvent extraction	1			7
after $Fe(OH)_3$ collection	$\leqslant 0.04$			8
after $Fe(OH)_3$ collection and solvent extraction			1	9
Anodic stripping voltammetry:				
after electrolytic deposition of Cu		0.1		10
after ion exchange	0.004		0.02	11, 12
Atomic absorption spectrometry:				
after collection on $La(OH)_3$ and hydride generation	0.002		0.004	13, 14
furnace, after dissolution	0.2	0.4	0.2	15—17
graphite cup, after collection on $Fe(OH)_3$	0.02	0.1	$\leqslant 0.04$	18

[22] in steels, and of bismuth [23], and silver and thallium [24] in nickel-base alloys. A review of the determination of volatile trace elements in metals by a.a.s. with the introduction of solid samples into furnaces will be published soon [25].

EXPERIMENTAL

Materials

Standard copper samples and dilute copper alloys were obtained from the Canada Centre for Mineral and Energy Technology (CANMET) and Johnson Matthey Chemicals Ltd., respectively. Analysed copper samples were supplied by BICC Metals Ltd. Samples for analysis should preferably be chips so that no more than three pieces need to be added to the furnace core at the same time. Chips should be degreased with a suitable solvent before use.

Apparatus and measurement procedure for a series of solid samples

These were identical to those previously described [19] except that the graphite core and side arms were made from Ultra F purity graphite type UF-4S (Ultra Carbon, U.S.A.) for bismuth and tellurium, and from nuclear-grade graphite (British Acheson Electrodes Ltd.) for lead; also the window mounts were modified so that a continuous flow of argon from six radial holes was directed onto the windows to minimise metal deposition on their surfaces. This is known as the window gas. It is only used in conjunction with the purge gas. The furnace temperatures and gas flow rates used are shown in Table 2.

TABLE 2

Experimental conditions for the induction furnace

Element determined	Core temp. (°C)	Flow rates of argon (ml min^{-1})		
		Purge gas	Stir gas	Window gas
Bismuth	2400	150	40	1500
Lead	2380	200	40	2000
Tellurium	2440	250	50	1500

Graphite cores, side arms and powder were baked under vacuum for 6 h (18 h for lead) at 1700°C before use. Absorbances were measured on a Perkin-Elmer 300S atomic absorption spectrometer using a bismuth (Pye Unicam Ltd.), lead (Activion Glass Ltd.) or tellurium (S. & J. Juniper Ltd.) hollow-cathode lamp at wavelengths of 306.8, 283.3 and 214.3 nm, respectively. All measurements were made without damping, i.e., with a time constant of 0.2 s. The masses of samples added to the furnace were determined with a 5-place balance.

Calibration graphs

For the determination of bismuth in copper containing 0.01—2.5 $\mu g\ Bi\ g^{-1}$, calibration graphs of peak area (absorbance × seconds) versus mass of bismuth were obtained by dropping increasing masses of copper SSC 3 (10—30 mg, 0.59 $\mu g\ Bi\ g^{-1}$) into the graphite core under conditions capable of producing absorbances up to 0.25. For the dilute copper alloys CA 5 and CA 6 with bismuth contents in excess of 2.5 $\mu g\ g^{-1}$, the calibration graph was prepared in a similar way with alloy CA 7 (2.3 $\mu g\ Bi\ g^{-1}$), which was standardised against SSC 3. No scale expansion was used with alloy CA 7 but × 5 scale expansion with alloy SSC 3. Peak areas were determined by multiplying the peak height (absorbance) by the peak width at half peak height (s).

For the determination of lead in copper specimens containing 0.8—15 $\mu g\ Pb\ g^{-1}$, calibration graphs of peak area versus mass of lead were obtained by dropping increasing masses of copper SSC 2 (5—20 mg, 6.1 $\mu g\ Pb\ g^{-1}$) into the graphite core. For the analysis of SEN 337—353, a calibration graph of peak height versus mass of lead was prepared using copper STD 1 (0.8 $\mu g\ Pb\ g^{-1}$), which was standardised against SSC 2. Scale expansion (× 10) was employed. Peak heights rather than peak areas were used for SEN 337—353 and the calibration graph, because with such a small absorbance for SEN 337—353, it was not possible to measure the areas of the peaks precisely enough.

For the determination of tellurium in copper containing 0.8—5 $\mu g\ Te\ g^{-1}$, calibration graphs of peak area versus mass of tellurium were obtained by dropping increasing masses of copper STD 2 (5—30 mg, 1.65 $\mu g\ Te\ g^{-1}$) into the graphite core. Peak heights rather than peak areas were used for SEN 337—353, SEN 399—416 and the calibration graph, for the same reason as given above for lead.

Procedure for the determination of bismuth, lead and tellurium in coppers

When a series of copper samples is to be analysed, suitable masses are dropped into the graphite core over a period of 2—3 h; during the same run but generally at the start of the run, various masses of SSC 3 or CA 7 (for bismuth), SSC 2 or STD 1 (for lead) or STD 2 (for tellurium) are also added for construction of a calibration graph. Scale expansion is not required when the concentrations of bismuth, lead and tellurium are expected to be in excess of 2.5, 0.8 and 0.5 $\mu g\ g^{-1}$, respectively. A scale expansion of $\times 5$ is used when the concentrations of bismuth and tellurium are expected to lie within the range 0.1—2.5 $\mu g\ g^{-1}$ or be less than 0.5 $\mu g\ g^{-1}$, respectively. A scale expansion of $\times 10$ is used when the concentrations of bismuth and lead are expected to be less than 0.1 and 0.8 $\mu g\ g^{-1}$, respectively. When the run has been completed, the calibration graph is drawn and the average concentrations of bismuth, lead or tellurium in the samples are calculated.

RESULTS AND DISCUSSION

The calibration graphs for bismuth, lead and tellurium were straight lines through the origin whether peak area or peak height was used. From typical graphs the masses of bismuth, lead and tellurium producing 1% absorption were 0.3, 1 and 0.2 ng, respectively. Results for the determination of bismuth, lead and tellurium in a range of copper and low-alloy copper samples are presented in Tables 3, 4 and 5, respectively.

As can be seen from Table 3, the results for bismuth obtained by using the induction furnace are in good agreement with the independent results for samples supplied by CANMET and BICC Metals, but those for samples

TABLE 3

Results for the determination of bismuth in copper

Copper sample[a]	Bi content ($\mu g\ g^{-1}$)		No. of samples	R.s.d. (%)
	Stated	Found		
SSC 1	1.15	1.10	6	6
SSC 2	0.10	0.09	11	20
SSC 4	0.23	0.27	6	11
STD 1	0.45	0.41	6	4
STD 2	0.90	0.91	6	5
SEN 337—353	$\leqslant$0.02	0.015	12	45
SEN 399—416	0.05	0.08	6	12
CA 5	12.5	10.7	6	14
CA 6	6.4	5.9	6	7
CA 7	2.7	2.3	12	4
CA 8	1.4	1.1	12	7

[a]SSC samples supplied by CANMET, SEN and STD samples by BICC, and CA5—8 by Johnson Matthey.

TABLE 4

Results for the determination of lead in copper

Copper sample	Pb content ($\mu g\ g^{-1}$)		No. of samples	R.s.d. (%)
	Stated	Found		
SSC 3	4.6	4.2	6	4
SSC 4	15.8	14.7	5	5
STD 1	0.8	0.8	6	9
STD 2	2.6	2.7	6	5
SEN 337—353	$\leqslant 0.1$	0.2[a]	10	26
SEN 399—416	0.9	0.8	12	8
CA 5	8	9.3	6	4
CA 6	4.5	5.2	12	8
CA 7	3	3.4	6	7
CA 8	3	3.8	6	8

[a]Peak height used.

CA 5—CA 8 supplied by Johnson Matthey are slightly lower than the stated results. However, CA 5—CA 8 form part of a series of spectrographic standards made and analysed twenty-seven years ago and the bismuth contents given on the certificates must be viewed with caution. The limit of detection for bismuth in copper with the induction furnace, taken as twice the standard deviation of the 12 results for SEN 337—353, was 0.014 $\mu g\ g^{-1}$.

As is evident from Table 4, the present results for lead are in good agreement with the independent results. The limit of detection for lead in copper was calculated to be 0.1 $\mu g\ g^{-1}$ by employing the ten results for lead in SEN 337—353.

The results obtained here for tellurium are in good agreement with the independent results except, at first sight, for copper SSC 2. However, the CANMET result for tellurium in SSC 2 has a standard deviation of 0.51 $\mu g\ g^{-1}$ and our result of 0.8 $\mu g\ g^{-1}$ is within one such standard deviation of the stated content (1.24 $\mu g\ g^{-1}$). Hence the agreement can be considered to be acceptable. The limit of detection for tellurium in copper was calculated to be 0.02 $\mu g\ g^{-1}$ by employing the twelve results for tellurium in SEN 399—416.

In the determination of bismuth, lead and tellurium in copper using the temperatures given in Table 2, a check for background absorption was made by replacing the hollow-cathode lamps with a hydrogen lamp and by dropping milligram samples of copper into the induction furnace. The maximum absorbances recorded were 0, 0.005 and 0.01 for bismuth, lead and tellurium, respectively. These were considered to be negligible and, therefore, no background corrector was used in this work. However, copper boils at 2567°C and the use of a background corrector would be advisable if core temperatures in excess of 2450°C were employed. An attempt was made to determine antimony and selenium in copper at 2450°C but the furnace temperature was obviously too low for a successful determination of these elements.

TABLE 5

Results for the determination of tellurium in copper

Copper sample	Te content ($\mu g\ g^{-1}$)		No. of samples	R.s.d. (%)
	Stated	Found		
SSC 1	4.6	4.9	11	9
SSC 2	1.2	0.8	12	7
SSC 3	2.5	2.5	6	4
SSC 4	1.4	1.2	5	8
STD 1	0.80	0.81	6	13
SEN 337—353	0.07	0.08[a]	6	10
SEN 399—416	0.04	0.04[a]	12	22

[a]Peak height used.

It is possible that antimony could be determined in copper by using the induction furnace, background correction and the maximum furnace temperature of 2640°C but even this temperature is likely to be too low for the determination of selenium. A switch to a resistively-heated furnace such as the Instrumentation Laboratory 555 furnace, which can attain temperatures in excess of 2640°C, might lead to the satisfactory determination of selenium in copper. Selenium can be determined in nickel-base alloys by adding chips to an IL 555 furnace in an atomic absorption spectrometer fitted with a background corrector, using a maximum furnace temperature of 3000°C [26].

Silver is not usually considered to be a detrimental trace element in copper but very low concentrations of silver in copper could be determined with the induction furnace if necessary. A straight-line calibration graph through the origin was obtained for silver when the lowest practicable temperature of 2120°C was used with the 338.3-nm resonance line and 0.5—3 mg samples of copper SSC 2 stated to contain 13.9 μg Ag g^{-1}. The mass of silver producing 1% absorption was 0.1 ng; this corresponds to a limit of detection of about 0.01 $\mu g\ g^{-1}$ for silver in a 10-mg sample of copper. Samples containing 0.01—2 μg Ag g^{-1} could be analysed by using the induction furnace. By employing the more usual 328.1-nm resonance line, which yields absorbances about double those for the 338.3-nm line, and a higher furnace temperature, it should be possible to determine silver in copper with a limit of detection of about 0.003 $\mu g\ g^{-1}$.

We are indebted to the Science Research Council for a Studentship (for A. A. B.) and to Materials Quality Assurance Directorate, Woolwich, for assistance with materials; to the British Steel Corporation for the gift of the Perkin-Elmer 300S atomic absorption spectrometer and to Dr. J. D. Mullen, BICC Metals Ltd., for analysed samples and much useful information.

REFERENCES

1 D. A. Reese and L. W. Condra, Wire Ind., (1969) 883.
2 L. K. Bigelow and J. H. Chen, Metall. Trans. B, 7 (1976) 661.
3 D. C. Hallam, Wire J., 10 (1977) 115.
4 J. D. Mullen, private communication, 1980.
5 W. E. Publicover, Anal. Chem., 37 (1965) 1680.
6 A. F. Ward and L. F. Manciello, Anal. Chem., 51 (1979) 2264.
7 E. M. Donaldson, Talanta, 25 (1978) 131.
8 G. Norwitz and M. Galan, Anal. Chim. Acta, 83 (1976) 289.
9 E. M. Donaldson, Talanta, 23 (1976) 823.
10 G. van Dijck and F. Verbeck, Anal. Chim. Acta, 54 (1971) 475.
11 G. A. P. van Dyck and F. Verbeck, Fresenius Z. Anal. Chem., 249 (1970) 89.
12 T. W. Hamilton, J. Ellis and T. M. Florence, Anal. Chim. Acta, 110 (1979) 87.
13 M. Bedard and J. D. Kerbyson, Anal. Chem., 47 (1975) 1441.
14 M. Bedard and J. D. Kerbyson, Can. J. Spectrosc., 21 (1976) 64.
15 F. Shaw and J. M. Ottaway, At. Absorpt. Newsl., 13 (1974) 77.
16 W. B. Barnett and E. A. McLaughlin, Anal. Chim. Acta, 80 (1975) 285.
17 B. W. Haynes, At. Absorpt. Newsl., 18 (1979) 46.
18 J. D. Mullen, Talanta, 23 (1976) 846.
19 D. G. Andrews and J. B. Headridge, Analyst, 102 (1977) 436.
20 D. G. Andrews, A. M. Aziz-Alrahman and J. B. Headridge, Analyst, 103 (1978) 909.
21 A. M. Aziz-Alrahman and J. B. Headridge, Talanta, 25 (1978) 413.
22 A. M. Aziz-Alrahman and J. B. Headridge, Analyst, 104 (1979) 944.
23 J. B. Headridge and R. Thompson, Anal. Chim. Acta, 102 (1978) 33.
24 A. A. Baker, J. B. Headridge and R. A. Nicholson, Anal. Chim. Acta, 113 (1980) 47.
25 J. B. Headridge, Spectrochim. Acta B, in press.
26 J. B. Headridge and R. A. Nicholson, unpublished results.

Analytica Chimica Acta, 125 (1981) 101—108
Elsevier Scientific Publishing Company, Amsterdam — Printed in The Netherlands

DEPTH PROFILES OF ARSENIC IN SEMICONDUCTOR SILICON BY CHEMICAL ETCHING AND NON-DISPERSIVE ATOMIC FLUORESCENCE SPECTROMETRY WITH HYDRIDE GENERATION

K. TSUJII* and E. KITAZUME
Central Research Laboratory, Hitachi Ltd., Kokubunji, Tokyo (Japan)
(Received 13th October 1980)

SUMMARY

An improved non-dispersive atomic fluorescence spectrometric determination of arsenic by sodium tetrahydroborate reduction is described. A new burner on which a small argon—hydrogen—entrained air flame can be maintained at a low hydrogen flow rate (0.15 l min^{-1}) is reported. The detection limit (S/N = 2) is 10 pg of arsenic, and the analytical working curve is linear over four decades of concentration from the detection limit. The system is applied to depth profiling of arsenic in silicon slices. The silicon is anodized, the silica film is removed by hydrofluoric acid and the arsenic in the etching solution determined. The depth of silicon removed is measured by determining the silicon content in the etching solution by inductively-coupled plasma atomic emission spectrometry. The method permits determinations of $\geqslant 10^{18}$ atoms As cm^{-3} in 30-nm sections of a silicon slice with a diameter of 5.1 cm.

Semiconductor characteristics depend critically on the depth concentration profile of dopant elements. Many efforts have been made to evaluate impurity profiles. The technique most commonly employed in semiconductor industries and research laboratories is based on differential sheet resistivity measurements by means of a four-point probe [1—4] or on the Hall effect [4—6], because these techniques are relatively simple in routine practice. These methods give the electro-active impurity concentration; however, there is no information on electro-inactive precipitates, and values are distorted when there are electrically compensating impurities.

The net concentration profiles of impurities have been attained by combining a sensitive analytical technique such as radioactivation analysis [4, 7—9] with a suitable chemical sectioning method. Anodic oxidation is known to be a useful technique for producing a homogeneous silicon oxide layer on the surface of a silicon slice, which can then be dissolved in dilute hydrofluoric acid.

Lanza et al. employed this technique for sectioning successive layers of silicon samples and determined the phosphorus [10] and arsenic [11] depth profiles for concentrations as low as 10^{19} atoms cm^{-3} by absorption spectrometry and polarography, respectively.

Arsenic is one of the most widely used doping donors. Non-dispersive atomic fluorescence spectrometry after hydride generation is well known as a sensitive method for the determination of arsenic, antimony, selenium, bismuth, etc. [12—19], and seems to be promising for evaluating arsenic depth profiles in silicon slices.

Previous workers [20, 21] reported that the height and volume of an argon—hydrogen—entrained air flame decreased with decreasing hydrogen flow rate, that a small argon—hydrogen—entrained air flame improved the signal-to-noise ratio in the non-dispersive atomic fluorescence spectrometric determination of arsenic, antimony and tin, when a sodium tetrahydroborate reduction technique was used, and that this system gave a detection limit of 50 pg of arsenic.

In the initial stages of this work, a further improvement of the arsenic detection limit was obtained by introducing a new burner that can maintain a small flame at a lower hydrogen flow rate than that previously employed (0.25 l min^{-1}). The improved system was applied to the depth profiling of arsenic in silicon slices. The sectioning depth was measured by determining the amount of silicon dissolved in hydrofluoric acid, with use of inductively coupled plasma atomic emission spectrometry (i.c.p.a.e.s.)

EXPERIMENTAL

Apparatus

The arrangement and specific components of the apparatus for non-dispersive atomic fluorescence spectrometry were similar to those reported previously [20, 21], except for the following points. First, a new burner (4 mm shorter slot) as shown in Fig. 1 was used, and the distance between the centre of the burner slots and the photocathode was decreased to 4.5 cm by using a rectangular burner head and eliminating the protruding part of the detector box. Secondly, the inner wall of the hydride generation cell was coated with paraffin wax to prevent etching by hydrofluoric acid. Thirdly, the sample injection volume was decreased from 500 μl to 200 μl.

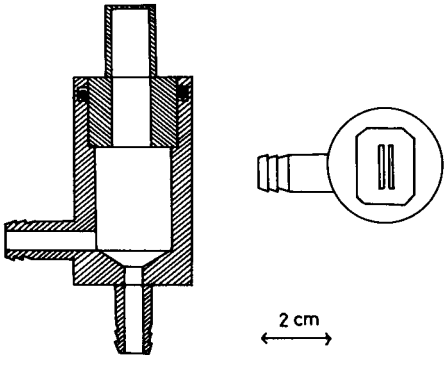

Fig. 1. New two-slot burner.

The burner head was situated so that the incident light beam from the source was parallel to the burner slots; the distance from the burner top to the centre of the light beam was 1 cm.

A Jarrell-Ash i.c.p. optical emission spectrometer (Model 975 Plasma Atomcomp) equipped with a data-processing unit was used for the determination of silicon.

Reagents

A commercially available arsenic(III) 1000 ppm standard solution (Kanto Chemicals Corp.) made from sodium arsenite was used. An arsenic(V) 1000 ppm standard solution was prepared by dissolving sodium dihydrogenarsenate in water. Sodium tetrahydroborate solution (1% w/v) was prepared just before use by dissolving sodium tetrahydroborate pellets (98% pure; Alfa Inorganics) in water. A potassium iodide solution (2.5 M) was used for the reduction of arsenic(V) to arsenic(III). The methanol, trichloroethylene and hydrofluoric acid used were of electronic grade. All other reagents were of analytical-reagent grade.

Procedures

Pretreatment of silicon slices. The silicon slice was washed in an ultrasonic cleaning vessel with methanol for 5 min, trichloroethylene for 10 min and methanol again for 5 min. The slice was rinsed in running deionized water for 5 min, treated in aqua regia for 10 min and rinsed again in running deionized water for 5 min. After being treated with (1 + 10) hydrofluoric acid for 1 min, the slice was washed in running deionized water for 5 min and dried in a nitrogen stream at room temperature.

Anodization of silicon slices. Silver paint (Silbest; Tokuriki Chemical Research Co. Ltd.) was applied to the back of the silicon slice to ensure good electrical contact between the slice and a copper electrode. The slice was fixed to a copper electrode by a wax (Electron Wax; Soh Denshi Kogyo Co. Ltd.) as shown in Fig. 2. Prior to anodic oxidation an initial four-point

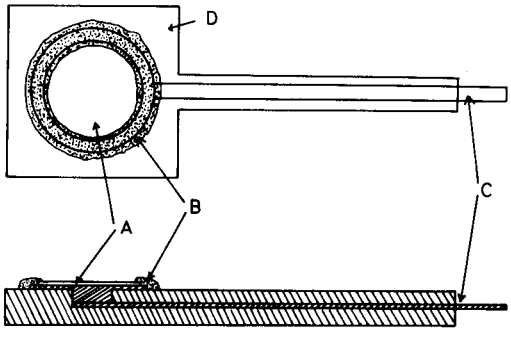

Fig. 2. Attachment of silicon slice to electrode: (A) silicon slice; (B) wax; (C) copper electrode; (D) acrylic resin.

probe resistivity measurement was made. The electrode was set in a vessel containing a saturated citric acid solution. Constant-current (50 mA) anodization was carried out for 6 min while the solution was stirred by a magnetic stirrer. After anodic oxidation, the silicon slice was rinsed in running deionized water for 5 min and dried in a nitrogen stream. The uniformity of the silicon oxide growth was checked by the colour uniformity of the slice surface before 1 ml of 0.1 M hydrofluoric acid was placed on the surface. After 10 min (to allow complete dissolution of the oxide layer) the solution was quantitatively transferred to a polyethylene bottle. The silicon slice was washed with deionized water, the washing solution was mixed with the etching solution, and the mixed solutions were diluted to 5 ml. The electrode was rinsed in running deionized water for 1 min and dried in a nitrogen stream. Next, a four-point probe resistivity measurement was made against the new silicon surface. The above procedure was repeated on successive surfaces of the silicon slice.

Atomic fluorescence measurements of arsenic. A 2.5 ml portion of each etching solution was taken, 1 ml of potassium iodide solution and 0.42 ml of hydrochloric acid solution were added, and the mixture was diluted to exactly 5 ml. A 200-μl portion was transferred by a Gilson pipette (Model P200) to a hydride generation cell containing 2 ml of 1% sodium tetrahydroborate solution as reported previously [20, 21]. The solution was injected into the cell and the atomic fluorescence signals (peak height) appearing on a recorder were measured under the conditions shown in Table 1.

Optical emission spectrometric measurements of silicon. A 2.5-ml portion of each etching solution was diluted to 25 ml, and aspirated into an inductively-coupled argon plasma. The measurements were made under the conditions shown in Table 2.

The silicon depth of each sectioning layer was obtained from the silicon content determined by the i.c.p. method and the silicon surface area.

RESULTS AND DISCUSSION

Effects of experimental conditions

The effects of different acids at various concentrations on arsenic fluorescence intensity were measured for arsenic(III) and arsenic(V). The results are shown in Fig. 3. To suppress the pressure increase in the cell, which caused the small argon—hydrogen—entrained air flame to be extinguished, all further measurements were made with 1 M hydrochloric acid, as previously [20, 21].

TABLE 1

Experimental conditions for non-dispersive atomic fluorescence spectrometry of arsenic

Lamp operating power	10 W	Argon flow rate	0.7 l min^{-1}
Chopping frequency	27 Hz	Hydrogen flow rate	0.15 l min^{-1}
Photomultiplier voltage	400 V	Time constant of lock-in amplifier	1.0 s

TABLE 2

Experimental conditions for i.c.p. atomic emission spectrometry of silicon

Operating frequency	27 MHz	Plasma observation point	16 mm above load coil
Incident power	1.1 kW		
Reflected power	3.0 W	Analytical line	288.1 nm
Argon flow rate: Coolant	17 l min^{-1}	Sample consumption rate	1.3 ml min^{-1}
Plasma	1.0 l min^{-1}		
Sample	0.5 l min^{-1}		

The effects of argon and hydrogen flow rates on arsenic fluorescence intensity were measured for arsenic(III). The effect of argon flow rate on arsenic fluorescence intensity was measured, at 0.25 l H_2 min^{-1}. The results are shown in Fig. 4. Subsequent measurements were made at an argon flow rate of 0.7 l min^{-1}.

Previous workers [20, 21] reported the effect of hydrogen flow rate (>0.25 l min^{-1}) on fluorescence intensity and noise level. In this study, these effects were measured at flow rates below 0.25 l min^{-1}. The noise level behaviour is similar to that reported previously, and the level decreased with decreasing hydrogen flow rates (Fig. 5). However, the signal behaviour is different from the previous results, in which a rapid signal increase was observed; here a gradual signal increase was observed (Fig. 6). Subsequent measurements were made at a hydrogen flow rate of 0.15 l min^{-1}. The visible portion of a flame from 0.7 l Ar min^{-1} and 0.15 l H_2 min^{-1} was about 1 cm high.

Detection limit, analytical working curve and repeatability

The detection limit of arsenic (S/N = 2) was 10 pg, which is 5 times better than the previously reported value [20]. The analytical working curve was

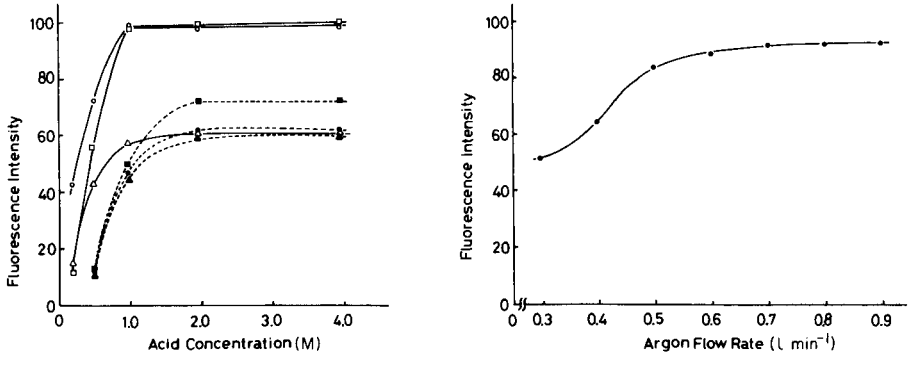

Fig. 3. Effect of acids at various concentrations on arsenic fluorescence intensity. Solid and broken lines represent As(III) and As(V), respectively. (□, ■) HCl; (○, ●) H_2SO_4; (△, ▲) HNO_3.

Fig. 4. Effect of argon flow rate on arsenic fluorescence intensity.

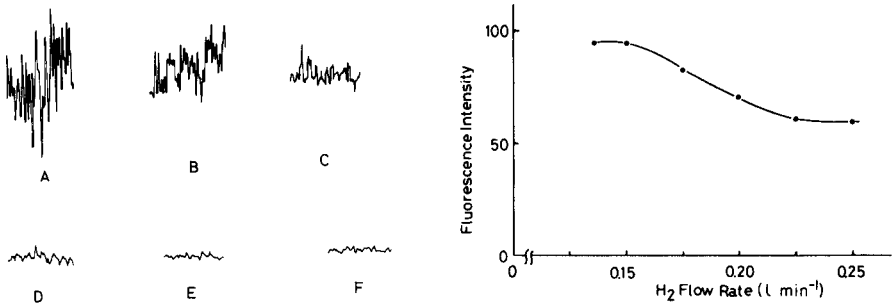

Fig. 5. Noise level dependence on hydrogen flow rate: (A) 0.25, (B) 0.23, (C) 0.20, (D) 0.18, (E) 0.15, (F) 0.13 l min^{-1}.

Fig. 6. Effect of hydrogen flow rate on arsenic fluorescence intensity.

linear up to 400 ng of arsenic, i.e. over four concentration decades from the detection limit. The relative standard deviations for 8 measurements each on 1, 10 and 100 ng As ml^{-1} were 4.5, 2.8 and 2.2%, respectively.

Reduction of arsenic(V) to arsenic(III)

As shown in Fig. 3, the fluorescence intensity from arsenic(V) is less than that from arsenic(III). Therefore, to apply this technique to practical analysis, all the arsenic must be converted to a single oxidation state prior to hydride generation. In this study, potassium iodide reduction was employed. The presence of 0.5 M potassium iodide was sufficient for complete reduction of arsenic(V) to arsenic(III) when using 1 M hydrochloric acid (Fig. 7).

Effect of silicon and hydrofluoric acid

The possible interfering effects of up to 10^5-fold amounts (by weight) of silicon and 0.1—4 M hydrofluoric acid were investigated. No interference was observed for either component in the range investigated.

Determination of arsenic in silicon

An arsenic-doped silicon slice was treated as described in the above procedure, and arsenic in the surface region of the slice, in which a high concentration of arsenic was present, was dissolved in dilute hydrofluoric acid. The etching solution was diluted to 5 ml, which was then divided into two parts. One was used for the non-dispersive atomic fluorescence measurements, the other for absorption spectrometry based on the formation of molybdoantimonylarsenic acid [22]. The results obtained by both methods agreed well, as shown in Table 3.

Determination of silicon

A silicon slice was treated as described in the above procedure. The silicon oxide film formed was dissolved in hydrofluoric acid solution and

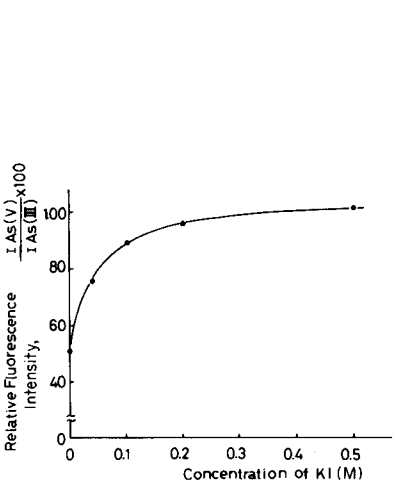

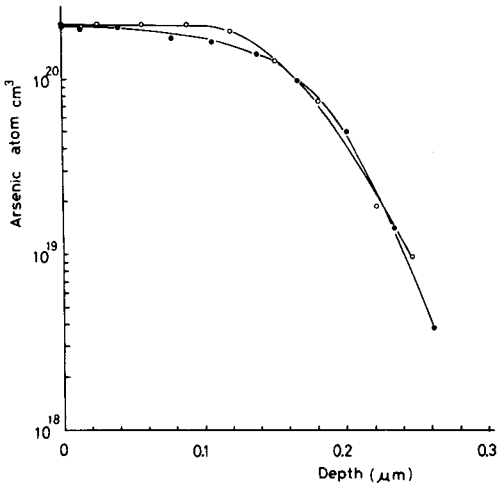

Fig. 7. Effect of potassium iodide concentration on arsenic(V) reduction to arsenic(III). Total arsenic concentration = 100 ng ml^{-1}.

Fig. 8. Typical depth profile of arsenic in a silicon slice. (•) Present method, (○) four-point probe resistivity method.

the etching solution was diluted to 5 ml. The solution was again divided into two parts. One was used for i.c.p.a.e.s., the other for absorption spectrometry, with a procedure similar to that reported by Lanza et al. [10, 11]. The analytical results agreed well with each other, as shown in Table 3, indicating that i.c.p.a.e.s. can be used for sectioning and depth profiles of silicon slices.

Depth profiles for arsenic

The technique developed was applied to a depth profiling of arsenic in silicon slices. A typical depth profile is shown in Fig. 8, which also shows the results obtained with a four-point probe resistivity method.

TABLE 3

Determination of arsenic and silicon in silicon slices

Sample no.	Arsenic concentration (μg ml^{-1})[a]		Silicon concentration (μg ml^{-1})[a]	
	Present method	Absorption spectrometry	i.c.p. method	Absorption spectrometry
1	0.13	0.13	4.6	4.7
2	0.60	0.53	4.3	4.4
3	0.60	0.63	4.3	4.4
4	0.73	0.70	5.2	5.2

[a]Concentration in the solution diluted to 5 ml after anodization and dissolution with HF.

The proposed method permits the determination of arsenic concentrations as low as 10^{18} atoms As cm^{-3} when a silicon slice of 5.1 cm diameter is used with sectioning at about 30-nm depth intervals of the slice. The limiting factors were the reagent blank (60 pg of arsenic) from hydrochloric acid and potassium iodide, and the gradual dissolution of arsenic from the wax-coated silicon slice surface, which has a high concentration of arsenic. Work is currently under way to overcome these limitations and determine arsenic profiles in the range of 10^{17}—10^{20} atoms As cm^{-3}.

We are grateful to Mr. N. Hashimoto for his encouragement, to Mr. M. Namba for providing arsenic-doped silicon slices, to Mr. H. Usui for his guidance in the anodization and resistivity measurements and for providing a computer program for calculating concentration profiles from resistivity data, and to Mr. K. Kuga for valuable discussions.

REFERENCES

1 F. M. Smits, Bell Syst. Tech. J., 37 (1958) 711.
2 E. Tannenbaum, Solid-State Electron., 2 (1961) 279.
3 P. J. Severin, Philips Res. Rep., 26 (1971) 279.
4 F. Mousty, P. Ostoja and L. Passari, J. Appl. Phys., 45 (1974) 4576.
5 L. V. van den Pauw, Philips Res. Rep., 13 (1958) 1.
6 N. G. E. Johansson and J. W. Mayer, Solid-State Electron., 13 (1970) 317.
7 Restelli, F. Girardi, F. Mousty and A. Ostidich, Nucl. Instrum. Methods, 112 (1973) 581.
8 F. Burkhardt, A. Mertens and C. Wagner, Phys. Status Solidi, A22 (1974) K45.
9 K. D. Beyer, J. Electrochem. Soc., 124 (1977) 630.
10 P. Lanza and P. L. Buldini, Anal. Chim. Acta, 104 (1979) 139.
11 P. L. Buldini, D. Ferri and P. Lanza, Anal. Chim. Acta, 106 (1979) 137.
12 K. Tsujii and K. Kuga, Anal. Chim. Acta, 72 (1974) 85.
13 K. Tsujii, K. Kuga and I. Sugaya, Chem. Lett., (1975) 695.
14 T. Nakahara, S. Kobayashi and S. Musha, Anal. Chim. Acta, 101 (1978) 375.
15 T. Nakahara, T. Tanaka and S. Musha, Bull. Chem. Soc. Jpn., 51 (1978) 2046.
16 J. Azad, G. F. Kirkbright and R. D. Snook, Analyst, 104 (1979) 232.
17 S. Kobayashi, T. Nakahara and S. Musha, Talanta, 26 (1979) 951.
18 T. Nakahara, S. Kobayashi and S. Musha, Anal. Chem., 51 (1979) 1589.
19 T. Nakahara, S. Kobayashi, T. Wakisaka and S. Musha, Appl. Spectrosc., 34 (1980) 194.
20 K. Tsujii and K. Kuga, Anal. Chim. Acta, 97 (1978) 51.
21 K. Tsujii and K. Kuga, Anal. Chim. Acta, 101 (1978) 199.
22 E. Kitazume, Bunseki Kagaku, to be published.

Analytica Chimica Acta, 125 (1981) 109—115
Elsevier Scientific Publishing Company, Amsterdam — Printed in The Netherlands

DETERMINATION OF LEAD AT THE ng ml^{-1} LEVEL BY REDUCTION TO PLUMBANE AND MEASUREMENT BY INDUCTIVELY-COUPLED PLASMA EMISSION SPECTROMETRY

MASAHIKO IKEDA*, JIRO NISHIBE, SETSUO HAMADA and RYUZO TUJINO[a]

Engineering Department, Nippon Jarrell-Ash Co. Ltd., 28 Joshungamae-cho, Shimotoba, Fushimi-ku, Kyoto 612 (Japan)

(Received 20th October 1980)

SUMMARY

A detection limit of 1 ng ml^{-1} for lead is obtained by the reported method. Samples are prepared in 0.5 M hydrochloric acid—0.8 M hydrogen peroxide. Plumbane is produced (with 64% efficiency) by the addition of 5% sodium tetrahydroborate in 0.5% NaOH, and is transported by the argon feed directly to an inductively-coupled argon plasma for emission spectrometry. Decreased hydrogen generation and greater stability of the plasma also contribute to the improved detection limit. The method is shown to be generally applicable to As, Sb, Bi, Sn, Te and Se, with detection limits at the ng ml^{-1} level.

Since 1972, when Braman et al. [1] reported that arsenic and antimony compounds were reduced to arsine and stibine, respectively, by the addition of aqueous 1% tetrahydroborate(III), hydride generation has been recognised to be very useful in measurements by atomic absorption spectrometry. Now, it is generally applied in trace determinations of As, Sb, Se, Te, Ge, Sn and Pb [2—6].

Greenfield et al. [7] have shown that an inductively-coupled plasma (i.c.p.) is a very effective excitation source for optical emission spectrometry (o.e.s.). More recently, the use of hydride generation instead of the conventional aqueous solution pneumatic-nebulization technique has produced good results for the determination of As, Sb, Se, Te, Bi, Sn and Ge [8—12]. Moreover, Vijan and Wood [3] have reported some advantages of this hydride generation technique for the determination of lead. They noted that plumbane decomposes easily, but the efficiency of its generation is poor, even in the presence of hydrogen peroxide. However, they reported that the sensitivity was improved compared to conventional nebulization and that physical interference from the nebulizer and spectral interference were significantly reduced. However, Thompson et al. [12] reported that a stable plasma could not be obtained for any concentration greater than 1.5%

[a]Present address: Yanagimoto Mfg. Co., Ltd., 28 Joshungamae-cho, Shimotoba, Fushimi-ku, Kyoto 612, Japan.

sodium tetrahydroborate, even for the condition of high r.f. power to the plasma. These last authors concluded that too much hydrogen was generated as a by-product and that its flow rate to the plasma should not exceed 150 ml min^{-1}. In order to avoid this problem, other authors [11, 13] employed low-temperature entrapment methods to eliminate the hydrogen. In the present paper, it is shown that the hydride generation method may be improved by increasing the efficiency of plumbane generation and decreasing the amount of hydrogen that is generated.

EXPERIMENTAL

An inductively-coupled argon-plasma optical emission spectrometer, Model ICAP-500 (Nippon Jarrell-Ash) equipped with a standard r.f. generator having a maximum output power of 2.0 kW at 27 MHz was used without any modification.

Figure 1 shows schematically the hydride generator and the i.c.p.—o.e.s. system. The hydride generator is similar to that previously reported [4] but it has two gas-liquid separators. The exhaust of the hydride generator was connected to the drain outlet of the conventional mixing chamber. In this manner, it was easily possible to interchange the conventional pneumatic nebulizer and the hydride generator as required.

The hydride generator functioned smoothly after some experimentation with its components. Initially hydrogen generation occurred in surges, even though the tetrahydroborate solution and the acidified sample were introduced slowly and evenly into the cross-joint that served as the initial mixing vessel. These surges sufficed to extinguish the plasma. However, stability of

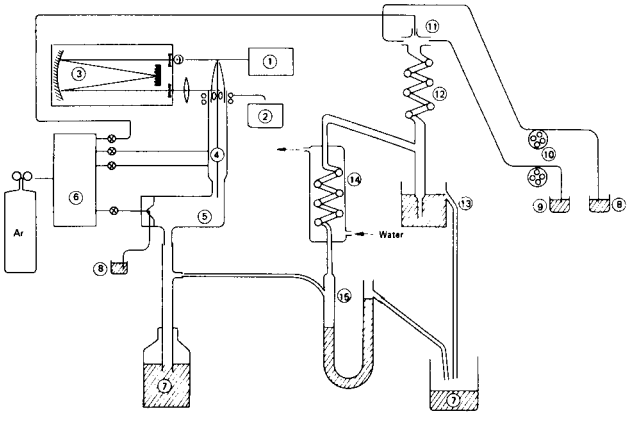

Fig. 1. Hydride generation i.c.p.—o.e.s. system. (1) Amp. and readout; (2) r.f. generator and matching box; (3) spectrometer; (4) torch; (5) mixing chamber; (6) gas flow regulator; (7) drain; (8) sample; (9) $NaBH_4$, (10) peristaltic pumps; (11) cross-joint; (12) mixing coil; (13) 1st gas-liquid separator; (14) condensor; and (15) 2nd gas-liquid separator.

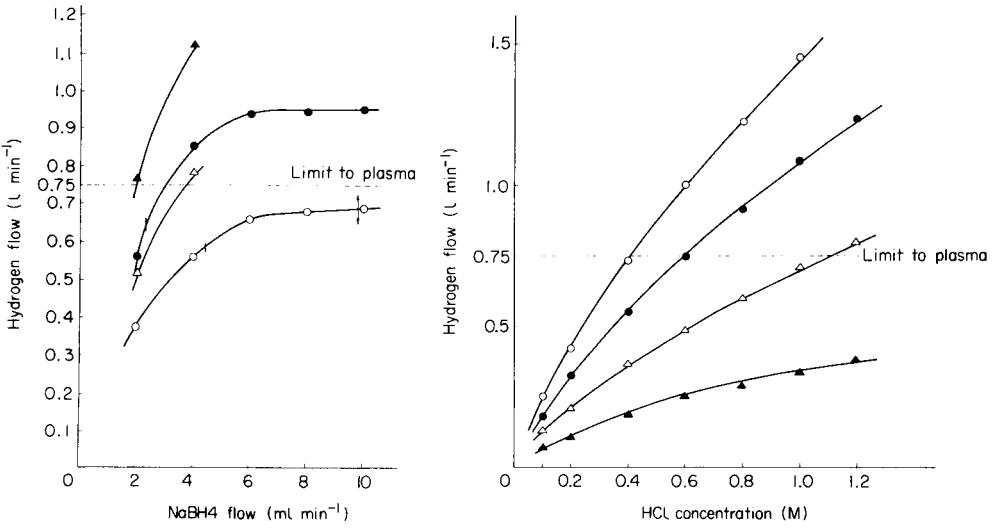

Fig. 2. Effect of $NaBH_4$ solution flow rate on amount of hydrogen evolved. (○) 5% $NaBH_4$, 3.5 ml min^{-1} sample flow; (●) 5% $NaBH_4$, 7.0 ml min^{-1} sample flow; (△) 10% $NaBH_4$, 3.5 ml min^{-1} sample flow; (▲) 10% $NaBH_4$, 7.0 ml min^{-1} sample flow.

Fig. 3. Effect of HCl concentration on amount of hydrogen evolved. $NaBH_4$ (5% in 0.1% NaOH) at a flow rate of 3.2 ml min^{-1}. HCl flow rate: (○) 5.6 ml min^{-1}; (△) 2.8 ml min^{-1}; (●) 4.2 ml min^{-1}; (▲) 1.4 ml min^{-1}.

hydrogen generation and of the plasma were achieved when a 10-mm i.d. cross-joint was substituted for the original 2 mm i.d. version.

In Fig. 1, the argon gas flows vertically down through the cross-joint carrying the solutions injected at either side and down through the spiral mixing coil, smoothly along the walls but not as bubbles. It then passes through the first gas-liquid separator, a condensor to remove excess water vapour, the second gas-liquid separator and finally to the plasma via the drain outlet. The mixing coil was made of a 100-mm long, 10-mm i.d. pyrex tubing wound tightly in 5 turns. This coil became hot because of the decomposition of hydrogen peroxide.

The hydride generation reaction occurred almost instantly. However, hydrogen continued to be generated for a while because the excess reductant decomposed only slowly. Excessive hydrogen generation was undesirable and therefore, the spent solution was allowed to drain rapidly from the first gas—liquid separator through a 3-mm i.d. discharge tube.

The reducing reagent was prepared daily with deionized water to contain 5% $NaBH_4$ and 0.5% NaOH; 33% hydrogen peroxide and 35% hydrochloric acid were used in the preparation of the sample and standard solutions. All reagents were of analytical grade (Nakarai Chemical Co. Ltd., Kyoto).

The operating conditions for the plasma were: torch, Fassel type; forward

power, 2.0 kW; viewing height, 13 mm; plasma support gas flow rate, 1.4 l min^{-1}; coolant gas flow rate, 18 l min^{-1}; carrier gas flow rate, 1.0 l min^{-1}; wavelength, 220.3 nm.

RESULTS AND DISCUSSION

Determination of conditions for maximum sensitivity

When hydrogen instead of argon was injected at the cross-joint, the plasma became unstable and extinguished at hydrogen flow rates exceeding 750 ml min^{-1}. This limit appeared to be independent of r.f. power from 1.2 to 2.0 kW and of coolant gas flow from 15 to 20 l min^{-1}. Therefore, it was reasonable to conclude that the feed rate of the reagents to the cross-joint should be such that hydrogen is generated at rates less than this limit. For example, as shown in Figs. 2 and 3, the maximum flow rates of hydrogen generated in the cross-tube were measured as a function of feed rates of the tetrahydroborate and hydrochloric acid solutions. The plasma became unstable at the predicted feed rate. In a separate experiment, the concentration of hydrogen peroxide in the hydrochloric acid solution was increased from 0.4 to 1.6 M, so that the plasma became unstable at smaller feed rates.

A sample solution containing 10 μg Pb ml^{-1}, 0.5 M HCl and 0.8 M H_2O_2 was prepared and, as shown in Fig. 4, the emission intensity of the analytical line was measured as a function of sample and tetrahydroborate feed rates. The onset of plasma instability was observed as a decrease in emission intensity as the sample feed rate exceeded 4.2 ml min^{-1} and above 5%

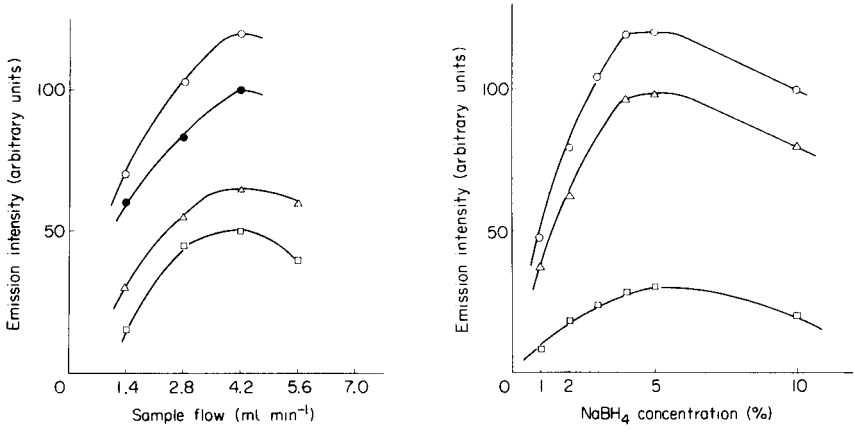

Fig. 4. Effect of sample flow rate on sensitivity for 10 μg Pb ml^{-1} in 0.5 M HCl—0.8 M H_2O_2. (○) 5% $NaBH_4$ at 3.2 ml min^{-1}; (△) $NaBH_4$ 2% at 5.5 ml min^{-1}; (●) 10% $NaBH_4$ at 2.2 ml min^{-1}; (□) 1% $NaBH_4$ at 7.5 ml min^{-1}.

Fig.5. Effect of $NaBH_4$ concentration on sensitivity for 10 μg Pb ml^{-1} at 4.2 ml min^{-1}, (○) 0.8 M H_2O_2; (△) 1.6 M H_2O_2; (□) 0.4 M H_2O_2; 0.5 M HCl in all cases.

sodium tetrahydroborate. In Figs. 5—7 the tetrahydroborate and hydrochloric acid concentrations and the carrier gas flow rate were varied. In each case, the emission intensity passed through a maximum. Therefore, the optimum conditions for maximum sensitivity were the following: 0.5 M HCl—0.8 M hydrogen peroxide at a flow rate of 3.8 ml min^{-1} for the lead solution; and 5% $NaBH_4$—0.5% NaOH at a flow rate of 3.2 ml min^{-1} for the reagent solution.

Calibration, accuracy and precision

Figure 8 shows a chart recording of the emission intensity from a 10 μg Pb ml^{-1} solution prepared as defined above. The mouth of the sample feed tube was placed alternately in the sample solution and in a blank solution. The small shoulder on the leading edge of each emission peak appeared to be due to the introduction of a small bubble of air into the sample feed tube when it was moved from one solution to another. Figure 9 shows a chart recording of the emission intensities for 5—100 ng Pb ml^{-1} in the optimum solutions described above. The measured intensities provided a usable calibration curve even at these low levels. The blank solution showed a signal equivalent to 2 ng Pb ml^{-1}.

The efficiency of hydride generation was determined simply by measuring the lead concentration in the fresh waste water obtained at the drain of the first gas-liquid separator. The recovery of lead in the drain was 36%. Therefore the efficiency of hydride generation was 64%. When the mixing coil was removed, this efficiency decreased to 30%.

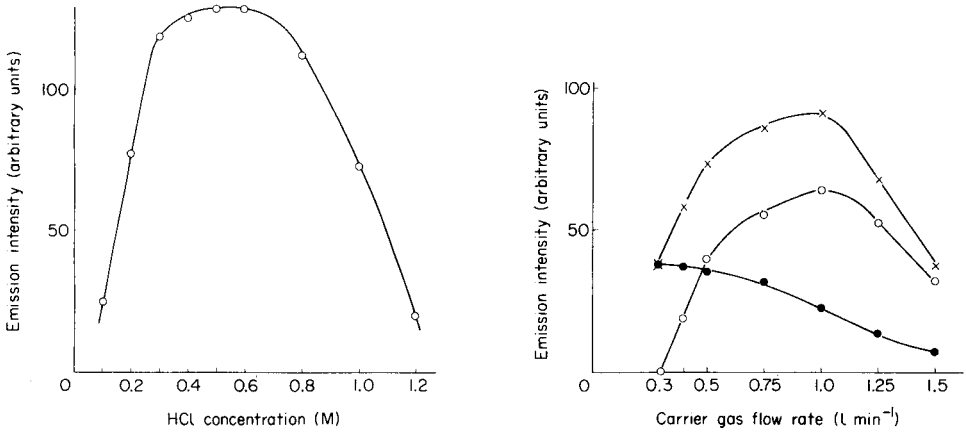

Fig. 6. Effect of HCl concentration on sensitivity for 10 μg Pb ml^{-1} at 3.8 ml min^{-1} with 5% $NaBH_4$ in 0.1% NaOH at 3.2 ml min^{-1}.

Fig.7. Effect of carrier gas flow rate on sensitivity for 10 μg ml^{-1} Pb at 3.8 ml min^{-1} with 5% $NaBH_4$ in 0.1% NaOH at 3.2 ml min^{-1}. (×) Total signal; (○) net signal; (•) background signal.

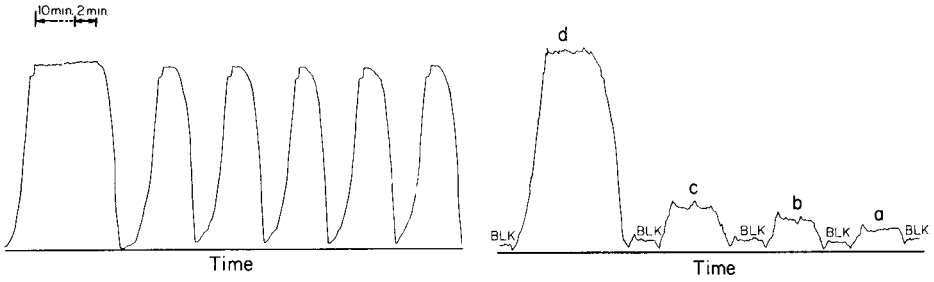

Fig. 8. Recorder tracings of stability and reproducibility for 10 μg Pb ml^{-1} (PMT high voltage, 400 V).

Fig. 9. Typical response curves. Lead concentrations: (a) 5 ng ml^{-1}; (b) 10 ng ml^{-1}; (c) 15 ng ml^{-1}; (d) 100 ng ml^{-1}; (BLK) blank solution. (PMT high voltage, 580 V).

Formation of other hydrides and interferences

The procedure described above was repeated to determine the optimum conditions and detection limits for As, Sb, Bi, Sn, Te and Se. The results are shown in Table 1. The measured efficiency of hydride generation for each of these elements was nearly 100%.

The effect of various interferents was studied by preparing sample solutions containing 10 μg Pb ml^{-1} and a measured concentration of interferent. Table 2 shows the apparent concentration of lead in the presence of interfering species. At high concentrations of silicon, a gel formed, presumably by the interaction of silica and the alkaline reductant solution. Copper and selenium interfered at the lowest levels tested.

Conclusions

The improved method appears to be generally applicable for the determination of Pb, As, Sb, Bi, Sn, Te and Se above 1 ng ml^{-1}. The improvements in the method for lead were the plumbane generation efficiency (64%), the

TABLE 1

Operating conditions and detection limits

Element	Wavelength (nm)	Concn. of $NaBH_4$ (%)	HCl (M)	Detection limit (ng ml^{-1})
Pb	220.3	5	0.5	1
As	234.9	1	0.5	1
Sb	206.8	3	1.0	5
Bi	306.8	1	0.5	2
Sn	326.2	1	0.5	0.5
Te	238.6	2	3.0	2
Se	204.0	1	3.0	1

TABLE 2

Effect of various ions on the recovery (percent) of lead (10 μg ml^{-1})
[Interferents were added as chloride salt except for Si (sodium silicate), Se (SeO_2 in water) and Bi (dissolved in nitric acid)]

Concn. (μg ml^{-1})	Cr	Cu	Fe	Si	Zn	Mg	Al	Mn	Ni	As	Sn	Sb	Te	Se	Bi
1	100	90	100	130	100	100	100	100	100	100	100	100	100	15	100
10	100	58	100	160	100	100	100	100	100	100	100	100	80	0	100
100	80	30	76	150	95	100	100	57	100	100	100	100	10	0	90
1000	30	8	40	—[a]	73	100	53	57	40	13	—[b]	100	0	0	80
10000	10	0	10	—[a]	10	100	—[b]	53	10	—[b]	—[b]	100	0	0	53

[a]Gel formation. [b]Plasma was extinguished.

decrease in hydrogen generation, and the improved stability of the plasma, leading to a much improved detection limit from that reported previously.

The authors sincerely thank Professor Y. Yamamoto of Hiroshima University and Dr. T. Nakahara of Osaka Prefectural University for their valuable suggestions.

REFERENCES

1 R. S. Braman, L. L. Justen and C. C. Foreback, Anal. Chem., 44 (1972) 2195.
2 K. C. Thompson and D. R. Thomerson, Analyst, 99 (1974) 595.
3 P. N. Vijan and R. Wood, Talanta, 23 (1976) 89.
4 P. N. Vijan and R. Wood, Analyst, 101 (1976) 966.
5 H. D. Fleming and R. G. Ide, Anal. Chim. Acta, 83 (1976) 67.
6 K. Jin, M. Taga, H. Yoshida and S. Hikime, Jpn. Analyst, 27 (1978) 759.
7 S. Greenfield, I. L. Jones, H. McD. McGeachin and P. B. Smith, Anal. Chim. Acta, 74 (1975) 225.
8 M. Thompson, B. Pahlavanpour, S. J. Walton and G. F. Kirkbright, Analyst, 103 (1978) 705.
9 M. Thompson and B. Pahlavanpour, Anal. Chim. Acta, 109 (1978) 251.
10 B. Pahlanvanpour, M. Thompson and S. J. Walton, J. Geochem. Explor., 12 (1979) 45.
11 R. L. Fricke, W. D. Robbins and J. A. Caruso, J. Assoc. Off. Anal. Chem., 61 (1978) 1118.
12 M. Thompson, B. Pahlavanpour and S. J. Walton, Analyst, 103 (1978) 568.
13 R. C. Fry, M. B. Denton, D. L. Windsor and S. J. Northway, Appl. Spectrosc., 33 (1979) 399.

Analytica Chimica Acta, 125 (1981) 117—130
Elsevier Scientific Publishing Company, Amsterdam — Printed in The Netherlands

DETERMINATION OF TRACE METALS IN SEA WATER BY CHELEX-100 OR SOLVENT EXTRACTION TECHNIQUES AND ATOMIC ABSORPTION SPECTROMETRY

LEIF RASMUSSEN

Superfos a/s, Frydenlundsvej 30, DK-2950 Vedbaek (Denmark)

(Received 6th October 1980)

SUMMARY

Determinations of cadmium, lead, nickel, copper and zinc in sea water are discussed. Two different methods of preconcentration are compared: the trace metals are preconcentrated either by extraction with ammonium pyrrolidinedithiocarbamate/diethylammonium diethyldithiocarbamate into freon followed by back-extraction into nitric acid, or by collection on a Chelex-100 resin followed by elution with nitric acid. Cd, Pb, Ni, and Cu are determined by graphite-furnace atomic absorption spectrometry, while zinc is determined by flame atomic absorption spectrometry. The comparison of methods shows that cadmium can be determined accurately whereas results for the other trace metals may be biased by reagent contamination in the Chelex-100 method. Recovery data are given for both methods of preconcentration. Filtering experiments with Chelex-100 method are described. Results are compared for sea-water samples preconcentrated immediately after sampling and some weeks after sampling, with only freezing for preservation. The present results are consistent with other recent work. The importance of blank values is discussed.

Many papers have been written which deal with the direct determination of trace metals in sea water by graphite-furnace atomic absorption spectrometry (g.f.a.a.s.) or by electrochemical methods. These methods are attractive, especially the latter because very little sample preparation is required. However, interferences are often troublesome. Direct g.f.a.a.s. requires virtually no addition of chemicals and is very fast. However, most pollutants and micro-nutrients are present in sea water near or only slightly above the detection limit. Consequently, many authors have focussed on preconcentration methods. This paper deals with preconcentration of trace metals on a Chelex-100 chelating resin, and with preconcentration by complexing with a mixture of ammonium-1-pyrrolidinedithiocarbamate (APDC) and diethylammonium diethyldithiocarbamate (DDDC), extraction with freon-TF, and back-extraction with nitric acid into a water phase.

The Chelex-100 preconcentration technique was originally described by Riley and Taylor [1], and later modified by many workers including Davey et al. [2, 3]. Kingston et al. [4] presented a very detailed description of the Chelex-100 preconcentration method, with special emphasis on the separa-

0003—2670/81/0000—0000/$02.50

tion of alkali and alkaline earth elements from the relevant heavy metals in sea water. The major advantage of this method is that sea-water samples can be transferred directly to the plastic bottle used in the preconcentration on Chelex-100. This step is carried out in a nearly closed system thereby eliminating the risk of sample contamination. In this closed system it is relatively simple to fit in an on-line plastic filter thus performing filtering experiments on sea water without the usual risk of contamination. The drawbacks are the use of relatively large amounts of reagents, an apparatus with many plastic fittings, and the necessity of careful flow control with each set of equipment.

The preconcentration method based on extraction with a mixture of ammonium pyrrolidinedithiocarbamate (APDC) and diethylammonium diethyldithiocarbamate (DDDC) as complexing agents and freon as solvent followed by back-extraction to an aqueous phase with nitric acid, was originally described by Danielsson et al. [5]. Nearly all experiments were done on synthetic sea water, but the utility of the method on real sea-water samples was later demonstrated [6, 7]. Advantages of this method are the few steps involved and the minimal use of reagents. The disadvantages are that some of the procedural steps are critical and that the method involves manual and very vigorous shaking which becomes tedious.

In the present paper, the techniques used with Chelex-100 preconcentration and with the APDC—DDDC—freon extraction are compared. The subsequent determinations of the trace elements Cd, Pb, Ni, Cu, and Zn in sea water are done by g.f.a.a.s. or by flame a.a.s. In addition, a comparison is made between these two methods for sea-water samples preconcentrated directly after sampling (on board ship) and with samples preserved by freezing only for subsequent preconcentration in the laboratory. The investigation was conducted during a cruise with "M/S Martin Knudsen" in April 1980.

EXPERIMENTAL

Apparatus

The Perkin-Elmer 5000 atomic absorption spectrometer used was equipped with a Perkin-Elmer 500 graphite furnace, an autosampler AS-40, and a D_2-background corrector. Instrumental settings were those generally recommended by the manufacturer, with only minor modifications. Perkin-Elmer hollow-cathode lamps were used for all elements. The sample volume pipetted by the autosampler AS-40 on to the graphite furnace was 20 μl. A standard single-slot burner head was used for the flame determination of zinc; background correction was used for the flame determination.

Preconcentration on Chelex-100

Reagents. The Chelex-100 resin was 200—400 mesh size (Bio-Rad Laboratories). The reagents were Merck Suprapur grade and dilutions were done with Millipore Q-grade water. Ammonium acetate buffer (7.5 M, pH 5.0)

was prepared by mixing ammonia liquor and anhydrous acetic acid, the pH being adjusted to 5.0 with concentrated nitric acid. A 1.0 M ammonium acetate buffer was prepared similarly with dilution. Solutions of 2.5 M and 1.5 M nitric acid and 2.0 M ammonia were prepared from the concentrated reagents. Dilution and mixing of reagents were done in acid-cleaned polyethylene bottles. All reagents were prepared in the laboratory, stored in polyethylene bottles in a freezer and thawed just before use.

Equipment. The equipment, shown in Fig. 1, is patterned after Kingston et al. [4]. A polyethylene bottle for the sea-water sample and the Chelex-100 separation column were mounted on a rack containing a total of 20 complete apparatuses. The rack was constructed from aluminium struts and PVC sheets. The distance between the polyethylene bottles and the Chelex-100 column was fixed, but chosen so that the free flow in all circumstances would be greater than the desired flow. This meant that a peristaltic pump had to be placed after the Chelex-100 column to provide flow restriction as required.

A 1-l polyethylene bottle served both as the container during pH adjustment and as the reservoir during preconcentration on the Chelex-100 resin.

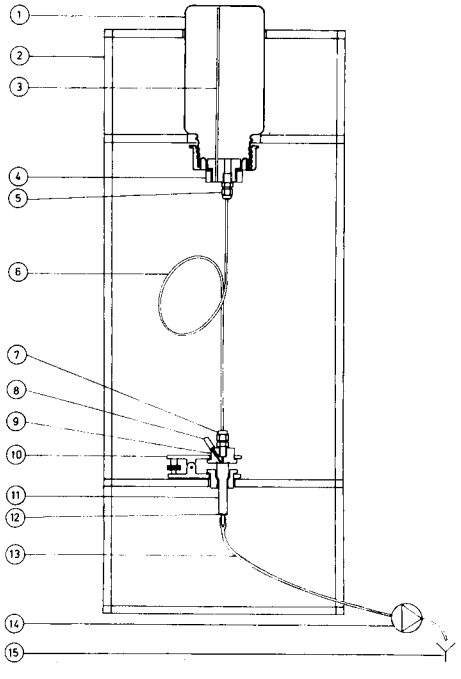

Fig. 1. Apparatus for Chelex-100 preconcentration: (1) Polyethylene bottle; (2) rack; (3) 3.2-mm teflon tubing; (4) lid with Delrin connector; (5) Swagelok fitting, teflon; (6) teflon tubing; (7) Swagelok fitting, teflon; (8) venting screw, Delrin; (9) upper part of entry port, Delrin; (10) clamp; (11) Isolab QS-Q polypropylene column; (12) polyethylene support; (13) silicone tubing; (14) multichannel pump; (15) waste.

The lid was modified by a Delrin connector (Delrin is a thermoplastic acetal resin). On this connector were mounted a 3.2-mm teflon tube for air venting (fixed mechanically) and a 3.2-mm teflon Swagelok fitting. The outlet was connected to the entry of the Chelex column by 3.2-mm teflon tubing with a teflon Swagelok fitting.

The Isolab QS-Q polypropylene column with porous polyethylene resin support was used for the Chelex-100 resin. On the upper part of the Delrin entry port for the Chelex-100 column is a venting screw (Delrin). The seal against the column is attained by a conical-shaped groove, thus expanding the column very slightly when held together by the clamp, and ensuring good sealing properties.

Only during the preconcentration step was the outlet from the column connected by silicone tubing to a multichannel pump. The pump acted as flow controller and/or flow restrictor.

Chelex-100 column preparation. The resin (200—400 mesh, sodium form) was slurried in a beaker with several large portions of 2.5 M nitric acid, rinsed several times by slurrying in Millipore Q-grade water to remove the excess of nitric acid, and finally transformed to the ammonium form by slurrying with 2.0 M ammonia solution. The column was then loaded nearly to the top with this slurry. The resin was next cleaned in the column by rinsing with Millipore Q-grade water, followed by 20 ml of 2.5 M nitric acid (resin transformed again to the hydrogen form), 10 ml of water, 15 ml of 2.0 M ammonia solution, and lastly 15 ml of water.

Columns, prepared at the laboratory before the cruise and stored under cool dark conditions, were sealed with the original seals from Isolab. Care was taken to seal all the columns "wet". On board ship, just before use, the columns were rinsed with 10 ml of water, 15 ml of 2.0 M ammonia solution, and 15 ml of water. The outlet of the column was sealed with a cap, and the column was mounted in the Delrin entry port and placed in the rack with teflon tubing and the modified lid for the polyethylene bottle.

Procedure for preconcentration on Chelex-100. Sea water was transferred directly from the sampler to the polyethylene bottle. The volume (normally 950—980 ml) was marked with a pen on the outside of the bottle only and measured after the preconcentration with a measuring cylinder. Acidity was adjusted to pH 5.0 with nitric acid and/or ammonia solution, and finally 0.5 ml of 7.5 M ammonium acetate buffer was added. The polyethylene bottle was screwed on the modified lid, inverted, and the air purged by means of the vent screw at the column entry port. The outlet from the column was then connected to the multichannel pump by the silicone tube. Care was taken to ensure that the flow rate was initially very slow (about 0.1 ml min^{-1}) to allow for shrinkage of the resin. When the shrinkage of all twenty Chelex-100 columns mounted in the rack had been completed, the multichannel pump was started and the process was left overnight at a flow rate of 1.0 ml min^{-1}.

After the sea water had passed through the Chelex-100 column, the entry port for the column was removed and replaced with a QS-R 12-ml poly-

ethylene extension funnel. Then 70 ml of 1.0 M ammonium acetate, added to the funnel by Finn pipette, was passed through the column, followed by 10 ml of water. The trace metals were eluted with 10 ml of 2.5 M nitric acid into 10-ml polyethylene bottles weighed previously.

Preconcentration by APDC—DDDC—freon extraction

Reagents. Freon TF (1,1,2-trichloro-1,2,2-trifluoroethane; Merck Uvasol) was used without purification.

Purified 1% APDC—DDDC solution was prepared by weighing 1.0 g of APDC and 1.0 g of DDDC into a 100-ml polyethylene bottle. Just before use, the complexing agents were dissolved in 100 ml of Millipore Q-grade water and purified by repeated extraction with 100 ml of freon in a separating funnel. The mixture of complexing agents was dissolved and purified just before use.

For the purified 0.5 M citrate buffer, citric acid was dissolved in water and the pH was adjusted to 5.0 by adding 10 M sodium hydroxide. This buffer was then purified by repeated extraction of 200-ml portions with 3 ml of 1% APDC—DDDC and 50 ml of freon. The purity was checked and the citrate buffer was stored in a freezer in a polyethylene bottle and first thawed on board the ship.

The 0.9 M hydrochloric acid was prepared by diluting the concentrated Merck Suprapur acid.

Procedure for APDC—DDDC—freon extraction. Sea water (500 ml) in a separating funnel (pyrex, teflon stopcock, polyethylene stopper) was adjusted to pH 5 with 0.9 M hydrochloric acid and/or 1 M sodium hydroxide. Then 3 ml of purified 0.5 M citrate buffer, 5 ml of purified 1% APDC—DDDC, and 20 ml of freon were added. The funnel was shaken vigorously for 180 s. The phases were allowed to separate and the lower phase, except for a few drops, was drained into a 50-ml polyethylene bottle. An additional 10 ml of freon was added to the funnel, and shaken repeatedly for 60 s. The lower phase was combined with the first extract. To the combined freon extracts 0.5 ml of concentrated nitric acid (Merck Suprapur) was added. The polyethylene bottle was closed tightly, shaken vigorously for 30 s, and allowed to stand for at least 5 min. Finally 10 ml of water was added and the phases were shaken vigorously for 30 s. After standing for phase separation, the upper phase was sucked out by means of a Finn-pipette directly from the 50-ml polyethylene bottle into a 25- or 10-ml polyethylene bottle and closed tightly.

This procedure was derived from the recommended procedure presented by Danielsson et al. [5] and was found from preliminary experiments to give more consistent results. Although the differences between the two procedures may seem to be minor, the effect measured in terms of recovery was very clear.

Cleaning procedures

All glass, polyethylene, polypropylene, and teflon equipment was cleaned by soaking it for at least one day (though more typically 1—2 weeks) in 7 M nitric acid and rinsing with Millipore Q-grade water, and stored in polyethylene containers in plastic bags. Delrin plastic parts were carefully rinsed several times with 2 M hydrochloric acid followed by Millipore Q-grade water.

The sea-water sampler has been used for several years and has always been stored under clean conditions so that rinsing several times in sea water was found to be adequate.

Additions of reagents and dilutions at sea and in the laboratory were made by extensive use of the adjustable Finn pipette. Disposable tips for these pipettes and plastic cups for the AS-40 autosampler were cleaned in the same manner as the equipment. Smoking was prohibited in the preconcentration area because of the risk of cadmium contamination. No equipment or laboratory aids had been used before except for sea-water analysis.

On board ship, the equipment used was cleaned either by soaking in Millipore Q-grade water or simply by rinsing with sea water.

Collection method

Sea-water samples were collected with a 4-l Delrin sampler (Oceanographic). Wire and contraweight were plastic-coated. The sampler was operated from the ship without other arrangements than a standard winch. Eleven sampling positions were spread over the northern Lille Belt to the east of Fredericia on mainland Denmark and northwest of Fyn Island and five sampling positions were in the more southerly Lille Belt area which is monitored by The National Agency of Environment Protection [8]. Sampling depth was generally of the order of 10—15 m (varying from 5 to 30 m), well above the bottom of the sea. The salinity at all positions was alike, generally 20—22‰, indicating average conditions.

Standards for a.a.s. measurements and spiking

Stock standard solutions (1000 mg l^{-1}) were prepared from Merck Titrisol. Intermediate solutions were prepared by dilution. Working standards were prepared daily. All standards used for graphite furnace measurements contained the same amount of nitric acid as the preconcentrated sea-water samples. Thus samples preconcentrated on Chelex-100 resin were eluted with 2.5 M nitric acid, but because of ion exchange the eluates corresponded to 1.5 M nitric acid. For samples preconcentrated by extraction, the standards were adjusted by adding 0.5 ml of concentrated nitric acid per 10 ml of working standard.

Typically, the working range used for g.f.a.a.s. measurements was 0—1.5 μg Cd l^{-1}, 0—50 (35) μg Pb l^{-1}, 0—100 μg Ni l^{-1}, and 0—50 (100) μg Cu l^{-1}.

During g.f.a.a.s. measurements, the signals of the working standards were checked periodically. Normally a slight decrease in signals was observed after approximately 50 firings. If the decrease or change was less than 10%, cal-

culations were based on the assumption that change in signals was equally distributed on firings between standards and a "moving average" was used. If the signal change was greater than 10%, samples were measured again.

The mixed standard used for spiking contained 2 μg Cd l^{-1}, 50 μg Pb l^{-1}, 100 μg Ni l^{-1}, and 100 μg Cu l^{-1}. The spiking solution was preserved by adding 5 ml of concentrated nitric acid per 100 ml. The spiking solution (10 ml) was added to sea water prior to preconcentration by Chelex-100; only 5 ml was used for preconcentration by extraction. The spiking solution was always analysed after appropriate dilution, together with normal working standards, as an extra check. Two independent spiking solutions were prepared for each method of preconcentration.

RESULTS AND DISCUSSION

The results for unfiltered sea water by APDC—DDDC—freon extraction and by Chelex-100 preconcentration are visualized as histograms in Figs. 2—6. In these histograms, outliers have not been excluded because in comparing methods it is very important to obtain an impression of probable contaminated samples, which must be excluded before data evaluation. Hatched blocks denote results for samples preconcentrated on board ship, while blank blocks denote results for samples frozen after collection and preconcentrated after the cruise under normal laboratory conditions.

As no significant differences in the trace metal concentrations of samples from different positions over the sampling area could be detected from the data, the results of the analyses are treated as if the sea water had been sampled from one uniform portion. Data evaluation is presented in Table 1. In Table 2 are given results from recovery experiments.

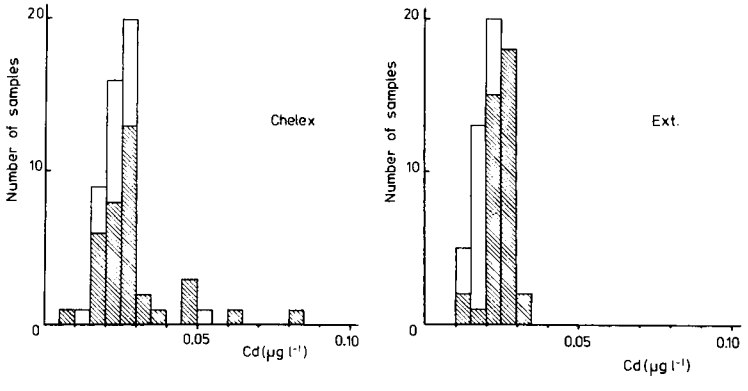

Fig. 2. Histogram of cadmium concentrations of samples by Chelex-100 (Chelex) and by extraction (Ext.). Hatched blocks denote samples preconcentrated on board the ship; blank blocks denote samples preconcentrated at the laboratory after the cruise.

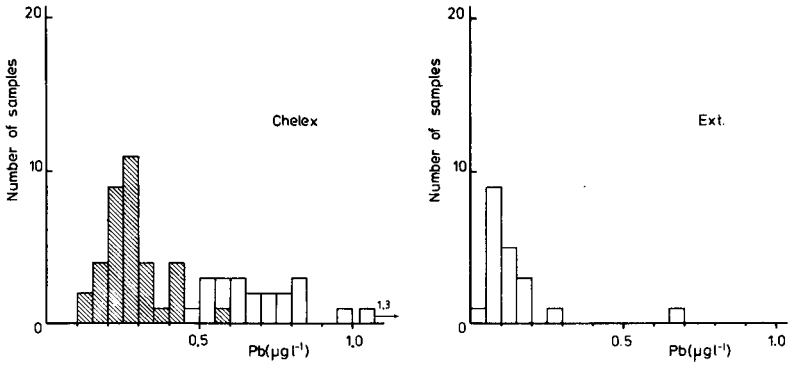

Fig. 3. Histogram of lead concentrations (refer to Fig. 2).

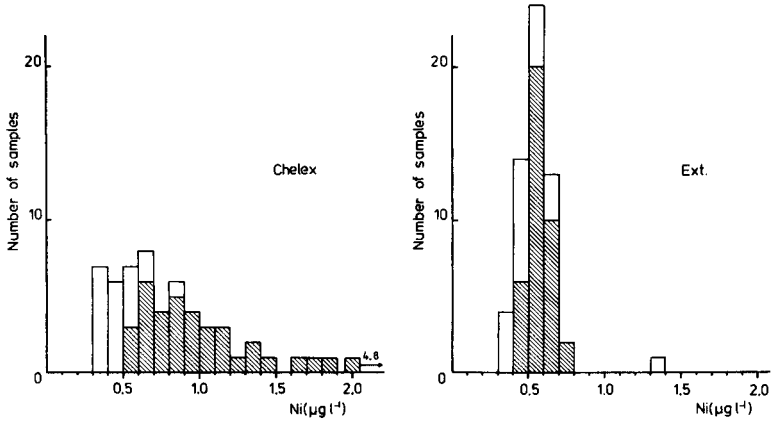

Fig. 4. Histogram of nickel concentrations (refer to Fig. 2).

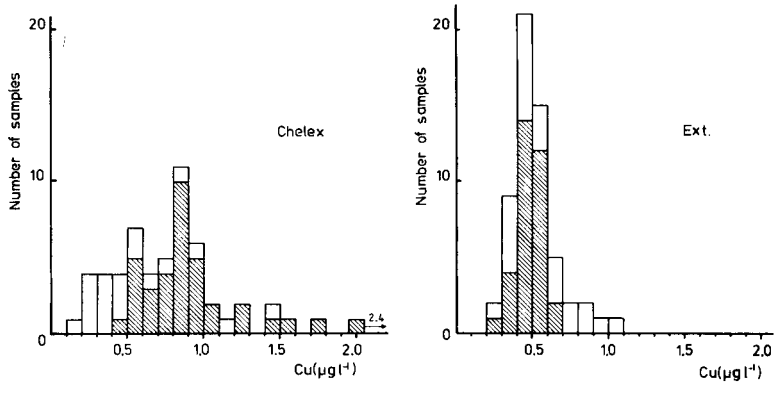

Fig. 5. Histogram of copper concentrations (refer to Fig. 2).

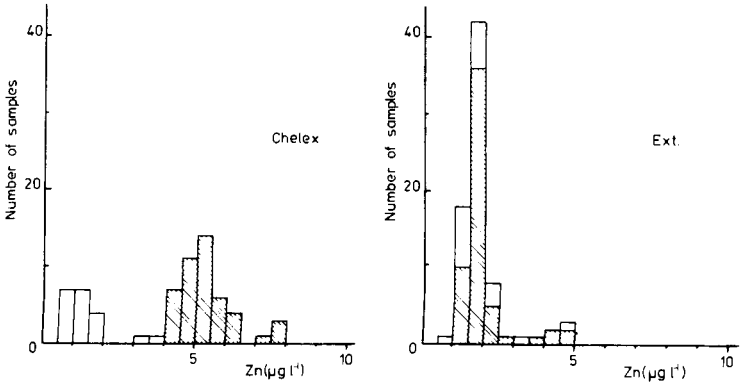

Fig. 6. Histogram of zinc concentrations (refer to Fig. 2).

Cadmium

The average cadmium concentration in the sea water tested seems to be 0.018—0.025 $\mu g\ l^{-1}$, with 0.024 μg Cd as the most probable average value. There is excellent agreement between the two methods of preconcentration both under field and laboratory conditions, though the results "at lab" tend to be slightly but insignificantly lower.

For data evaluation, six results were discarded from the Chelex-100 preconcentration whereas no results were discarded for the APDC—DDDC—freon method. During the cruise sea-water samples were spiked with 0.020 μg Cd l^{-1} corresponding to an amount quite close to the original cadmium content (Table 2). Based on 19 spiked samples with the extraction and on 10 with Chelex-100 preconcentration method, recoveries of 93% and 91%, respectively, were achieved.

The precision of the two methods was derived from replicate samples and calculated as the pooled standard deviation. Based on 38 samples with the

TABLE 1

Comparison of preconcentration methods for trace metals in sea water (All data are given in $\mu g\ l^{-1}$)

Preconcentration		Cd	Pb	Ni	Cu	Zn
		Mean ± s.d. (n)[a]	Mean ± s.d. (n)	Mean ± s.d. (n)	Mean ± s.d. (n)	Mean ± s.d. (n)
Method	Place					
Ext.	at sea[b]	0.025 ± 0.004 (38)	—	0.57 ± 0.08 (38)	0.52 ± 0.16 (38)	1.9 ± 0.7 (56)
Ext.	at lab[b]	0.018 ± 0.003 (20)	0.12 ± 0.06 (19)	0.49 ± 0.11 (19)	0.50 ± 0.15 (20)	1.7 ± 0.9 (20)
Chelex	at sea[b]	0.024 ± 0.005 (31)	0.26 ± 0.08 (35)	0.96 ± 0.34 (35)	0.87 ± 0.28 (35)	5.3 ± 0.9 (46)
Chelex	at lab[b]	0.023 ± 0.004 (19)	0.68 ± 0.14 (19)	0.47 ± 0.12 (20)	0.54 ± 0.34 (20)	1.4 ± 0.8 (20)

[a]Mean ± s.d. (standard deviation) and the total number (n) of samples included in the statistical treatment. [b]"At sea" means that samples were processed on board immediately after sampling. "At lab" denotes that samples were frozen after sampling, stored in a freezer, and preconcentrated at the laboratory about three weeks after sampling.

TABLE 2

Recovery of trace metals from spiked sea water by the two methods of preconcentration (Sea-water samples were spiked and preconcentrated on board ship)

Element	Method	Present[a] ($\mu g\ l^{-1}$)	Added ($\mu g\ l^{-1}$)	Found Mean ± s.d.[c] ($\mu g\ l^{-1}$)	Recovery (average) (%)
Cd	Ext.	0.025	0.020	0.042 ± 0.005	93
	Chelex	0.024	0.020	0.040 ± 0.004	91
Pb	Ext.	0.12[b]	0.50	0.65 ± 0.12	105
	Chelex	0.26	0.50	0.62 ± 0.08	82
Ni	Ext.	0.57	1.00	1.51 ± 0.08	96
	Chelex	0.96	1.00	2.78 ± 0.51	142
Cu	Ext.	0.52	1.00	1.52 ± 0.08	100
	Chelex	0.87	1.00	2.01 ± 0.59	107

[a] Values taken from the average of all sea-water samples preconcentrated on board ship. [b] Data from sea-water samples preconcentrated at the laboratory (see text). [c] Mean ± s.d. (standard deviation) for Ext. (extraction) and Chelex were calculated from 19 and 10 spiked samples, respectively.

extraction and on 31 with the Chelex-100 preconcentration method, the relative standard deviations were 7% and 11%, respectively (Table 3). Thus the two methods of preconcentration are equal with respect to average value for cadmium concentration, recovery and precision. Bearing in mind that the two methods involve entirely different types of reagents and that the natures of the preconcentrations are different, it is very unlikely that the average values obtained are biased. Both methods, therefore, function well for cadmium determination in sea water.

In the Kattegat and the eastern Baltic Sea, Magnusson and Westerlund [6] found 0.03—0.06 μg Cd l^{-1}. This is somewhat higher than the data presented here, though a proper comparison is not possible because of the much lower salinity in that part of the Baltic Sea. In the western part of the Baltic Sea, Schmidt [9] found his "data clustering around about 0.02 μg Cd l^{-1}", which is in excellent agreement with the present data.

TABLE 3

Estimated precision for trace metals in sea water by the two methods of preconcentration [Relative standard deviations (%) from replicate determinations. In the calculations, only samples preconcentrated on board ship were considered, except for lead (see text).]

Method	Cd	Pb	Ni	Cu	Zn
Ext.	7	31	5	12	13
Chelex	11	33	24	27	10

Lead

After the cruise, the hydrochloric acid that had been used for pH adjustment of sea water was found to be contaminated by lead. Therefore, all preconcentrations by extraction on board the ship were discarded, except those spiked with trace metals because the spiking solution was preserved with nitric acid thus eliminating the need for another acid for pH adjustment. No lead was found in the hydrochloric acid used with the Chelex-100 preconcentration.

The lead concentration in the sea water (at the laboratory) was 0.12 μg Pb l^{-1} based on the extraction method, while Chelex-100 preconcentration on board indicated a level of 0.26 μg Pb l^{-1} and under laboratory conditions 0.68 μg Pb l^{-1}. The clear shift in concentration level shown by the latter result indicates reagent contamination. The results obtained on spiked samples (Table 2) indicate recoveries of 105% and 82%, respectively, for preconcentration by extraction and by Chelex-100. The corresponding precisions expressed as pooled relative standard deviations for replicate samples were 31% and 33% (Table 3). Even though the spiking chosen for lead is high compared with original lead concentrations, the average lead present is not consistent. Because ionic lead was used for spiking, it is tempting to conclude that lead in sea water is present in at least two different available forms, thereby giving different averages for natural sea water and satisfactory recoveries. The present data do not provide clear evidence for the true available lead concentrations, and it seems likely that these differences in lead concentration reflect the considerable amount of reagents used in the Chelex-100 method, rather than a true speciation. Thus the average lead concentration is probably of the order of 0.12 μg Pb l^{-1}, or even lower, which is similar to results obtained for the eastern part of the Baltic Sea [6].

Nickel

The average nickel concentrations, based on samples preconcentrated on board and at the laboratory, were 0.57 μg Ni l^{-1} and 0.49 μg Ni l^{-1}, respectively. These levels are consistent with samples preconcentrated at the laboratory with Chelex-100, i.e., 0.47 μg Ni l^{-1}, whereas samples preconcentrated on board showed great dispersion (Fig. 4). Results for spiked samples (Table 2) indicated a mean recovery of 96% by extraction, while the recovery by Chelex-100 preconcentration was 142%. The corresponding precisions (pooled relative standard deviations) were 5% and 24%, respectively (Table 3). The differences in the average nickel concentrations by the two methods can clearly be explained by an undetected reagent contamination.

Considering the differences in salinity, the average nickel concentration of 0.6—0.9 μg Ni l^{-1} found by Magnusson and Westerlund [6] in the eastern Baltic Sea, is in fair agreement with the concentration found here, 0.5—0.6 μg Ni l^{-1}. In the western Baltic Sea, Schmidt [9] found nickel contents in the range 0.2—1.2 μg Ni l^{-1}; the data presented here showed clustering around the average.

Copper

The average copper concentrations obtained are similar to the results for nickel. Samples preconcentrated by extraction on board and at the laboratory contained 0.52 μg Cu l^{-1} and 0.50 μg Cu l^{-1}, respectively. These results are in fine agreement with those for samples preconcentrated by Chelex-100 at the laboratory (0.54 μg Cu l^{-1}) whereas samples preconcentrated on board were probably contaminated by one of the reagents used, showing 0.87 μg Cu l^{-1}. The dispersion for copper is somewhat greater than the nickel dispersion, which may mean that copper is more unevenly distributed in the mass of sea water than nickel, or it might mean that copper presents a greater analytical problem than one might expect. Spiked samples (Table 2) indicated recoveries of 100% and 107%, respectively, for preconcentration by extraction and by Chelex-100. The corresponding pooled standard deviations were 12% and 27%, respectively (Table 3), the latter results indicating a problem similar to that found with lead.

Although the present data do not provide clear evidence for the true available copper concentration, it is unlikely that they reflect speciation problems because ionic copper is tightly bound by the Chelex resin making it difficult to elute and recover quantitatively. Magnusson and Westerlund [6] found average copper concentrations of 0.6—1.0 μg Cu l^{-1} in the eastern Baltic Sea, which is somewhat higher than the present average of 0.52 μg Cu l^{-1}. In the western Baltic Sea, Schmidt [9] found values in the range 0.3—1.2 μg Cu l^{-1}.

Zinc

The average zinc concentrations found in the sea water based on extraction on board and at the laboratory, and by Chelex-100 at the laboratory, were 1.9 μg Zn l^{-1}, 1.7 μg Zn l^{-1}, and 1.4 μg Zn l^{-1}, respectively. The reagents used with Chelex-100 on board contained an undetected contaminant. No spiking experiments were done. The precision of the two methods based on pooled standard deviations for replicate samples were 13% for extraction and 10% for Chelex-100.

Data from the eastern Baltic Sea [6] were in the range 1.5—3.5 μg Zn l^{-1}, whereas the present results were 1.4—1.9 μg Zn l^{-1}.

Filtering experiments with Chelex-100

Filtering experiments were done only with the Chelex-100 method because it is easy to establish contamination-free conditions, i.e., freedom from dust and other foreign particles. For the filtering experiments, a standard Millipore filter holder was simply screwed into the teflon tubing as shown in Fig. 1; a Millipore HA, 0.45 μm, was used.

The results from seven replicate experiments are shown in Table 4. There was no significant tendency for metal to be removed by membrane filtration. Even though the average values for lead, nickel, copper, and zinc are biased, the means for cadmium are not.

TABLE 4

Filtering experiments with Chelex-100 preconcentration
(Concs. are given in $\mu g\ l^{-1}$)

	Cd Mean ± s.d.	Pb Mean ± s.d.	Ni Mean ± s.d.	Cu Mean ± s.d.	Zn Mean ± s.d.
Unfiltered[a]	0.024 ± 0.005	0.26 ± 0.08	0.96 ± 0.34	0.87 ± 0.28	5.3 ± 0.9
Filtered[b]	0.022 ± 0.003	0.27 ± 0.06	0.79 ± 0.11	1.22 ± 0.27	5.8 ± 0.7

[a] All samples preconcentrated on board ship by the Chelex method. [b] Calculated from seven samples taken at one sampling position.

Blank values

It is not clear why only cadmium should have been relatively easy to determine without contamination problems. Rigorous cleaning procedures and checking of reagents as potential sources of contamination, such as have been described by Smith and Windom [10] are applied regularly, yet reliable blank values are very difficult to obtain. Smith and Windom [10] used pre-extracted sea water to establish blank values, whereas Danielsson et al. [5] determined reagent blank and total blank; total blank was defined as the metal found when the reagents used were poured into the separatory funnel as in the normal extraction procedure. Kingston et al. [4] demonstrated excellent recoveries from their radiochemical tracer study but only stated the blank values for the Chelex-100 procedure. Davey and Soper [3] used a double Chelex technique where the first column served for preconcentration and the following column for the blank and standard matrix.

Because a synthetic sea-water sample free from trace metals cannot be prepared for blank determinations, it becomes necessary to choose between estimating reagent blanks and so probably underestimating the true blanks because real sample manipulations are not included, or using pre-extracted sea water (solvent extraction or ion exchange) and so overestimating the true blank values. This last point seems not to be widely realised yet, but is rather elementary: the theoretical maximum recovery is 100% whereas even a good procedure for trace metals will usually give recoveries of only 90%. Adding reagents to an extracted sample and re-extracting the trace metals will then produce 9% of the original amount. Results corrected for blanks in this way will clearly be underestimates.

The importance of the blank values can be assessed, as in the present work, by using quite different methods of preconcentration with different reagents. However, as demonstrated, it proved very difficult to achieve consistent results, which were obtained only for cadmium. Blank values, in this work, were estimated only by extraction of Millipore Q-grade water with APDC—DDDC—freon on a few samples and are to be considered only as a guide line. Blank values by this method were found to be 0.0011 μg Cd l^{-1}, $<0.021\ \mu g$ Pb l^{-1}, $<0.05\ \mu g$ Ni l^{-1}, $0.024\ \mu g$ Cu l^{-1}, and $0.24\ \mu g$ Zn l^{-1}.

Conclusion

When the different methods of preconcentration were used, consistent and reliable results were obtained only for cadmium. No significant differences were observed between samples preconcentrated directly after sampling on board and samples frozen and then preconcentrated some weeks after sampling. Preconcentration by the extraction procedure described proved to be more reliable and robust than the Chelex-100 procedure.

The author thanks Per Eichner for his comments and for the company's permission to publish this work, Pia Eigil and Uffe Hald for practical assistance, and Michael Fischer for construction of the equipment.

REFERENCES

1 J. P. Riley and D. Taylor, Anal. Chim. Acta, 40 (1968) 479.
2 E. W. Davey, J. H. Gentile, S. J. Erickson and P. Betzer, Limnol. Oceanogr., 15 (1970) 486.
3 E. W. Davey and A. E. Soper, Limnol. Oceanogr., 20 (1975) 1019.
4 H. M. Kingston, I. L. Barnes, T. J. Brady, T. C. Rains and M. A. Champ, Anal. Chem., 50 (1978) 2064.
5 L. G. Danielsson, B. Magnusson and S. Westerlund, Anal. Chim. Acta, 98 (1978) 47.
6 B. Magnusson and S. Westerlund, Mar. Chem., 8 (1980) 231.
7 L. G. Danielsson, Mar. Chem., 8 (1980) 199.
8 The Belt Project, The National Agency of Environmental Protection, Denmark, January 1980.
9 D. Schmidt, Helgoländer Meeresuntersuchungen, 33 (1980) 576; 14th European Marine Biology Symposium 1979, in O. Kinne and H. P. Bulnhien (Eds.) Protection of Life in the Sea, Helgoland 23—29 Sept. 1979.
10 R. G. Smith, Jr. and H. L. Windom, Anal. Chim. Acta, 113 (1980) 39.

Analytica Chimica Acta, 125 (1981) 131—137
Elsevier Scientific Publishing Company, Amsterdam — Printed in The Netherlands

THE EFFECT OF WASHING PROCEDURES ON TRACE ELEMENT CONTENT OF HUMAN HAIR†

SEPPO SALMELA*, ERKKI VUORI and JUKKA O. KILPIÖ[a]

Department of Public Health Science, University of Helsinki, Haartmaninkatu 3, SF-00290 Helsinki 29 (Finland)

(Received 23rd September 1980)

SUMMARY

The effects of four washing procedures on the concentrations of manganese, iron, copper, zinc and cadmium and were investigated for three pooled samples of human head hair. The solutions evaluated were a non-ionic detergent (Triton X-100), an ionic detergent (sodium lauryl sulfate), acetone and a complexing agent (EDTA). The results indicate that for every element determined there is a level below which the concentration cannot be reduced by further washings. The numbers of washings required to reach these levels vary considerably. This effect must be considered in the trace element analysis of hair.

In trace element analyses of human head hair, interest is usually focused on the endogenous trace elements. Because grease and dust on the surface of hair may contribute most of the element concentrations of hair, the hair sample must be washed. The importance of a standardized washing procedure is widely acknowledged. Nevertheless, different laboratories use different washing procedures and there is no consensus on how the washing should be done [1, 2]. For example, the following washing solutions with variable volumes and washing times have been used: distilled water, ionic or nonionic detergents, combinations of aqueous detergents and organic solvents, chelating agents and even mineral acids. However, the effects of washing procedures have been stated to differ [3—9]. Moreover, mammalian hair may continue to lose material for an indefinite number of washes [10]. It has been emphasized that washing experiments should be performed for various but fixed periods of time [9]. The problem in hair analysis, therefore, is not the reliability of the measurement but the preparation of the hair samples [11]. This is a source of discrepancy between the results of various workers.

The purpose of this study was to investigate systematically the effects of different washing procedures and successive washings on the concentrations of manganese, iron, copper, zinc and cadmium in human scalp hair.

---

†Presented in part at the 27th IUPAC Congress, Helsinki, Finland, 1979.
[a]Present address: Labsystems Oy, Pulttitie 9, SF-00810 Helsinki 81, Finland.

EXPERIMENTAL

Samples

The effects of different procedures were studied with head hair obtained from three females. The hair had had no chemical treatment except ordinary shampoo washing. Each sample was homogenized by cutting it into small pieces (2—3 mm) and by mixing with a glass rod on a filter paper. The homogenized samples were numbered as hair pools 1, 2 and 3, which will be cited in the text. The weights of the hair pools were 25, 25 and 10 g, respectively.

Procedures

Four different washing procedures were selected. An organic solvent wash (acetone, Merck), a complex-forming agent (1% disodium EDTA, Merck), an ionic detergent (1% sodium lauryl sulfate, BDH) and a nonionic detergent (1% Triton X-100, BDH). The washings were done in a 50-ml test tube fitted with a ground-glass stopper on a three-dimensional mechanical shaker (Desaga, Heidelberg) at the minimum available speed at room temperature. Each wash period was 20 min and the amount of washing agent was 30 ml. The first step in the washing procedures, except in the acetone wash, was a hexane (95%, J. T. Baker) rinse (20 min, 30 ml) in order to remove surface grease.

Six 600-mg portions of hair were weighed. After the hexane rinse, the samples were allowed to dry at 75°C to remove the hexane. Five of them were then washed successively 1, 2, 4, 8 and 12 times with the selected wash solution, rinsed with deionized water until a clear solution was obtained, and allowed to dry at 105°C. Each sample was divided into two equal portions, weighed, dry-ashed at 450°C, dissolved in 2 M nitric acid and diluted with deionized water to give 1 M HNO_3 solutions. Concentrations were measured (Table 1) by atomic absorption spectrometry utilizing both flame and graphite furnace techniques (Perkin—Elmer 300 and HGA-2100 with deuterium background correction). The final concentration in the hair after each washing step was calculated as the arithmetic mean of the duplicate ashed samples.

RESULTS

The precision of the analytical method was checked by making 6—10 parallel determinations for each element from each unwashed hair pool. The results (Table 1) showed good precision. Literature reports indicate that loss of zinc and cadmium during ashing at 450°C is negligible [12—14]. The precision of each wash method was checked by performing duplicate washings for hair pool 1. The agreement between duplicate results was excellent, so that further duplicate washings were regarded as unnecessary.

The effects of the four washing procedures on the concentrations of iron, zinc, manganese and cadmium in hair pool 1 are presented in Fig. 1. The copper determinations of this hair pool had to be rejected because of slight

TABLE 1

Concentration of trace metals in each hair pool before and after 12 successive acetone washes[a]

Element	Hair pool 1 ($\mu g\ g^{-1}$)		Hair pool 2 ($\mu g\ g^{-1}$)		Hair pool 3[b] ($\mu g\ g^{-1}$)	
	Unwashed ($n = 6$)	After 12 washes	Unwashed ($n = 10$)	After 12 washes	Unwashed ($n = 6$)	After 12 washes
Mn	3.89[c] (3.7)[e]	2.74[c]	1.41[d] (8.2)	1.16[d]	1.83[d] (8.5)	1.25[d]
Fe[c]	19.0 (5.8)	9.8	19.0 (5.5)	9.6	13.8 (5.9)	11.4
Cu[c]	—	—	40.6 (3.0)	40.3	12.8 (3.0)	10.4
Zn[c]	568 (2.2)	406	138 (2.0)	130	94.5 (2.0)	94.3
Cd[d]	1.18 (2.9)	0.87	1.03 (5.4)	0.18	5.11 (3.5)	0.43

[a]I.A.E.A. procedure (see text). [b]Sodium lauryl sulfate wash. [c]Flame technique. [d]Graphite furnace. [e]Relative standard deviation (%) in parentheses.

contamination from the porcelain crucibles during the dry ashing stage. In the analysis of hair pools 2 and 3, quartz crucibles were used and no copper contamination was apparent. The acetone wash proved least effective; EDTA was somewhat stronger but the two detergents were strongest. After 1–4 washings a constant trace metal level was reached, which greatly depended on the washing procedure used. The difference between the acetone and the detergent washes was, at most, about 40% (for manganese and cadmium). There was a continuously slightly decreasing trend in the Triton X-100 wash for zinc, manganese and cadmium, in the sodium lauryl sulfate wash for zinc and manganese, and in the acetone wash for zinc.

The effects of washing on the concentrations of the five elements in hair pool 2 are presented in Fig. 2. Here the procedures are equally effective except for manganese, for which the acetone wash was significantly less effective than the others. For cadmium, there was no difference between the washing methods, and the level remained the same as after the hexane rinse, even after twelve washings. In all cases where the concentration became constant, this level was reached after no more than four washings.

Only the effect of sodium lauryl sulfate washing was investigated in hair pool 3 (Fig. 3), because of the small size of this hair pool. Figure 3 also shows that this particular method removed different amounts of different elements, varying from zero (Zn) to 90% (Cd) in hair pool 3, as for the other hair samples. Again, a constant level was reached after not more than four washings (Fe).

Figure 4 presents the effect of the sodium lauryl sulfate wash on cadmium concentrations in the three hair pools. For pool 1 the washes removed about 55% of the initial cadmium; this was achieved after about four washes.

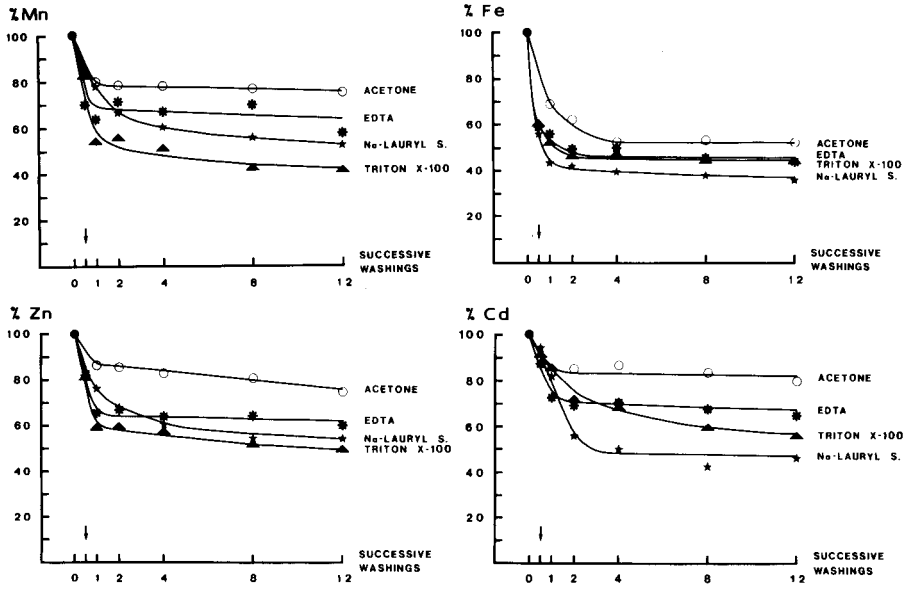

Fig. 1. The percentages of the trace elements remaining in hair pool 1 after each wash. The arrow indicates the hexane rinse.

For pool 2 a constant level was reached after the hexane rinse, and successive washings with sodium lauryl sulfate had no effect on the cadmium content. A third kind of effect was seen in hair pool 3. The hexane rinse removed about 5% of the cadmium, but after a single wash with sodium lauryl sulfate only about 10% of the initial cadmium content of the hair, remained. This level remained constant on further washing.

DISCUSSION

The repetitive results obtained with the parallel determinations of the unwashed hair pools demonstrate that the pools were homogeneous. These results support the recommendation of Hilderbrand and White [7] that the hair should be cut into short pieces ($\leqslant$0.5 cm) to obtain a representative sample.

The problem in washing hair samples is to separate the internal (endogenous) and external (exogenous) trace elements. Chittleborough [15] outlined and supported a no-wash policy, which is well suited to forensic and environmental purposes, but not appropriate for scrutinizing the biomedical or metabolic history of the individual.

Most pretreatments mentioned in the literature may roughly be divided into three categories: organic solvents, detergents, and complex-forming agents. The present selection thus included an organic solvent, an ionic and a nonionic detergent, and a complex-forming agent. This study does not reveal which of the four washing procedures, if any, is the ideal one, i.e.

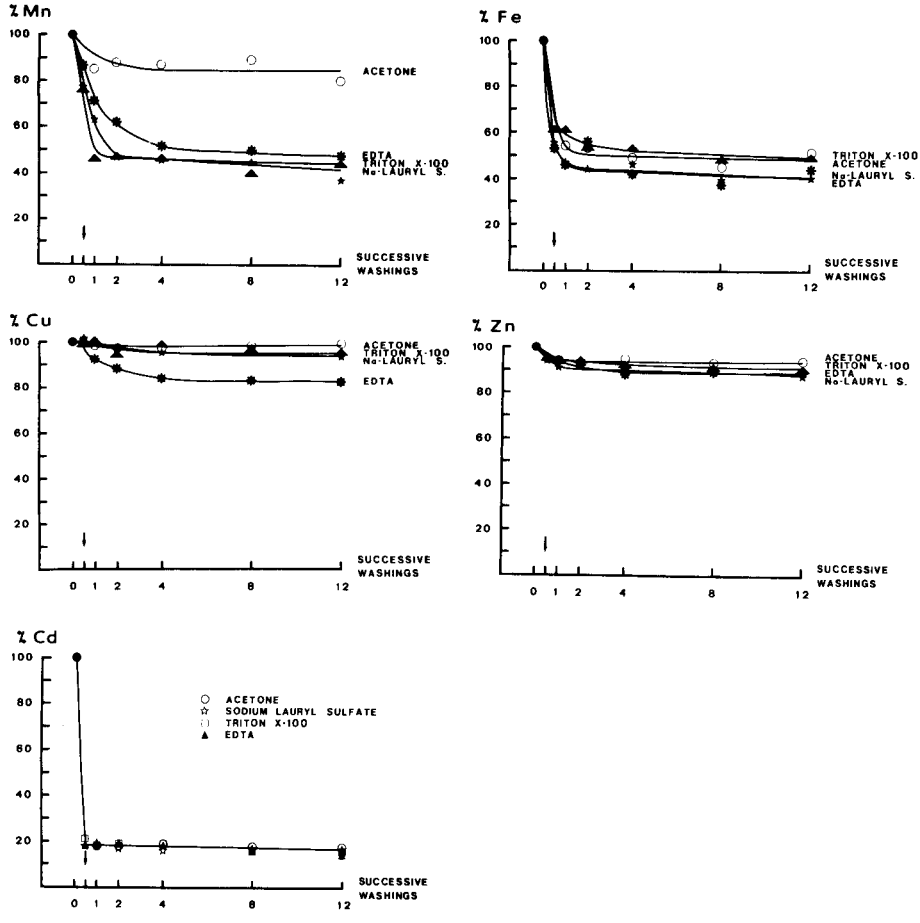

Fig. 2. The percentages of the trace elements remaining in hair pool 2 after each wash. The arrow indicates the hexane rinse.

removes only the external contamination and leaves the structure unchanged. The results indicate that for every element determined there is a level below which the concentration cannot be reduced by further washing. For every element, however, this level is strongly dependent on the washing procedure used.

The results for cadmium in hair pools 1 and 2 represent extreme possibilities. First, the percentage of the element remaining after each wash in hair pool 1 was less than 50% with sodium lauryl sulfate and was about 85% for the acetone wash, i.e. the results obtained with the acetone wash would be more than 50% higher than the results obtained with sodium lauryl sulfate wash, provided that the levels mentioned above are reached (Fig. 1). Secondly, the percentage of the element remaining after washing is independent of the wash procedure used in hair pool 2 (Fig. 2). The acetone wash removes the least of the trace element content of the two hair pools.

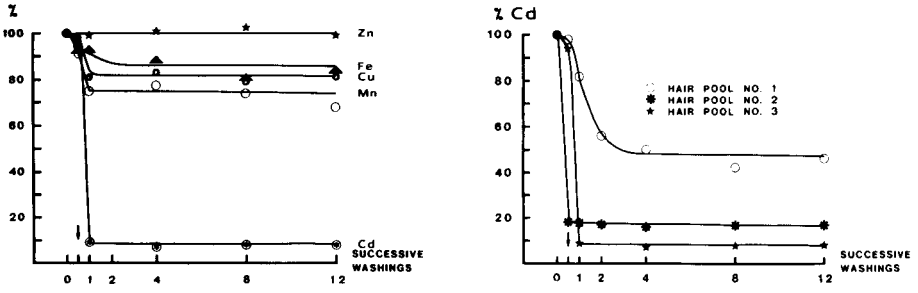

Fig. 3. The percentages of the trace elements remaining after each sodium lauryl sulfate wash for hair pool 3.

Fig. 4. The percentage of cadmium remaining after each sodium lauryl sulfate wash for different hair pools.

The difference between the acetone and other methods is clearest in hair pool 1, but the difference between the washing effects is dramatic for manganese in hair pool 2. According to the present results it seems reasonable to state that the acetone wash cannot be used as a standard method in the pretreatment of human head hair, although this principle has been recommended by the International Atomic Energy Agency (I.A.E.A.) for neutron activation analysis (5—20 mg of hair in 10-min contacts with 25-ml portions of acetone, water, water, water and acetone, successively [16]).

The number of washes required to reach constant trace element levels also varies considerably. In hair pool 1 after the hexane rinse and four successive washes with washing agent, constant levels are reached for all elements. In hair pool 2, a constant level is already reached for cadmium after the hexane rinse, but in some cases four washes are still needed (EDTA for Mn and Cu).

The present results reveal two washing parameters which affect the efficiency of the pretreatment of human head hair, i.e., the washing agent and the number of successive washes. The effects of these parameters reflect the nature of different contaminants or different leaching speeds for human head hair. When data obtained from different laboratories are compared, the results should be interpreted with the greatest caution, because the effect of washing time has not been taken into consideration. This may even invalidate the comparison of values obtained by the same technique, contrary to the statement of Shapcott [9].

In conclusion, it seems reasonable that an additional criterion be recommended as a prerequisite in the pretreatment of human hair: that the duration of washing should be so long that further washes do not change the concentration of the element to be determined. The leaching effect may occur in all the washing methods used, and this should be investigated.

REFERENCES

1 T. H. Maugh, II, Science, 202 (1978) 1271.
2 K. Nishiyama and G. F. Nordberg, Arch. Environ. Health, 25 (1972) 92.
3 L. C. Bate, J. Forensic Sci., 10 (1965) 60.
4 R. F. Coleman, Modern Trends in Activation Analysis, International Conference Proceedings, Texas A. and M. University, 1966, p. 302.
5 W. W. Harrison, J. P. Yurachek and C. A. Benson, Clin. Chim. Acta, 23 (1969) 83.
6 K. M. Hambidge, M. L. Franklin and M. A. Jacobs, Am. J. Clin. Nutr., 25 (1972) 384.
7 D. C. Hilderbrand and D. H. White, Clin. Chem., 20 (1974) 148.
8 G. S. Assarian and D. Oberleas, Clin. Chem., 23 (1977) 1771.
9 D. Shapcott, Clin. Chem., 24 (1978) 391.
10 H. J. M. Bowen, Trace elements in Biochemistry, Academic Press, London, 1976, p. 61.
11 C. R. Alvarez, Am. J. Med. Techn., 44 (1978) 1011.
12 T. T. Gorsuch, Analyst, 84 (1959) 135; The Destruction of Organic Matter, Pergamon, Oxford, 1970.
13 J. G. van Raaphorst, A. W. van Weers and H. M. Haremaker, Analyst, 99 (1974) 523.
14 S. R. Koirtyohann and C. A. Hopkins, Analyst, 101 (1976) 870.
15 G. Chittleborough, Sci. Total Environ., 14 (1980) 53.
16 Activation analysis of hair as an indicator of contamination of man by environmental trace element pollutants, Report IAEA/RL/41 H (1977), p. 10.

Analytica Chimica Acta, 125 (1981) 139—147
Elsevier Scientific Publishing Company, Amsterdam — Printed in The Netherlands

ADSORPTION BEHAVIOUR OF SCANDIUM, YTTRIUM, CERIUM AND URANIUM FROM XYLENOL ORANGE SOLUTIONS ONTO ANION-EXCHANGE RESINS

HSUAN-ERH CHAO and NOBUO SUZUKI*

Department of Chemistry, Faculty of Science, Tohoku University, Sendai, 980 (Japan)

(Received 2nd June 1980)

SUMMARY

The effects of concentration, pH and anions on the adsorption behaviour of xylenol orange (XO) on the strong anion exchangers, Amberlite IRA-400 and Hitachi 2632 are described. The adsorption behaviour of the XO complexes of Ce(III), Y(III), Sc(III) and U(VI) on the Amberlite IRA-400 resin as a function of XO concentration and pH is reported. A continuous-flow radiometric detector is used to investigate the separations of the Ce(III)—Sc(III), Y(III)—Sc(III), and Ce(III)—Y(III) pairs on the XO-form Hitachi 2632 resin column by pH control. Satisfactory separations of the Ce(III)—Sc(III) and Y(III)—Sc(III) pairs are achieved.

Many complexing agents which form negatively charged complexes have been employed for the separation of metal ions on anion-exchange resins. The separations are based on the different stabilities of the complexes, and their different affinities for the resins [1—5]. Recently, chelating groups have been introduced into resins via synthetic techniques or by simple loading, and the modified resins have been used for the selective recovery or preconcentration of metal ions [6—13].

Xylenol orange (XO) has been widely used as a chromogenic agent in determinations of metal ions by complexiметric titrations [14] or spectrophotometry [15]. Metal—XO complexes have been little used in separations of metal ions by chromatography. Quantitative information about the complexation equilibria with many metal ions is available [15]. The complexes formed are negatively charged, coloured and quite stable in aqueous solutions of appropriate pH.

In order to examine the feasibility of chromatographic separation of metal ions by using metal—XO complexation, the adsorption behaviour of the XO complexes with Sc(III), Y(III), Ce(III) and U(VI) on strongly basic anion exchanger was investigated. For convenience, an on-line radiometric detector system was used to monitor the chromatographic separations.

EXPERIMENTAL

Ion-exchange resins

Amberlite IRA-400 (Rohm and Haas) and Hitachi 2632 (16—20 μm) resins with quaternary ammonium functional groups were employed. The exchange capacity of the Hitachi resin was determined by converting a known amount of resin to the chloride form with an excess of 1 M NaCl solution. After washing the resin thoroughly with deionized water, chloride ions were eluted with 1 M $NaNO_3$ solution and measured by the mercury(II) thiocyanate method. The exchange capacity was found to be 4.20 meq g^{-1} of dry resin (60°C, oven). The exchange capacity of Amberlite IRA-400 is stated to be 3.1 meq g^{-1}.

Radioactive tracers and reagents

The following radioactive tracers were used: ^{139}Ce ($t_{1/2}$ = 140 d), ^{88}Y($t_{1/2}$ = 108.1 d), ^{46}Sc($t_{1/2}$ = 84.0 d), and ^{237}U($t_{1/2}$ = 6.75 d). The ^{46}Sc tracer was obtained from New England Nuclear Co.; the others were produced by 20-MeV bremsstrahlung bombardment of CeO_2, Y_2O_3 and U_3O_8, respectively, in a 300-MeV linear accelerator. After bombardment, ^{139}Ce and ^{88}Y were used without further purification, and ^{237}U was purified by the TBP—benzene—HNO_3 extraction to remove the fission products. The purity of the tracers was checked by comparing the γ-ray spectra against literature data.

All the chemicals used were of reagent-grade purity. Xylenol orange (Dotite Reagent Co.) was used as received. Working XO solutions were prepared by diluting aliquots of stock solutions of the disodium salt: hydrochloric acid, acetic acid and sodium acetate solutions were added to adjust the pH. Formation of XO complexes is reasonably rapid for the elements studied except uranium(VI), which forms only a weak complex at room temperature [16]. All the experiments were carried out at ca. 20°C.

Apparatus

The chromatographic system used is outlined in Fig. 1. All connections were made by 1 mm i.d. teflon tubing. The glass eluent reservoir was equipped with an elution exchange valve. Eluent was pumped from the reservoir by a constant flow pump (JOEL P-2705S) at a rate of 0.50 ml min^{-1}. The sample injection valve was fitted with a calibrated sample loop, which allowed injection of a volume of 507.6 ± 3.3 μl. The chromatographic column (8 mm i.d., 140 mm long) was prepared by slurry-packing Hitachi 2632 resin. The radiometric flow cell (volume 137.0 μl) was coiled up in the well of a NaI(Tl) 3 × 3-in. scintillation detector (NAIG D-421) and shielded with a lead block. The detector was equipped with a NAIG E-541 dual counter timer and E-594 printer, reading the integrated counts every 30 s.

Procedures

Resins in the XO-form were prepared by treating the chloride forms with a large excess of XO solution followed by washing with deionized water to

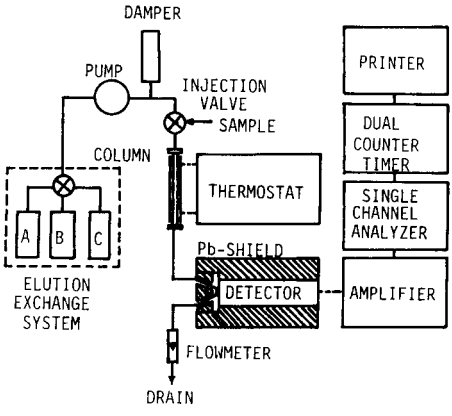

Fig. 1. Schematic diagram of ion-exchange chromatograph.

remove excess of reagent. (It was shown (see below) that the ratio of the amount of XO (in mmol) to exchangeable chloride (in meq) on the resin had to exceed 0.51.) Resins were dried in a vacuum desiccator for a week and stored in the dark.

The exchange capacities of the XO-form resins were determined by weighing ca. 100 mg of resin equilibrated with 10 ml of XO solution of various concentrations. The quantity of XO adsorbed was determined from the difference in XO concentrations, determined at 578 nm (pH 6.0).

Distribution coefficients were determined by a batch technique. Batches (ca. 100 mg) of XO-form resin were added to solutions (10 ml) containing different amounts of XO, tracers and buffers, then gently shaken until equilibrium was attained. Aliquots were counted before and after equilibration. The K_d values were calculated from

$$K_d = [(A_i - A_f)/A_f]\,[\text{Volume of solution (ml)/Weight of resin (g)}]$$

where A_i and A_f were the activities in cpm of the solution initially, and after equilibrium, respectively.

Column separations were performed using the XO-form of Hitachi 2632 resin. Before injection of samples, columns were equilibrated with the eluent to be used.

RESULTS AND DISCUSSION

Adsorption of xylenol orange on anion-exchange resin

According to Rehák and Körbl [17] the acid—base equilibria of xylenol orange (3,3′-bis[N,N′-di(carboxymethyl)-aminomethyl]-o-cresolsulphonphthalein) are as follows

$$H_9XO^{3+} \overset{pK^a_{IV}=-1.74}{\rightleftharpoons} H_8XO^{2+} \overset{pK^a_{III}=-1.09}{\rightleftharpoons} H_7XO^{+} \overset{pK^a_{II}=-0.76}{\rightleftharpoons}$$

$$H_6XO^{0} \overset{pK^a_{I}=1.15}{\rightleftharpoons} H_5XO^{1-} \overset{pK^c_{1}=2.58}{\rightleftharpoons} H_4XO^{2-} \overset{pK^c_{2}=3.23}{\rightleftharpoons}$$

$$H_3XO^{3-} \overset{pK^c_{3}=6.40}{\rightleftharpoons} H_2XO^{4-} \overset{pK^c_{4}=10.46}{\rightleftharpoons} HXO^{5-} \overset{pK^c_{5}=12.28}{\rightleftharpoons} XO^{6-}$$

— and the general formula of XO is expressed as H_pXO^{p-6} (p = 0 to 9).

On a strongly basic resin, the equilibrium between XO and the resin is given by

$$RB + \frac{1}{p-6} H_pXO^{p-6} \rightleftharpoons \frac{1}{p-6} R_{p-6}H_pXO + B \quad (1)$$

where B and H_pXO^{p-6} are exchangeable ions and R is the resin matrix. The distribution coefficient, K_d^{XO}, of eqn. (1) is defined as

$$K_d^{XO} = [R_{p-6}H_pXO]/[H_pXO^{p-6}]_f = ([H_pXO^{p-6}]_i - [H_pXO^{p-6}]_f)/[H_pXO^{p-6}]_f$$

$$= ([H_pXO^{p-6}]_i/[H_pXO^{p-6}]_f) - 1 = (\bar{n}\,[RB]/[H_pXO^{p-6}]_f) - 1 \quad (2)$$

where $[H_pXO^{p-6}]_i$ and $[H_pXO^{p-6}]_f$ are the initial and final concentration of XO in solution, respectively. The term $\bar{n}$ is the apparent molar ratio of eqn. (1) expressed as

$$\bar{n} = \sum_{j=0}^{9} n_j\alpha_j = [H_pXO^{p-6}]_i/[RB] = \text{Total mmol of XO in solution/}$$

Total meq of functional group B in resin (3)

where $j = 9 - p$, α_j and n_j are the mole fraction and molar ratio of species j, $[H_pXO^{p-6}]/\Sigma_{p=0}^{9}[H_pXO^{p-6}]$ and $1/(p-6)$, respectively. Consequently, $\bar{n}$ can be obtained from the slope of a plot of K_d^{XO} vs. $[RB]/[H_pXO^{p-6}]_f$, given an apparent molar ratio in eqn. (1). In the case of both Amberlite IRA-400 and Hitachi 2632 resins, $\bar{n}$ was ca. 1/3 (Fig. 2). In this experiment, carried out without addition of buffer, the pH fell from 3.7 to 3.1 during equilibration. Considering the main species and their distribution at pH 3.7 (H_3XO^{3-} (α_6 = 0.73), H_4XO^{2-} (α_5 = 0.248), and H_5XO^{-} (α_4 = 0.019)), the fall in pH may be ascribed to H^+ release from H_5XO^{+} and H_4XO^{2-} to H_3XO^{3-}. Comparison of the experimental value of $\bar{n}$ with eqn. (3) shows that the predominant XO species adsorbed is H_3XO^{3-}, and the possible adsorption reaction can be written

$$RB + \frac{1}{3} H_3XO^{3-} \rightleftharpoons \frac{1}{3} R_3H_3XO + B^{-} \quad (4)$$

Figure 3 shows that the maximum exchange capacity for XO reaches 1.0 and 1.01 mmol g^{-1} for the Amberlite IRA-400 and Hitachi 2632 resins, respectively, at a molar ratio of ca. 0.51.

Figure 4 illustrates the pH dependence of the exchange capacity for the XO-form resins; the maximum capacity is observed in the pH range 2.7—3.1.

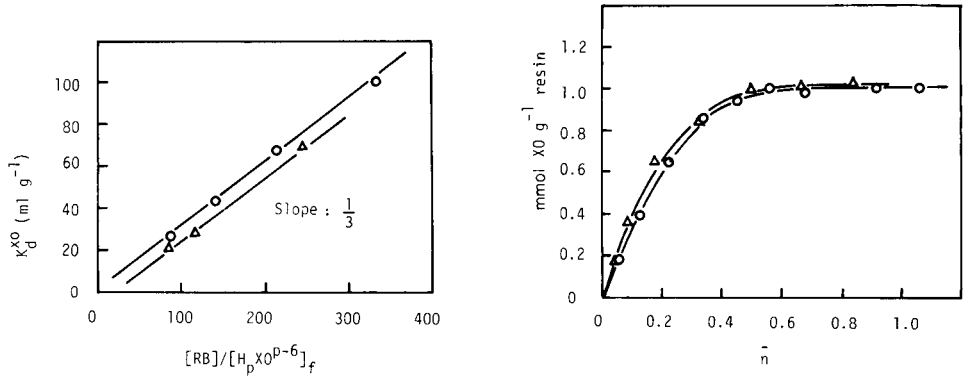

Fig. 2. Equilibrium between the XO solution and anionic exchange resin (pH 3.1, without buffer): (○) Amberlite IRA-400; (△) Hitachi 2632.

Fig. 3. Effect of XO concentration on adsorption on anion-exchange resin at pH 2.7—3.1: (○, △) as in Fig. 2.

The noticeable reduction of capacity at lower and higher pH may be caused by a shrinkage of the resin matrix or (at higher pH) by a capacity change for more highly charged XO species. To avoid such interferences, the pH range 2.7—3.1 was chosen to study the adsorption of metal complexes.

When the maximum adsorption capacity for XO in Amberlite IRA-400 resin is compared with those for other complexing agents — tiron (3.1 mmol g^{-1}) [8], sulphonated dithizone (1.9 mmol g^{-1}) [9], and XO (1.0 mmol g^{-1}) — it is apparent that the capacity decreases with increasing molecular size.

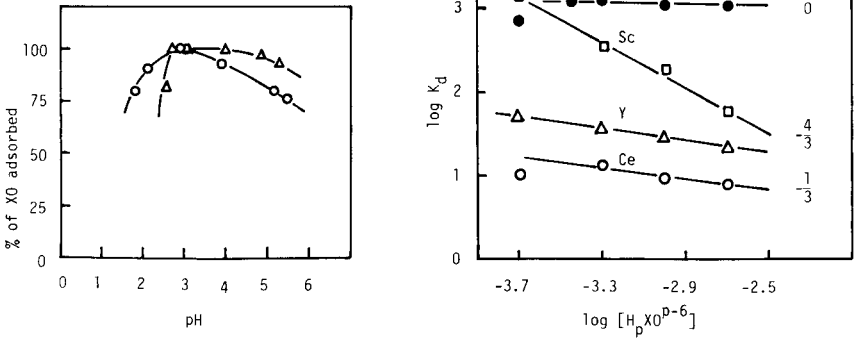

Fig. 4. pH dependence of the exchange capacity for XO in a 0.1 M HCl—HOAc—NaOAc buffer system: (○, △) as in Fig. 2.

Fig. 5. Adsorption of U(VI), Sc(III), Y(III) and Ce(III) from XO solution buffered at pH 2.8 with a 0.1 M HCl—HOAc—NaOAc system.

TABLE 1

Effects of anions and acidity on XO adsorption on Amberlite IRA-400 resin (100 mg) from 10-ml solutions

Acid	Conc. (M)	XO adsorbed (%)	Acid	Conc. (M)	XO adsorbed (%)
HOAc	0.02	100.0	HCl	0.02	91.3
H_2SO_4	0.02	91.2		0.10	83.8
HNO_3	0.02	89.9		0.20	77.0
$HClO_4$	0.02	87.2		0.50	74.0
				1.0	73.4

The effects of anions and of HCl acidity on XO adsorption on the resin were studied by the batch method (Table 1). The effects of the anions in the sequence $ClO_4^- > NO_3^- > SO_4^{2-} \geqslant Cl^- > CH_3COO^-$ are quite similar to their affinities for anion-exchange resins. Some XO was still retained on the resin even in 1 M HCl because of the π—π interaction between the benzene ring of XO and the divinylbenzene of the resin matrix.

Adsorption of metal complexes on resin

Negatively charged complexes of metal ions with XO will be adsorbed on to XO-equilibrated resin by the following steps: dissociation of complexing agent, complex formation, and ion exchange. The reaction of an m-valent metal ion with XO can be written as

$$a\,M^{m+} + b\,H_pXO^{p-6} \rightleftharpoons M_a(H_{p-q}XO)_b^{b(p-q-6)+ma} + bq\,H^+ \quad (5)$$

If $x = b(p - q - 6) + ma$ (for simplification), the formation constant is

$$K_f = [M_a(H_{p-q}XO)_b^x][H^+]^{bq}/[M^{m+}]^a[H_pXO^{p-6}]^b \quad (6)$$

Then the equilibrium of the negatively charged complex on the XO-form resin can be described by

$$M_a(H_{p-q}XO)_b^x + x/(p-6)R_{p-6}H_pXO \rightleftharpoons R_xM_a(H_{p-q}XO)_b + x/(p-6)H_pXO^{p-6} \quad (7)$$

If the mass of metal ions is very small compared with the capacity of the resin, i.e., $[R_xM_a(H_{p-q}XO)_b] \ll [R_{p-6}H_pXO]$, and the ionic strength is constant, then the exchange constant, K_{ex}, is independent of concentration

$$K_{ex} = [R_xM_a(H_{p-q}XO)_b][H_pXO^{p-6}]^{x/p-6}/[M_a(H_{p-q}XO)_b^x][R_{p-6}H_pXO]^{x/p-6}$$

$$= K_d[H_pXO^{p-6}]^{x/p-6}/\Phi_{MXO}[R_{p-6}H_pXO]^{x/p-6} \quad (8)$$

where Φ_{MXO} is the mole fraction of the complex in the solution, $[M_a(H_{p-q}XO)_b^x]/\{[M^{m+}] + \Sigma[M_a(H_{p-q}XO)_b^x]\}$, and can be calculated from the XO concentration and the stability constant.

If the total amount of metal ion and complexes is much less than $[H_pXO^{p-6}]$, then the distribution coefficient K_d can be written as

$$K_d = K_{ex}\Phi_{MXO}[R_{p-6}H_pXO]^{x/p-6}[H_pXO^{p-6}]^{-x/p-6} \quad (9)$$

All the subsequent experiments were carried out at trace metal concentrations, low ionic strength, and fixed pH: hence the slopes of log—log plots of K_d vs. $[H_pXO^{p-6}]$ should closely approximate the charge ratio $-x/p-6$. Adsorption of U(VI), Sc(III), Y(III) and Ce(III) from XO solutions at pH 2.8—3.1 was examined by using the equilibrated resin essentially in the H_3XO^{3-} form (p = 3). As shown in Fig. 5, the slopes were approximately −1/3 for Ce(III) and Y(III), −4/3 for Sc(III), and 0 for U(VI). From these results, it is concluded that the compositions of the complexes are $Ce(H_2XO)^-$, $Y(H_2XO)^-$ (a = b = q = 1, m = 3), and $Sc_2(HXO)_2^{4-}$ (a = b = q = 2, m = 3). However, adsorption of U(VI) was independent of XO concentrations, suggesting that a complex was not formed between U(VI) and XO: the strong adsorption of U(VI) on the resin is probably due to a U(VI)—acetate complex. Consequently, the predominant exchange reactions can be expressed as follows: for Ce(III) and Y(III), a = b = q = 1 and m = 3

$$M(H_2XO)^- + 1/3\ R_3H_3XO \rightleftharpoons RM(H_2XO) + 1/3\ H_3XO^{3-} \quad (10)$$

and for Sc(III), a = b = q = 2 and m = 3

$$Sc_2(HXO)_2^{4-} + 4/3\ R_3H_3XO \rightleftharpoons R_4Sc(HXO)_2 + 4/3\ H_3XO^{3-} \quad (11)$$

The adsorption of U(VI), Sc(III), Y(III) and Ce(III) on an XO-form resin as a function of pH at constant XO concentration is summarized in Fig. 6. The experiments were carried out at trace metal concentrations (10^{-4}—10^{-5} M) with 2×10^{-4} M XO and 0.1 M HCl—acetate buffer. The formation constants (pK_f) of $Sc_2(HXO)_2^{4-}$, $Y(H_2XO)^-$ and $Ce(H_2XO)^-$ are 18.4 [18], 7.7 and 6.01 [19], respectively. However, the sequence of the adsorbability for these complexes is dependent on their stability: the characteristic rapid

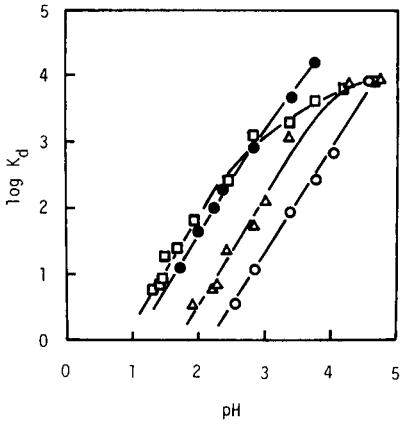

Fig. 6. Adsorption as a function of acidity in 2×10^{-4} M XO solutions for (•) U(VI), (□) Sc(III), (△) Y(III), and (○) Ce(III).

decreases in adsorption at low pH reflect the instability of the complexes under such conditions.

Column separations

On the basis of the data obtained from the batch method, the separation factors (K_{d_2}/K_{d_1}) for Sc/Ce, Sc/Y and Y/Ce were estimated as 124, 22 and 5.6, respectively, at 2×10^{-4} M XO and pH 2.5. It was expected that the separation would be facilitated by the use of column methods. The mutual separation of the Ce(III)—Sc(III), Y(III)—Sc(III), and Ce(III)—Y(III) combinations was attempted on a column packed with Hitachi 2632 resin in the XO-form. Examples of the chromatograms for these separations are shown in Figs. 7 and 8. The Ce/Sc and Y/Sc separations were easily performed by changing the pH of the eluents during the elution. In the examples shown in Fig. 7, the eluents were changed about 15 min after the emergence of the previous components, in order to prove the absence of undesirable baseline distortion. It is safe to say that, in practice, the eluent can be changed without this 15-min gap.

In the case of Ce/Y, the separation was adequate (Fig. 8), and could not be improved by changing the eluent. According to the results shown in Figs. 5 and 6, the separation factor for the Ce/Y combination is almost independent of either pH or XO content of the eluent. Higher resolution for the Ce/Y separation could be obtained with a longer column.

The elution order, Ce(III) > Y(III) > Sc(III), is the converse of the order of the formation constants of their XO complexes. Similar behaviour has been reported in work concerned with the chromatography of those metal ions with commonly used complexing agents such as EDTA [20].

The authors gratefully acknowledge the gift of Hitachi 2632 resin from the Nissei Sangyo Co., and thank Dr. K. Saitoh for his keen interest in this work.

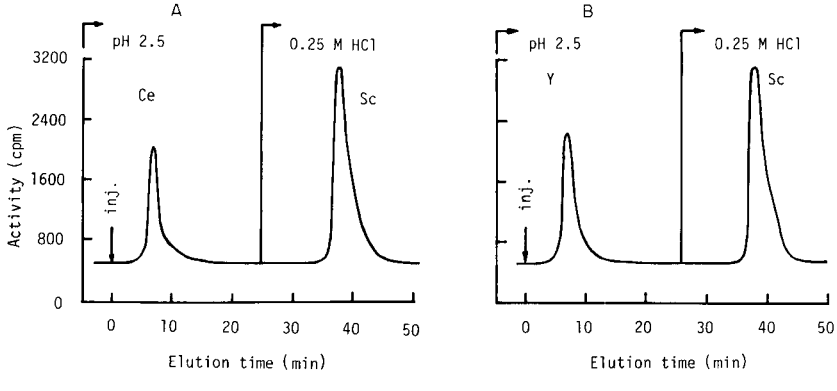

Fig. 7. (A) Separation of 35.1 μg of Ce(III) and 20.7 μg of Sc(III) in 2×10^{-4} M XO solutions; (B) separation of 35.5 μg of Y(III) and 20.7 μg of Sc(III) in 2×10^{-4} M XO solutions. Hitachi 2632 resin column in XO-form (8 mm i.d. × 140 mm); flow rate of eluent, 0.5 ml min^{-1}).

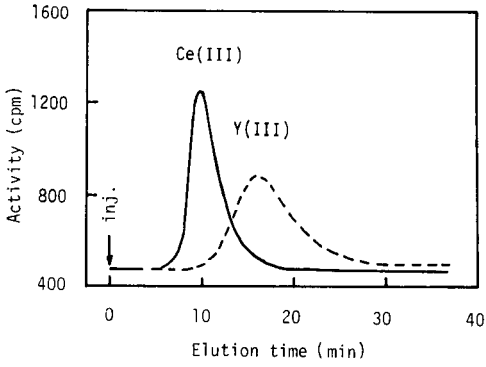

Fig. 8. Separation of Ce(III) and Y(III) in 2×10^{-4} M XO at pH 2.75. Column and flow rate of eluent as in Fig. 7.

REFERENCES

1 F. Nelson, R. A. Day, Jr. and K. A. Kraus, J. Inorg. Nucl. Chem., 15 (1960) 140.
2 L. Wódkiewicz and R. Dybczyński, J. Chromatogr., 32 (1968) 394.
3 R. Dybczyński, J. Chromatogr., 50 (1970) 487.
4 L. Balsenc, R. Beeler, W. Haerdi and D. Monnier, Anal. Chim. Acta, 55 (1971) 253.
5 J. P. Faris, J. Chromatogr., 26 (1967) 232.
6 J. E. Going, G. Wesenberg and G. Andrejat, Anal. Chim. Acta, 81 (1976) 349.
7 K. S. Lee, W. Lee and D. W. Lee, Anal. Chem., 50 (1978) 255.
8 K. Brajter and E. Dabek-Zbotorzyńska, Talanta, 27 (1980) 19.
9 H. Tanaka, M. Chikuma, A. Harada, T. Ueda and S. Yube, Talanta, 23 (1976) 489.
10 H. Loewenschuss and G. Schmuckler, Talanta, 11 (1964) 1399.
11 H. Eccles and F. Vernon, Anal. Chim. Acta, 66 (1973) 231.
12 S. B. Savvin, I. I. Antokolskaja, G. V. Myasedova, L. I. Bolshakova and O. P. Shvoeva, J. Chromatogr., 102 (1974) 287.
13 J. S. Fritz, Pure Appl. Chem., 49 (1977) 1547.
14 K. Ueno, Chelatometric Titration, Nankodo, Tokyo, 1960, p. 133.
15 M. Otomo, Jpn. Analyst, 21 (1972) 436.
16 M. Otomo, Bull. Chem. Soc. Jpn., 36 (1963) 140.
17 B. Rehák and J. Körbl, Collect. Czech. Chem. Commun., 25 (1960) 806.
18 B. Budesínský, Collect. Czech. Chem. Commun., 28 (1963) 1863.
19 R. Nayan and A. K. Dey, J. Indian Chem. Soc., 54 (1977) 197.
20 R. Dybczyński, J. Chromatogr., 14 (1964) 79.

Analytica Chimica Acta, 125 (1981) 149—153
Elsevier Scientific Publishing Company, Amsterdam — Printed in The Netherlands

Short Communication

SEPARATION AND DETERMINATION OF BISMUTH(III) AND COPPER(II) DIETHYLDITHIOCARBAMATES IN CHLOROFORM WITH HYDROBROMIC ACID

B. KARADAKOV* and M. SAKHARIEVA
High Institute of Chemical Technology, Sofia-1156 (Bulgaria)

(Received 13th June 1980)

Summary. Bismuth and copper diethyldithiocarbamates are extracted into chloroform. Bismuth is selectively re-extracted with 3 M hydrobromic acid and determined spectrophotometrically as a bromide complex at 376 nm. Bismuth can be determined in the presence of large quantities of copper and iron.

In the presence of EDTA and citrate in an ammoniacal medium, organic solvents extract only the diethyldithiocarbamates of copper(II), bismuth(III), mercury(II) and silver(I) [1, 2]. Only the first two metal ions give coloured extracts. The spectrophotometric determination of copper(II) and bismuth(III) with sodium diethyldithiocarbamate is possible either by preventing copper extraction with appropriate masking agents, or with subsequent separation in the organic phase. Copper can be held in the aqueous phase by adding cyanide [3, 4] to the solution before extraction. The separation of copper and bismuth diethyldithiocarbamates is possible by treatment of the organic phase with cyanide [5], 1 M sodium hydroxide [6, 7] or 5—6 M hydrochloric acid [2, 7, 8]. Complete re-extraction of the bismuth diethyldithiocarbamate complex is achieved with 5 M hydrochloric acid. Above this concentration of the acid, partial re-extraction of copper [8] occurs.

The present investigation aimed at clarifying whether it is possible to separate copper(II) and bismuth(III), extracted as their diethyldithiocarbamate complexes, by re-extraction with hydrobromic acid, as well as showing the maximum amount of copper to which this separation is applicable. The determination of bismuth in the presence of large quantities of copper and iron is also investigated.

Experimental

Reagents. Standard solutions of bismuth nitrate and perchlorate contained 100 mg Bi l^{-1}. Standard copper nitrate solutions contained 1.000 and 10.000 g Cu l^{-1} and the iron(III) nitrate solution contained 100.0 g Fe l^{-1}. Hydrobromic acid (8.00 M) was used from which 1.00—5.00 M solutions were prepared by dilution. The 1 M ammonium citrate solution was of pH 8.4—8.5. This solution was tested for copper, which if present, was removed by extraction with sodium diethyldithiocarbamate. The solutions of sodium

0003—2670/81/0000—0000/$02.50

diethyldithiocarbamate, 0.1—20% in twice-distilled water at pH 8.5—9.0, were kept in a brown-glass bottle. All reagents were of analytical grade.

Apparatus. A Perkin-Elmer model 137 u.v.-visible recording spectrophotometer and a LPU-01 pH meter (USSR) were used.

General procedure for bismuth. To 5—100 μg of bismuth as bismuth nitrate or perchlorate in a separating funnel were added 1 ml of 0.1 M EDTA and 1 ml of ammonium citrate solution, and the pH of the solution was adjusted to 8.0—8.8 with ammonia (1 + 9). A 0.1% (w/v) sodium diethyldithiocarbamate solution (5 ml) was added and the total volume was brought to 25 ml with distilled water. The solution was extracted with chloroform (10 + 5 + 5 ml) for 2 min each time. The combined extracts were transferred to a dry separating funnel and re-extracted for 30 s with 20 ml of 3 M hydrobromic acid. After separation, both phases were put into dry 25-ml volumetric flasks. The aqueous phase was diluted to volume with 3 M hydrobromic acid and the absorbance was measured at 376 nm in 4-cm cells against a water reference.

In preliminary tests, the organic phase was diluted to 25 ml with chloroform and its absorbance measured at 365 nm against a chloroform reference in 4-cm cells.

Determination of bismuth and copper in the presence of iron. EDTA solution (0.1 or 1 M) was added to the sample solution to give a 50—70% excess over the amount necessary to complex all the metals present. The 1 M ammonium citrate was also added in 50—70% excess. The pH was adjusted with ammonia (1 + 9) if necessary. A 50—70% excess of sodium diethyldithiocarbamate was added (extraction of 1 mg of copper requires 5 mg of sodium diethyldithiocarbamate, extraction of 1 mg of bismuth requires 7.5 mg). The solution was then extracted with chloroform and back-extracted with 3 M hydrobromic acid as described in the above procedure for bismuth. The organic phase, containing the copper, was collected in a dry 25-ml volumetric flask, diluted to volume with chloroform and the absorbance measured at 600 nm in a 1-cm cell against a chloroform blank. If the extract was turbid, part of it was filtered through a dry filter directly into the cell. When larger quantities of copper were present, an aliquot of the organic phase was measured. The aqueous phase, containing the bismuth, was collected and measured at 376 nm as described above.

Determination of bismuth in ores. A 2-g sample was decomposed with 6 ml of aqua regia under moderate heating, evaporating to give a volume of 1—1.5 ml. The solution was evaporated several times with concentrated nitric acid nearly to dryness. After cooling, 3 ml of concentrated nitric acid were added, the walls of the vessel were washed with distilled water, and the mixture was heated nearly to boiling (to dissolve any soluble salts completely). The solution and residue were transferred to a 100-ml volumetric flask after cooling, made up to volume with distilled water and filtered twice through a double "blue strip" filter. Bismuth was determined on aliquots of this solution as described in the first procedure.

Calibration. The calibration graph for 5—100 μg of bismuth in 25 ml was established by using bismuth perchlorate and an appropriate amount of 8 M hydrobromic acid so that its final concentration was 3.0 M. The absorbance of the bismuth bromide complex was measured at 376 nm in 4-cm cells against a water blank. The calibration graph for 0.10—2.2 mg of copper in 25 ml was established by using copper nitrate and diethyldithiocarbamate [9]; the absorbance was measured at 600 nm in a 1-cm cell against a chloroform blank.

Results and discussion

Influence of hydrobromic acid concentration. The influence of hydrobromic acid on the distribution of bismuth diethyldithiocarbamate between the aqueous and organic phases was studied by using the conditions described above for the determination of bismuth alone. Re-extractions were tested with 1—5 M hydrobromic acid. The aqueous phase was diluted to volume with an amount of concentrated hydrobromic acid calculated to give a final acid concentration of 3.0 M. The absorbance of each phase as a function of hydrobromic acid concentration is given in Fig. 1. It is obvious that complete re-extraction of bismuth is achieved into $\geqslant$3 M hydrobromic acid. A similar set of experiments was carried out with 1.20 mg of copper. Figure 1 shows that no re-extraction of copper diethyldithiocarbamate occurred from $\leqslant$5 M hydrobromic acid.

The duration of the re-extraction was also investigated, using the above reaction conditions. The time of re-extraction into 3 M hydrobromic acid was varied from 2.5 to 30 s and the absorbance of each phase was measured afterwards. The results obtained are shown in Fig. 2, which indicates that re-extraction must continue for at least 10 s in order to achieve complete conversion to the bismuth—bromide complex. Re-extraction of the copper

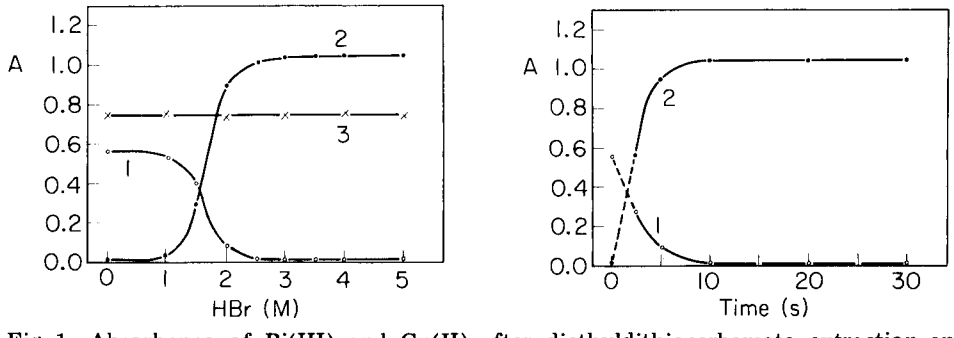

Fig. 1. Absorbance of Bi(III) and Cu(II) after diethyldithiocarbamate extraction and re-extraction with HBr of various concentrations: (1) organic phase, 365 nm; (2) aqueous phase, 376 nm, 80 μg Bi/25 ml; (3) organic phase, 600 nm, 1.20 mg Cu/25 ml.

Fig. 2. Variation of the bismuth absorbance for 80 μg Bi/25 ml with re-extraction time: (1) organic phase, 365 nm; (2) aqueous phase, 376 nm.

complex does not occur at this acid concentration. This is the advantage of hydrobromic acid over hydrochloric acid [2, 7, 8] in the determination of bismuth.

Determination of bismuth in the presence of copper and iron. Mixtures of bismuth(III), copper(II) and iron(III) were analysed by the method described above. The pH of the solution was adjusted to 8.0—8.8, because copper extraction at pH >9 is very slow [7]. Some results are given in Table 1. These satisfactory results indicate that it should be possible to determine bismuth in copper ($\geqslant 10^{-3}$%) and in iron ($\geqslant 10^{-4}$%).

The possibility of bismuth determination in the presence of iron and several other elements (Ni, Co, Zn, Al, Mn) was also investigated. The results obtained were satisfactory in the presence of $\leqslant 100$ mg of each element, except manganese. The errors become considerable when >2 mg of manganese is present.

The method was applied to the determination of bismuth in standard copper samples. The results are shown in Table 2. The method was also

TABLE 1

Determination of bismuth and copper in the presence of iron(III)

Bi taken (mg)	Cu taken (mg)	Bi found (mg)	Cu found (mg)	Bi taken (mg)	Cu taken (mg)	Fe taken (mg)	Bi found (mg)	Cu found (mg)
0.0100	0.040	0.0101	0.040	0.0100	—	5.0	0.0101	—
0.0100	1.00	0.0099	0.998	0.0050	—	10.0	0.0049	—
0.0100	5.00	0.0101	5.01	0.0050	—	25.0	0.0051	—
0.0100	10.00	0.0103	10.0	0.0050	—	50.0	0.0052	—
0.0050	20.0	0.0048	20.0	0.0050	—	100.0	0.0050	—
0.0050	50.0	0.0051	50.0	0.0050	—	500.0	0.0048	—
0.0050	100.0	0.0051	—	0.0050	—	1000	0.0051	—
				0.0050	—	2500	0.0054	—
				0.0050	—	5000	0.0056	—
				0.0050	0.50	500	0.0050	0.50
				0.0050	1.00	2500	0.0052	0.99
				0.0050	2.50	5000	0.0053	2.48

TABLE 2

Determination of bismuth in official Bulgarian standard copper samples

Sample	Bi (%)	
	Certificate value	Found[a]
SOD 11/1-77	0.050 ± 0.005	0.052 ± 0.004
SOD 11/2-77	0.025 ± 0.002	0.026 ± 0.002
SOD 11/3-77	0.016 ± 0.001	0.015 ± 0.001
SOD 11/4-77	0.0080 ± 0.0006	0.0078 ± 0.0006

[a]Mean of 6 results ± 95% confidence limits.

TABLE 3

Determination of bismuth in ores

Bi (%)						
	Taken[a]	0.011	0.049	0.088	0.125	0.197
	Found[a]	0.012	0.046	0.089	0.126	0.195

[a]Measured by the thiocarbamide method [9].

successfully applied to the determination of bismuth in ores containing many metals. The results are given in Table 3.

REFERENCES

1 V. Šedivec and V. Vašak, Collect. Czech. Chem. Commun., 15 (1950) 260.
2 A. Claasen and Z. Bastings, Fresenius Z. Anal. Chem., 153 (1956) 30.
3 H. Bode, Fresenius Z. Anal. Chem., 143 (1954) 182.
4 K. L. Cheng, R. H. Bray and S. W. Melsted, Anal. Chem., 27 (1955) 24.
5 D. Z. Drabkin, Fresenius Z. Anal. Chem., 134 (1951) 204.
6 E. N. Jenkins, Analyst, 79 (1954) 209.
7 T. Kuroha and S. Schibuya, Jpn. Analyst, 21 (1972) 1197, 1505.
8 M. Sakharieva and B. Karadakov, C. R. Acad. Bulg. Sci., 32 (1979) 9.
9 E. B. Sandell, Colorimetric Determination of Traces of Metals, (Russian translation) Moscow, 1964, pp. 402, 299.

Analytica Chimica Acta, 125 (1981) 155—159
Elsevier Scientific Publishing Company, Amsterdam — Printed in The Netherlands

Short Communication

SPECTROFLUORIMETRIC DETERMINATION OF HAFNIUM WITH 3-HYDROXYCHROMONE

TAKUSHI ITO*

Junior College of Engineering, Shizuoka University, 3-5-1, Johoku, Hamamatsu-shi, Shizuoka (Japan)

AKIRA MURATA

Faculty of Engineering, Shizuoka University, 3-5-1, Johoku, Hamamatsu-shi, Shizuoka (Japan)

(Received 3rd December 1980)

Summary. The fluorescence of the 1:1 hafnium—3-hydroxychromone complex in 4—0.5 M hydrochloric acid is used to determine 0.4—9.0 μg of hafnium in 25 ml of solution; the relative standard deviation is 0.15%. Zirconium does not interfere in 2-fold amounts.

The spectrofluorimetric determination of zirconium with 3-hydroxychromone was reported previously [1]. Zirconium reacts with the reagent in dilute hydrochloric acid to form a faintly fluorescent complex, which exhibits strong u.v. absorption. However, in the presence of a large amount of sulfate, the absorbance of the zirconium complex decreases, whereas the fluorescence intensity increases so that 0.5—8 μg of zirconium per 25 ml can be determined spectrofluorimetrically at an apparent pH of 1.5—2.0 in aqueous 30% (v/v) methanol, 0.2 M in sulfate. This communication describes the fluorimetric determination of hafnium with 3-hydroxychromone. Under the above conditions, the fluorescence intensities of the hafnium and zirconium complexes per mole are the same so that the sum of zirconium and hafnium can be determined. However, the hafnium complex also exhibits an intense fluorescence in dilute hydrochloric acid containing no sulfate, so that hafnium can be determined in the presence of about 2-fold molar amounts of zirconium. Quercetin [2—4], morin [5], myricetin [6] and quercetin sulfonic acid [7], which are all polyhydroxy derivatives of flavone, a 2-phenyl chromone, have previously been reported as reagents of the fluorimetric determination of hafnium. Quercetin, for example, can be applied in the presence of zirconium.

Experimental

Reagents and apparatus. A hafnium solution was prepared by dissolving dichlorooxohafnium (Johnson Matthey Chemicals, Specpure) in 4 M hydrochloric acid and was standardized by EDTA titration (0.883 mg Hf ml^{-1}).

Working solutions were prepared by dilution with 4 M hydrochloric acid. 3-Hydroxychromone, synthesized as described earlier [8], was used as a methanolic solution. All other chemicals were of analytical-reagent grade.

Fluorescence spectra were recorded with a Shimadzu Model 500 spectrofluorimeter equipped with a quantum counter; excitation spectra were corrected, but emission spectra were not. A Hitachi Model 204 spectrofluorimeter fitted with a 120-W medium-pressure mercury lamp was used for quantitative measurements. Absorption spectra and absorbance measurements were obtained with a Hitachi Model 340 spectrophotometer. A Toadenpa pH meter, Model HM-20B, served for pH measurements.

Procedure. To a sample solution containing 0.4—9.0 μg of hafnium, add 3 ml of a methanolic 1×10^{-2} M solution of 3-hydroxychromone, 4.5 ml of methanol (the final methanol content should be 30% v/v) and sufficient 6 M hydrochloric acid to adjust its concentration in the final solution to 2 M. Dilute the mixture to 25 ml with water. After about 30 min, irradiate the solution with the 366-nm mercury line and measure the fluorescence intensity at 415 nm. Adjust the sensitivity of the fluorimeter with an aqueous 1.0-μg ml^{-1} solution of sodium fluorescein.

Results and discussion

Hafnium reacts with 3-hydroxychromone in solutions of pH <3 up to 6 M hydrochloric acid to form a water-soluble complex. The effect of the concentration of hydrochloric acid on the absorbance and fluorescence intensity is shown in Fig. 1. The hafnium complex has an absorbance maximum at 350 nm. Maximum absorbance is obtained in the pH range 1.4—1.8. The complex shows an intense fluorescence in 0.5—4 M hydrochloric acid and has maximum intensity in 2 M hydrochloric acid. However, constant fluorescence intensity is not obtained over any range of acidity. Over a similar pH range, zirconium forms a water-soluble complex, which has an absorption maximum at 347 nm and only a faint fluorescence (Fig. 1). The hafnium complex also shows an intense fluorescence in perchloric acid, but the maximum intensity (achieved in 2 M perchloric acid) is about 80% of that in 2 M hydrochloric acid.

Fluorescence spectra. The excitation and emission spectra of the hafnium complex and the reagent in 2 M hydrochloric acid are shown in Fig. 2. The excitation and emission spectra have maxima at 353 nm and 418 nm, respectively. When excitation is carried out by a mercury lamp, the 366-nm mercury line is suitable.

Effect of reaction variables. The effect of the concentration of the reagent was examined (Fig. 3). The optimum concentration of the reagent is $1.0—1.4 \times 10^{-3}$ M; larger reagent concentrations cause some decrease of the fluorescence intensity, probably because of an inner filter effect. A 1.2×10^{-3} M reagent solution is recommended for the determination of hafnium.

A study of the effect of methanol content showed that an increase in methanol concentration increases the fluorescence intensity to a limited

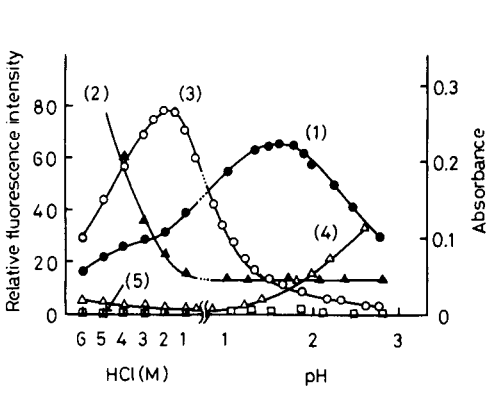

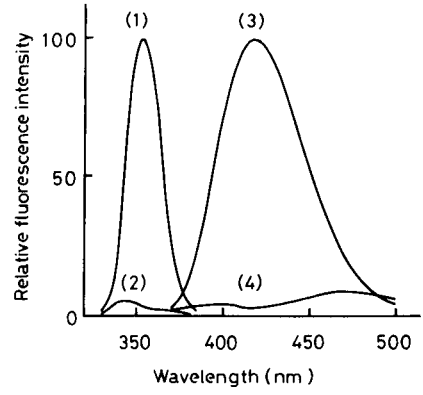

Fig. 1. Effect of hydrochloric acid concentration on absorbance and relative fluorescence intensity. (1, 2) Absorbance at 350 nm for (1) the hafnium complex (2.0×10^{-5} M Hf) and (2) the reagent (4.0×10^{-4} M). (3—5) Relative fluorescence intensity for (3) the hafnium complex (1.0×10^{-6} M Hf), (4) the reagent (1.2×10^{-3} M reagent) and (5) the zirconium complex (1.0×10^{-6} M Zr).

Fig. 2. Fluorescence spectra of the hafnium complex and 3-hydroxychromone in 2 M hydrochloric acid: excitation spectrum of (1) the hafnium complex and (2) the reagent blank; (3) and (4) are the corresponding emission spectra.

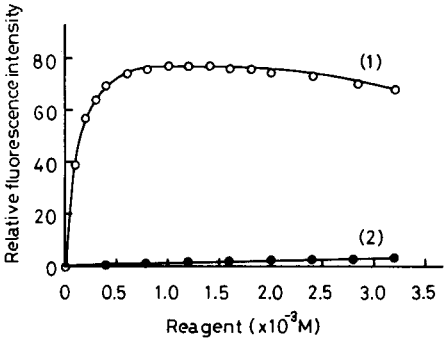

Fig. 3. Effect of reagent concentration for (1) hafnium complex (1.0×10^{-6} M Hf); (2) reagent blank.

extent; a 30% (v/v) methanol content is recommended. The fluorescence intensity increases slightly for 30 min after mixing the solutions (e.g., for 1.0×10^{-6} M hafnium the intensity of 75.1 after 3 min became 78.0 after 30 min), after which it remains constant for at least 3 h.

Calibration. Under the recommended conditions, the calibration graph was linear over the range $0.1—2.0 \times 10^{-6}$ M (0.4—9 μg/25 ml) hafnium. The coefficient of variation obtained from seven measurements of 4.46 μg of hafnium was 0.15%.

Effect of diverse ions. The effects of ions which interfere in the determination of 5.00 μg of hafnium when present in <100-fold amounts (by weight)

are summarized in Table 1. EDTA, fluoride, phosphate and oxalate cause negative errors, whereas at least 2000-fold amounts of sulfate, nitrate, perchlorate, acetate, tartrate and citrate are without effect.

The positive interferences of gallium, zirconium, thorium, scandium, aluminium and germanium can be attributed to the fact that these elements also form fluorescent complexes. Various cations give negative errors probably by formation of non-fluorescing complexes. Maximum tolerable concentrations of other cations are as follows: tin(IV), palladium, 0.5 mg; silver, copper, indium, antimony(III), 1 mg; thallium(III), bismuth, manganese(II), 5 mg; strontium, barium, zinc, cerium(III), arsenic(III, V), cobalt, nickel, 10 mg.

Up to about 2-fold amounts (about 4-fold molar amounts) of zirconium do not interfere with the determination of hafnium. Thus the proposed method tolerates less zirconium than the method based on quercetin [2, 3], the spectrofluorimetric method which is the most discriminatory between zirconium and hafnium so far reported. The sensitivity of the present method is greater than that of the quercetin method, and the fluorescence intensity of the reagent is far less.

Composition of the complex. Spectrophotometric and spectrofluorimetric continuous variation methods were examined in 2 M hydrochloric acid. The mole ratio of hafnium to ligand was found to be 1:1 by both methods. It was found that the mole ratio of hafnium to ligand was 1:3.0 and 1:1.70,

TABLE 1

Effect of diverse ions on the determination of 5.00 μg of hafnium

Ion	Amount added (μg)	Hf found (μg)	Ion	Amount added (μg)	Hf found (μg)
EDTA	1	4.61	Sc	100	5.07
F^-	1	4.81		500	5.97
	5	4.38	Al	100	4.94
PO_4^{3-}	10	4.92		500	5.37
	50	4.46	Ge(IV)	100	5.06
$C_2O_4^{2-}$	10	4.83		500	5.31
	50	4.49	Mo(VI)	100	4.87
Ga	10	5.14		500	3.75
	25	5.43	W(VI)	100	4.88
	50	5.86		500	4.50
Zr	10	5.15	Au(III)	100	4.91
	25	5.23		500	4.59
	50	5.48	V(V)	100	4.95
Th	10	5.10		500	4.70
	50	5.35	Pt(IV)	100	4.97
Fe(III)	10	4.88		500	4.74
	50	4.64			
Cr(VI)	50	4.86			
	100	4.69			

respectively, at pH 1.64 and 0.83 by the spectrophotometric method. It is therefore likely that two of the ligands bound to hafnium are replaced by chloride ions when the concentration of hydrochloric acid increases.

In the presence of a large excess of sulfate, hafnium exhibits an intense fluorescence at an apparent pH of 1.5—2.0. The fluorimetric continuous variation method under these conditions showed that the mole ratio of hafnium to ligand was 1:1. In this instance, it is thought that two of the ligands bound to hafnium are replaced by sulfate ions.

Determination of the sum of hafnium and zirconium. In a 0.2 M sulfate solution at apparent pH 1.5—2.0, the hafnium complex with 3-hydroxychromone exhibits an intense fluorescence similar to that obtained in the zirconium reaction (excitation and emission maxima, 355 nm and 418 nm, respectively). The intensity of the hafnium complex is about 70% of that in 2 M hydrochloric acid and is the same as that of the zirconium complex at the same molar concentration. Consequently, the sum of hafnium and zirconium can be determined up to about 3.0×10^{-6} M under the conditions recommended for the determination of zirconium [1]. Some results of such determinations are summarized in Table 2.

TABLE 2

Determination of the sum of hafnium and zirconium

Concentration (M) of		Fluorescence intensity	Concentration (M) of		Fluorescence intensity
Hf	Zr		Hf	Zr	
1.5×10^{-6}	0	75.2	3.0×10^{-6}	0	150.0
1.0×10^{-6}	0.5×10^{-6}	75.6	2.0×10^{-6}	1.0×10^{-6}	151.0
0.5×10^{-6}	1.0×10^{-6}	75.8	1.0×10^{-6}	2.0×10^{-6}	152.1
0	1.5×10^{-6}	75.6	0	3.0×10^{-6}	151.0

REFERENCES

1 T. Ito and A. Murata, Bunseki Kagaku, 23 (1974) 274.
2 A. Brookes and A. Townshend, Analyst, 95 (1970) 781.
3 T. Kouimtzis and A. Townshend, Analyst, 98 (1973) 40.
4 A. T. Pilipenko, T. U. Kukibaev and A. I. Volkova, Zh. Anal. Khim., 28 (1973) 510.
5 A. T. Pilipenko, T. U. Kukibaev, A. I. Volkova and T. E. Get'man, Zh. Anal. Khim., 27 (1972) 1787.
6 S. T. Talipov, L. E. Zel'tser, L. A. Morozova and A. T. Tashkhodzhaev, Zavod. Lab., 44 (1978) 1052; Chem. Abstr., 89 (1978) 225547.
7 A. T. Pilipenko, T. U. Kukibaev and A. I. Volkova, Zh. Anal. Khim., 29 (1974) 710.
8 A. Murata, T. Ito, T. Suzuki and K. Fuziyasu, Bunseki Kagaku, 15 (1966) 143.

Analytica Chimica Acta, 125 (1981) 161—164
Elsevier Scientific Publishing Company, Amsterdam — Printed in The Netherlands

Short Communication

LASER FLUORIMETRIC SYSTEMS FOR ULTRA-TRACE ANALYSIS

KAZUHIKO MIYAISHI, MIKIO KUNITAKE, TOTARO IMASAKA, TEIICHIRO OGAWA and NOBUHIKO ISHIBASHI*

Faculty of Engineering, Kyushu University, Hakozaki, Fukuoka 812 (Japan)

(Received 12th November 1980)

Summary. Laser fluorimetric systems with different exciting sources and signal processing systems are compared with rhodamine B as the standard, and detection limits are discussed. The combination of a nitrogen laser-pumped dye laser, a monochromator and a pulse-gated photon counter provides the highest sensitivity (0.04 ng l^{-1}). Optical filters, a boxcar detection system, or an argon laser with high average power are also effective when fast response times are required.

In laser fluorimetry, many combinations of laser sources and signal processing systems have been used for ultra-trace analysis [1—4]. Detection of rhodamine 6G at the sub-ng l^{-1} level was achieved with a nitrogen laser and interference and Corning filters instead of a monochromator in the detection system [5]. Richardson and George [6] recently discussed various instrumental methods in laser fluorimetry, using rhodamine B as a fluorophor, and detected 0.5 ng l^{-1} with a cavity-dumped argon ion laser and a long pass filter combined with a boxcar integrator. Their conclusions were that a nitrogen laser-pumped dye laser is the preferable source because of its tunability, although the dye laser excitation did not improve the limit of detection (1 ng l^{-1}); that a monochromator in the detection system yielded a poorer detection limit (15 ng l^{-1}); and that a photon counting system also gave a poor detection limit (15 ng l^{-1}). In contrast, fluorescein was recently detected at the 0.02 ng l^{-1} level, by using a dye laser with an identical power output [7]; a tunable dye laser and double monochromator combined with a sensitive photon counting system was found to be essential for ultra-trace analysis. These apparently contradictory results encouraged further studies to clarify the best combination of exciting source and detection system for ultra-trace measurements of rhodamine B.

Experimental

Two fluorimetric systems were studied. In the first system, a sample was excited by a nitrogen laser-pumped dye laser (ca. 0.5 mW), and fluorescence was measured by a double monochromator. The signal from a photomultiplier was processed by a pulse-gated photon counter. Details of this apparatus have been given elsewhere [8]. Alternatively, the 514.5-nm line of a CW argon ion laser (NEC GLG 3200, 800 mW) was used as the exciting source.

The fluorescence signal was amplified by a d.c. amplifier (BB 3421 K) or a commercially available picoammeter (Keithley 417).

Results

The background and fluorescence spectra were measured and signal-to-noise ratios were calculated to find optimum experimental conditions [7]. The highest signal-to-noise ratio was observed at exciting and emission wavelengths of 560 nm and 592 nm, respectively: the detection limit of rhodamine B was thus determined at these wavelengths. Table 1 shows the experimental conditions and the detection limits obtained. Sources of noise are also listed. A detection limit of 0.04 ng l^{-1} was achieved by combining the dye laser system with a pulse-gated photon counter. When the latter was replaced by a d.c. amplifier, a poorer detectability (1 ng l^{-1}) was obtained, because of dark current noise. A change of the exciting wavelength to 514.5 nm (dye laser—photon counting system) gave about 5 times higher detection limits, as expected. This shows that a tunable source is effective for detection at ultra-trace levels, when the source of noise is the solution blank. In comparison with dye laser excitation at 514-5 nm, argon ion laser excitation (514.5 nm) gave a slightly lower detection limit. The dark current noise in this case was again negligible (as in the gated detection system) because of the high average power of the argon ion laser. The slight improvement of the detection limit may thus be obtained, because the power output is stable and there is minimal statistical fluctuation of the photoelectron signal. The average power of the dye laser is 10^2—10^3 times lower than that of the argon ion laser. Nevertheless, the use of sensitive detection equipment such as the pulse-gated photon counter compensates for this disadvantage of the dye laser, and gives a lower detection limit at the optimum exciting wavelength.

The use of a high-power argon laser makes it possible to reduce the time constant of the detection system. Such a system has distinct advantages for

TABLE 1

Detection limits of rhodamine B

Exciting source	Detection apparatus	λ_{ex} (nm)	$\Delta\lambda_{ex}$ (nm)	λ_{em} (nm)	$\Delta\lambda_{em}$ (nm)	Detection limit (ng l^{-1})	Source of noise
Dye laser	Pulse-gated photon counter	560.0	0.66	592	1.3	0.04	Blank
Dye laser	D.c. amplifier	560.0	0.66	592	5.0	1	Dark current
Dye laser	Pulse-gated photon counter	514.5	0.33	585	1.0	0.21	Blank
Argon laser	D.c. amplifier	514.5	0.01	585	1.3	0.16	Blank
Xe lamp	D.c. amplifier	560.0	16.5	585	15.5	2.5	Dark current

the application of laser fluorimetry to continuous flow procedures, because the signal response time should be several seconds at most. In a preliminary investigation of a flow system, the detectable concentration of rhodamine B obtained with argon laser excitation was 1.4 pg, about 20 times lower than that obtained with dye laser excitation and d.c. amplifier detection.

Discussion

To achieve ultra-trace analysis of fluorescent samples, it is essential to use the most sensitive and specific equipment. Tunable CW dye lasers with high average power (ca. 100 mW) have recently become available; alternatively, the wavelength of an argon laser may coincide with the optimum excitation wavelength of the sample. When these sources are combined with a monochromator detection system, the sensitivity of the fluorimeter is usually sufficient, dark current noise is negligible in comparison with the blank signal. It is thus possible to optimize the excitation and emission wavelengths and obtain high sensitivity. Samples at very low concentrations (0.03—0.015 ng l^{-1}) can be detected in about 1 s. Wide bandpass or long pass filters give higher detection limits because of poor specificity.

Nitrogen laser-pumped dye lasers are convenient sources for ultra-trace analysis. However, the average power of 0.5 mW used here is hardly sufficient and a very sensitive detection system is needed. Pulse-gated photon counting is very promising, because the dark count noise from the photomultiplier can be completely removed, but the time constant becomes relatively long. Nonetheless, detection of strongly fluorescent samples (e.g., fluorescein, rhodamine B) at concentrations of 0.02—0.04 ng l^{-1} can be achieved. In this system, the precision of the measurement, which depends on the number of photoelectron signals observed, is limited by the repetition rate of the nitrogen laser. A higher-power dye laser provides no advantage except for increasing specificity by narrowing the resolution of the fluorescence monochromator. However, the present resolution (1.3 nm) is good enough for the measurement of organic samples in the condensed phase.

If a short response time (several seconds at most) is required for the measurement, a boxcar integrator may be useful. In this case, the sensitivity of the instrument is not sufficient because of the low average power of the dye laser (0.5 mW). The detection limit is thus relatively high (15 ng l^{-1}) [2]. In order to increase sensitivity, the monochromator may be replaced by optical filters; this can improve the detection limit to 1 ng l^{-1} [6]. In this configuration, the detection limit is dependent on the solution blank. If a tunable dye laser is available, the wavelength should be adjusted to the optimum value for the detection of the samples at yet lower levels. Otherwise, the higher-power laser (e.g. cavity-dumped argon laser at ca. 60 mW [6]) may provide slightly better detection limit [1]. The use of sensitivity signal-processing equipment such as a photon counter gives much poorer detection limits because of statistical fluctuation of the signals [3].

The conclusions reached earlier [6, 7] can thus be consistently explained. One remaining problem is the discrepancy in the detection limits obtained

by measurements with a dye laser and a monochromator. The detection limit of 1—2 ng l^{-1} obtained with a d.c. amplifier are much lower than those (15 ng l^{-1}) obtained with a boxcar integrator [6]. The gate operation of the boxcar integrator reduces the dark current noise, and so should provide the lower detection limit. The improved detection limit in this study may originate partly from the optimization of the excitation wavelength (cf. Table 1) and partly from the improvement of the optical system for fluorescence collection; the line image of fluorescence is exactly adjusted to the slit of the monochromator.

This research was partly supported by a Grant-in-Aid for Scientific Research (Grant No. 347054) and for Environmental Science (Grant No. 543041) from the Ministry of Education.

REFERENCES

1 T. F. V. Geel and J. D. Winefordner, Anal. Chem., 48 (1976) 335.
2 G. J. Diebold and R. N. Zare, Science, 196 (1977) 1439.
3 J. H. Richardson and M. E. Ando, Anal. Chem., 49 (1977) 955.
4 T. Imasaka, H. Kadone, T. Ogawa and N. Ishibashi, Anal. Chem., 49 (1977) 667.
5 A. B. Bradley and R. N. Zare, J. Am. Chem. Soc., 98 (1976) 620.
6 J. H. Richardson and S. M. George, Anal. Chem., 50 (1978) 616.
7 N. Ishibashi, T. Ogawa, T. Imasaka and M. Kunitake, Anal. Chem., 51 (1979) 2096.
8 T. Imasaka, T. Ogawa and N. Ishibashi, Anal. Chem., 51 (1979) 502.

Analytica Chimica Acta, 125 (1981) 165—169
Elsevier Scientific Publishing Company, Amsterdam — Printed in The Netherlands

Short Communication

LIQUID ANION-EXCHANGE SEPARATION OF VANADIUM(V) AND NIOBIUM(V) FROM SUCCINATE SOLUTION

S. D. SHETE and V. M. SHINDE*

Analytical Laboratory, Department of Chemistry, Shivaji University, Kolhapur 416 004 (India)

(Received 22nd August 1980)

Summary. Tri-n-octylamine is used for the extraction and mutual separation of V(V), Nb(V) and Ta(V) from succinate solution. Niobium and vanadium are determined spectrophotometrically in the organic phase with thiocyanate and PAR, respectively. Tantalum is determined with PAR in an aqueous phase.

Various methods for the extraction of vanadium, niobium and tantalum have been summarized and critically reviewed [1—3]. In this communication, a new method is proposed for extraction and separation of vanadium, niobium and tantalum from succinate solution using tri-n-octylamine (TOA) as the extractant. The proposed method is suitable for the mutual separation of the three metals at microgram levels.

Experimental

Apparatus. A Zeiss spectrophotometer (Jena) with 1-cm quartz cells and a Philips precision pH meter were used.

Reagents. For the standard vanadium(V) solution, dissolve 1.14 g of ammonium metavanadate in the requisite amount of hydrochloric acid, dilute with distilled water to 1 l, and standardize titrimetrically [4]. For the standard niobium(V) solution, fuse 0.071 g of Nb_2O_5 (Koch-Light) with 3 g of potassium pyrosulphate, dissolve the cooled melt in 1 M tartaric acid and dilute to 100 ml with this solution. For the standard tantalum(V) solution, fuse 2.5 g of Ta_2O_5 (Koch-Light) with potassium nitrate and potassium carbonate in the weight ratio 2:5:5. Dissolve the cooled melt in concentrated sulphuric acid, evaporate to almost dryness and dissolve the residue in 20% tartaric acid solution. Standardize the niobium and tantalum solutions with N-benzoyl-N-phenylhydroxylamine [5]. Prepare working solutions by suitable dilution of the stock solutions.

Prepare a 5% (w/v) solution of TOA (Koch-Light) in benzene, and equilibrate with 2 M sodium succinate before use.

Prepare a 15% (w/v) tin(II) chloride solution in 4 M hydrochloric acid—1 M tartaric acid solution. For the acetate buffer, dissolve 27.2 g of sodium acetate in water, add 17 ml of glacial acetic acid and dilute to 1 l.

Procedure for TOA extraction and determination of vanadium(V). To 10—25 μg of vanadium(V) in aqueous solution, add enough sodium succinate to make its concentration 0.01 M in a total volume of 25 ml, adjust the pH to 4.0 with dilute sodium hydroxide and hydrochloric acid solutions and transfer to a 100-ml separatory funnel. Equilibrate the aqueous solution for 5 min with two 5-ml portions of 5% TOA in benzene. To the combined organic phases, add 1 ml of an aqueous 0.01% solution of 4-(2-pyridylazo)-resorcinol. Shake the mixture and allow to stand for 10 min; vanadium(V) forms a red complex with PAR. Dry the organic phase with anhydrous sodium sulphate and measure the absorbance at 560 nm, against a reagent blank prepared analogously.

Procedure for TOA extraction and determination of niobium(V). Take 10—40 μg of niobium(V) in an aliquot of aqueous solution prepared as above, and extract once as for vanadium, but omitting the pH adjustment. Separate the organic phase and shake it well for 2 min with the reagents added in the following order: 5 ml of freshly prepared 20% potassium thiocyanate solution, 2 ml of 15% tin(II) chloride solution and 5 ml of 9 M hydrochloric acid—1 M tartaric acid solution (freshly prepared); niobium forms a yellow complex. Dry the organic phase with anhydrous sodium sulphate and measure the absorbance at 430 nm against a reagent blank prepared analogously.

Separation and determination of vanadium(V), niobium(V) and tantalum(V). To an aqueous solution containing 10—40 μg each of vanadium(V) and niobium(V) and 100—400 μg of tantalum(V), add succinate, adjust to pH 4, and extract twice as described for vanadium(V). Tantalum(V) is not extracted at all under these conditions. Evaporate the aqueous phase almost to dryness, add 2 ml of hydrogen peroxide and 2 ml of 0.01% PAR solution, adjust the pH to 5.5 with tartaric acid and sodium hydroxide solutions to give a total volume of 25 ml, and measure the absorbance of the tantalum complex at 490 nm against a reagent blank [6]. From the combined organic phases, selectively strip vanadium with 5 ml of pH 4.7 acetate buffer and determine it spectrophotometrically with PAR after oxidation with bromine water [7]. Niobium remains in the organic phase; determine as described in the above procedure for niobium.

Results and discussion

Extraction conditions. The extraction of vanadium(V) and niobium(V) was investigated at pH 2—8, from 0.002—0.02 M sodium succinate solution and by 0.05—5% TOA. The pH for quantitative extraction of vanadium(V) and niobium(V) is 4 ± 0.2. Figure 1 shows that vanadium (10—25 μg) and niobium (10—40 μg) are quantitatively extracted into 5% TOA solution from 0.01 M sodium succinate (this has a pH of 4). Tantalum(V) is not extracted into TOA from succinate solutions. The percentage extraction (% E), and distribution ratio for vanadium and niobium were calculated after spectrophotometric measurement in the TOA phase with PAR and thiocyanate,

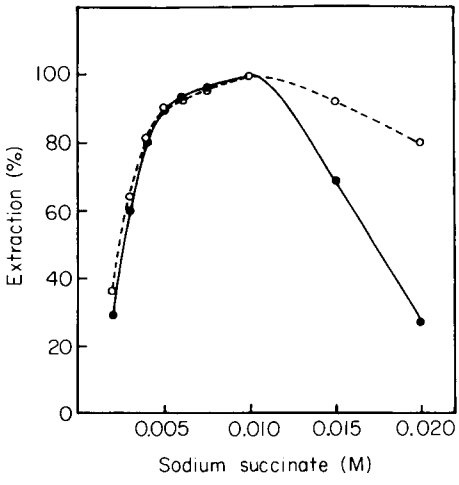

Fig. 1. Extraction of (○) vanadium, and (●) niobium with 5% TOA in benzene as a function of sodium succinate concentration.

respectively. Variation in the concentration of TOA in benzene showed that 5% TOA is needed for quantitative extraction of vanadium and niobium. The log—log plots of the distribution ratio vs. succinate concentration at fixed pH and TOA concentrations gave slopes of 3.1 and 3.3 for vanadium and niobium, respectively, indicating a metal-to-succinate mole ratio of 1:3 in the extracted species. Similarly, log—log plots of distribution ratio vs. TOA concentration at fixed pH and succinate concentration gave a slope of 0.9 for both vanadium and niobium which shows that the metal-to-TOA ratio in the extracted species is 1:1.

The amine-succinate salt thus acts as a liquid anion exchanger, reacting with the anionic metal succinate complex and resulting in extraction into the organic phase. The extraction mechanism could be written as

$$\{R_3NH^+S^-\}_{org} + [M(C_4H_4O_4)_3]^-_{aq} \rightleftharpoons \{R_3NH^+[M(C_4H_4O_4)_3]^-\}_{org} + S^-_{aq}$$

where M is vanadium(V) or niobium(V), S^- represents the succinate ion and R_3N is TOA.

Spectral characteristics. The extracted vanadium and niobium may be determined spectrophotometrically in the TOA phase, with PAR and thiocyanate, respectively. The red vanadium(V)-PAR complex in TOA shows maximum absorbance at 560 nm (Fig. 2); the absorbance is stable for more than 24 h. The colour system conforms to Beer's law for 5—25 μg of vanadium per 10 ml of organic phase. The yellow niobium—thiocyanate complex in TOA absorbs appreciably at 430 nm and obeys Beer's law for 5—40 μg of niobium per 5 ml of organic phase. The absorbance is again stable for more than 24 h. The characteristic spectrophotometric data for vanadium and niobium are reported in Table 1.

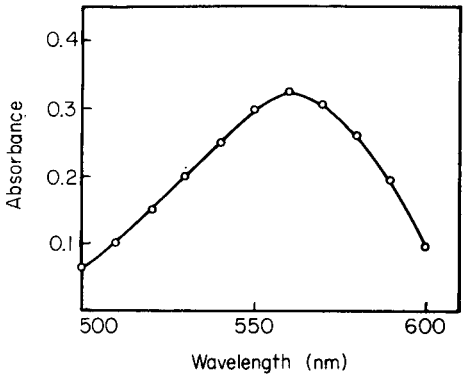

Fig. 2. Absorption spectrum of vanadium(V)—PAR in 5% TOA in benzene.

TABLE 1

Spectrophotometric data for the determination of vanadium(V) and niobium(V) after extraction with TOA

	Vanadium (PAR)	Niobium (Thiocyanate)
Molar absorptivity ($\times 10^4$ l mol^{-1} cm^{-1})	1.65	1.34
Sandell sensitivity (ng cm^{-2})	3.1	6.9
Mean absorbance[a]	0.325	0.29
Standard deviation	0.0045	0.0035
Coefficient of variation (%)	1.4	1.2

[a] 6 determinations of 10 μg of V or Nb.

Interferences. For the extraction and spectrophotometric determination of vanadium (10 μg), 100 μg of Hf(IV), 250 μg of Bi(III), 500 μg of Mn, Sn(II), Sb, Zr(IV) or Te(IV), 1 mg of Pb, Se(IV), Nb, citrate or oxalate, and 5 mg of chloride, fluoride, nitrate or tartrate did not interfere. However, cadmium, EDTA and phosphate interfered seriously. Interference of iron(III) in vanadium and niobium extractions is eliminated by selective pre-extraction with mesityl oxide [8].

For the extraction and spectrophotometric determination of niobium (10 μg), 100 μg of Bi(III), Sb(III), Zr(IV) or Hf(IV), 500 μg of Mn, Sn(II) or Pb, 1 mg of Cd, Te(IV) or Se(IV), 2.5 mg of V(V) or ascorbate and 5 mg of chloride, fluoride, nitrate, citrate, tartrate, phosphate or oxalate did not interfere. EDTA interfered seriously.

By suitable combination of extraction and back-extraction procedures, tantalum, vanadium and niobium can be determined in admixture. The results of some determinations done in this way are given in Table 2. The

TABLE 2

Analysis of synthetic mixtures

Vanadium(V)			Niobium(V)			Tantalum(V)		
Taken (μg)	Found (μg)	Recovery (%)	Taken (μg)	Found (μg)	Recovery (%)	Taken (μg)	Found (μg)	Recovery (%)
10	10.4	104	10	9.9	99	100	99.6	99.6
20	19.8	99	20	20.2	101	200	19.8	99
40	40.4	101	40	39.6	99	400	400	100

average recoveries of vanadium, niobium and tantalum are 101.3%, 99.6% and 99.6%, respectively. The method permits the separation and determination of each metal ion in 30 min.

The authors thank the University Grants Commission, New Delhi, for financing this project and awarding a fellowship to one of them (S. D. S.).

REFERENCES

1 J. Korkisch, Modern Methods for the Separation of Rare Metal Ions, Pergamon, Oxford, 1969.
2 J. Starý, The Solvent Extraction of Metal Chelates, Pergamon, Oxford, 1964.
3 A. K. De, S. M. Khopkar and R. A. Chalmers, Solvent Extraction of Metals, Van Nostrand, London, 1970.
4 V. M. Shinde and S. M. Khopkar, Chem. Anal. (Warsaw), 14 (1969) 749.
5 A. K. Majumdar and A. K. Mukherjee, Anal. Chim. Acta, 19 (1958) 23.
6 S. V. Elinson and T. Rezova, Z. Anal. Khim., 19 (1964) 1078.
7 E. Gagliardi and B. Ilmaier, Mikrochim. Acta, (1967) 180.
8 V. M. Shinde and S. M. Khopkar, Sep. Sci., 4 (1969) 161.

Analytica Chimica Acta, 125 (1981) 171—174
Elsevier Scientific Publishing Company, Amsterdam — Printed in The Netherlands

Short Communication

η^6-ARENE-η^5-CYCLOPENTADIENYLIRON CATIONS AND THEIR APPLICATION IN THE IDENTIFICATION OF AROMATICS IN PETROLEUM

C. I. AZOGU

Department of Chemistry, University of Ibadan, Ibadan (Nigeria)

(Received 17th July 1980)

Summary. The ligand-exchange reaction between arenes and ferrocene to form η^6 arene-η^5-cyclopentadienyliron cations is utilized for the selective complexation of aromatics. Pyrolytic mass spectral analysis then gives qualitative information on the aromatic composition of the samples. Thin-layer chromatography can be used in some cases.

In 1963, Nesmeyanov et al. [1] reported the preparation of η^6-arene-η^5-cyclopentadienyliron cations by the reaction of benzene and substituted benzenes with ferrocene and aluminium chloride, with aluminium powder added to convert any ferricinium ion formed to ferrocene. Many polycyclic aromatics [2] and polycyclic heteroaromatic systems [3—6] have since been shown to undergo the ligand-exchange reaction. These complexes disproportionate to give the arene and ferrocene on irradiation at 253—577 nm [6—9] or by pyrolytic sublimation under reduced pressure [9, 10].

The apparent generality of this reaction prompted an investigation of the possibility of its use in the selective complexation of aromatics in petroleum followed by a pyrolytic mass spectral analysis of the mixed complexes for their aromatic components. This analytical approach for identification of aromatics in petroleum offers some advantages over conventional methods because there is no interference from non-aromatic components. The sample can thus be used directly for the identification without the need for fractionation and in relatively short time.

Experimental

Apparatus and reagents. All reagents used were of analytical grade. These included ferrocene (Aldrich), $AlCl_3$ (BDH), aluminium powder (BDH), ammonium hexafluorophosphate (Alfa Products) and decahydronaphthalene (decalin; Aldrich), which were used as received. n-Hexane, petroleum ether (b.p. 40—60°C), diethyl ether, dichloromethane, and acetone were distilled before use. The arenes and oil samples were thoroughly dried over anhydrous calcium chloride and magnesium sulphate before each ligand-exchange reaction. Authentic samples of η^6-arene-η^5-cyclopentadienyliron hexafluorophosphates for benzene, toluene, *p*-xylene and naphthalene were

0003—2670/81/0000—0000/$02.50

prepared as described in the literature [1, 8].

The mass spectral analyses were done with a Varian MAT 112 double-focussing mass spectrometer. Thin-layer chromatography was done on Selecta F1500 silica gel plates (Schleicher and Schuell). Column chromatography was on Merck silica gel-60 activated at 120°C for 3 h.

Preparation of arenecyclopentadienyliron salts of a mixture of arenes. Ferrocene (9.3 g, 50 mmol), $AlCl_3$ (13.3 g, 100 mmol), Al (1.35 g, 50 mmol), benzene (3.9 g, 50 mmol), toluene (4.6 g, 50 mmol), *p*-xylene (5.3 g, 50 mmol) and naphthalene (6.4 g, 50 mmol) in decalin (80 ml) were heated at 135°C with vigorous stirring under reflux in an atmosphere of nitrogen for 5 h. The reaction mixture was allowed to cool and was gradually decomposed by pouring onto ice (50 g). After being stirred for 30 min, the mixture was filtered through celite, and the aqueous filtrate was extracted with n-hexane or diethyl ether (40 × 4 ml) to remove unreacted ferrocene, aromatics and decalin. A yellow precipitate was obtained by the addition (with stirring) of a concentrated aqueous solution of ammonium hexafluorophosphate (5 g) to the aqueous layer. The precipitate was filtered and dried under vacuum to give yellow crystals (5.2 g) which were stored under vacuum, protected from light.

Preparation of arenecyclopentadienyliron salts from crude oil samples W-1 and W-2. Ferrocene (9.3 g, 50 mmol), $AlCl_3$ (15 g, 110 mmol), Al (1.35 g, 50 mmol) and the crude oil sample (10 g) in decalin (30 ml) were heated under reflux with stirring at 135°C for 6 h in an atmosphere of nitrogen. After work-up, following the procedure described above, W-1 gave a green solid (2.1 g) while W-2 gave a light-brown solid (3.9 g) after an initially-formed oily product had been pumped under high vacuum.

Thin-layer chromatography of the arene complexes. The complexes dissolved in acetone were spotted on the plates and developed in acetone–dichloromethane (1:4). The spots were located in iodine vapour and identified by comparison with authentic samples. R_f values obtained were: $[C_6H_6FeC_5H_5]PF_6$ (0.15), $[C_6H_5CH_3FeC_5H_5]PF_6$ (0.23), $[C_{10}H_8FeC_5H_5]PF_6$ (0.32) and $[p\text{-}C_6H_4(CH_3)_2FeC_5H_5]PF_6$ (0.35).

Column chromatography of the crude oil samples, W-1 and W-2. The crude oil samples (4 g) were chromatographed on Merck silica gel-60 (200 g) and eluted successively with petroleum ether (500 ml) and benzene (1000 ml). The benzene eluate was concentrated at 50°C and 1.5 mm.

Results and discussion

In preliminary experiments, the ligand-exchange reaction between ferrocene and a mixture of benzene, toluene, *p*-xylene and naphthalene was tested. The yellow solid obtained was subjected to pyrolytic mass spectral analysis at 250°C and 15 eV. Peaks were observed at *m/z* 78 ($C_6H_6^+$), 92 [$C_6H_5CH_3^+$], 106 [$C_6H_4(CH_3)_2^+$], 128 ($C_{10}H_8^+$), 132 and 186 [$(C_5H_5)_2Fe^+$] as expected. The peak at *m/z* 132 corresponded to tetralin from the tetralin complex resulting from hydrogenation of the naphthalene ligand during the

ligand-exchange reaction [8]. Thin-layer chromatography of the solid gave a clean separation of the individual complexes and by comparison with authentic samples, the R_f values were found to be in the order $[C_5H_5FeC_6H_4(CH_3)_2]PF_6 > [C_5H_5FeC_{10}H_8]PF_6 > [C_5H_5FeC_6H_5CH_3]PF_6 > [C_5H_5FeC_6H_6]PF_6$. No spot corresponding to the tetralin complex was observed, possibly because of overlap between this band and that of the naphthalene or *p*-xylene complexes.

The ligand exchange procedure was then applied to petroleum samples W-1 and W-2 from two Nigerian oil wells. The solids obtained for the two samples were analysed by mass spectrometry at 250°C and 15 eV. The spectra revealed a wide range of aromatics (Table 1). These data were compared with those obtained from mass spectral analyses of the benzene eluates of the two crude oil samples, also presented in Table 1. Benzene was used for the elution since it had already been identified by the complexation method. The agreement between the two sets of data is striking and points to the efficacy of the complexation method.

Thin-layer chromatography of the complexes from W-1 and W-2, however, could separate only benzene, methylbenzenes, naphthalene and fluorene; other components of mixture were bunched up close to the solvent front. Further work on improving the t.l.c. analytical procedure is in progress.

TABLE 1

Mass spectral data for arene complexes and benzene eluates from crude oil samples

m/z	W-1		W-2	
	Complex	Eluate	Complex	Eluate
	Arene	Arene	Arene	Arene
78	Benzene	(Benzene)	Benzene	(Benzene)
92	Toluene	Toluene	Toluene	Toluene
106	Xylene	Xylene	Xylene	Xylene
118	Indan	Indan	—	Indan
120	Mesitylene	Mesitylene	Mesitylene	—
128	Naphthalene	Naphthalene	Naphthalene	Naphthalene
132	—	—	Tetralin	—
142	Methylnaphthalene	Methylnaphthalene	—	Methylnaphthalene
154	Acenaphthene	Acenaphthene	Acenaphthene	Acenaphthene
156	Dimethylnaphthalene	Dimethylnaphthalene	Dimethylnaphthalene	Dimethylnaphthalene
166	—	Fluorene		Fluorene
170	Trimethylnaphthalene	Trimethylnaphthalene	Trimethylnaphthalene	Trimethylnaphthalene
178	Phenanthrene	—	—	—
186	Ferrocene	—	Ferrocene	—

REFERENCES

1 A. N. Nesmeyanov, N. A. Vol'kenau and I. N. Bolesova, Dokl. Akad. Nauk SSSR, 149 (1963) 615.
2 R. G. Sutherland, J. Organomet. Chem. Libr., 3 (1977) 311.
3 C. C. Lee, B. R. Steele and R. G. Sutherland, J. Organomet. Chem., 186 (1980) 265.
4 J. F. Helling and W. A. Hendrickson, J. Organomet. Chem., 141 (1977) 99.
5 P. Bachmann and H. Singer, Z. Naturforsch B, 31 (1976) 525.
6 R. G. Sutherland, B. R. Steele, K. J. Demchuk and C. C. Lee, J. Organomet. Chem., 181 (1979) 411.
7 A. N. Nesmeyanov, N. A. Vol'kenau and L. S. Shilovtseva, Dokl. Akad. Nauk SSSR, 190 (1970) 857.
8 R. G. Sutherland, S. C. Chen, W. J. Pannekoek and C. C. Lee, J. Organomet. Chem., 101 (1975) 221.
9 R. G. Sutherland, W. J. Pannekoek and C. C. Lee, Can. J. Chem., 56 (1978) 1782.
10 C. C. Lee, K. J. Demchuk and R. G. Sutherland, Can. J. Chem., 57 (1979) 933.

Analytica Chimica Acta, 125 (1981) 175—178
Elsevier Scientific Publishing Company, Amsterdam — Printed in The Netherlands

Short Communication

COMPARISON OF A CONVENTIONAL EXTRACTOR WITH TWO UNCONVENTIONAL EXTRACTORS

WALTER A. AUE*, PALITHA P. WICKRAMANAYAKE and JÜRGEN MÜLLER
Department of Chemistry, Dalhousie University, Halifax, Nova Scotia (Canada)
(Received 9th September 1980)

Summary. Two specially-made extractors are compared against a standard Soxhlet by using test samples simulating adsorptive and non-adsorptive conditions and containing coarse and fine particles. The unconventional extractors, one with a fixed thimble and the other with a removable thimble, proved considerably faster than the Soxhlet.

Among continuous extractors [1], the Soxhlet ranks high as an efficient and widely used laboratory tool. It has therefore been chosen as a standard against which to compare two specially-made high-purity extractors. These units can be built in a wide range of configurations and capacities [2]. The ones tested here are shown in Fig. 1. They are designed to maintain a solvent head [3] and quasi-chromatographic flow aided by considerable hydrostatic pull.

The relative speed of extractors depends not only on solvent flow but also on various physical characteristics of the sample. The model systems examined here contained adsorbed or non-adsorbed solute on matrices of low or high flow resistance. Other parameters such as intraparticle diffusion or swelling were not investigated.

Experimental

The matrices were a high-resistance (200-mesh) silica gel 62 with a surface area of about 300 $m^2\ g^{-1}$ and an average pore diameter of about 135 Å, and a low-resistance (70—230 mesh) silica gel 60 with 550 $m^2\ g^{-1}$ and 60 Å. The solute was quinoline; the two solvents were hexane and ethanol. Quinoline was determined by ultraviolet absorption. It was strongly retained on silica gel when chromatographed with hexane, but migrated with the solvent front when developed with ethanol. The sample was prepared by dissolving a known amount of quinoline in the extraction solvent and depositing it onto a known amount of silica by rotary evaporation.

The conventional extractor used was a Soxhlet (Kontes model K-585100, size 21, in which hot solvent vapors ascend around the thimble chamber), operated with specially-made or commercial (Fisher) 25 × 80 mm thimbles (both thimbles gave the same performance) and a conventional Kontes model K456500 size 21 reflux condenser.

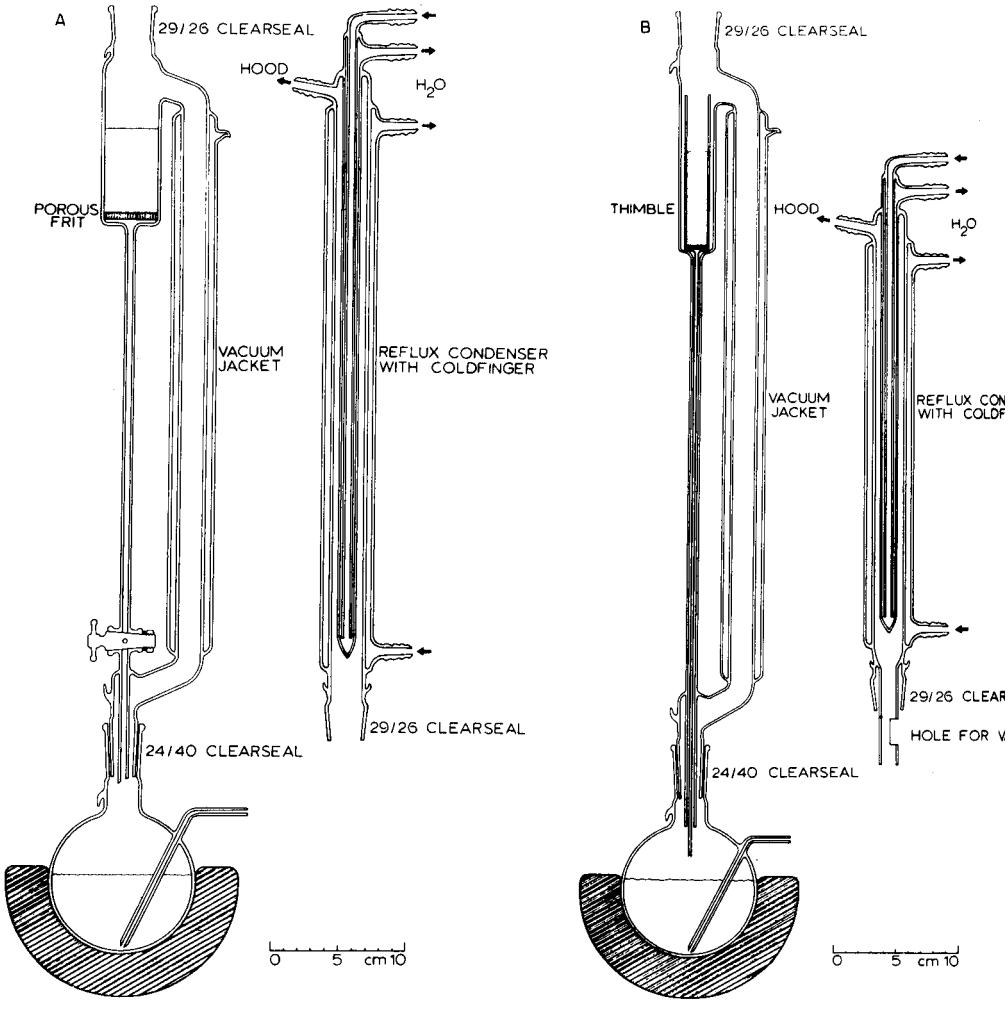

Fig. 1. Extractor models: (A) "integral thimble" unit; (B) "removable thimble" unit.

With one exception, 500-ml flasks were used for all extractors. These flasks had a side-arm through which, by means of a stationary PTFE capillary with outside Luer-lock, samples could be withdrawn for measurements and returned with a syringe. (This sampling port replaced the regular side-arm for nitrogen introduction that is shown in Fig. 1.) The solvents were heated by "Thermowells" (Laboratory Craftsman) at the percent of maximum power listed in Table 1.

The cross-sections (and inner diameters) of the sample compartments were as follows: Soxhlet thimble 4.9 cm^2 (2.5 cm), Soxhlet thimble container 7.1 (3.0); model A thimble 10.8 (3.7); model B thimble 2.5 (1.8), and model B thimble chamber 4.5 cm^2 (2.4 cm).

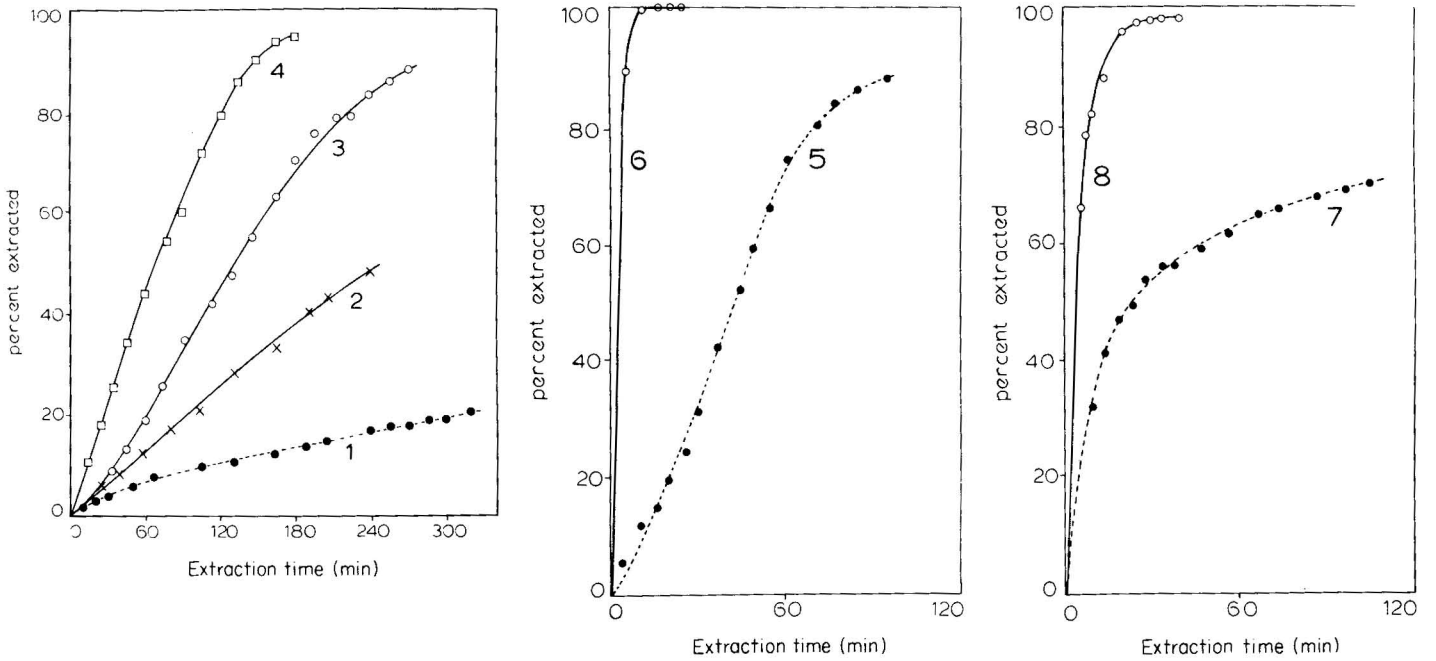

Fig. 2. Extraction curves for an adsorptive system with low flow resistance: quinoline on 70—230 mesh silica gel 60, extracted by hexane close to boiling point. Curves, extractor models and heat inputs: (1) Soxhlet, 30%/325 W; (2) model B, 30%/325 W; (3) model A, 30%/325 W; (4) model A, 100%/500 W. Other data in Table 1.

Fig. 3. Extraction curves for a non-adsorptive system with low flow resistance: quinoline on 70—230 mesh silica gel 60, extracted by ethanol close to boiling point. Curves: (5) Soxhlet, 55%/325 W; (6) extractor A, 55%/325 W. Other data in Table 1.

Fig. 4. Extraction curves for a non-adsorptive system with high flow resistance: quinoline on 200-mesh silica gel 62, extracted by ethanol close to boiling point. Curves: (7) Soxhlet, 55%/325 W; (8) extractor A, 40%/325 W. Other data in Table 1.

TABLE 1

Extraction conditions

Run number[a]	1	2	3	4	5	6	7	8
Extractor model	Soxhlet	B[b]	A[c]	A[c]	Soxhlet	A[c]	Soxhlet	A[c]
Quinoline (mg)	14	14	13	16	12	11	12	11
Silica gel (g)	15	15	15	15	15	14	7	7
Particle mesh	70/230	70/230	70/230	70/230	70/230	70/230	200	200
Solvent	Hexane	Hexane	Hexane	Hexane	Ethanol	Ethanol	Ethanol	Ethanol
Flask (ml)	500	500	500	1000	500	500	500	500
Heat setting (%)	30[d]	30[e]	30[f]	100[f]	55[d]	55	55[d]	40[e]
100% power (W)	325	325	325	500	325	325	325	325
Fig. no.	2	2	2	2	3	3	4	4

[a]Corresponds to curve numbers in Figs. 2—4. [b]Model B is the extractor with removable thimble shown in Fig. 1B. [c]Model A is the extractor with integral thimble shown in Fig. 1A. [d]Maximum for Soxhlet before solvent backs up in reflux condenser. [e]Small amount of overflow. [f]Necessary to restrict flow with stopcock to maintain solvent head.

Results and discussion

Table 1 lists the extraction conditions and Figs. 2—4 present the resulting extraction curves. The conditions had been chosen to provide a fair comparison of performance, to accommodate the different model systems, and to include a high-speed run.

Such extraction curves represent the best way to express quantitatively the results of this and similar studies. Clearly, the two unconventional extractors evaluated here were considerably faster than the quite efficient Soxhlet.

This research was supported by NSERC grant A-9604.

REFERENCES

1 L. C. Craig and D. Craig, in A. Weissberger (Ed.), Technique of Organic Chemistry, Vol. III, Interscience, New York, 1956, p. 149.
2 W. A. Aue, M. M. Daniewski, J. Müller and J. P. Laba, Anal. Chem., 49 (1977) 1465.
3 C. E. Browne, W. L. Buchanan and E. J. Eisenbraun, Chem. Ind., 1977, p. 35.

Analytica Chimica Acta, 125 (1981) 179—181
Elsevier Scientific Publishing Company, Amsterdam — Printed in The Netherlands

Short Communication

A PROPRANOLOL-RESPONSIVE COATED-WIRE ELECTRODE

TAKESHI YAMADA[a] and HENRY FREISER*
Department of Chemistry, University of Arizona, Tucson, AZ 85721 (U.S.A.)

(Received 22nd October 1980)

Summary. Propranolol-responsive electrodes of both the coated wire and conventional types based on the didodecylnaphthalene sulfonic acid salt were prepared and their operating characteristics were compared. The detection limit of the coated-wire electrodes is about 10^{-6} M; interferences from common inorganic ions and from the analagous product isoproterenol are small. The response time varies from 15 s to 30 min depending on concentration; readings are reproducible to within 0.5 mV. Electrodes are still operational after six months of intermittent use.

Recently the efficacy has been demonstrated of using dinonylnaphthalene sulfonate as a counter-ion for developing highly selective coated-wire electrodes for higher molecular weight substituted ammonium ions [1] that can be usefully adapted to trace level assay of drugs and medicinals [2]. This report presents the results of a study of a coated-wire electrode designed to respond to propranolol.

Propranolol {1-[(1-methylethyl)amino]-3-(1-naphthalenyloxy)-2-propanol}

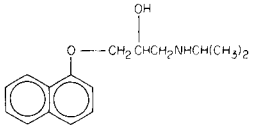

was introduced in the sixties [3] as a β-adrenergic blocking agent [4, 5] useful in treating hypertension and cardiac arrhythmia. Various analytical approaches to its determination including high-performance liquid chromatography [6], gas chromatography [7], fluorimetry [8], radioimmunoassay [9], have been reported but these methods require the use of sophisticated instrumentation and more complex or time-consuming procedures than would be needed with the potentiometric approach of ion-selective electrodes (i.s.e.).

Selinger and Staroscik [10] prepared a working propranolol electrode using tetraphenylborate as counter-ion and observed a relatively low slope (—50 mV) and short lifetime (3—5 weeks). This study was undertaken in the expectation of developing an electrode with significantly improved characteristics.

[a]On study leave from the Faculty of Textile Science, Kyoto Technical University, Kyoto, Japan.

0003—2670/81/0000—0000/$02.50

Experimental

Reagents. Propranolol-HCl was kindly donated by Ayerst Laboratories (New York), and l-isoproterenol by Dr. T. Mimaki, Osaka University, Japan. Didodecylnaphthalene sulfonic acid (DDNS) was obtained from Henkel (Minneapolis, MN) and quaternary ammonium salts from Eastman (Rochester, NY). All other reagents were analytical-reagent grade.

E.m.f. measurements. All electrode potentials were measured vs. a double-junction saturated Ag/AgCl reference electrode with 0.1 M NH_4NO_3 junction solution.

Calibration experiments were performed with a microcomputer-controlled potentiometric system [11]. Calibration solutions were thermostatted at 25.0 ± 0.1°C using a Forma Scientific (Marietta, OH) circulating bath. Selectivity coefficients and i.s.e. detection limits were determined as described previously [12].

Preparation and handling of electrodes. Coated-wire and conventional polymer membrane i.s.e.'s were prepared as previously described [1]. The internal reference solution of the conventional polymer membrane i.s.e.'s was 10^{-3} M propranolol-hydrochloride. All propranolol—HCl solutions used were buffered at pH 5.0 with 10^{-2} M acetate buffers. The DDNS in the polymer membrane was converted to the propranolol—DDNS ion-pair form by soaking the electrodes in 10^{-3} M propranolol—HCl for a week. When not in use, coated-wire electrodes were stored in 10^{-3} M propranolol; conventional electrodes were stored in 10^{-4} M propranolol.

Results and discussion

The response characteristics of both the conventional polymer membrane and coated-wire i.s.e.'s are summarized in Table 1. Both types exhibited near Nernstian response down to 10^{-5} M with a lower limit of detection at approximately 10^{-6} M. It should be pointed out that at the lower concentrations, the electrodes should be equilibrated for 30 min to obtain the proper response. Although the conventional membrane electrode has a somewhat greater sensitivity than the coated-wire electrode, the response times of the latter are significantly shorter. It should be noted that the reproducibility measures reported in Table 1 represent averages of data obtained from at least eight electrodes, collected over a period of a month, demonstrating the high stability and reproducibility of these electrodes.

The selectivity ratios (K_{ij}) of the propranolol electrodes, determined by a standard procedure [12], are shown in Table 2. They show, as did other DNNS-based electrodes for DTA [1] and PCP [2], negligible interference from common inorganic cations, indicating that determination of propranolol in physiological fluids can be readily accomplished using this electrode. Furthermore, the K_{ij} of l-isoproterenol, a dihydroxylated analagous product of isopropranolol, is small and significant interference does not occur. Propranolol electrodes made more than six months ago are still performing well and have essentially unchanged operating parameters.

TABLE 1

Critical response characteristics of propranolol electrodes

	Coated-wire	Conventional
Slope (mV/log a)[a]	59.51 ± 0.71	59.70 ± 0.42
Standard deviation (mV)[b]	0.11	0.16
Intercept (mV)[c]	528 ± 12	392.6 ± 5.1
Lower limit of linear range (M)	$10^{-5.00}$	$10^{-5.40}$
Detection limit (M)	$10^{-5.80}$	$10^{-6.00}$

[a]Standard deviation in slopes obtained for multiple calibrations over 30-day period. [b]Average of standard deviations obtained from least-squares analysis of individual calibration curves. [c]Standard deviation in intercept obtained for multiple calibration.

TABLE 2

Selectivity ratios for propranolol electrodes

Interference	K_{ij} values		Interference	K_{ij} values	
	Coated-wire	Conventional		Coated-wire	Conventional
Mg^{2+}, Ca^{2+} K^+, NH_4^+	$<10^{-4}$	$<10^{-4}$	Tetramethyl-ammonium	1.1×10^{-3}	1.8×10^{-3}
H^+	-2.2×10^{-4}	1.3×10^{-4}	Tetraethyl-ammonium	0.010	0.017
Dimethylammonium	2.4×10^{-4}	2.1×10^{-4}	Tetrapropyl-ammonium	0.90	1.9
Dipropylammonium	0.026	0.036	Tetrabutyl-ammonium	49	120
Dibutylammonium	0.31	0.32	Decyltri-methylammonium	19	29
Triethylammonium	3.2×10^{-3}	4.6×10^{-3}	Dodecyltri-methylammonium	130	170
Tripropylammonium	0.042	0.072	l-isoproterenol	2.6×10^{-3}	1.5×10^{-3}
Tributylammonium	4.0	5.8			

This research was financially supported by a grant from the Office of Naval Research.

REFERENCES

1 C. R. Martin and H. Freiser, Anal. Chem., 52 (1980) 562.
2 C. R. Martin and H. Freiser, Anal. Chem., 52 (1980) 1772.
3 A. F. Crowther and L. H. Smith, Belg. pat. 640312 (1964), U.S. pat. 3337628 (1967).
4 A. M. Barrett and V. A. Cullum, Brit. J. Pharmacol., 34 (1968) 43.
5 P. A. Bond, Nature, 213 (1967) 721.
6 J. F. Prithard, D. W. Schneck and A. H. Hayes, Jr., J. Chromatogr., 162 (1979) 47.
7 R. E. Kates and C. L. Jones, J. Pharm. Sci., 66 (1977) 1490.
8 P. S. Rao, L. C. Quesada and H. S. Mueller, Clin. Chim. Acta, 88 (1978) 355.
9 K. Kawashima, A. Levy and S. Spector, J. Pharmacol. Exp. Ther., 196 (1976) 517.
10 K. Selinger and K. Staroscik, Pharmazie, 33 (1978) 208.
11 C. R. Martin and H. Freiser, Anal. Chem., 51 (1979) 803.
12 C. R. Martin and H. Freiser, J. Chem. Educ., 57 (1980) 512.

Analytica Chimica Acta, 125 (1981) 183—186
Elsevier Scientific Publishing Company, Amsterdam — Printed in The Netherlands

Short Communication

TIME RESOLUTION OF INTERFERENCES IN ELECTROTHERMAL ATOMIC ABSORPTION SPECTROMETRY

JOHN P. MANEY*
Energy Resources Co. Inc., 185 Alewife Brook Parkway, Cambridge, MA 02138 (U.S.A.)
VINCENT J. LUCIANO
Jarrell-Ash Division, Fisher Scientific Co., 590 Lincoln Street, Waltham, MA 02154 (U.S.A.)
(Received 25th April 1980)

Summary. A fast detector-amplifier-readout system is used for studying interferences in electrothermal graphite atomizers. The effects of different matrix components (K, B, Ca, Mg, and Cl), and graphite tube surfaces significantly alter the atomization processes of lead.

While electrothermal graphite atomization (e.g.a.) is a proven technique which expands the capabilities of atomic absorption spectroscopy, the technique is subject to substantial interferences [1—9]. This communication describes the use of a fast detection system [10, 11] to study the influences of selected matrix elements (K, B, Ca, Mg, Cl) on the time-dependent atomization of lead. The system used has a sample-hold design which produces discrete data points with a time resolution of 4.2 ms for a double beam absorbance data point or an update rate of 238 data points per second with a time constant less than 1 ms. Operated in the background correction mode, the system has a time resolution of 8.4 ms for each double beam background-corrected absorbance data point. The fast electronics permits the study of the time-dependent characteristics of the atomization process. This is especially important when determining the more volatile elements, such as lead and cadmium, for which atomization can occur in 0.5 s.

Experimental

All data were obtained with a Jarrell-Ash Model 850 double beam atomic absorption spectrometer, a model FLA-100 electrothermal graphite atomizer, a model 867 data translator, and a Tektronix T912 dual-channel storage oscilloscope. A battery-operated switching device was used to trigger the oscilloscope at the time of atomization. A Tektronix camera attachment and Polaroid film were used to record data. Ringsdorff graphite tubes were used for all but one study which used an Ultracarbon pyrolytically coated graphite tube. The optimum dry ash and atomization temperatures were determined for each sample type and remained unchanged throughout a study.

The inductively-coupled plasma data were obtained by the use of a Jarrell-Ash Model 975 plasma spectrometer which had 43 fixed-wavelength channels and an additional variable-wavelength channel. All data were collected with the system working in the background correction mode.

Standards were prepared from Fisher Scientific or Ventron atomic absorption standards. J. T. Baker Ultrex acids and reagent-grade phosphoric acid were used in the acid studies. A wastewater sample was supplied by a Pennsylvania wastewater treatment plant.

Results and discussion

This discussion deals solely with lead determination, although similar results were observed for cadmium. Coordinates for all figures are 200 ms/scale division (abscissa) and 0.1 absorbance units/scale division (ordinate). Figure 1A shows the lead atomization profile for a wastewater sample prepared according to the EPA approved method [12] that involves addition of nitric acid, evaporating to dryness followed by a nitric acid digestion and dissolving in a minimum of hydrochloric acid. This sample yielded the observed two-humped atomization peak which persisted regardless of ashing or atomization conditions. It can be assumed that most of the organic materials were destroyed by the wet digestion and the acid content was known to be less than 1%; thus inorganic materials became suspect. Inductively-coupled plasma emission spectrometry was used to determine 43 elements in the sample.

Individual 100-ppb lead standards were then prepared in the presence of individual matrix elements at concentrations near those found in the water sample, and Fig. 1B shows the atomization profiles for these standards. The peak for the standard with calcium is similar to a peak for pure lead. It is suggested that the double peak observed in Fig. 1 is a composite of all the effects observed in Fig. 1B.

Effects of sodium and potassium were studied in greater depth. The chlorides and carbonates of these ions gave virtually identical results, suggesting that the cations rather than the anions were involved. It was also noted that the interference resulting from KCl was not observed when a lead sample containing 250 ppm of calcium nitrate was previously atomized. The interference recurred, however, with successive runs as shown in Fig. 1C. If a high-temperature clean-up of the graphite tube is done after the atomization of the calcium nitrate/lead standard and before introduction of the KCl/Pb standard, the interference of KCl is seen to its fullest degree. One possible explanation of this loss and recurrence of the KCl interference may be a temporary residual calcium compound altering the graphite surfaces.

It has been proposed [7, 8] that reactions with, or catalyzed by, graphite surfaces can affect the atomization process. A study was performed in which the previously discussed wastewater sample was atomized on a new graphite tube and then atomized again after the tube had been artificially aged. New graphite tubes were subjected to an initial high-temperature clean-up,

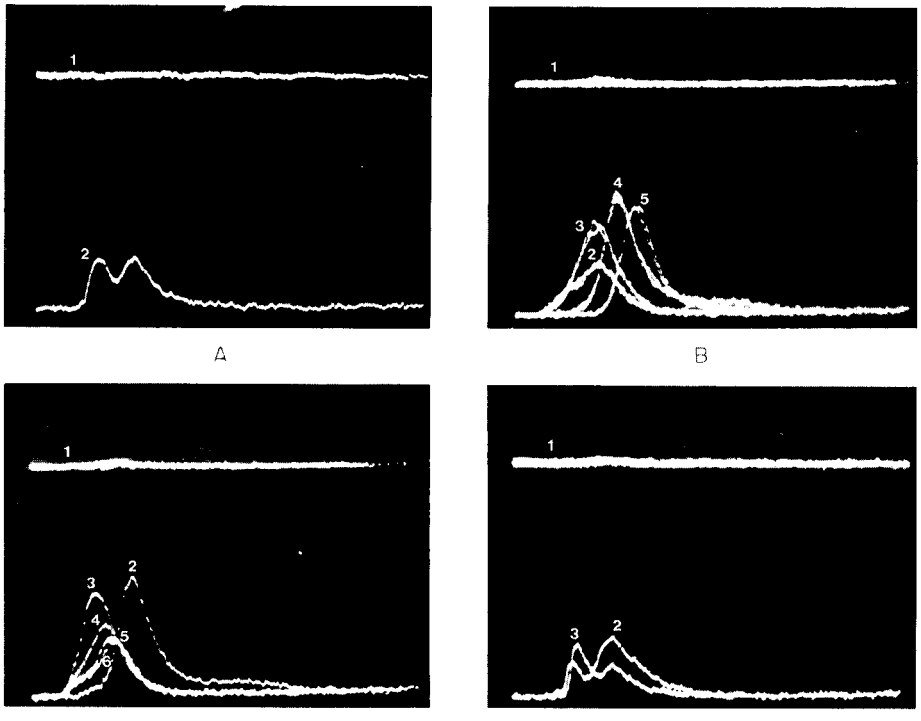

Fig. 1. Oscilloscope recordings of time-dependent absorbance for lead in selected matrices. For all frames: Ordinate = 0.1 A/div; abscissa = 200 ms/div; λ = 283.3 nm. A: (1) Background; (2) background-corrected peak for lead in digested wastewater sample. B: (1) Background; (2—5) background-corrected peaks for a 100 ppb lead standard in: (2) 100 ppm of K as KCl, (3) 10 ppm of B as H_3BO_3, (4) 250 ppm of Ca as $Ca(NO_3)_2$, (5) 100 ppm of Mg as $Mg(NO_3)_2$. C: (1) Background; (2—6) background-corrected peaks for a 100 ppb lead standard in: (2) 250 ppm of Ca as $Ca(NO_3)_2$, (3, 4, 5, 6) 100 ppm of K as KCl. D: (1) Background; (2, 3) background-corrected signal for lead in a digested wastewater sample using: (2) a new graphite tube, (3) an artificially aged graphite tube.

followed by three consecutive atomizations of the wastewater sample with the third atomization peak being recorded. The graphite tubes were then artificially aged by exposing them to maximum temperature in the absence of purge gas and the atomization process was repeated. Figure 1D depicts atomization peaks for the wastewater sample treated as described above. Both atomizations consist of dual peaks; however, with the fresh tube the first peak is the larger of the two, while the reverse is true for the peaks obtained on the aged tube. An identical study was performed with a pyrolytically coated tube. With the aged pyrolytically coated graphite tube, the second peak was completely eliminated.

When the method of standard additions was applied to the wastewater sample, it was observed that the added lead suffered from the same interference as the original lead. Thus, the standard addition method could be

used to determine lead in the sample. A second and less time-consuming method of quantifying the lead concentration was by the addition of phosphoric acid to a final concentration of 0.01—0.1%. The analytical results obtained by the two methods agreed with each other and with the results obtained by inductively-coupled plasma emission spectrometry.

Interferences in flameless atomic absorption are shown to be more complex than originally expected and more work must be done to explain the interference processes.

REFERENCES

1 D. C. Manning and W. Slavin, Anal. Chem., 50 (1978) 1234.
2 G. M. Hieftje and T. R. Copeland, Anal. Chem., 50 (1978) 300.
3 G. Horlick, Anal. Chem., 52 (1980) 290.
4 E. J. Czobik and J. P. Matousek, Anal. Chem., 50 (1978) 1.
5 J. Smeyers-Verbeke, Y. Michotte, P. van den Winkel and D. Massart, Anal. Chem., 48 (1976) 125.
6 D. J. Churella and T. R. Copeland, Anal. Chem., 50 (1978) 309.
7 D. J. Hodges, Analyst, 102 (1977) 66.
8 K. C. Thompson, K. Wagstaff and K. C. Wheatstone, Analyst, 102 (1977) 310.
9 J. Smeyers-Verbeke, Y. Michotte, and D. Massart, Anal. Chem., 50 (1978) 10.
10 R. E. Sturgeon and C. L. Chakrabarti, Prog. Anal. At. Spectrosc., 1:5, Pergamon, Oxford, 1978.
11 E. Lundberg, Chem. Instrum., 8 (1978) 197.
12 U.S. Environmental Protection Agency, Methods for Chemical Analysis of Water and Wastes, EPA-625-/-6-74-003A, 1976.

Analytica Chimica Acta, 125 (1981) 187—191
Elsevier Scientific Publishing Company, Amsterdam — Printed in The Netherlands

Short Communication

DETERMINATION OF TRACE MERCURY IN MILK PRODUCTS AND PLASTICS BY COMBUSTION IN AN OXYGEN BOMB AND COLD-VAPOUR ATOMIC ABSORPTION SPECTROMETRY

HISATAKE NARASAKI

Department of Chemistry, Faculty of Science, Saitama University, Shimo-Okubo, Urawa 338 (Japan)

(Received 29th October 1980)

Summary. Samples (ca. 1 g) are ignited by a nickel wire after the oxygen bomb has been charged with acidic peroxodisulphate solution. Precautions needed for measurements at the ng g^{-1} level are described. Accuracy, tested with a standard reference material, is satisfactory. The relative standard deviations for samples of butter, margarine, milk powder and polyethylene are in the range 19—5%.

As the mercury levels in the environment rise [1], the mercury contents of many materials have been investigated, mainly by neutron activation analysis (n.a.a.) [2] and cold-vapour atomic absorption spectrometry (a.a.s.) [3]. Both techniques usually require mineralization of the samples. Non-destructive n.a.a. does not require a radiochemical separation but separation is still needed for samples (e.g. milk and bone) containing large amounts of alkali metals, calcium and phosphorus [4].

Wet digestion is not recommended for samples consisting almost entirely of fat, since some fat may remain in the digest [5]. The undecomposed fats have been removed by petroleum ether extraction for determinations of, for example, trace copper [6—8] and iron [6, 7, 9] in butter. For reliable results, however, the whole sample should be decomposed completely, even if the required element cannot be detected in the fats. Likewise, ashing of polythenes is difficult without loss of mercury.

The oxygen bomb is suitable for rapid ignition of combustible materials such as milk products and polythenes, and has been used in determinations of trace mercury in samples such as paper [10], food, human hair [11, 12], cereals [13] and alfalfa [14].

Experimental

Apparatus. An Ogawa Sampling pellet press was used to press powder samples into tablets. The Rigosha oxygen bomb (capacity, 300 ml) used had stainless steel electrodes and capsule. The Nippon Jarrell-Ash AA-782 atomic absorption spectrometer used was fitted with an AMD-B2 pump and was attached to a Yanagimoto YR-110 chart recorder. The a.a.s. operating parameters were: wavelength, 253.7 nm; lamp current, 4 mA; damping, 1;

sensitivity, 1; air flow, 2.3 l min^{-1}; quartz absorption tube, 20 cm long, 17 mm i.d.; chart speed, 5 mm min^{-1}. The generating apparatus was of conventional design: a magnesium perchlorate-containing tube was inserted between the generator cell and absorption tube, and a charcoal-containing tube placed after the exit from the absorption tube.

Reagents. All chemicals used were of analytical grade; deionized and distilled water was used throughout. All reagents were stored in glass bottles.

For the stock mercury solution (1000 mg Hg l^{-1}), dissolve 0.3384 g of mercury(II) chloride in 50 ml of sulphuric acid (1 + 1) and dilute to 250 ml with water. For the working solution (1 mg Hg l^{-1}), dilute a suitable aliquot of the stock solution several times with 20 ml of sulphuric acid (1 + 2) and finally dilute to 100 ml with water; this standard is stable for a month without addition of preservatives. The addition of chloride or dichromate decreased the peak heights.

Potassium peroxodisulphate solution (0.05 M) must be stored in glass, because storage in polythene bottles leads to absorption of mercury from the atmosphere [15].

To purify the hydroxylammonium chloride solution (20% w/v), shake with portions of 0.001% (w/v) dithizone solution in chloroform until the colour remains constant in three extracts. To purify the tin(II) chloride stock solution (10% w/v) in sulphuric acid (1 + 2), bubble nitrogen through it for 2 h with stirring.

Preparation of sample solutions. Weigh 1 g of butter or margarine into the capsule of the bomb, and melt the sample under an infrared lamp. Make a coil in the middle of a 10-cm length of nickel wire (0.1 mm diameter) using a rod 3 mm in diameter. Wind the ends of the wire round the boss of the electrodes, so that the coil is clear of the capsule. Insert a thick cotton thread (5 cm long) through the coil and stick the ends of the thread into the sample. For powder samples, place about 1 g of the sample in the pellet press including the uncoiled nickel wire and make a tablet 13 mm in diameter by pressing the punch strongly. Wind the free ends of the wire around the electrodes so that the tablet will be above the crucible.

Place 10 ml of the peroxodisulphate solution and 10 ml of 10% (w/v) sulphuric acid in the bomb. Assemble the bomb and charge with oxygen to a pressure of 25 kg cm^{-2}. Apply 10 V a.c. to the electrodes, behind the safety shield. Cool the bomb in ice-water for 10 min. Shake the bomb on a horizontal shaker for 2 min, after placing the bomb in a wooden frame specially constructed to hold the screw cap in position. Release the gas gradually and transfer the contents with water to a 300-ml stoppered Erlenmeyer flask. Add 8 ml of (1 + 2) sulphuric acid and make up to 120 ml with water.

Measurement. To the flask add 2 ml of the hydroxylammonium chloride solution and 5 ml of the tin(II) chloride solution. Shake the flask for 2 min. Insert the bubbler into the flask with the air blowing through a by-pass via a three-way stopcock, and the recorder running. Turn the stopcock so

that the mercury vapour passes into the absorption tube and, after the peak has been recorded, turn back to the by-pass situation [16]. Wash the bubbler by bubbling through 100 ml of water after each measurement.

For calibration, place 100-ml portions of water in the flasks and add 10 ml of (1 + 2) sulphuric acid, 10 ml of the peroxodisulphate solution and up to 150 ng of mercury. Reduce the solution and measure as described above.

Results and discussion

Preparation of sample solutions. Rice paper has been used for wrapping samples [17]. Each sheet, however, was found to contain about 100 ng of mercury, which could not be removed uniformly at 190°C under reduced pressure. Polyethylene films likewise contained mercury, and no suitable wrapping materials could be found. Thus the fused or pressed samples were ignited with the nickel wire. Solid butter or margarine could not be burned. Among the powder samples studied, polyethylene and Orchard Leaves (NBS SRM 1571) were not easily pelleted, so the tablets were reweighed after pressing. In standard methods [18], flammable liquids (e.g., white oil) are mixed with samples to aid combustion; low results were obtained here when methyl ethyl ketone was mixed with the Orchard Leaves, because of incomplete oxidation of mercury.

Since platinum absorbs mercury [19], stainless steel electrodes and capsule were used in the present procedure.

Acidic solutions of potassium permanganate [10, 12] and ammonium cerium(IV) nitrate [13] and nitric acid [11] have been tried in the bomb as oxidants for mercury. Potassium peroxodisulphate has given good recoveries of mercury from many types of samples and so was preferred here.

For successive determinations on a sample, the analytical results decreased, presumably because atmospheric mercury adsorbed on the interior of the bomb was released by the heat of combustion. This mercury could not be removed by washing the bomb with detergent [13], or by blank determinations. Therefore, at least two portions of a sample were burned to clean the bomb before a series of determinations. A clean laboratory would be desirable for this determination.

When coal (NBS SRM 1630) was ignited, erroneous results were obtained and the electrodes were corroded. This arose because coal contains some sulphur, which forms mercury sulphide and oxidation with peroxodisulphate is incomplete [20]. Hence the bomb method is not suitable for determining mercury in coal or crude petroleum.

Results. Table 1 shows the results obtained for mercury determinations in various samples. The result for Orchard Leaves is within the certified value. As can be seen, the mercury contents of butter, margarine and milk powder range from 20 to 30 ng g^{-1}. In West Germany, the values reported for butter and margarine are 2.8 and 5.3 ng g^{-1} [21], or a maximum of 10 or 20 ng g^{-1} [22] and the values for milk powder range from 3 to 29 ng g^{-1} [23].

TABLE 1

Determination of mercury in milk products, plastics and Orchard Leaves (SRM 1571) for 1-g samples

Sample	Mercury found[a] ($ng\ g^{-1}$)	R.s.d. (%)
Butter 1	22—34 (30)	19
Butter 2	14—22 (19)	15
Margarine 1	17—22 (18)	11
Margarine 2	21—30 (25)	16
Milk powder	22—29 (26)	15
Polyethylene	21—25 (23)	9
Polyvinyl alcohol	67—74 (71)	5
Orchard Leaves[b]	141—158 (150)	5

[a]Range for 5 determinations with the average result in parentheses. [b]NBS certified value, $155 \pm 15\ ng\ g^{-1}$; for this sample only, a 0.5-g sample was taken.

In Great Britain, 10 $ng\ g^{-1}$ has been reported for butter [24]. In the United States the mercury content of dry milk ranges from 4 to 27 $ng\ g^{-1}$ [25]. In Japan, the values for butter range from 10 to 40 $ng\ g^{-1}$ and those for margarine from 10 to 20 $ng\ g^{-1}$ [26]. The present results for milk products are close to these ranges.

This work was partly supported by a grant from the Ministry of Education, Japan, grant number 364191.

REFERENCES

1 P. A. Krenkel, Crit. Rev. Environ. Control, 3 (1973) 303; 4 (1974) 251.
2 W. Zmijewska, J. Radioanal. Chem., 35 (1977) 389.
3 A. M. Ure, Anal. Chim. Acta, 76 (1975) 1.
4 G. H. Morrison, Crit. Rev. Anal. Chem., 8 (1979) 287.
5 N. T. Crosby, Analyst, 102 (1977) 225.
6 H. Timmen and J. Blütgen, Z. Lebensm.-Unters.-Forsch., 153 (1973) 283.
7 H. Hänni, J. Hulstkamp and A. Rothenbühler, Mitt. Geb. Lebensmittelunters. Hyg., 67 (1976) 448.
8 T. E. H. Downes and J. H. Labuschagne, S. Afr. J. Dairy Technol., 7 (1975) 167.
9 J. Koops, H. Klomp and R. H. C. Elgersma, Neth. Milk Dairy J., 33 (1979) 112.
10 L. G. Borchardt and B. L. Browning, Tappi, 41 (1958) 669.
11 M. Fujita, Y. Takeda, T. Terao, O. Hoshino and T. Ukita, Anal. Chem., 40 (1968) 2042.
12 T. Ukita, T. Osawa, N. Imura, M. Tonomura, Y. Sayato, K. Nakamuro, S. Kanno, S. Fukui, M. Kaneko, S. Ishikura, M. Yonaha and T. Nakamura, Eisei Kagaku, 16 (1970) 258.
13 R. Tkachuk and F. D. Kuzina, J. Sci. Food Agric., 23 (1972) 1183.
14 E. W. Bretthauer, A. A. Moghissi, S. S. Snyder and N. W. Mathews, Anal. Chem., 46 (1974) 445.
15 J. H. Cragin, Anal. Chim. Acta, 110 (1979) 313.
16 H. Narasaki, J. L. Down and R. Ballah, Analyst, 102 (1977) 537.

17 S. Fujiwara and H. Narasaki, Anal. Chem., 40 (1968) 2031.
18 ASTM D 129-64; ASTM D 808-63, Am. Soc. Testing Mat. Philadelphia, PA, U.S.A., 1966.
19 A. M. Ure and C. A. Shand, Anal. Chim. Acta, 72 (1974) 63.
20 L. W. Jacobs and D. R. Keeney, Environ. Sci. Technol., 8 (1974) 267.
21 R. Schelenz and J. F. Diehl, Z. Lebensm.-Unters.-Forsch., 151 (1973) 369.
22 A. Thomas, Fette, Seifen, Anstrichm., 78 (1976) 141.
23 K. Heine and A. Wiechen, Milchwissenschaft, 27 (1972) 688.
24 Working Party on the Monitoring of Foodstuffs for Mercury and Other Heavy Metals, First Report Survey of Mercury in Food, Her Majesty's Stationery Office, London, 1971, p. 31.
25 J. T. Tanner, M. H. Friedman, D. N. Lincoln, L. A. Ford and M. Jaffee, Science, 177 (1972) 1102.
26 K. Ikebe, Y. Tanaka, R. Tanaka and N. Kunita, Shokuhin Eiseigaku Zasshi, 18 (1977) 62.

Analytica Chimica Acta, 125 (1981) 193—198
Elsevier Scientific Publishing Company, Amsterdam — Printed in The Netherlands

Short Communication

ROTARY SAMPLE COMPARISON VALVE FOR FLAME SPECTROMETRY

J. E. PATTERSON

Chemistry Division, Department of Scientific and Industrial Research, Lower Hutt (New Zealand)

(Received 10th October 1980)

Summary. A motor-driven valve designed for the repeated (0.2 Hz) alternating introduction of sample and blank solutions into an atomic absorption spectrometer, improves detection limits and precision at the expense of greater sample consumption and elapsed time. It is applied in low level determinations of boron, the precise comparison of standard rocks, and the safe analysis of liquid hydrocarbons for lead by avoiding aspiration of air between samples.

Repeated manual introduction of sample and blank solutions into an atomic absorption spectrometer is sometimes employed to improve the precision of determinations at low concentrations by averaging the readings. The rotary sample comparison valve described here is a simple device which enables this task to be performed automatically and is intended for use with spectrometers which have some user-programmable data-processing capacity. Benefits obtained from the modulation of sample uptake have been discussed previously [1—3] but the rapid modulation rate meant that restrictions [4] were placed on the type of burner and flame employed. For the technique to be of general value, it would be desirable if premix burners, as normally found on commercial instruments, could be used.

Near the detection limit the use of very long time constants to resolve small signals from background is often frustrated by random baseline drift caused, for example, by changes in source intensity or flame background. The approach described here, where sample and blank are alternated at 0.2 Hz is more effective in reducing drift over long time intervals. The relatively slow cycle rate of 0.2 Hz is determined by limitations in the response time of premix burner systems. This is not necessarily a disadvantage as modern spectrometers employ either source modulation or double-beam optics which discriminate against noise, and some, but not all, causes of drift. An improvement in performance is required when long time constants are employed. Sample and blank then become separated by a substantial time interval, increasing the effect of any drift.

Experimental

The rotary sample comparison valve (Fig. 1) is connected to the nebuliser of an atomic absorption spectrometer. It is a simple, reliable device comprising a machined titanium shaft rotated by a synchronous motor inside a machined teflon block. As well as accommodating the titanium shaft, two side entrance apertures 180° apart and one axial exit aperture are drilled in the block, the bore being that of the uptake tubing. The block is enclosed by a brass ring to provide a compressive seal onto the titanium shaft. The shaft is milled and drilled (Fig. 1B) to allow continuous flow from one or

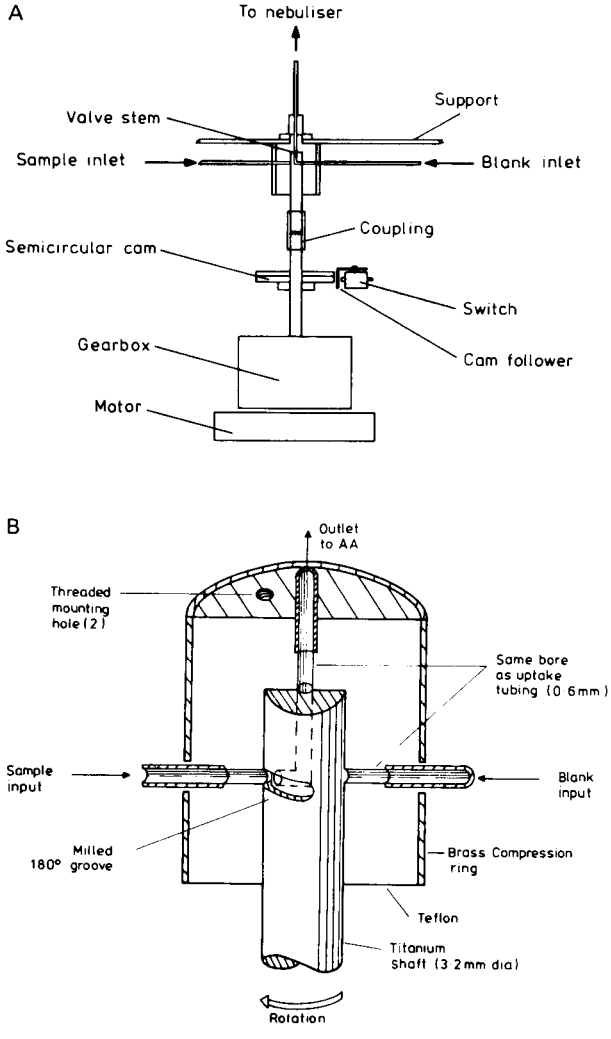

Fig. 1. (A) Rotary sample comparison valve showing a sectional view of the relationship between components. (B) Sectional detail of valve. The titanium shaft, which rotates with respect to the teflon block, is polished, after milling to remove any burrs.

other of the entrance apertures to the exit aperture, during shaft rotation. Stream changeover occurs every 180° of rotation without interruption of flow at any point because of the groove milled half-way around the shaft. The groove carries the solution from one inlet to the outlet while the shaft rotates 180°; the other inlet then supplies solution for the remaining 180°. The most important features of the valve are reliable sealing, minimum dead volume, symmetrical operation and continuous flow.

The titanium shaft is connected to the synchronous motor by a secure flexible coupling made from PVC tubing. Just below the coupling, a split synchronising cam is provided which can be adjusted to operate a microswitch giving a contact changeover for each 180° of shaft rotation. Each contact changeover initiates a read cycle in the atomic absorption spectrometer (Perkin-Elmer Model 403). This is achieved by connecting both the normally open and normally closed contacts to the trigger inputs of a monostable oscillator (SN74121N) while the common contact is grounded. The momentary opening of the contacts during changeover has the effect of triggering the monostable which provides the complementary output signals necessary to start a read cycle in the spectrometer. A variable delay can also be provided to synchronise sample input to the flame, with the start of the read cycle.

A program [5] written for an interfaced Hewlett-Packard 9815A desktop calculator averages the incoming data and calculates standard errors. Concentration differences between the inputs and corresponding standard errors are calculated with reference to a previously run standard. To counter drift more effectively, especially when there are few cycles, the difference between sample readings and the mean of two blank readings is summed into memory. The blank readings are taken immediately before and after the sample, the second blank reading also serving as the first blank reading for the next sample. Program use is simple. The concentration of the standard is entered and the RUN/STOP key on the calculator is pressed to load the data into the memory. Next the number of readings required is entered but the pressing of the RUN/STOP key is delayed until a pointer on the motor shaft matches an index mark. The timing required is not critical because readings are not started until the next contact changeover. After the specified number of readings has accumulated, the average and a standard error are printed. The sample is then run in the same way resulting in a printout of concentration difference between sample and blank and a composite standard error.

Results

Determinations at low concentrations. In this laboratory boron is determined in geothermal waters and in surface waters influenced by geothermal systems. In the latter case, low-level determinations may be required in which case preconcentration of boron on Amberlite XE-243 boron-selective ion-exchange resin may be necessary. Direct determinations are more rapid

and convenient, but the detection limit is poor, being 2—4 μg B cm^{-3}. Detection limits below 1 μg cm^{-3} are obtainable if the sample comparison valve is used. Table 1 shows some results obtained with the valve for a sample containing 4 μg B cm^{-3} obtained under conditions where this was just detectable by direct atomic absorption. A 10 μg cm^{-3} standard was used; the diminishing return with $n^{1/2}$ is noteworthy. The trace shown in Fig. 2 was obtained under the same analytical conditions, except that the valve was omitted; the analytical difficulties with manual determinations are obvious.

Comparison of nearly identical samples. The sample comparison valve is useful for the unbiased comparison of similar samples. A standard is run first so that differences may be expressed in suitable concentration units. The samples to be compared are then presented, one to each input, and the program restarted when the reference marks on the valve match. The

TABLE 1

Improvement in the precision of boron determinations (4 μg cm^{-3}) with increasing number of readings. The 150 readings took 12.5 min. The improvement is approximately related to $n^{1/2}$.

No. of readings (n)	10	30	60	75	150
Concentration (μg cm^{-3})[a]	2.98	4.27	3.88	3.37	3.97
Standard error (μg cm^{-3})[b]	1.0	0.73	0.53	0.45	0.39

[a]Average of 325 readings was 3.81 μg cm^{-3}. [b]Standard deviation/$n^{1/2}$.

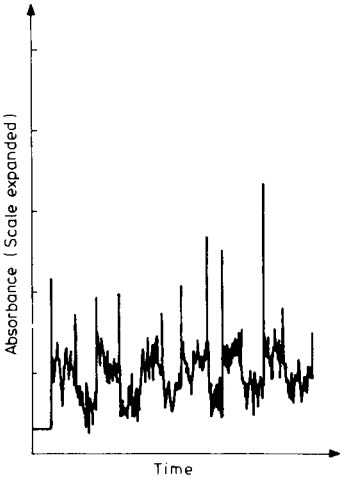

Fig. 2. Response from 4 μg B cm^{-3} solution manually aspirated into the nitrous oxide—acetylene flame. The flame conditions (fuel-rich) were optimised using a higher standard (e.g. 500 μg cm^{-3}).

output is a positive or negative difference in concentration. A positive result means that the sample with the higher concentration was applied to the same input as the calibrating standard, the converse being true for a negative result.

An important application has been the comparison of closely similar geochemical rock standards. The nearly depleted rock standard BR and a proposed replacement standard BE-N were compared. Small compositional differences were clearly resolved and the results (Table 2) were contributed to a cooperative study [6] involving 122 laboratories belonging to the International Working Group "Analytical Standards of Minerals, Ores and Rocks" (IWG).

For this work, six 0.1-g samples of BR and six of BE-N were fused with lithium tetraborate and lithium carbonate, and the beads were dissolved in 2% perchloric acid to give 200 $\mu g\ cm^{-3}$ solutions of dissolved rock. The sample comparison valve was used with one BR solution taken as a standard and as a reference to obtain concentration differences for the remaining eleven solutions. For each element determined, the five BR solutions showed concentration differences close to zero, while small deviations from zero were observed for the six BE-N solutions. The results were averaged and weight corrections made. Concentrations were evaluated by using known values for BR and calculating the average BE-N values from the mean concentration differences.

Aspiration of liquid hydrocarbons. A third application of the valve is to use it when liquid hydrocarbons are being aspirated. Direct switching from a wash solvent to a sample can be made without the usual interruption of flow and possible extinguishing of the flame during transfer. It is possible to run solvent/oxidant flames with the acetylene supply turned off. In this case the valve rotation is stopped so that the desired intake is open, changeover simply requiring a further rotation of 180 degrees. The program is not required. This procedure was used as part of an exercise in identifying fuels from different sources on the basis of their lead content. Quantifying the lead content would have required a more sophisticated procedure, usually

TABLE 2

Results for % oxides in BE-N submitted to the co-operative study [6] compared with proposed values obtained from the study. Standard errors ranged from 0.06% for SiO_2 to 0.002% for Na_2O. In each case 30 readings were accumulated (180 for 6 replicates).

Oxide	Sample comparison valve	Proposed values [6]	Oxide	Sample comparison valve	Proposed values [6]
SiO_2	38.00	38.20	Na_2O	3.21	3.18
Al_2O_3	10.14	10.07	TiO_2	2.60	2.61
MgO	13.15	13.15	Fe_2O_3(T)	12.90	12.84
CaO	14.00	13.87			

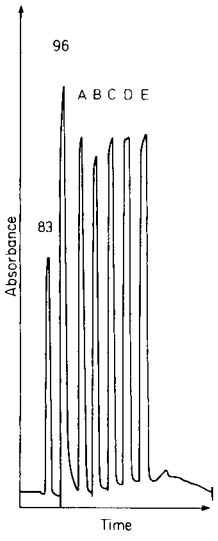

Fig. 3. Lead in aviation gasolines aspirated using a nitrous oxide oxidant; 83 and 93 octane fuels were used as references.

involving an extraction. Figure 3 shows some results for aviation gasolines where lead contents were compared to assist in determining if the correct fuel was used in a helicopter which had crashed. The oxidant used in the determination was nitrous oxide, acetylene being used only for lighting the flame by normal ignition procedures. Samples A, C, D, and E appear to have similar tetraethyl lead contents.

The cancellation of drift obtained with the rotary sample comparison valve will be of even more benefit where single-beam spectrometers are employed or the use of background correction requires single-beam operation. It would, of course, be unwise to use the valve to compensate for serious instrument defects.

The author thanks Mr. Murray Jones, DSIR, Physics and Engineering Laboratory for constructing the valve, and Mr. Mark Dwyer for preparing and running the standard rocks.

REFERENCES

1 K. Rüdiger, B. Gutsche, H. Kirchhof and R. Herrmann, Analyst, 94 (1969) 204.
2 M. Marinkovic and T. J. Vickers, Anal. Chem., 42 (1970) 1613.
3 V. G. Mossotti, F. N. Abercrombie and J. A. Eakin, Appl. Spectrosc., 25 (1971) 331.
4 R. L. Cochran and G. M. Hieftje, Anal. Chem., 49 (1977) 98.
5 J. E. Patterson, Atomic Spectrometry Programs for the HP 9815A computing controller, Report No. CD2309, New Zealand Department of Scientific & Industrial Research, Chemistry Division, Wellington, 1980.
6 K. Govindaraju, Geostandards Newsl., 4 (1980) 49.

Analytica Chimica Acta, 125 (1981) 199—202
Elsevier Scientific Publishing Company, Amsterdam — Printed in The Netherlands

Short Communication

AN AUTOMATED EXTRACTION SYSTEM FOR FLAME ATOMIC ABSORPTION SPECTROMETRY

LAGE NORD

Department of Analytical Chemistry, Royal Institute of Technology, S-100 44 Stockholm (Sweden)

BO KARLBERG*

Bifok AB, Box 5024, S-19405 Upplands-Väsby (Sweden)

(Received 6th October 1980)

Summary. A manifold is described which allows continuous liquid/liquid extraction of aqueous solutions of metal ions. A fraction of the organic stream is separated and led into the sample loop of an injector. The injector is situated in an aqueous carrier stream which is pumped into the nebulizer. The organic extract enters as an undispersed plug into the carrier when the valve is actuated. A preconcentration factor of 5.5 resulting in a correspondent sensitivity increase is readily obtained for aqueous samples.

Flame atomic absorption is frequently used for determinations of traces of metal ions. In order to lower the limit of detection the sample can be preconcentrated by extraction. Suitable metal complexes are extracted into a small portion of organic phase, which, after separation, is aspirated into the flame. The distribution ratio of the metal complex must be sufficiently high that an almost complete extraction is obtained even in cases when the phase volume ratio aqueous/organic is high. Ammonium pyrrolidinedithiocarbamate (APDC) is widely used as extracting agent in conjunction with atomic absorption [1].

Manual extraction is rather tedious and so mechanization of this sample pretreatment procedure is desirable. Jones et al. [2] used an AutoAnalyzer system for this purpose and a concentration factor of about 4 was attained. The consumption of sample was 16 ml min^{-1} while the aspiration rate of the separated organic phase was just less than 4 ml min^{-1}. In order to achieve as high a flow as 16 ml min^{-1} two identical sets of pump tubes had to be used resulting in an ingenious but rather complex flow pattern.

The optimum aspiration rate for most commercial nebulizers exceeds 4 ml min^{-1}; below this rate the sensitivity drops drastically [3]. This is probably the reason why two parallel manifolds were used by Jones et al. in order to create a high flow rate [2]. The principle of continuous feeding of the nebulizer by the organic phase must consequently be abandoned in a situation when the extraction manifold is characterized by a low consumption, less than 2 ml min^{-1}, of the organic phase. This communication

describes a simple, low-flow manifold by which addition of complexing agent to the aqueous sample as well as subsequent extraction can be performed, and also a new means of connecting this low-flow manifold to the high-flow feed of the nebulizer.

Experimental

Reagents. All chemicals were of reagent grade. Copper methyl isobutyl ketone (MIBK) test solutions were prepared by shaking aqueous solutions of copper–APDC with MIBK.

Apparatus. A Varian 875 atomic absorption spectrometer with an adjustable nebulizer was used throughout. The acetylene flow was reduced as much as possible, without the flame being extinguished on aspiration of water. Instrument settings were according to the standard procedure for determination of copper.

The flow system comprised a peristaltic pump (FIA 08, Bifok, Sweden), a flow injection analyzer provided with an injection valve with variable volume (FIA 05, Bifok) and an extraction manifold, parts of which have been described in detail previously [4].

Direct pumping of MIBK with a peristaltic pump is at present an unsolved problem, so a displacement bottle was constructed to deliver a smooth, unsegmented stream. A teflon stopper was pierced by two teflon tubings. The outlet tubing should not protrude into the bottle, otherwise an air bubble would be trapped and its compressibility would inevitably cause pulsing. A simple variable gauge was made from a standard tube union into which a hole was drilled perpendicularly. The tube was inserted and could be squeezed variably by means of two PVC connectors.

Manifold design. Figure 1 shows the flow diagram of the two interconnected flow systems, i.e., the nebulizer feed system (upper part) and the extraction system (lower part). The sample, **x**, is pumped continuously and mixed with the APDC solution, **y**, segmented by the MIBK stream by the aid of segmentor **b**, and extracted in the extraction coil **c**. A fraction of the organic phase is separated by the membrane separator **d** and led into the injector **f**. The variable gauge **e** is adjusted so that this fraction is kept constant. The rest of the organic phase is expelled through restrictor **g** to waste together with all of the aqueous phase.

In the filling position of the injector **f**, the extract fills the loop. In the injection position the loop is transferred to and interposed in the carrier stream of the nebulizer feed system. In this way a discrete, undispersed plug of the organic extract is transported by the aqueous carrier stream up to the nebulizer. The output signal is a peak, the shape of which depends on the volume of the plug.

Results and discussion

Figure 2 shows a calibration graph for copper. Linearity does not prevail above 0.15 ppm, because of the limited solubility of the APDC–copper

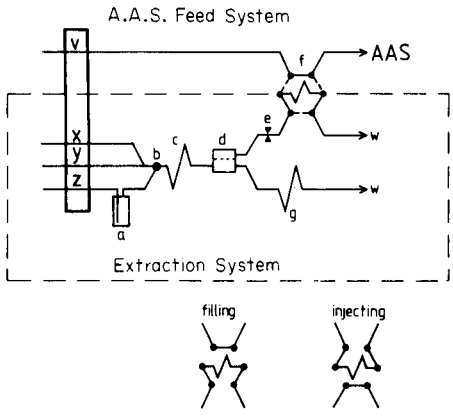

Fig. 1. Manifold for extraction of aqueous samples. Flows: v is the aqueous carrier to the spectrometer (4.4 ml min^{-1}), x the sample (4.4 ml min^{-1}), y the APDC reagent (1.0 ml min^{-1}) and z the water to the displacement bottle, a, providing the stream of MIBK (0.8 ml min^{-1}). b is the phase segmentor, c the extraction coil (2 m × 1 mm i.d. teflon), d the phase separator, e the variable gauge, f the injector with 200-µl sample loop, and g the restrictor (0.5 m × 0.5 mm i.d.). W denotes waste. The two modes of operation of injector f are indicated below the manifold.

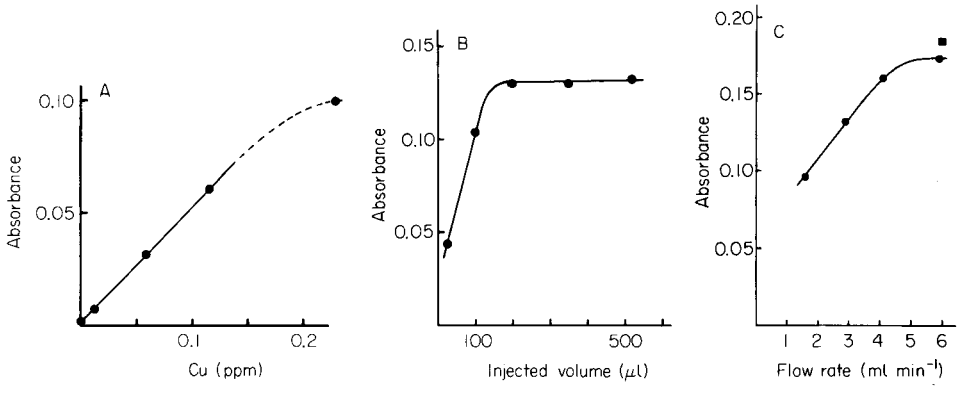

Fig. 2. (A) Calibration plot for aqueous copper solutions with the proposed manifold. (B) Injection of different volumes of 1 ppm Cu—MIBK standard into a pumped stream of aqueous carrier at a flow rate of 4.1 ml min^{-1}. (C) Injection of 1 ppm Cu—MIBK standard into a pumped stream of aqueous carrier (•) with aspiration set to 6.0 ml min^{-1}; aspiration of 1 ppm Cu—MIBK standard (▪).

complex in water which results in precipitation in the extraction system prior to introduction of organic phase. The repeatability (r.s.d.) was 1—2% in the linear range. The gain in sensitivity for a 0.1 ppm solution was about a factor of 6 compared with continuous aspiration of the aqueous sample. A concentration factor of 5.5 may be calculated from the flow rates of the sample stream and the organic stream. The present construction of the separator [4] limits the flow ratio aqueous/organic to less than about 7.

The nebulizer feed system. It is evident that the volume of the injector loop will influence both the peak height and the peak shape for a constant flow rate of the carrier. Figure 2(B) illustrates the peak height as a function of the volume of the injected Cu—MIBK solution (1 ppm). The carrier flow rate was 4.1 ml min^{-1}. The loop was manually filled with the MIBK solution. The peaks attained steady-state for volumes larger than 200 μl; for smaller volumes the peaks were sharp.

As mentioned previously most commercial nebulizers require a feed rate of analyte solution of at least 4 ml min^{-1} to avoid significant loss in sensitivity. To verify this in the case of sample injection in a pumped stream (instead of aspiration) 350 μl of Cu—MIBK solution was injected into the aqueous carrier stream; Fig. 2(C) shows the results. Different flow rates of the carrier were studied. For comparison the Cu—MIBK solution was aspirated at a rate of 6.0 ml min^{-1} until a steady-state signal was obtained. This signal was slightly larger than the signal resulting from the 350-μl portion of the organic sample transported at the same rate by the carrier. The MIBK plug caused an incidental fuel enrichment; however, injection of pure MIBK did not give any detectable peak. The baseline noise was about 0.002 units.

The repeatability (r.s.d.) was 0.6% calculated on 10 injections of the 1 ppm Cu—MIBK solution (carrier flow rate 5.9 ml min^{-1}).

Conclusions

A new way of performing an integrated preconcentration extraction with a.a.s. detection has been developed. It enables the extraction system to work independently from the nebulizer feed system which requires a high flow rate to take full advantage of the a.a.s. sensitivity. The flow rate of the organic solvent in the extraction system can be less than 1 ml min^{-1}. This concept of connecting a low-flow system with a high-flow system might be used for other applications within the field of continuous flow systems.

This work was supported by the Swedish National Board for Technical Development.

REFERENCES

1 M. S. Cresser, Solvent Extraction in Flame Spectroscopic Analysis, Butterworth, London, 1978, p. 63.
2 M. Jones, G. F. Kirkbright, L. Ranson and T. S. West, Anal. Chim. Acta, 63 (1973) 210.
3 Nebulizers for Atomic Absorption, Varian, Australia, 1979.
4 L. Nord and B. Karlberg, Anal. Chim. Acta, 118 (1980) 285.

Analytica Chimica Acta, 125 (1981) 203—207
Elsevier Scientific Publishing Company, Amsterdam — Printed in The Netherlands

Short Communication

DETERMINATION OF LEAD IN GEOSTANDARD ROCKS BY ELECTROTHERMAL ATOMIC ABSORPTION SPECTROMETRY AFTER ISOLATION OF LEAD WITH YIELD MONITORING

HAJIME SUGISAKI, HISAKO NAKAMURA, YOSHIMITSU HIRAO* and KAN KIMURA

College of Science and Engineering, Aoyama Gakuin University, 6-16-1 Chitosedai, Setagayaku, Tokyo 157 (Japan)

(Received 29th October 1980)

Summary. Lead contents in geochemical rock standards of the Geological Survey of Japan and the U.S. Geological Survey, were determined with coefficients of variation less than 5%. After dissolution of the rock by hydrofluoric and nitric acids, and spiking with ^{212}Pb, lead was purified by extraction with dithizone, appropriate corrections being applied to the final results.

Atomic absorption spectrometry (a.a.s.) has been extensively used for the determination of lead in geochemical standard rock samples. According to Ando et al. [1], 22 out of 46 analyses of the standard rocks JB-1 and JG-1 from the Geological Survey of Japan (G.S.J.) were done by a.a.s. Although the coefficient of variation of the method for lead determination is generally less than 5% [2], those for the lead contents of JB-1 and JG-1 obtained by a.a.s. are 34 and 13%, respectively. These values are larger than would be expected, and may be attributed to the inhomogeneity of the sample, incomplete sample dissolution, interference of other elements, contamination by lead, and variation in chemical yield during lead separation. In the work described here, special attention was paid to these five factors. The lead contents of geostandard rocks were determined by graphite-furnace a.a.s. after careful dissolution and purification for lead, with ^{212}Pb as yield monitor [3] in a clean room.

Experimental

Reagents. Hydrofluoric acid (special grade, Wako Pure Chemical Industries Ltd., Wako) was used as received. Water was distilled twice in a clean room in a quartz distillation system. Nitric and hydrochloric acids (super special grade, Wako) were purified twice by distillation in a standard quartz apparatus. Chloroform (special grade, Wako) was distilled in a teflon subboiling system [4]. Ammonia solution was prepared by absorbing the commercially available high-purity gas in the purified water after passing the gas through a Millipore filter and water trap. The dithizone solution in

0003—2670/81/0000—0000/$02.50

chloroform and the ammonium citrate solution were purified as described elsewhere [5], as was the ^{212}Pb solution [3].

A stock solution of 500 ppm lead in 0.1 M hydrochloric acid was prepared from lead metal (99.999% purity, Wako). This solution was diluted to appropriate concentrations with 0.1 M hydrochloric acid for a.a.s. calibration.

Apparatus. To avoid contamination and a high blank, polyethylene and teflon vessels were used for the chemical procedures. Polyethylene was washed with hot 2 M and 0.1 M nitric acids, and teflon with hot concentrated and 0.1 M nitric acids. When weighing was necessary, this equipment was dried under vacuum.

An atomic absorption spectrometer, AA-1 Mark-II, with a graphite furnace system, FLA-10 (Nippon Jarrell-Ash Co. Ltd.) was used. The lead hollow-cathode lamp (Hamamatsu TV Co. Ltd.) was run at 9 mA. The 283.3-nm lead line was used.

Analytical procedure. To avoid lead contamination, the complete procedure was carried out in a clean room with polyethylene-gloved hands. Weigh about 100 mg of finely-powdered rock sample in a teflon beaker. Add 3 ml of concentrated nitric acid and, after several hours, 1 ml of concentrated hydrofluoric acid, and digest overnight at room temperature. Slowly evaporate the solution to dryness and dissolve the residue completely in 10 ml of 2 M nitric acid. Add about 0.05 μCi of ^{212}Pb tracer solution and stir for 10 min to attain complete isotope exchange. Purify the lead (including the ^{212}Pb) by dithizone extraction and back-extraction [5, 6], as follows. Add 1 ml of 25% (w/v) ammonium citrate solution to the sample solution and adjust the pH to 9—10 with ammonia solution. Add 1 ml of 0.1% dithizone in chloroform and extract the lead complex with 5 ml of chloroform. Wash the lead extract with very dilute ammonia. Back-extract the lead with 10 ml of 0.1 M hydrochloric acid. Adjust the pH of the lead solution to 9—10 with ammonia and repeat the extraction and back-extraction steps.

Allow the back-extract to stand for more than 4 h to attain radioactive equilibrium between ^{212}Pb and ^{212}Bi, and measure the total γ-ray activity with a NaI(Tl) scintillation counter, in order to calculate the chemical yield. After diluting to an appropriate volume, measure the lead concentration by g.f.a.a.s., by dispensing 20 μl of the solution into the furnace. The power supply program for the furnace was: drying, 25 A for 20 s (ca. 200°C); ashing, 70 A for 20 s (ca. 800°C); atomizing, 200 A for 5 s (ca. 2000°C). During this time argon was passed through the furnace at 3 l min^{-1}.

Results and discussion

Five analyses of JB-1 and four analyses of JG-1 were carried out; the results are given in Table 1. From the sample weight, M, and the total amount of lead calculated, T, the concentration of lead in the sample, a, and the amount of blank lead, b, were calculated for a single analysis assuming the relationship $T = aM + b$, by least-squares fitting [7]. The blank lead is defined as the total, constant amount of lead introduced from the reagents

TABLE 1

Lead concentration in geochemical standard rocks by the proposed method

Sample	Weight (mg)	Yield (%)	Wt. of final soln. (g)	Pb content			
				Total		Net[a] concn. (ppm)	Mean[b] concn. (ppm)
				(ppb)	(ng)		
JB-1	40.5	86.8	5.62	57.2	370	8.5	
	43.0	77.9	10.68	29.0	398	8.7	
	103.2	57.8	10.54	48.2	879	8.3	
	126.4	19.3	14.90	14.6	1130	8.7	
	167.1	33.0	15.38	31.0	1440	8.5	8.5 ± 0.2
JG-1	19.0	89.9	20.89	19.0	442	21.9	
	50.2	87.7	35.17	28.3	1130	22.0	
	89.1	86.4	54.30	33.6	2110	23.4	
	203.1	86.3	85.74	46.5	4620	22.6	22.5 ± 0.7
JA-1	145.9	37.0	24.65	19.1	1270	8.5	
	148.8	70.4	26.91	33.2	1270	8.4	
	161.2	37.1	23.72	20.7	1320	8.1	8.3 ± 0.3
JB-2	174.5	47.1	18.37	24.7	963	5.4	
	195.0	41.6	18.48	23.6	1050	5.3	5.3 ± 0.1
G-2	53.4	87.6	29.93	49.0	1670	30.9	
	54.2	83.6	29.48	49.9	1760	32.0	
	94.3	61.4	25.66	70.4	2940	30.9	31.3 ± 0.9
BCR-1	46.3	43.8	15.88	18.2	660	13.7	
	74.7	25.7	16.30	17.7	1120	14.7	14.2 ± 0.7
AGV-1	91.5	71.8	24.78	101	3490	37.8	37.8 ± 1.9

[a]After deduction of the blank (25 ng Pb). [b]Mean concentration and standard deviation.

and equipment used, and by handling during the analytical procedure. The calculation of a and b for JB-1 gave a lead concentration in the sample of 8.5 ppm and 26 ng of blank lead and, for JG-1, 22.7 ppm and 24 ng. Thus, it is reasonable to assume 25 ng of lead as the blank for a single analysis. On this basis, the arithmetical mean lead concentrations were calculated to be 8.5 and 22.5 ppm for JB-1 and JG-1, respectively. The value for JB-1, 8.5 ppm, is the same as the value obtained by the least-squares method, and that for JG-1, 22.5 ppm, is lower than the least-squares value by only 0.2 ppm, which is within the statistical uncertainty. Thus, for the other standard rocks, the arithmetical means were calculated, and a blank value of 25 ng was used.

The coefficients of variation of 2 and 3% for JB-1 and JG-1 are explained by the combination of uncertainties in the radioactivity measurement and g.f.a.a.s. A statistical error of about 1% is included in the measurement of radioactivity of ^{212}Pb for the calculation of chemical yield, and g.f.a.a.s. has an uncertainty of 3—4% for a single analysis. Repeated analyses reduced the uncertainty to the values in Table 1.

Other geochemical standard rocks were analysed by the same procedure.

TABLE 2

Comparison of lead concentrations reported for the standard rocks

Rock		Pb concentration (ppm)		
		This work	Literature values	I.d.m.s.
G.S.J.	JA-1	8.3	No report	
	JB-1	8.5 ± 0.2	11.5 [8]	
	JB-2	5.3	No report	
	JG-1	22.5 ± 0.7	25.9 [8]	
U.S.G.S.	G-2	31.3	31.2 [9]	30.8 [10]
	BCR-1	14.2	17.6 [9]	13.56 [11], 13.53 [12]
	AGV-1	37.8	35.1 [9]	36.53 [11]

These results are also shown in Table 1. A comparison with literature values is given in Table 2. The values obtained by the present method are generally lower than most recommended or literature values except for AGV-1, but the values for G-2, BCR-1 and AGV-1 agree fairly well with the values obtained by isotope dilution mass spectrometry (i.d.m.s.), which is thought to be one of the most accurate methods. For standards from the G.S.J., no values have been obtained i.d.m.s.

The present method requires about 100 mg of sample, which is more convenient for handling than the 1-g samples required in the usual methods [13, 14]. As regards inhomogeneity of the sample, as shown in Table 1, five analyses of JB-1 and four of JG-1 gave linear calibration relationships, indicating good homogeneity for lead at least within each bottle of sample, although the homogeneity among bottles may still be open to question. Incomplete sample dissolution might be a cause of low results. However, there was no visible residue after dissolution. Furthermore, preliminary experiments showed that the lead values obtained by this simple nitric–hydrofluoric acid treatment were almost the same as those obtained by hydrofluoric and perchloric or sulphuric acid dissolution. The simple dissolution with a small volume of acids lowers the blank, and tedious purification of perchloric and sulphuric acids by distillation was avoided.

Interferences in the a.a.s. were avoided by using the dithizone extraction which is simple and introduces only very low blanks. Any variation in chemical yield during purification was corrected by the yield tracer technique with ^{212}Pb.

Contamination with lead is defined here as an indefinite amount (frequently extraordinarily large compared to the blank) of lead introduced during handling. The experiments with JB-1 and JG-1 gave constant blank values, indicating that there was no contamination by lead.

The method described in this communication should prove useful for the determination of lead in silicate rocks with high accuracy and should be valid for all samples which can be dissolved in acids, such as soils, sediments and biological materials.

REFERENCES

1 A. Ando, H. Kurasawa, T. Ohmori and E. Takeda, Geochem. J., 8 (1974) 175; A. Ando, private communication, 1978.
2 C. Iida, Jpn. Analyst, 23 (1974) 842.
3 Y. Hirao, K. Fukumoto, H. Sugisaki and K. Kimura, Anal. Chem., 51 (1979) 651.
4 J. M. Mattinson, Anal. Chem., 44 (1972) 1715.
5 C. C. Patterson and D. M. Settle, Natl. Bur. Stand. Spec. Publ., 422 (1976) 321.
6 E. B. Sandell, Colorimetric Determination of Traces of Metals, Interscience, New York, 1950, p. 107.
7 M. Tatsumoto and C. C. Patterson, Earth Science and Meteoritics, North-Holland, Amsterdam, 1963, p. 74.
8 A. Ando, Bunseki, 44 (1976) 526.
9 F. J. Flanagan, Geochim. Cosmochim. Acta, 37 (1973) 1189.
10 B. R. Doe, M. Tatsumoto, M. Delevaux and Z. E. Peterman, U.S. Geol. Surv. Prof. Paper, 575-B (1967) 170.
11 M. Tatsumoto, 1968, cited from F. J. Flanagan, Geochim. Cosmochim. Acta, 33 (1969) 81.
12 N. H. Gale, 1972, cited from F. J. Flanagan, U.S. Geol. Surv. Prof. Paper, 840 (1976) 131.
13 C. Iida and K. Yamazaki, Anal. Lett., 3 (1970) 251.
14 S. Terashima, Jpn. Analyst, 20 (1971) 321.

Analytica Chimica Acta, 125 (1981) 209—213
Elsevier Scientific Publishing Company, Amsterdam — Printed in The Netherlands

Short Communication

THE DETERMINATION OF CADMIUM, COPPER, LEAD AND THALLIUM IN HUMAN LIVER AND KIDNEY TISSUE BY FLAME ATOMIC ABSORPTION SPECTROMETRY AFTER ENZYMATIC DIGESTION

R. C. CARPENTER

Home Office Central Research Establishment, Aldermaston, Reading, Berkshire RG7 4PN (Gt. Britain)

(Received 15th December 1980)

Summary. Digestion of human liver and kidney tissue by the proteolytic enzyme subtilisin provides suitable solutions for direct determinations of Cd, Cu, Pb and Tl. Good precision and accuracy are demonstrated. Normal concentrations of Cd and Cu can be determined in these tissues; the poorer sensitivity for Pb and Tl precludes determinations of normal levels but typical concentrations found in acute poisoning can be measured. The metal concentrations in tissue digest solutions are stable for at least one month at 5°C.

Flame atomic absorption spectrometry (a.a.s.) is often used for the determination of trace elements in human liver tissue for toxicological evaluation [1]. The preferred method of sample preparation is low-temperature ashing (oxygen plasma), although wet oxidation is necessary for the determination of certain volatile elements (e.g. Sb, As, Hg). Both methods of preparation, however, are time-consuming for routine use and specialised equipment is required for low-temperature ashing.

Although the chemical stability afforded by acidic solutions is generally desirable for trace metal determinations, sample destruction techniques using strong bases have also been used successfully. These have the advantages of speed, simplicity and good analyte recovery. The use of tetramethylammonium hydroxide is typical, and in aqueous or organic solvents can solubilise a wide variety of tissues for determinations by either flame or flameless a.a.s. [2—5]. Enzymes are efficient reagents for protein destruction and the potent proteolytic enzyme, subtilisin Carlsberg, has been shown to degrade tissue rapidly for the isolation of the main chemical classes of drugs (basic, neutral and acidic) in high yields [6—8]. These features together with ease of use have led to its acceptance by forensic toxicologists in routine drug determinations.

The solubilised tissue produced by subtilisin digestion may be directly nebulised into an atomic absorption spectrometer. The high source temperature degrades the complexed metal ions, in solution with amino acids and polypeptides, to atomic species. In this communication, the technique of

enzymatic digestion followed by a.a.s. is described for the determination of four toxic metals of interest to the forensic toxicologist. The method is rapid and offers considerable advantages as it employs the standard enzymatic degradation used for drug extraction.

Experimental

Reagents and apparatus. Crystalline subtilisin A (Novo Enzymes, Windsor) and Trizma base [2-amino-2-(hydroxymethyl)propane-1,3-diol; Sigma Chemical Co., London] were used. These materials have been examined for trace element content by spark-source mass spectrometry and atomic absorption spectrometry [9] and found to contain very low levels of the elements of major toxicological interest.

Standard stock solutions (1 g l^{-1}; Hopkin and Williams) were used for cadmium, copper and lead. A stock solution of thallium (1 g l^{-1}) was prepared from thallium(I) sulphate (Johnson Matthey, Specpure) dissolved in water.

A Perkin-Elmer 303 atomic absorption spectrometer fitted with a Boling three-slot 11-cm burner was used for the determinations, the output being recorded on a Telsec 700 series potentiometric chart recorder. Fuel-lean air—acetylene mixtures were used throughout, together with a height of 8 mm from burner top to beam centre. Instrumental details are shown in Table 1.

Enzymatic digestion of human liver and kidney tissue. Portions of liver or kidney tissue (5 g) were mechanically blended with Trizma base (20 ml, 121 g l^{-1}) and distilled water (10 ml) in 100-ml conical flasks. Crystalline subtilisin A (5 mg) was added to the blended tissue prior to incubation at 55°C for 60 min with continuous shaking in a thermostatted water bath.

After completion of the incubation the solutions were filtered through glass wool (to remove residual connective tissue and thus avoid nebuliser blockage) into 50-ml volumetric flasks. When the solutions had cooled, they were made up to 50 ml with distilled water. Duplicate preparations were normally carried out together with samples which had been doped with appropriate quantities of the metals of interest for recovery studies.

TABLE 1

Instrumental details

Element	Cd	Cu	Pb	Tl
Wavelength (nm)[a]	228.8	324.7	283.3	276.8
Expansion	x 1	x 1	x 3	x 3

[a]Spectral bandwidth 0.7 nm.

Results and discussion

Development of the method. Preliminary experiments were carried out to investigate the most suitable matrix for the standards by adding known amounts of the metals to a liver digest solution and checking the recoveries. Initially, partial matching of concomitants in the tissue solutions and the standards was achieved by preparing the standards in the same concentrations of Trizma base as for the samples. This procedure was adequate for copper and cadmium but addition of potassium dihydrogenphosphate was necessary to ensure maximum recovery of lead and thallium. Thus, standards prepared in Trizma base plus potassium dihydrogenphosphate (1 g l^{-1}) gave good recoveries for all elements from additions made to tissue digests. Based on earlier work [1], this concentration of phosphate approximates the phosphorus and total alkali metal content of the tissue digest solutions. The calibrations obtained with these standards show a slight curvature towards the concentration axis. The sensitivities obtained are as follows (mg l^{-1} for 1% absorption): Cd 0.04, Cu 0.09, Pb 0.5 and Tl 0.5. Multi-element standard solutions were prepared with the following concentration ranges: 0—5 mg Cd l^{-1}, 0—10 mg Cu l^{-1}, 0—20 mg Pb l^{-1}, and 0—20 mg Tl l^{-1}. These standards were found to be stable for at least 2 months.

Tissue analysis. Determinations of Cd, Cu, Pb and Tl were carried out on three human livers and one kidney. Comparative data were obtained by low-temperature plasma ashing followed by atomic absorption spectrometry [1] and spark-source mass spectrometry [10]. The results of duplicate determinations are shown in Table 2. In general, good agreement was obtained between the enzymatic digestion and plasma ashing preparation techniques. These results clearly show that the simple matrix matching of standards to samples is adequate for the determination of these elements in enzyme tissue digests.

With the exception of copper in Liver B, the cadmium and copper results are within the range quoted for normal tissue [11]; the copper results for

TABLE 2

Analytical data on liver and kidney samples
(Results expressed as $\mu g\ g^{-1}$ in wet tissue)

Sample	Preparation	Cd	Cu	Pb	Tl
Liver A	Plasma ash	0.9	5.1	0.8	—
(Sudden death, physical causes)	Subtilisin	0.9	4.5	<2	<2
Liver B	Plasma ash	2.5	18.4	1.4	—
(As Liver A)	Subtilisin	2.3	17.7	<2	<2
Liver C	Plasma ash	3.1	4.8	13.4	—
(Acute, toxic poisoning)	Subtilisin	2.9	4.6	12.4	<2
Kidney	Plasma ash	28.0	2.6	8.3	—
(As Liver C)	Subtilisin	26.0	2.5	8.9	<2

Liver B are slightly higher. The concentrations of lead in Livers A and B are within the range quoted for normal tissue, which is below the limit of detection for this technique. Liver C and the kidney sample arose from a case of acute toxic poisoning and the lead levels observed are typical. As expected, thallium was not detected in the liver and kidney samples, normal levels for this element being $<0.1\ \mu g\ g^{-1}$. It is expected from recovery studies that this element could be determined when present at concentrations associated with cases of acute poisoning.

Results from recovery studies of metal additions made to tissue samples before the subtilisin digestion are shown in Table 3. These results were obtained during the analysis of the tissue samples shown in Table 2 and are the means of duplicate additions.

Precision of method. The precision of this technique was estimated by determining cadmium and copper in five separate digests of the same liver sample. The mean results obtained were $1.22\ \mu g\ Cd\ g^{-1}$ and $4.62\ \mu g\ Cu\ g^{-1}$, with standard deviations of 0.06 and 0.12, respectively. Insufficient sample was available to determine the precision for lead. The precision of these determinations is considered to be good as the variation includes both sampling and measurement errors.

Estimation of detection limits. Detection limits for this technique were estimated by using the criterion of twice the peak-to-peak background noise, expressed as $\mu g\ g^{-1}$ in wet tissue. They are as follows: Cd 0.25, Cu 0.4, Pb 2 and Tl $2\ \mu g\ g^{-1}$. As demonstrated earlier, cadmium and copper can be determined at normal levels in liver and kidney whereas lead and thallium can be determined only at concentrations typically seen in acute poisoning cases.

Stability of subtilisin digests. Cadmium, copper and lead were redetermined in the digests, from the Liver B and kidney samples after storage for 1 month at 5°C. The digests were allowed to reach room temperature before the determinations. The results obtained agreed with the original data within the limits of experimental error, indicating no significant losses of these elements.

The standard subtilisin tissue degradation technique is thus shown to provide stable solutions for the direct determination of trace metals in human liver and kidney tissue by a.a.s. The technique offers good precision and the results agree well with samples prepared by low-temperature ashing (oxygen

TABLE 3

Recovery of metal additions to tissue samples

Metal	Concentration added ($mg\ l^{-1}$)	Recovery (%)			
		Liver A	Liver B	Liver C	Kidney
Cd	1	98	96	96	98
Cu	2	100	98	98	99
Pb	4	99	99	102	102
Tl	4	96	99	95	99

plasma). This rapid enzyme degradation offers considerable advantages to toxicologists in operational laboratories investigating cases of suspected metal poisoning.

REFERENCES

1 J. Locke, Anal. Chim. Acta, 104 (1979) 225.
2 A. J. Jackson, L. M. Michael and H. J. Schumacher, Anal. Chem., 44 (1972) 1064.
3 P. D. Kaplan, M. Blackstone and N. Richdale, Arch. Environ. Health, 27 (1973) 387.
4 L. Murthy, E. E. Menden, P. M. Eller and H. G. Petering, Anal. Biochem., 53 (1973) 365.
5 S. B. Gross and E. S. Parkinson, Atom. Absorpt. Newsl., 13 (1974) 107.
6 M. D. Osselton, M. D. Hammond and P. J. Twitchett, J. Pharm. Pharmacol., 29 (1977) 460.
7 M. D. Osselton, J. Forensic Sci. Soc., 17 (1977) 189.
8 M. D. Osselton, I. C. Shaw and H. M. Stevens, Analyst, 103 (1978) 1160.
9 J. Locke, R. Carpenter and M. D. Osselton, Med. Sci. Law, in press.
10 J. Locke, D. R. Boase and K. W. Smalldon, Anal. Chim. Acta., 104 (1979) 233.
11 G. V. Iyengar, W. E. Kollmer and H. J. M. Bowen, The Elemental Composition of Human Tissues and Body Fluids, Verlag Chemie, New York, 1978, p. 65.

Analytica Chimica Acta, 125 (1981) 215—218
Elsevier Scientific Publishing Company, Amsterdam — Printed in The Netherlands

Short Communication

TITRIMETRIC DETERMINATION OF MICROGRAM AMOUNTS OF LEAD BY THIOCYANATE AMPLIFICATION AFTER PRECIPITATION AS LEAD HEXATHIOCYANATOCHROMATE(III)

MOUAYED Q. AL-ABACHI*, NAZLI A. SHAHBAZ and S. T. SULAIMAN
Department of Chemistry, College of Education, University of Mosul, Mosul (Iraq)
(Received 31st October 1980)

Summary. Lead (25—200 μg) is precipitated as $Pb_3[Cr(SCN)_6]_2$. The filtered precipitate is treated with 10% carbonate solution, and the thiocyanate dissolved is oxidized by iodine to sulphate at pH 8.2. After acidification, the excess of iodine is extracted into chloroform, and the iodide ion retained in the aqueous solution is amplified by bromine oxidation and subsequent treatment with more iodide. The method provides 152 iodine atoms for each original lead ion. Only Bi^{3+} and Cu^{2+} interfere seriously.

Present day demands on analytical chemistry include the necessity of detecting and determining smaller amounts and at lower concentrations than ever before. Among the approaches to meet these challenges is chemical multiplication or amplification. As shown in Belcher's review [1], most known amplification procedures are based on iodide and not bromide amplification, because iodide amplification is simple, rapid and stoichiometric. Generally, the determination of iodate or bromate is completed simply by addition of iodide and titration of the liberated iodine with thiosulphate. Belcher et al. [2] developed an indirect method for the determination of thiocyanate (2.7—90 μg) and thiosulphate (4.5—90 μg), by oxidation with iodine in alkaline solution to sulphate. After acidification, the excess of iodine was extracted into chloroform, and the iodide ions formed in the redox reaction were amplified by bromine oxidation. Either a titrimetric or a spectrophotometric finish could be used. Each thiocyanate ion results in the ultimate production of 19 and 24 iodine molecules, respectively. The thiocyanate amplification was later applied to the indirect determination of bismuth after its precipitation as bismuth hexathiocyanatochromate(III) [3]. Méndez et al. [4] recently developed an indirect method for the determination of lead (15—120 μg) by precipitation as $(C_4H_9)_4N[Pb(SCN)_3]$; after filtration, the precipitate was treated with hydrogencarbonate solution and the thiocyanate released was determined by the above amplification reaction. In this communication, the thiocyanate amplification is applied to the more sensitive determination of lead (25—200 μg) after precipitation as $Pb_3[Cr(SCN)_6]_2$.

0003—2670/81/0000—0000/$02.50

Experimental

Reagents. All the chemicals used were of analytical-reagent grade except where otherwise stated. For the stock lead(II) solution (500 μg ml^{-1}) dissolve 0.3996 g of lead nitrate in 500 ml of distilled water. Recrystallize potassium hexathiocyanatochromate(III) from absolute ethanol and dry in a vacuum desiccator until required.

Determination of lead. To 1 ml of cold solution containing 25—200 μg of lead in a 4-ml test tube, add 50—60 mg of solid potassium hexathiocyanatochromate(III). After precipitation is complete (see Results and discussion), filter off the precipitate on a porosity-4 sintered-glass filter and wash it with 2 ml of 1 M nitric acid followed by four 2-ml portions of cold distilled water. Treat the precipitate with 10 ml of 10% sodium carbonate solution, transfer the solution to a 50-ml separating funnel, adjust the pH of the solution to 8.2 with 2 M sulphuric acid, add 0.4 ml of saturated iodine solution in chloroform, and shake well. After 5 min, acidify the solution with 4 ml of 2 M sulphuric acid and extract the iodine with four 10-ml portions of chloroform, shaking consistently for 1 min each time. Transfer the aqueous layer to a 100-ml stoppered flask, add 1 ml of saturated bromine water, mix for 5 min (using an electric shaker), destroy excess of bromine with 3 ml of 90% formic acid, and add 1 g of potassium iodide. Leave in the dark for 5 min for complete liberation of iodine, and then titrate the liberated iodine with standard 0.002 M sodium thiosulphate using starch as indicator. Run a blank through the whole process. (1 ml of 0.002 M thiosulphate = 2.726 μg of Pb^{2+}.)

Results and discussion

Lead(II) precipitates with hexathiocyanatochromate(III) ions as $Pb_3[Cr(SCN)_6]_2$ [5]. On treatment of the precipitate with 10% sodium carbonate solution, $[Cr(SCN)_6]^{3-}$ ions are released and lead carbonate is formed

$$Pb_3[Cr(SCN)_6]_2 + 3CO_3^{2-} \rightarrow 3PbCO_3 + 2[Cr(SCN)_6]^{3-}$$

In the carbonate medium (pH 8.2), the thiocyanate in the hexathiocyanatochromate(III) ions is oxidized to sulphate by an excess of iodine [4]; the chromium(III) is not oxidized

$$[Cr(SCN)_6]^{3-} + 24I_2 + 24H_2O \rightarrow 6SO_4^{2-} + 6ICN + 42I^- + 48H^+ + Cr^{3+}$$

Since each thiocyanate ion gives rise to 38 iodine atoms [3], each hexathiocyanatochromium(III) ion gives rise to 228 iodine atoms, and thus each lead ion gives rise to 152 iodine atoms.

The influence of varying amounts of chromium(III) and lead(II) on the determination of 10 μg of thiocyanate was investigated in order to establish the feasibility of the suggested procedure. The results showed that neither ion interfered, even when present in a 50-fold weight ratio to the thiocyanate ion.

The effect of addition of various amounts of solid potassium hexathio-

TABLE 1

Effect of amount of potassium hexathiocyanatochromate(III) on the precipitation of lead (50 μg)

Amount of reagent added (mg)	Pb found[a] (μg)	Recovery (%)	Amount of reagent added (mg)	Pb found[a] (μg)	Recovery (%)
7	35.2	70.4	50	49.9	99.8
10	39.9	79.8	60	50.0	100.0
20	44.5	89.0	70	50.1	100.2
30	50.0	100.0	90	50.5	101.0
40	50.1	100.2	130	52.3	104.6

[a]Average of 3 determinations after subtraction of the blank value.

TABLE 2

Results for the indirect amplification of lead

Pb taken (μg)	Titrant volume (ml)	Pb found[a] (μg)	Mean recovery (%)	Pb taken (μg)	Titrant volume (ml)	Pb found[a] (μg)	Mean recovery (%)
25	9.20	25.0	100.0	130	47.80	130.3	100.2
40	14.70	40.0	100.0	150	55.00	149.9	99.9
50	18.40	50.1	100.2	170	62.30	169.8	99.8
70	25.70	70.0	100.0	200	73.30	199.8	99.9
100	36.70	100.0	100.0				

[a]Average of 5 determinations after subtraction of the blank value.

cyanatochromate(III) on the precipitation of 50 μg of lead is shown in Table 1. The addition of a moderate amount of potassium hexathiocyanatochromate(III) (50—60 mg) provided the best recovery of lead; large excesses of reagent (>90 mg) should be avoided in order to decrease the number of washings needed to avoid high results. It proved possible to precipitate quantitatively 25—200 μg of lead in 1 ml of sample solution. Quantitative precipitation of 25 μg Pb required 30—35 min, 50 μg Pb required 15—20 min, but 100—200 μg Pb required only 5 min. The results in Table 2 show recoveries ⩾99.8%. The blank was always 1.4—2.0 ml of 0.002 M thiosulphate solution; the coefficient of variation for seven determinations of 50 μg of lead was 0.14%.

The presence of up to 50-fold weight ratio (to lead) of Cd^{2+}, Zn^{2+}, Cr^{3+}, Co^{2+}, Th^{4+}, Mg^{2+}, Mn^{2+}, Al^{3+}, Fe^{3+}, CO_3^{2-} and SO_4^{2-} did not interfere in the determination of 50 μg of lead. The presence of a 50-fold weight ratio (to lead) of Hg^{2+}, Cu^{2+} or Bi^{3+} introduced negative errors of 3.6, 17.1 or 20.0%, respectively.

REFERENCES

1 R. Belcher, Talanta, 15 (1968) 357.
2 R. Belcher, S. S. T. Liao and A. Townshend, Talanta, 23 (1976) 541.
3 R. Belcher, S. Liawruangrath and A. Townshend, Talanta, 24 (1977) 590.
4 J. H. Méndez, A. A. Mateos and E. J. M. Mateos, Anal. Chim. Acta, 111 (1979) 327.
5 K. Jørgensen, Inorganic Complexes, Academic Press, London, 1966.

Analytica Chimica Acta, 125 (1981) 219—220
Elsevier Scientific Publishing Company, Amsterdam — Printed in The Netherlands

Short Communication

DETERMINATION OF THE DISSOCIATION CONSTANT AND LIMITING EQUIVALENT CONDUCTANCE OF A WEAK ELECTROLYTE FROM CONDUCTANCE MEASUREMENTS ON THE WEAK ELECTROLYTE

LEONARD S. LEVITT

Chemistry Department, College of Science, The University of Texas at El Paso, El Paso, TX 79968 (U.S.A.)

(Received 27th October 1980)

Summary. A method is described for computing the dissociation constant and equivalent conductance at infinite dilution, Λ_0, for a weak electrolyte from as few as two conductance measurements at different concentrations. The iterative procedure applied to acetic acid data yielded a dissociation constant of 1.80×10^{-5} and an average value ($n = 4$) of Λ_0 of 389.5 compared with an expected value of 390.7.

It is well known that a plot of the equivalent conductance, Λ, vs. $c^{1/2}$ for a strong electrolyte gives a straight line (Kohlrausch's Law) which can readily be extrapolated to zero concentration to obtain Λ_0, the equivalent conductance at infinite dilution. For a weak electrolyte the same plot is curved and approaches the Λ axis asymptotically, thus making it impossible to determine Λ_0 by extrapolation. Consequently, Λ_0 for a weak electrolyte is computed as the sum of the individual ionic conductances at infinite dilution, λ_0, which in turn are determined from conductance measurements on strong electrolytes by the application of Kohlrausch's second Law ($\lambda_{0(+)} + \lambda_{0(-)} = \Lambda_0$).

It is shown below that both Λ_0 and the concentration dissociation constant, K_c, can be calculated accurately for weak electrolytes from as few as two conductance measurements at two different concentrations. Neither graphical extrapolation nor individual ionic conductivities at infinite dilution are required for these calculations. The accuracy of the method is limited by the accuracy of the Ostwald—Arrhenius dilution law [1]

$$K_c = \Lambda^2 C/\Lambda_0(\Lambda_0 - \Lambda) \tag{1}$$

In principle it is necessary only to solve two equations for two unknowns (Λ_0 and K_c) which seems trivial and obvious enough, except for the fact that it is never done. Equation (1) can be solved for Λ_0 to yield

$$\Lambda_0 = (\Lambda/2)\,[1 + (1 + 4c\,K_c^{-1})^{1/2}] \tag{2}$$

Substituting Λ_1 and Λ_2 at concentrations c_1 and c_2, respectively, it is shown that

$$K_c = \{[\Lambda_2(4c_2 + K_c)^{1/2} - \Lambda_1(4c_1 + K_c)^{1/2}]/[\Lambda_1 - \Lambda_2]\}^2 \tag{3}$$

Equation (3) can be solved for numerical data by an iterative procedure in which it is assumed that $4c \gg K_c$, or by regression methods.

When K_c has been determined in this manner, it can be used to calculate Λ_0 with eqn. (2). The values obtained for Λ_0 for two or more experimental concentrations should agree. The equilibrium constant and conductance at one concentration can also be used to compute the conductance at any other concentration using eqn. (2).

The applicability of these relations was evaluated using the conductance data of MacInnes and Shedlovsky [2] for acetic acid at 25°C. From the data for two low concentrations ($c_1 = 2.801 \times 10^{-5}$; $\Lambda_1 = 210.4$; and $c_2 = 1.028 \times 10^{-3}$; $\Lambda_2 = 48.15$), the iterative procedure yielded $K_c = 1.80 \times 10^{-5}$. This is the usual value for acetic acid when K_c is not corrected for activity coefficients [3].

Values of Λ_0 computed with $K_c = 1.80 \times 10^{-5}$ and $c = 2.801 \times 10^{-5}$, 1.028×10^{-3}, 5.911×10^{-3}, and 1.0×10^{-1} M were 388, 389, 391, and 390, respectively, compared with the accepted thermodynamic value of 390.7 for acetic acid [3].

It should be clear that for higher concentrations, where $4c/K_c \gg 1$, eqn. (2) can be simplified [4] to $\Lambda_1/\Lambda_2 \simeq (c_2/c_1)^{1/2}$, which gives quite accurate results at all concentrations [4] above 0.01 M.

REFERENCES

1 L. S. Levitt and H. Widing, Chem. Ind., (1974) 781.
2 D. A. MacInnes and T. Shedlovsky, J. Am. Chem. Soc., 54 (1932) 1429.
3 G. M. Barrow, Physical Chemistry, McGraw-Hill, 2nd edn., 1966, p. 652.
4 L. S. Levitt, Chem. Ind., (1961) 1621.

ANALYTICA CHIMICA ACTA, Vol. 125 (1981)

AUTHOR INDEX

(continued from back cover)

(continued on facing page)

Printed in The Netherlands.

CONTENTS

Short Communications

(continued on inside page of cover)